EXPRESSION PROFILING REVEALS KEY REGULATORS OF SYNAPTIC SPECIFICITY AND FUNCTION IN THE *C. ELEGANS* MOTOR CIRCUIT

By

Rebecca Marie Fox

Dissertation

Submitted to the Faculty of the

Graduate School of Vanderbilt University

in partial fulfillment of the requirements

for the degree of

DOCTOR OF PHILOSOPHY

in

Cell and Developmental Biology

December 2006

Nashville, Tennessee

Approved:

David M. Miller, III

Kathleen L. Gould

Bruce H. Appel

Kendal S. Broadie

Daniela Drummond-Barbosa

For my family

ACKNOWLEDGEMENTS

I would first like to thank my mentor David Miller for his support and encouragement during my time in graduate school. He has been incredibly patient and taught me the importance of taking risks to achieve my scientific goals. David is an excellent teacher and has encouraged me to become independent and he has always been confident in my abilities as a scientist. I would also like to thank David Greenstein, who was like a second mentor. His enthusiasm for science is unmatched, and I am indebted to him for taking the time to help me out early on when I was struggling. I would also like to thank the additional members of my committee: Kathy Gould, Kendal Broadie, Bruce Appel, Daniela Drummond-Barbosa, and Peter Kolodziej for challenging me, and guiding me throughout my graduate career.

I need to thank the members of the Miller lab, both past and present, for making work a fun place to be. I am incredibly lucky that I get to go to work each day with my best friends. I especially want to thank Steve Von Stetina and Joseph Watson. Graduate school is hard enough, but it would have been ten times harder without you guys there every step of the way. You two provided endless entertainment, sometimes very early into the morning, and I think we can all agree that together, we made one hell of a graduate student.

My friends have provided a constant support system throughout my graduate career. I need to thank especially, Julie, JJ, Laurie, Jessica, Steve, Mary, Joe, Macy, Joseph, Kathy, Clay, Kylee, and Leigh. We have suffered through freezing cold bike rides, dirty nasty lake water, and sweltering heat to complete several endurance sporting

events. We have also enjoyed many random spontaneous road trips to baseball games, football games and concerts that were good for a much-needed retreat from Nashville. I also want to thank my "Mountain Therapy" friends (Leigh, Nellie, Nicole, Efrain, Jenn) for providing a weekend of relaxation every winter in Gatlinburg. I will never forget the evening in the Sevierville ER, the hot tub and of course Moulin Rouge.

I am incredibly grateful for my family and the love and support they have given me throughout my life. My parents, Richard and Susan Fox, have been incredibly supportive, both financially and emotionally, and have always encouraged me to pursue my goals. This past year they have been extremely generous with their time in coming to Tennessee and helping me to recover from some serious health problems. I also need to thank my sister, Carolyn, and my brother Jonathan for their unending support.

Finally, I need to thank Michael Anderson for his continued love and support. We have endured some pretty rough times this past year, and I admire you for the strength you have shown in these situations. I am also very grateful that I had you by my side through everything. Given everything we have overcome this year, I know that together, we can tackle anything that may challenge us. These last couple of years have been amazing and I look forward to our future together.

Finally, I need to acknowledge my funding sources. I was fortunate enough to be on the Developmental Biology training grant, and I have also received support from a predoctoral NRSA from the NIH/NINDS.

TABLE OF CONTENTS

PAGE

LIST OF TABLES

LIST OF FIGURES

CHAPTER I

INTRODUCTION

Coordinated locomotion depends on the motor circuit. The brain processes sensory inputs to signal command interneurons, which in turn control motor neuron activity in an axial nerve cord. Motor neurons innervate skeletal muscles, instructing them to contract or relax, thereby regulating movement. To better understand the molecular determinants that drive locomotion it is necessary to characterize the individual components that comprise this circuit. Generating a comprehensive description has been difficult, however, given the complexity of the vertebrate nervous system. To circumvent this problem we have adopted the nematode *Caenorhabditis elegans* (*C. elegans*) for our studies, an organism with a simple, well-defined nervous system. A complete electron microscopic (EM) reconstruction of the nervous system has revealed exactly 302 neurons that make ~7000 synapses, (White, Southgate et al. 1986). Furthermore, the complete cell lineage is known (Sulston and Horvitz 1977; Sulston, Schierenberg et al. 1983), and with the use of green fluorescent protein (GFP) reporters, individual types of neurons can be visualized as they are generated as well as in the mature nervous system (Chalfie, Tu et al. 1994). Thanks to the development of methods to isolate individual cell types (Christensen, Estevez et al. 2002; Zhang, Ma et al. 2002), it is now possible to obtain molecular fingerprints that define the properties of cells that function in this circuit (Colosimo, Brown et al. 2004; Cinar, Keles et al. 2005; Fox, Von Stetina et al. 2005; Touroutine, Fox et al. 2005).

This introduction provides an overview of what is known about motor neuron specification and the mechanisms that govern the choice of synaptic partners. I will first introduce the components that constitute the *C. elegans* motor circuit. The next section will focus on motor neuron specification and will feature information obtained from vertebrates and from Drosophila since detailed pathways that govern motor neuron differentation in the spinal cord and insect nervous system have been delineated in these organisms. Our work shows that many of the same players are involved in motor neuron specification in *C. elegans* as well. In the final section I will describe molecules that have been implicated in specifying synaptic choice.

The *C. elegans* Motor Circuit

C. elegans locomotion is characterized by sinusoidal waves generated by the coordinated firing of neurons and the muscle cells they innervate. The opposing actions of inhibitory and excitatory motor neurons lead to the alternation of dorsal and ventral body wall muscle contractions thus producing body bends that drive movement. Below is an overview of the anatomical components that comprise the *C. elegans* motor circuit.

Body Wall Muscle (BWM)

There are 95 BWM cells in the adult nematode; 81 of these cells are generated in the embryo, while the additional 14 are added postembryonically. BWM cells appear striated, as the contractile apparatus in each cell is assembled from a well-ordered array of sarcomeres, the basic functional units of striated muscles from nematodes to mammals (Waterston 1988; Moerman and Fire 1997). Body muscle cells are arrayed in four

quadrants, with paired rows of cells flanking the ventral and dorsal nerve cords (Figure 1.1). Nematode body wall muscles extend cytoplasmic extensions or "muscle arms", to synapse with motor axons in the ventral nerve cord. A detailed description of the molecular components that drive muscle cell function is included in Chapter III.

The Ventral Cord Motor Circuit

Command interneurons, located in the head region, extend processes into the ventral nerve cord to synapse with motor neurons. Motor neuron soma are located in the ventral nerve cord (VNC). These motor neurons are either excitatory or inhibitory and are the key regulators of muscle contraction. There are five major classes of motor neurons (A, B, D, AS and VC) in the ventral nerve cord. Within each class are dorsal subtypes (DA, DB, DD, AS) which extend processes or commissures around the animal to innervate dorsal muscles; ventral subclasses (VA, VB, VD, VC) synapse with ventral muscles with the exception of the VCs which innervate the vulval muscles required for egg laying (Figure 1.2). Below, is a summary of the circuits that are responsible for mediating coordinated backward and forward locomotion.

Command Interneurons

Coordinated locomotion results from the propagation of waves, either anterior or posterior, to drive backward and forward locomotion, respectively. Laser ablation studies have been used to identify neurons that are required for either forward or backward locomotion (Chalfie, Sulston et al. 1985). There are five pairs of interneurons that contribute to motor activity: AVA, AVB, AVD, AVE and PVC (White, Southgate et al.

1976; White, Southgate et al. 1986; Chalfie and White 1988). The axonal processes of AVA (backward) and AVB (forward) interneurons are the largest in diameter in the ventral nerve cord, and ablation of these interneurons results in severe movement defects. AVA ablation preferentially impairs backward locomotion; this defect is enhanced when AVD and AVE are also ablated. Similarly, removal of PVC enhances the forward movement defect of an AVB ablated animal (Chalfie, Sulston et al. 1985). These results suggest that AVA and AVB are the major regulators of locomotion, with the additional interneurons (i.e. AVD, AVE vs PVC) functioning to modify either forward or backward locomotory activity (Chalfie and White 1988).

Excitatory motor neurons

The A and B class motor neurons are responsible for inducing muscle contraction thereby leading to the propagation of the sinusoidal waves that result in locomotion. These neurons are excitatory and signal using the neurotransmitter acetylcholine (Rand and Nonet 1997).

Backward Locomotion

Backward locomotion depends on A-class motor neurons, the DAs and VAs (Chalfie, Sulston et al. 1985). These motor neurons extend anteriorly directed processes and receive inputs from the AVA, AVD and AVE command interneurons (Figure 1.3. The AVD and AVE interneurons form chemical synapses with the A-class motor neurons, while AVA signals via both chemical and electrical synapses (White, Southgate et al. 1986).

Forward Locomotion

Forward locomotion is mediated through the actions of the B-class motor neurons, DBs and VBs. In contrast to DA and VA motor neurons, the B-class motor neurons extend posteriorly directed axons and receive inputs from AVB and PVC (Figure 1.3). AVB makes gap junctions only with these neurons and PVC, chemical synapses (White, Southgate et al. 1986).

Inhibitory motor neurons

The inhibitory DD and VD motor neurons extend processes along both the dorsal and ventral nerve cord, and utilize the neurotransmitter GABA (Chalfie and White 1988). DD motor neurons provide outputs to dorsal muscles whereas the VDs innervate ventral muscles. Inputs to DD and VD motor neurons are provided by excitatory motor neurons (White, Southgate et al. 1976; White, Southgate et al. 1986). The DDs enhance the actions of the VA and VB motor neurons by inducing dorsal muscle relaxation in response to ventral muscle contraction that results from the firing of VA and VB motor neurons. Conversely, the VDs function to promote ventral muscle inhibition in response to the excitatory actions of DA and DB motor neurons. (Figure 1.4) (McIntire, Jorgensen et al. 1993; Von Stetina, Treinin et al. 2006) The importance of this mechanism to movement is evident in mutants with defects in GABAergic motor neuron function. The simultaneous loss of of both DD and VD function leads to the dorsal and ventral muscles contracting simultaneously, causing the animal to "shrink" following touch stimulation (McIntire, Jorgensen et al. 1993).

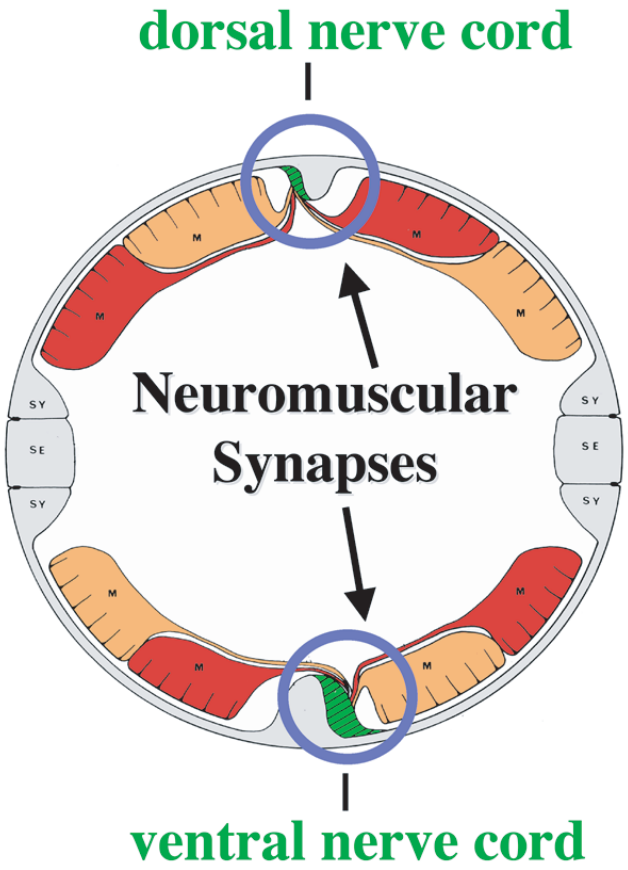

Figure 1.1. Cross-section of the *C. elegans* motor circuit. Body wall muscle cells (orange/red) send out muscle arms to form neuromuscular synapses with motor neuron processes in the ventral and dorsal nerve cords. Figure adapted from White, et al., 1986.

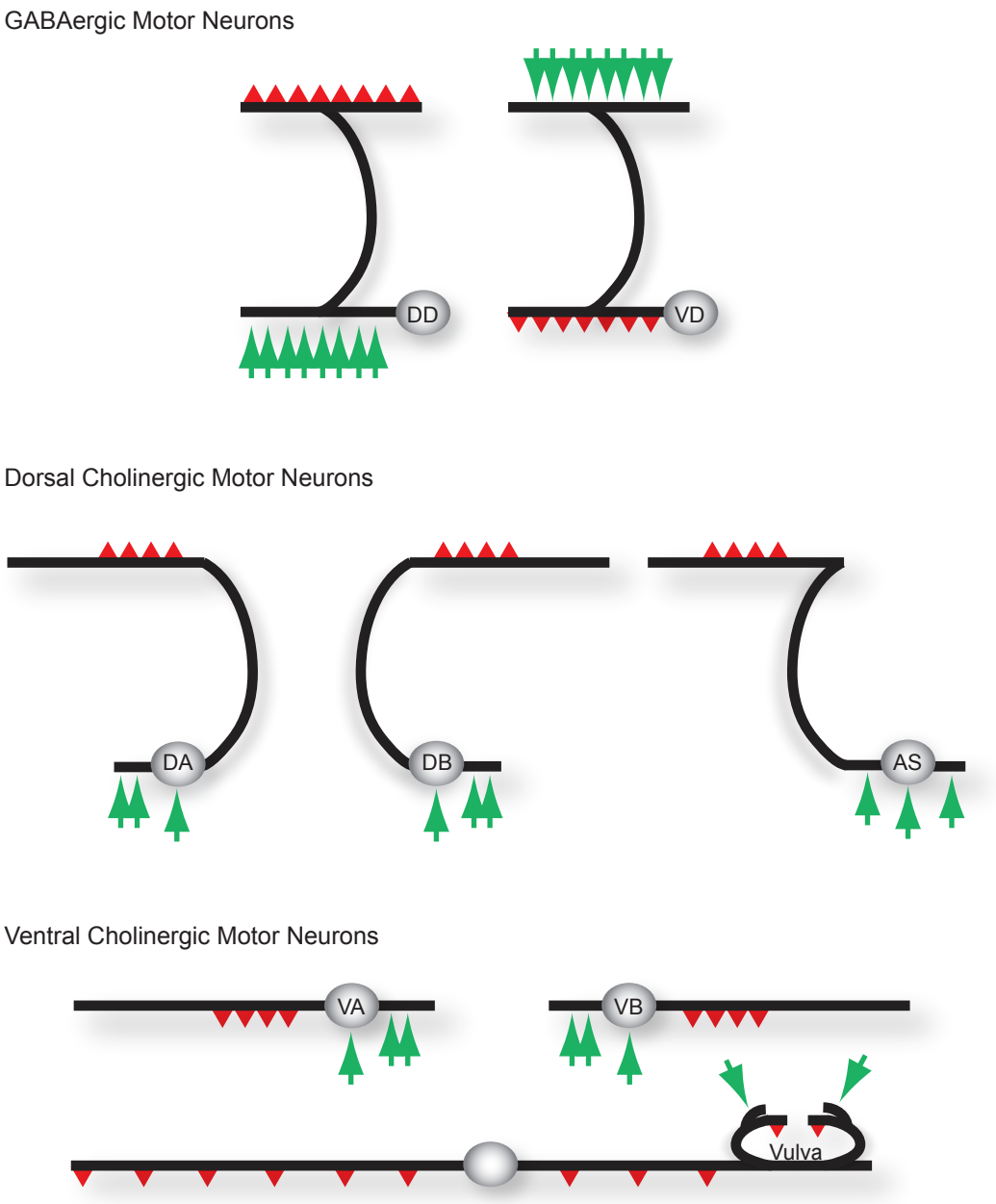

Figure 1.2. The anatomy of the ventral nerve cord motor neurons. A. The GABAergic motor neurons (DD/VD) both extend processes anteriorly and posteriorly along both the ventral and dorsal nerve cords. DDs receive inputs from ventral motor neurons and innervate dorsal muscles, whereas VD motor neurons receive dorsal inputs and signal to ventral muscles. B. The dorsal cholinergic motor neurons (DA, DB, AS) all extend commissures from the ventral cord and provide excitatory signals to dorsal body wall muscles. C. The ventral cholinergic motor neurons (VA, VB, VC) innervate the ventral body wall muscles, with the exception of the VC motor neurons, which innervate the vulval muscles. Green arrows indicate inputs from other neurons, while red triangles depict NMJs with body wall muscle. Figure reprinted from Von Stetina et al., 2006.

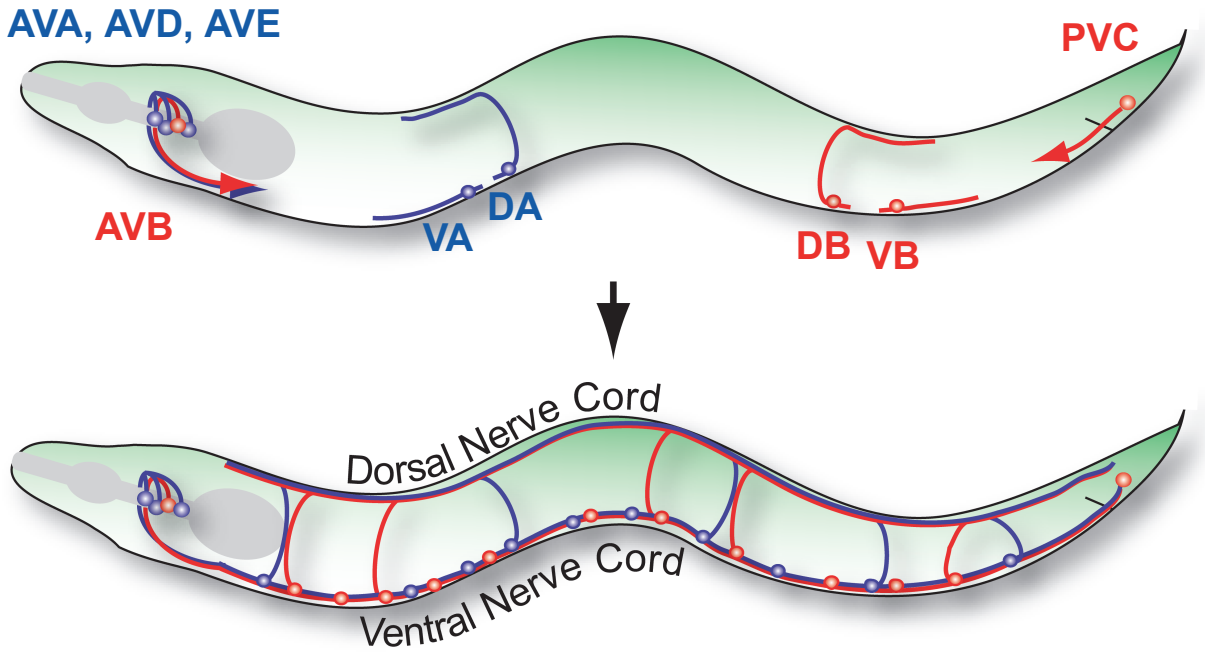

Figure 1.3. The *C. elegans* locomotory circuit. Interneurons in the head and tail extend processes into the ventral nerve cord and synapse with specific motor neurons. For example, the AVA, AVD, and AVE interneurons connect to the DA and VA motor neurons to comprise the "blue circuit" while AVB and PVC synapse with VB and DB motor neurons in the "red circuit." VA and VB motor neurons control ventral muscle cells; DA and DB motor neurons send commissural processes to synapse with dorsal muscle cells.

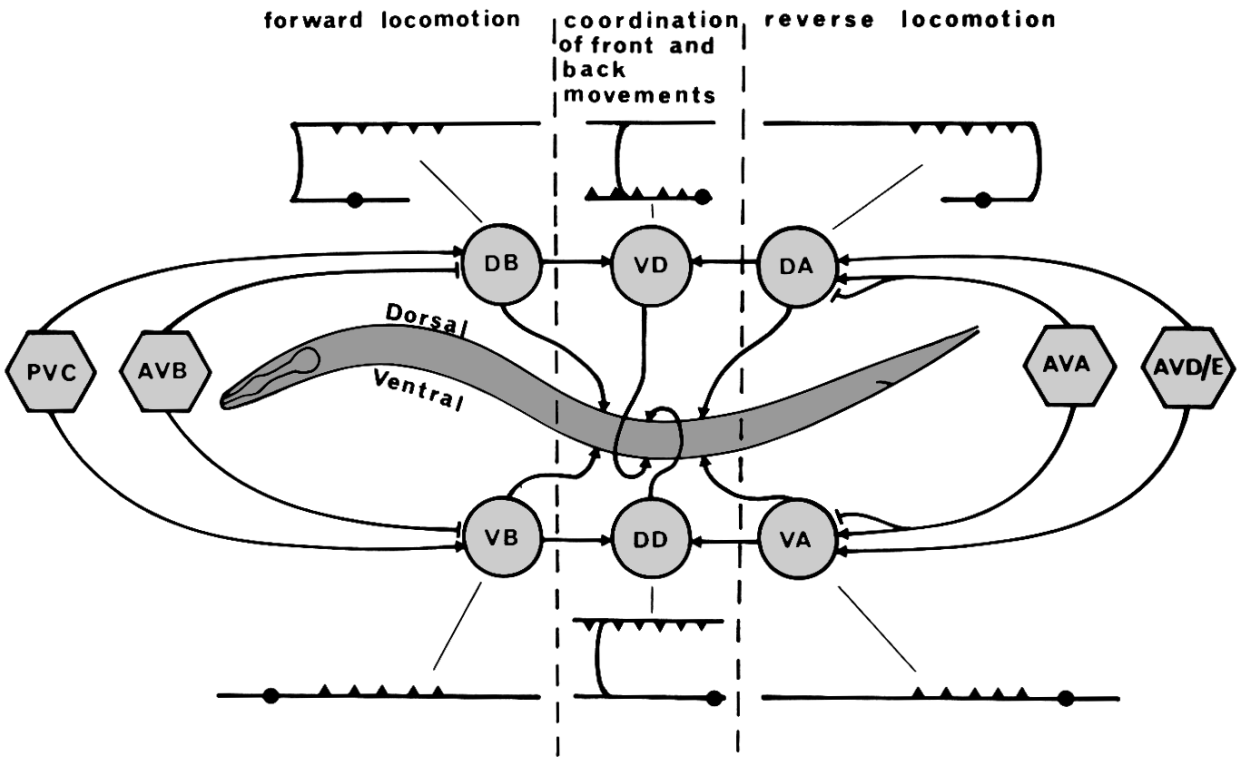

Figure 1.4. Wiring diagram of the *C. elegans* motor circuit. Hexagons denote interneurons while circles depict motor neurons; arrows indicate chemical synapses while blunt ends refer to gap junctions. The AVA, AVD, and AVE interneurons form chemical and electrical synapses (AVA only) with VA and DA motor neurons to mediate backward movement. The AVB and PVC interneurons form synapses with the VB and DB motor neurons to regulate forward movement. The DD and VD motor neurons receive inputs from A and B class motor neurons to provide cross-inhibitory signals to body wall muscle cells thereby coordinating the alternation of muscle contraction and relaxation that propels sinusoidal locomotion. Figure reprinted from Von Stetina et al., 2006.

Chemical vs. Electrical synapses

The *C. elegans* nervous system contains ~2000 neuromuscular junctions, ~5000 chemical synapses and ~600 electrical gap junctions between neurons (White, Southgate et al. 1986). Chemical synapses are comprised of the active zone of a presynaptic cell directly opposite a membrane density of the postsynaptic cell (except that in *C. elegans*, no postsynaptic density is evident in EMs of the nervous system). The active zone is traditionally defined as a region in which a presynaptic density forms surrounded by a cluster of synaptic vesicles. Synaptic vesicles release neurotransmitter into the synaptic cleft adjacent to the postsynaptic membrane (Figure 1.5) (Chalfie and White 1988; Driscoll and Kaplan 1997). Specific receptors are activated by neurotransmitter binding leading to ion flow that modifies the electrical activity of the postsynaptic cell. In the ventral nerve cord, chemical synapses are formed *en passant* between adjacent processes (White, Southgate et al. 1986; Chalfie and White 1988). Based on the EM reconstruction, some cells make one large synapse with the neighboring neuron whereas others make multiple smaller synapses. These synapses are highly specific, however, as the patterns of synaptic connections are similar between individuals (White, Southgate et al. 1986; Chalfie and White 1988). Interestingly, many neurons with adjacent processes do not form synapses with each other, suggesting that there are intrinsic mechanisms that are required for synaptic specificity. This choice is probably genetic in origin, and likely to depend on regulated gene expression. To better understand the mechanism of specificity, it will be necessary to identify the membrane components that signal for active zone formation and facilitate the alignment of the pre- and post-synaptic areas. Thus far, the molecular properties that regulate these processes are poorly understood.

Gap junctions facilitate rapid transmission of signals by electrically coupling adjacent cells. In the ventral nerve cord, motor neurons of the same class are connected by gap junctions (White, Southgate et al. 1986; Chalfie and White 1988). Gap junctions are also formed between the command interneurons and specific motor neurons. In addition to their formation between specific pairs of neurons, gap junctions may also be placed at particular cellular locations. For example, gap junctions with the AVA interneurons can occur throughout the length of their A-class motor neuron partners whereas AVB interneurons typically place gap junctions on the cell soma of B-class motor neurons (White, Southgate et al. 1986). The principle components of gap junction channels are the innexin proteins which are functionally related to the connexin and pannexin proteins, the building blocks of vertebrate gap junctions (Phelan and Starich 2001; Bruzzone, Hormuzdi et al. 2003; Panchin 2005). Gap junctions form by apposition of hemichannels located in the plasma membranes of adjacent cells. Each hemichannel contains six subunits and may be homomeric (all subunits are the same) or heteromeric (subunits are of multiple subtypes). In addition, these hemichannels can form either homotypic (hemichannels are identical) or heterotypic (hemichannels differ in subunit composition) gap junctions (Phelan and Starich 2001). The *C. elegans* genome encodes ~25 innexin subunits (Bargmann 1998). It is reasonable to believe that synaptic choice could be achieved by the specific expression of certain innexin proteins in adjacent cells. For instance, channel formation between two neighboring cells only occurs when certain hemichannels encounter a specific partner hemichannel. An example of this comes from genetic and cell biological data suggesting that the innexins UNC-7 and UNC-9 are likely to form heterotypic gap junctions between AVB and B-class motor neurons in the

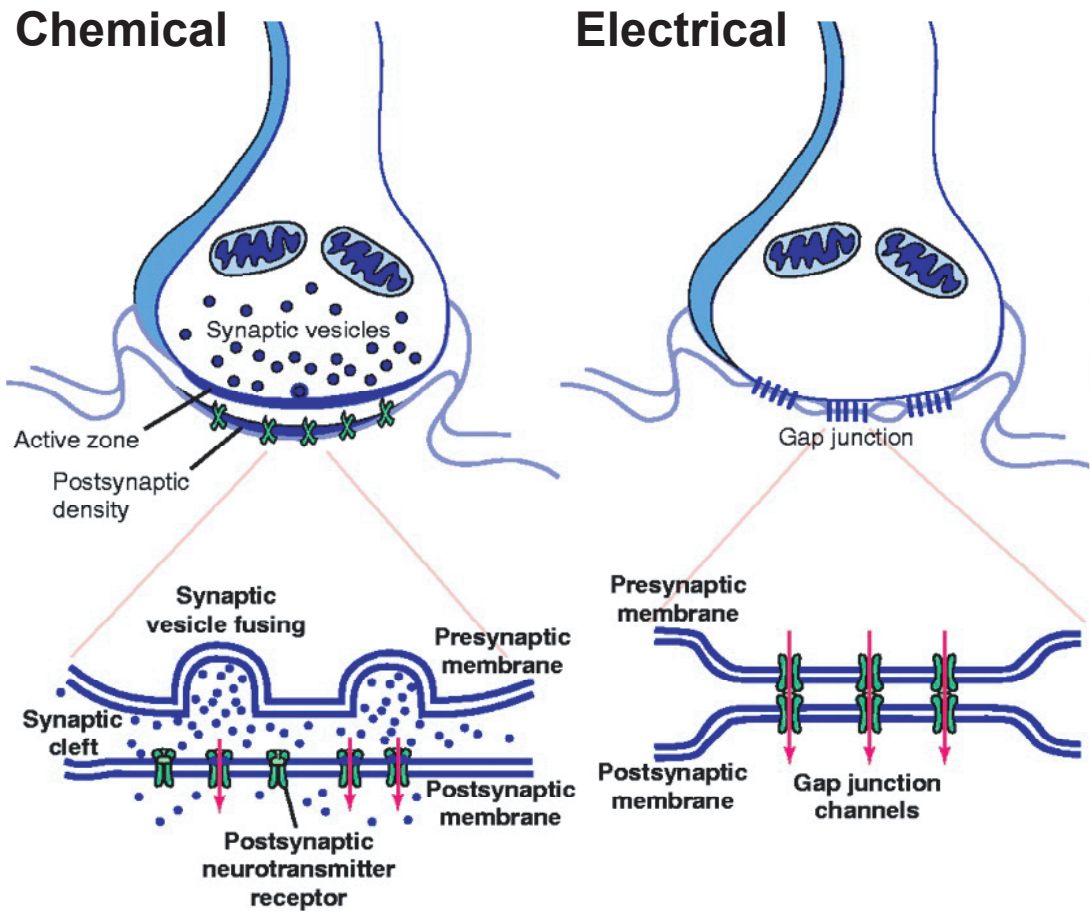

Figure 1.5. Chemical and Electrical synapses facilitate signaling between neurons. (Left) At the chemical synapse, neurotransmitter vesicles are released at the active zone of the pre-synaptic cell. Receptors, located at the postsynaptic density of the receiving neuron, bind the neurotransmitters allowing ion flow into the cell, thereby propagating an action potential. (Right) The electrical synapse is composed of gap junction channels that directly couple the pre- and post-synaptic membranes. These channels allow for passive flow of electrical current as well as additional signaling molecules (i.e. ions, ATP). Figure adapted from Cohen-Cory (2002).

ventral cord. UNC-7 is highly expressed in the command interneurons, whereas *unc-9* is primarily detected in ventral cord motor neurons (T. Starich, J.Shaw unpublished; Von Stetina, Fox et al., submitted)(Fox, Von Stetina et al. 2005). Mutations in *unc-9* phenocopy *unc*-7; both mutants display similar "jerky" uncoordinated movements (Starich, Herman et al. 1993). Furthermore, loss of *unc-9* leads to the failure of UNC-7 to assemble into gap junctions; instead UNC-7 is diffusely distributed along the plasma membrane. This finding is consistent with the proposal that both of these subunits are required for heterotypic gap junction formation between the command interneurons and motor neurons (T. Starich, J. Shaw, unpublished results). However, UNC-9 is expressed in several classes of motor neurons (i.e. A and D classes), where it does not form specific channels with the AVB, thus suggesting that additional mechanisms are required to control the localized development of gap junction channels. In this regard, understanding the mechanisms that regulate the formation and localization of these channels may provide insight into the components critical for synaptic specificity.

The Neuromuscular Junction (NMJ)

The NMJ is defined as a synapse in which the postsynaptic partner is a muscle cell (Chalfie and White 1988). In *C. elegans*, neuromuscular junctions are chemical synapses between membrane extensions ("muscle arms") and motor axons (Chalfie and White 1988; Driscoll and Kaplan 1997). Electrophysiological analysis of specific *C. elegans* mutants has determined that three pharmacologically distinct receptors function in the BWM cells at the NMJ. One of these is an inhibitory GABA receptor, while the other two are excitatory acetylcholine receptors (Richmond and Jorgensen 1999).

unc-49: The GABA receptor

GABA receptors are heteromeric and are typically composed of three distinct subunits that function as anion channels to inhibit muscle contraction. In *C. elegans*, three GABA receptor subunits (UNC-49A, UNC-49B, UNC-49C) are encoded by alternatively spliced transcripts from the *unc-49* locus. Only UNC-49B and UNC-49C, however, show overlapping expression at neuromuscular synapses, and they are sufficient to form a functional heteromeric channel in *Xenopus* oocytes. Furthermore, *in vivo* recordings suggest that only UNC-49B and UNC-49C are required to form the functional GABA receptor in BWM (Bamber, Beg et al. 1999; Bamber, Richmond et al. 2005). This UNC-49B/C heteromeric channel accounts for all of the GABA-evoked currents at the NMJ, as mutations in *unc-49(e407)* completely eliminate this response (Richmond and Jorgensen 1999).

Nicotinic Acetylcholine Receptors (nAChRs)

In contrast to the GABA receptor, in which a single gene encodes multiple subunits, nAChR subunits at the NMJ are encoded by separate genes. In fact, the *C. elegans* genome contains ~40 predicted nAChR subunits, of which at least 27 are functional (Bargmann 1998; Mongan, Baylis et al. 1998). nAChRs are composed of 5 subunits that surround a cation-permeable channel and are activated by nicotine. Subunits required for ACh binding are referred to as "α subunits", whereas the additional subunits (β, δ, ε, γ) are known collectively as non-α subunits. In *C. elegans*, nAChR subunits can be classified into 5 groups based on homology: DEG-3-like, ACR-16-like,

UNC-38-like, ACR-8-like, and UNC-29-like (Mongan, Baylis et al. 1998; Jones and Sattelle 2004). The ACR-16-like group is most closely related to the vertebrate α7 receptors, with the founding member, ACR-16, sharing 47% homology with the vertebrate α7 receptors. Additionally, ACR-16 can form homomeric channels in heterologous cells, a characteristic that is also shared with vertebrate α7 receptors (Ballivet, Alliod et al. 1996). The UNC-38 group is most similar to insect nAChRs, whereas the UNC-29 group is most closely related to non-α receptors from both flies and vertebrates. Finally, the DEG-3 and ACR-8 groups show significant sequence divergence from nAChRs in other species and may be nematode-specific (Jones and Sattelle 2004).

C. elegans BWM cells express two classes of nAChRs that can be distinguished on the basis of their response to the nAChR agonist, levamisole (Richmond and Jorgensen 1999). A genetic screen for levamisole-resistant mutants (Lewis, Wu et al. 1980) identified three essential subunits (*unc-29, unc-38* and *unc-63*) (Fleming, Squire et al. 1997; Richmond and Jorgensen 1999; Culetto, Baylis et al. 2004), as well as two non-essential subunits (*lev-1* and *lev-8*) (Fleming, Squire et al. 1997; Towers, Edwards et al. 2005) of a levamisole-sensitive receptor (Figure 1.6). Each of these genes shows overlapping expression in BWM, and encode subunits capable of forming functional ACh receptors in *Xenopus* oocytes (Fleming, Squire et al. 1997; Culetto, Baylis et al. 2004; Towers, Edwards et al. 2005). The potential existence of an additional BWM nAChR was suggested by the discovery that genetic ablation of the

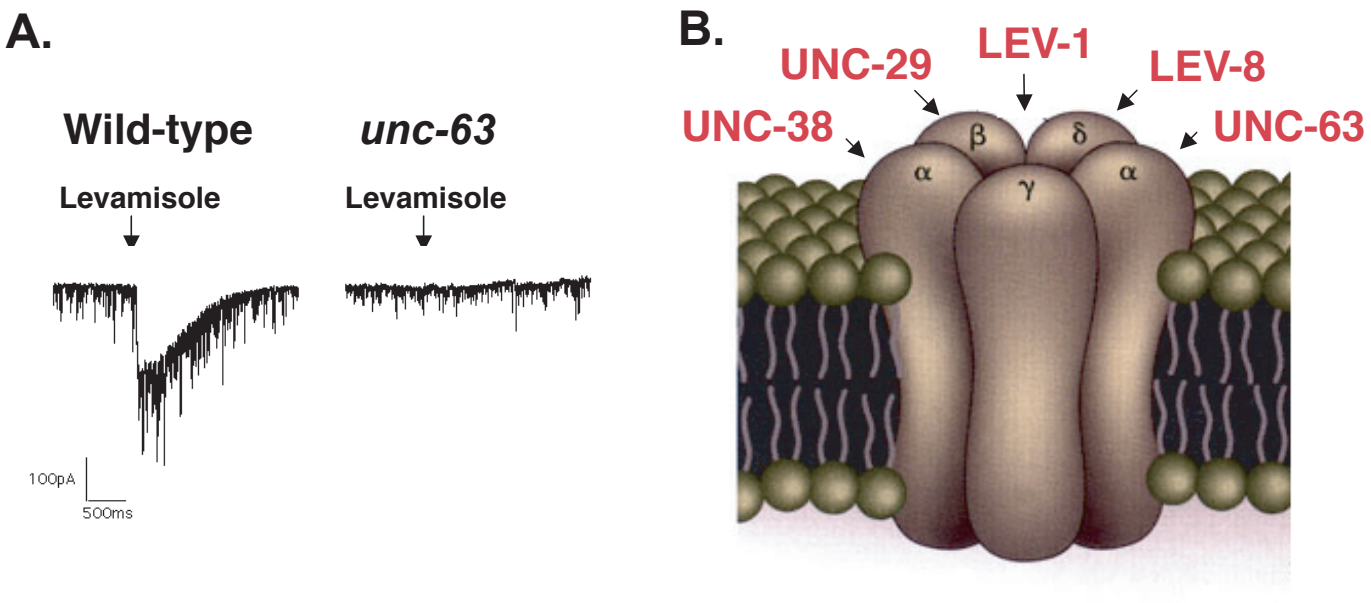

Figure 1.6. The components of the Levamisole-sensitive acetylcholine receptor (AChR) at the neuromuscular junction. A. Electrophysiological recordings from the NMJ reveal an AChR that is sensitive to the ACh agonist levamisole. Loss of this channel, in the *unc-63* mutant, leads to complete elimination of the levamisole response. B. The five subunits that compose this channel are UNC-38, UNC-29, LEV-1, LEV-8 and UNC-63. Figure provided by Janet Richmond and adapted from Richmond and Jorgensen, 1999.

levamisole-sensitive receptor does not eliminate the acetylcholine response at the NMJ. Pharmacological data indicate that this putative additional nAChR is insensitive to levamisole (Richmond and Jorgensen 1999). In collaboration with Janet Richmond, we have now identified an essential component of this receptor, *acr-16*, by testing uncharacterized AChR subunits identified in a gene expression profile from the BWM cells (Touroutine, Fox et al. 2005). A full description of this work is presented in Chapter III.

Motor Neuron Specification

Transcription factors play a critical role in determining cell fate. This section focuses on the role of transcription factors that specify the differentiation of motor neurons within developing vertebrate and invertebrate nervous systems.

Vertebrate motor neuron development

A "de-repression" model specifies neuron progenitor domains in the developing spinal cord

The vertebrate spinal cord is organized into neuron progenitor domains that are defined by expression of distinct combinations of transcription factors. Progenitor domains arise in response to a gradient of the morphogen, Sonic hedgehog (Shh). Shh release from the notochord and floorplate leads to differential expression of patterning factors that define the different progenitor domains (Lee and Pfaff 2001; Shirasaki and Pfaff 2002). These transcription factors are either repressed (class I) or induced (class II) in response to the Shh signal. In this context, unique combinations of transcription

factors arise in response to this graded signal effectively patterning each progenitor domain (Figure 1.7) (Lee and Pfaff 2001; Shirasaki and Pfaff 2002). A majority of these factors (8/11) contain a conserved eh1 (engrailed homology) domain that mediates interactions with Groucho/TLE, a transcriptional co-repressor. This Groucho/TLE interaction is required for neuronal specification, as disruption of Groucho/TLE function leads to defects in ventral patterning (Muhr, Andersson et al. 2001). Thus, a model of "de-repression" has been proposed wherein Class I and Class II transcription factors cross-repress each other to delineate specific boundaries between progenitor domains. This model is substantiated by the findings that the loss of one factor leads to the expansion of the opposing factor, which in turn represses domain-specific determinants, thereby inducing changes in cell fate. For example, the motor neuron progenitor domain (pMN) normally expresses Pax6, Olig2, Nkx6.1 and Nkx6.2. Mutations in Pax6 lead to the expansion of Nkx2.2/2.9 expressing cells, which are normally confined to the adjacent p3 interneuron progenitor domain, thus repressing MN determinants and converting these cells to interneurons (Lee and Pfaff 2001; Shirasaki and Pfaff 2002). In effect, the wildtype pathway functions to "de-repress" downstream genes in the appropriate domain to specify neuronal subtypes.

MNR2/HB9 define postmitotic motor neurons

This phenomenon of cross-repression is maintained as motor neurons begin to express additional sets of transcription factors to define postmitotic motor neuron fate (Lee and Pfaff 2001). In the chick, two closely related homeodomain transcription

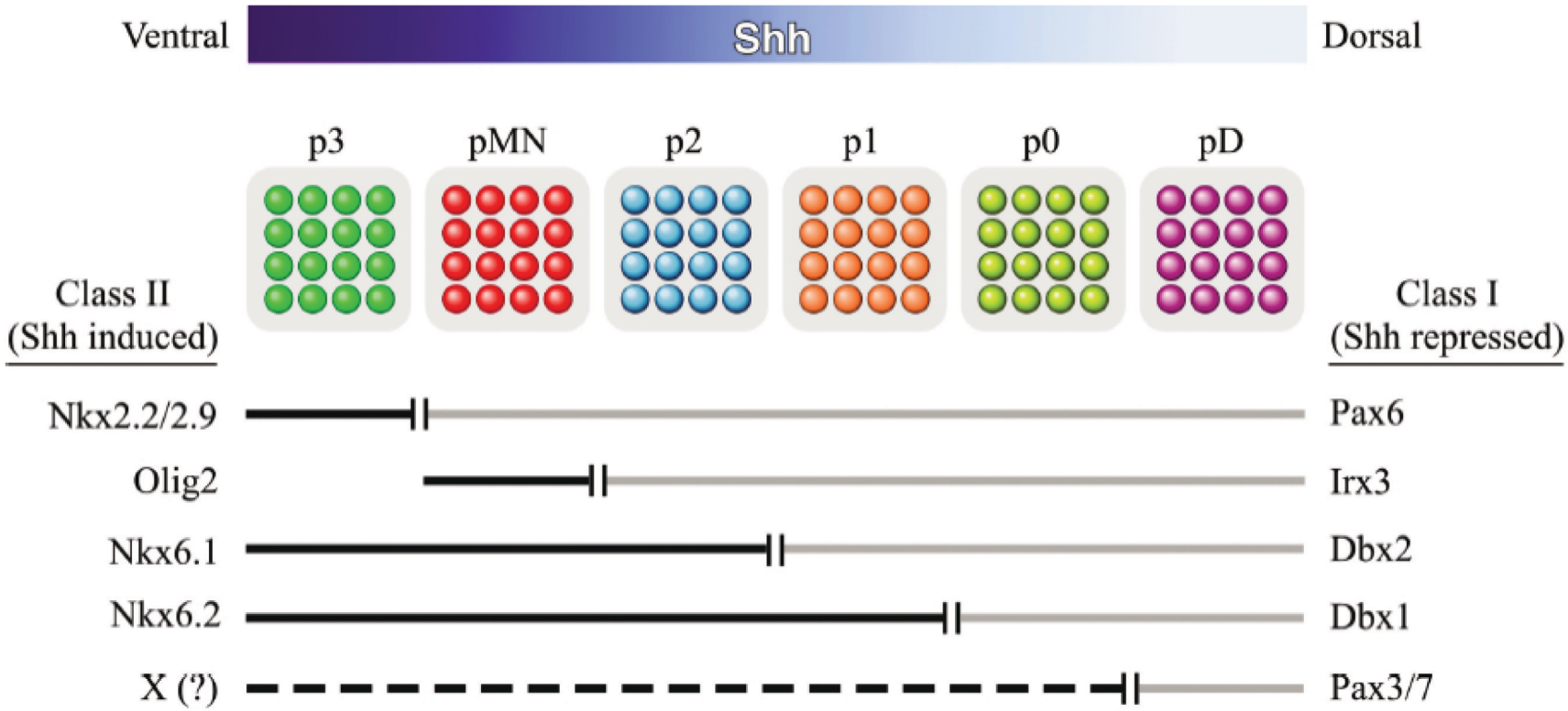

Figure 1.7. A sonic hedgehog gradient defines progenitor domains in the developing vertebrate spinal cord. A high ventral to low dorsal gradient of Shh activates class II genes while repressing class I factors. Groucho-mediated cross-repression between these two classes of transcription factors establishes distinct progenitor domain boundaries. pMN gives rise to motor neurons, while p0-p3 define interneuron progenitors. pD denotes the dorsal spinal cord region. Figure reprinted from Lee and Pfaff, 2002.

factors, MNR2 and HB9, function to define motor neuron fate. MNR2 is first expressed by motor neuron progenitors as they enter their final division cycle. Once they have achieved a postmitotic state, they begin to express HB9 (Tanabe, William et al. 1998; Shirasaki and Pfaff 2002; William, Tanabe et al. 2003). Interestingly, in the mouse, a single gene encodes an MNR2/HB9-like protein that is expressed during both of these developmental periods. HB9 expression is required in postmitotic motor neurons to specify motor neuron fate by preventing the adoption of interneuron traits. Loss of HB9 causes ectopic expression of the V2 interneuron marker, Chx10, in motor neurons and leads to aberrant motor neuron migrations and axon projections, in addition to loss of motor neuron subtype identity (Arber, Han et al. 1999; Thaler, Harrison et al. 1999).

The LIM code defines postmitotic motor neuron subtypes

Whereas all motor neurons in the vertebrate spinal cord express HB9, motor neuron subtypes are defined by a combinatorial code of LIM homeodomain transcription factors. The LIM code directs motor neuron migrations into spinal columns, axon pathfinding, and target muscle innervation (Tsuchida, Ensini et al. 1994; Appel, Korzh et al. 1995). For example, in the chick spinal cord, all motor neurons express Isl1 and Lhx3/4 upon exit from the cell cycle. However, motor neurons that express Isl2 in combination with these factors extend axons that exit from the ventral end of the neural tube, while cells that do not express Isl2 exit dorsally (Ericson, Thor et al. 1992; Shirasaki and Pfaff 2002). These motor neurons are classified based on target muscle innervation; for example, those that form the medial motor column (MMC) synapse with trunk muscles while those that constitute the lateral motor column (LMC) innervate limb

muscles. These groups are further subdivided into neurons that project medially (MMCm and LMCm) or laterally (MMCl and LMCl) (Shirasaki and Pfaff 2002).

Upon axonal exit from the neural tube, ventral motor neurons undergo dynamic changes in gene expression. Those that retain Lhx3/4 expression go on to become MMCm motor neurons (Sharma, Sheng et al. 1998; Sharma, Leonard et al. 2000), whereas other subtypes arise from neurons that lose this expression but gain expression of other transcription factors. For example, LMCl neurons begin to express Lim1 (Figure 1.8)(Kania, Johnson et al. 2000). The transcriptional code leads to the differential expression of receptors that respond to guidance molecules, thereby leading to appropriate axon trajectory. Recently, this idea was substantiated by the discovery that the fibroblast growth factor receptor 1 (FGFR1) is specifically expressed in MMCm motor neurons and that loss of FGFR1 leads to axon guidance defects in MMCm neurons. Importantly, overexpression of Lhx3 in ectopic areas leads to an expansion of neurons that respond to FGF signaling (Shirasaki, Lewcock et al. 2006). Furthermore, LMCm neurons are directed ventrally by repulsion from semaphorin (Huber, Kania et al. 2005), while LMCl neurons project dorsally in response to ephrin signals (Helmbacher, Schneider-Maunoury et al. 2000; Eberhart, Swartz et al. 2002). Thus, motor neuron subtypes are proposed to express guidance molecules that ensure correct target pathfinding and recognition based on the differential expression of LIM homeodomain transcription factors.

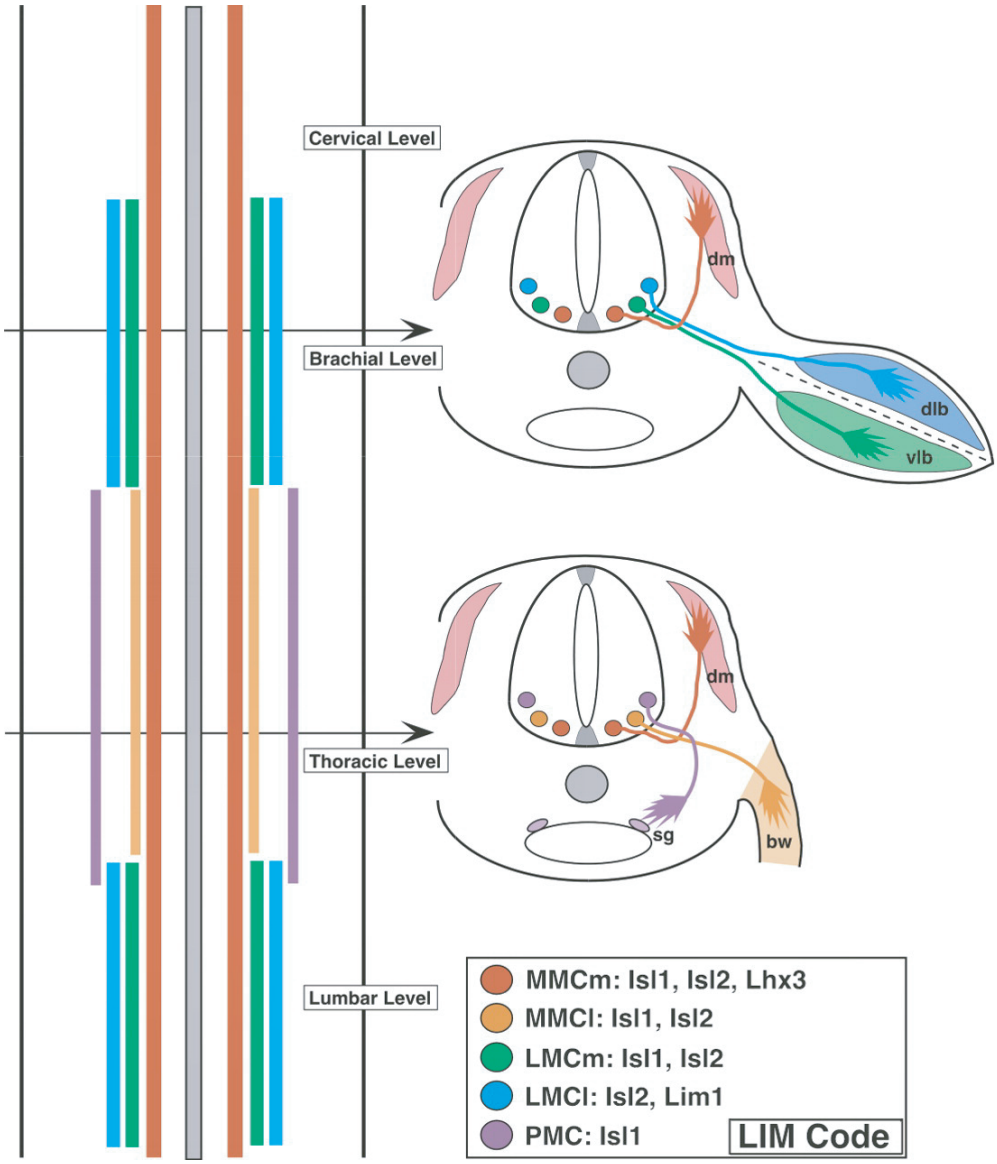

Figure 1.8. The LIM-code defines motor neuron subtypes in the ventral spinal cord. Motor neurons are arranged into distinct columns based on the combinations of LIM-HD transcription factors, as shown in the open book whole mount view of the chick spinal cord shown on the left. Each specific subtype expresses a unique combination of factors that defines axonal trajectory and the specificity of target recognition. For example the MMC (medial motor column) neurons express Lhx3 and Isl1/2 as they exit the ventral end of the spinal cord. Those that lose Lhx3 expression are directed to the lateral (MMCl) half of the MMC to connect with bodywall muscle (bw) while those that retain Lhx3 expression are directed to the median half (MMCm) where they innervate the dermomyotome (dm). A similar scenario occurs with the lateral motor column (LMC) neurons. Those that express Isl1/2 (LMCm) connect to the ventral limb bud (vlb) whereas those that express Isl2 and Lim1 (LMCl) innervate the dorsal limb bud (dlb). Figure reprinted from Shirasaki and Pfaff, 2002.

Invertebrate motor neuron specification

Motor neuron determination in Drosophila

Similar to vertebrate motor neuron specification, transcriptional codes define motor neuron subtypes in Drosophila as well. Unlike the vertebrate spinal cord where HB9 defines all developing motor neurons, no single factor has been identified that is required for general motor neuron specification in Drosophila. A candidate motor neuron specifier, Zfh1, was recently identified as a zinc finger transcription factor that is expressed in all somatic motor neurons; however, it does not appear that *zfh-1* is required for general motor neuron specification given that mutations in *zfh1* lead to mild neuronal defects, most noticeably a reduction in the ventrally projecting motor axons from the CNS. Since only a subset of motor neurons exhibits this defect, additional transcription factors are likely required to specify axonal exit from the CNS (Layden, Odden et al. 2006). Along these lines, further evidence from Drosophila suggests that while multiple cells express the same transcription factors, unique cascades of these factors determine cell identity. For example, all ISN motor neurons express *eve*, *zfh1* and the GATA transcription factor Grain encoded by *grn* (Garces and Thor 2006). Nevertheless, the specific transcriptional cascade of *eve→grn→zfh1* is required to define a single ISN motor neuron, the aCC. Interestingly, these transcription factors are co-expressed in other motor neurons, including RP2 and pCC, but distinct transcriptional mechanisms specify these cell types (Garces and Thor 2006).

Similar to the vertebrate model of motor neuron specification, a conserved mechanism of cross-repression is required to determine the fates of ventrally versus dorsally directed axon projections in Drosophila. In particular, dorsal-projecting motor

axons exit the CNS via the ISN (intersegmental nerve) and express the homeodomain transcription factor Even-skipped, encoded by *eve* (Landgraf, Roy et al. 1999). Ventrally projecting motor neurons exit the ISNb/d or SNa/c (segmental nerve) branches and express *Islet*, *dHb9*, *Lim3* and *Nkx6* (Figure 1.9) (Broihier and Skeath 2002; Broihier, Kuzin et al. 2004). Genetic analysis has determined that *eve* functions to repress dHb9 expression in dorsally projecting motor neurons, whereas dHb9, in concert with Nkx6, prevents *eve* expression thereby specifying ventrally projecting motor neurons (Broihier and Skeath 2002; Fujioka, Lear et al. 2003; Broihier, Kuzin et al. 2004). Loss of function of any of these transcription factors leads to alterations in motor axon outgrowth; for example, loss of *dHb9* leads to ectopic expression of *eve* and subsequent adoption of dorsally directed projections (Broihier and Skeath 2002).

As described above, transcription factors are required to determine axonal trajectory in both vertebrate and invertebrate systems. The problem now is to identify the downstream target genes that mediate these responses. One possibilitity is that differential expression of transcription factor-regulated target genes could account for responses of specific neurons to different signaling molecules. As described above, vertebrate motor neurons are directed either ventrally (LMCm) or dorsally (LMCl) depending on their responsiveness to ephrin (Helmbacher, Schneider-Maunoury et al. 2000; Eberhart, Swartz et al. 2002) or semaphorin (Huber, Kania et al. 2005) signals. An obvious model to explain this effect would link a unique combination of transcription factors to expression of specific receptors to axon guidance cues. A potential example of this mechanism has been revealed from studies in Drosophila. Axon guidance is mediated through the actions of the netrin guidance cues. There are two characterized netrin

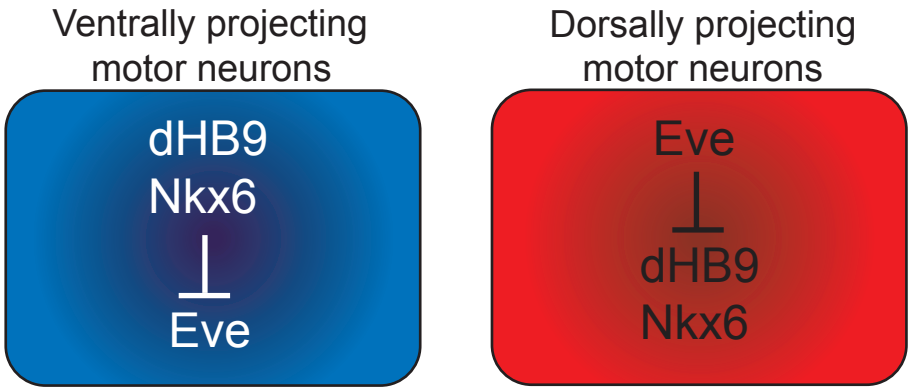

Figure 1.9. Reciprocal repression determines motor neuron fate in Drosophila**.** (Left) dHB9 and Nkx6 function in parallel to repress Eve and specify the fate of ventrally projecting motor neurons. (Right) Conversely, Eve represses dHB9 and Nkx6 to determine dorsally projecting motor neurons

receptors, Frazzled, encoded by *fra,* and Unc-5. Labrador et al., (2005) have determined that the dorsally projecting motor neurons, that express *eve*, also express *unc-5* and *fra*. Conversely, the *dHB9* expressing neurons that project ventrally only express *fra*. Furthermore, loss of *eve* leads to a reduction in *unc-5* expressing cells, thereby suggesting that it is the transcriptional regulation of the *unc-5* receptor that leads to the adoption of dorsal axonal trajectory (Labrador, O'Keefe et al. 2005).

Specification of Motor neuron fate in C. elegans

A common theme throughout evolution is the use of transcription factors to define cell type identity. Given the simplicity of the *C. elegans* nervous system, a number of genes required for motor neuron specification and fate have been identified (Von Stetina, Treinin et al. 2006). In this section, I will focus on the transcription factors that are required to establish motor neuron fate, as well as those required to determine motor neuron subtype identity. Although many of these factors are conserved in the vertebrate nervous system, it is likely that we may uncover new roles for these genes in neuronal development using *C. elegans*.

Transcription factors required for general aspects of motor neuron specification

cnd-1

cnd-1 encodes the nematode homolog of NeuroD/Neurogenin, bHLH transcription factors implicated in vertebrate neurogenesis. CND-1 is detected at the 14 cell stage of development in the AB lineage, which gives rise to most neurons. Later in development, *cnd-1* is detected in mitotically active motor neuron precursors as well as

their postmitotic daughter cells (Hallam, Singer et al. 2000). As expected, given its expression in VNC motor neurons, mutations in *cnd-1* lead to defects in embryonic motor neuron development. Specifically, the number of motor neurons is reduced, the placement of motor neurons is altered, cell-type specific transcription factor expression is disrupted, and there are defects associated with axon outgrowth. *cnd-1* mutations affect all classes of embryonic motor neurons, DA, DB and DD, and based on the mutant phenotypes described above, *cnd-1* is predicted to function as a regulator of mitotic exit, as well as a mediator of cell-type specific transcriptional programs (Hallam, Singer et al. 2000). However, the incomplete penetrance and the variability of mutant phenotypes associated with *cnd-1* suggest that there are likely other redundant factors required to specify motor neuron fate.

pag-3

While the fate of embryonic neurons relies on *cnd-1*, postembryonic VA, VB and VC motor neurons require *pag-3* to acquire their normal fates. *pag-3* mutants are characterized by an increase in cell corpses, which are generated following apoptosis (Cameron, Clark et al. 2002). Analysis of cell-type specific markers revealed a significant decrease in VA motor neurons, the virtual absence of VB motor neurons and an increase in the number of VC motor neurons. The increase in VC motor neurons is attributed to a reiteration in cell divisions, likely due to PAG-3 function in the Pn.aa progenitor (Cameron, Clark et al. 2002). Normally, the Pn.aa neuroblast gives rise to Pn.aaa and Pn.aap (VC motor neuron). Pn.aaa goes on to produce a VA and a VB motor neuron (Sulston and Horvitz 1977). However, in *pag-3* mutants, Pn.aaa divides to give

rise to a VC motor neuron, and often an abnormal VA motor neuron; VB motor neurons are never produced (Cameron, Clark et al. 2002). Therefore, in this model, a transcription factor is required to define the lineage of a particular cell type by specifying the fate of motor neuron progenitor cells.

zag-1

zag-1 encodes the *C. elegans* homolog of ZFH-1/δEF1 Zinc finger transcription factors. ZAG-1 is expressed transiently in all motor neurons as they are beginning to differentiate and send out axonal projections. Similar to *zfh-1* in Drosophila (see above) (Layden, Odden et al. 2006), *zag-1* does not regulate the adoption of neuronal fates, but instead is required to specify the differentiated properties of neurons. In *zag-1* mutants, there are defects in axon branching and guidance in most motor neurons, as well as the command interneurons and several additional neurons in the head, tail, and lateral nerve cord (Clark and Chiu 2003; Wacker, Schwarz et al. 2003). In addition to maintaing axonal branching and guidance, ZAG-1 also regulates the levels of neurotransmitter biosynthesis and reuptake genes. In particular, loss of *zag-1* leads to increases in transcription of *unc-25* (GABA biosynthetic enzyme, glutamic acid decarboxylase), *tph-1* (serotonin biosynthetic enzyme, tryptophan hydroxylase), *dat-1* (dopamine transporter) and the glutamate receptor, *glr-1* (Clark and Chiu 2003; Wacker, Schwarz et al. 2003). Thus, it appears that *zag-1* is not functioning to specify particular cell fate, but is instead required to confer a range of different neuronal traits.

Specification of the GABAergic motor neurons, DDs and VDs

unc-30

unc-30 encodes a homeodomain transcription factor of the Pitx family. UNC-30 is the "master regulator" of DD and VD motor neuron fate, as it is required for expression of genes required for D-motor neuron function and release of GABA (Jin, Hoskins et al. 1994). In particular, *unc-30* regulates the expression of *unc-25* (glutamic acid decarboxylase), and *unc-47* (GABA vesicular transporter) (Eastman, Horvitz et al. 1999; Cinar, Keles et al. 2005). Consistent with the important role for UNC-30 in GABAergic motor neuron differentiation, the mammalian homolog, Pitx2 is also required in GABAergic neurons to promote and regulate the synthesis of GABA (Westmoreland, McEwen et al. 2001).

unc-55

In *C. elegans*, the DD motor neurons arise in the embryo and initially synapse onto ventral muscles. When the postembryonic VD motor neurons are born during the late L1 larval stage, they initiate connections with ventral muscles, whereas the DDs undergo synaptic remodeling to innervate the dorsal muscles (White, Albertson et al. 1978; Walthall and Plunkett 1995). *unc-55*, a nuclear receptor transcription factor, is expressed in VD motor neurons, where it is required to specify synaptic connections with ventral body wall muscles (Walthall and Plunkett 1995; Zhou and Walthall 1998). The coexpression of *unc-30* and *unc-55* in VD motor neurons leads to the adoption of ventral inputs, whereas the lack of *unc-55* in the DD motor neurons leads to the creation of dorsal connections. Consistent with this idea, mutations in *unc-55* lead to the innervation

of dorsal muscles by VD motor neurons, a trait normally exhibited by the DDs (Walthall and Plunkett 1995). Conversely, overexpression of *unc-55* in DD motor neurons induces synaptic connections with ventral muscles (Shan, Kim et al. 2005). Recently, it was discovered that *unc-55* is likely functioning in VDs to repress DD specific traits. For example, the FMRF-amide peptide gene, *flp-13*, is normally expressed in DD motor neurons; however, in *unc-55* mutants, there is ectopic expression of *flp-13* in the VD motor neurons. Interestingly, *flp-13* is activated by *unc-30* in the DDs, and the authors propose that *unc-55* functions in VDs to restrict the activation of *unc-30* target genes, since both transcription factors are expressed in these cells (Shan, Kim et al. 2005). Identifying the genes that act downstream of *unc-55* should reveal interesting pathways that have conserved functions in synaptic remodeling.

alr-1

The *aristaless*/ARX family of homeodomain proteins have been implicated in a variety of human diseases including epilepsy and mental retardation (Stromme, Mangelsdorf et al. 2002; Sherr 2003). In *C. elegans*, *alr-1* is the closest relative of *aristaless*, and has important roles in specifying the fate of AWA chemosensory neurons, maintaining the structural integrity of the amphid sensory neurons, as well as defining VD motor neuron fate (Melkman and Sengupta 2005; Tucker, Sieber et al. 2005). Loss of *alr-1* leads to the adoption of a subset of DD motor neuron traits. For example, *flp-13*::GFP is ectopically expressed in the VD motor neurons of the *alr-1* mutants, but the synaptic connectivity of these neurons is not compromised, as observed in *unc-55* mutants. These findings suggest that *unc-55* and *alr-1* may function in parallel pathways

to repress *flp-13* expression in VD motor neurons (Melkman and Sengupta 2005) but that *alr-1* is not required for the UNC-55 function that maintains VD polarity. Given the high incidence of X-linked mental retardation attributed to mutations in human ARX (Stromme, Mangelsdorf et al. 2002; Sherr 2003), identifying the targets of *C. elegans alr-1* could provide important insights into the downstream pathways that govern differentation of GABA neurons in the mammalian brain.

Transcription factors that define cholinergic motor neuron fate

unc-3

unc-3 is a member of the Olf/EBF family of transcription factors first identified for their role in olfactory neuron development (Wang and Reed 1993). In *C. elegans*, *unc-3* is expressed in the ASI chemosensory neuron as well as in the developing motor neurons, as they are beginning to send out axonal projections (Prasad, Ye et al. 1998; Kim, Colosimo et al. 2005). *unc-3* is detected in the A and B class motor neurons, where it is required for proper fasciculation of axonal projections. Mutations in *unc-3* also result in synaptic defects; EM reconstruction has revealed ectopic neuromuscular junctions and improper interneuron inputs to motor neurons (J. White, unpublished) (Prasad, Ye et al. 1998). *unc-3* is also required for expression of cholinergic traits; UNC-17 (vesicular choline transporter) and CHA-1 (choline acetyltransferase) are not expressed in *unc-3* mutants (Von Stetina, Treinin et al. 2006)(K. Lickteg, D. Miller, unpublished results). Thus, *unc-3* is necessary to specify cholinergic traits and possibly regulate synaptic input to the A- and B- class motor neurons.

vab-7

As discussed above, the homeodomain *even-skipped* (*eve*) is expressed in dorsally projecting motor neurons in Drosophila (Landgraf, Roy et al. 1999). Interestingly, *vab-7*, the *C. elegans eve* homolog, also controls the trajectory of axonal outgrowth of a specific class of embryonic motor neurons. *vab-7* is expressed in the embryonic DB motor neurons as well as the post-embryonic VC motor neurons (Esmaeili, Ross et al. 2002). Commissures from DB motor neurons enter the dorsal nerve cord and project posteriorly. In *vab-7* mutants, the DB motor neurons instead adopt anteriorly directed projections, similar to the DA motor neurons (Figure 1.10). Furthermore, loss of *vab-7* in DB motor neurons also results in the loss of DB markers, including *acr-5* and *acr-16* (Esmaeili, Ross et al. 2002)(RMF, S. Von Stetina, D. Miller, unpublished results). Our lab, in collaboration with Julie Ahringer's group, has discovered that *vab-7* functions to repress *unc-4* in DBs and that this repression of *unc-4* is required to maintain posterior axonal polarity. *unc-4*, which is normally expressed in VA and DA motor neurons, is expressed ectopically in the DB motor neurons of *vab-7* mutants. Furthermore, double mutants of *vab-7* and *unc-4* rescue the axonal polarity defect (Figure 1.10), thus suggesting that ectopic UNC-4 is sufficient to promote DA-like anterior axon outgrowth in *vab-7* mutant DB motor neurons (Esmaeili, Ross et al. 2002).

The UNC-4 homeodomain protein specifies synaptic inputs to VA class motor neurons

UNC-4 is a paired-like homeodomain protein expressed in DA and VA motor neurons (Miller, Shen et al. 1992; Miller and Niemeyer 1995). Mutations in *unc-4* result in a characteristic backing defect; when tapped on the head, mutant animals coil dorsally

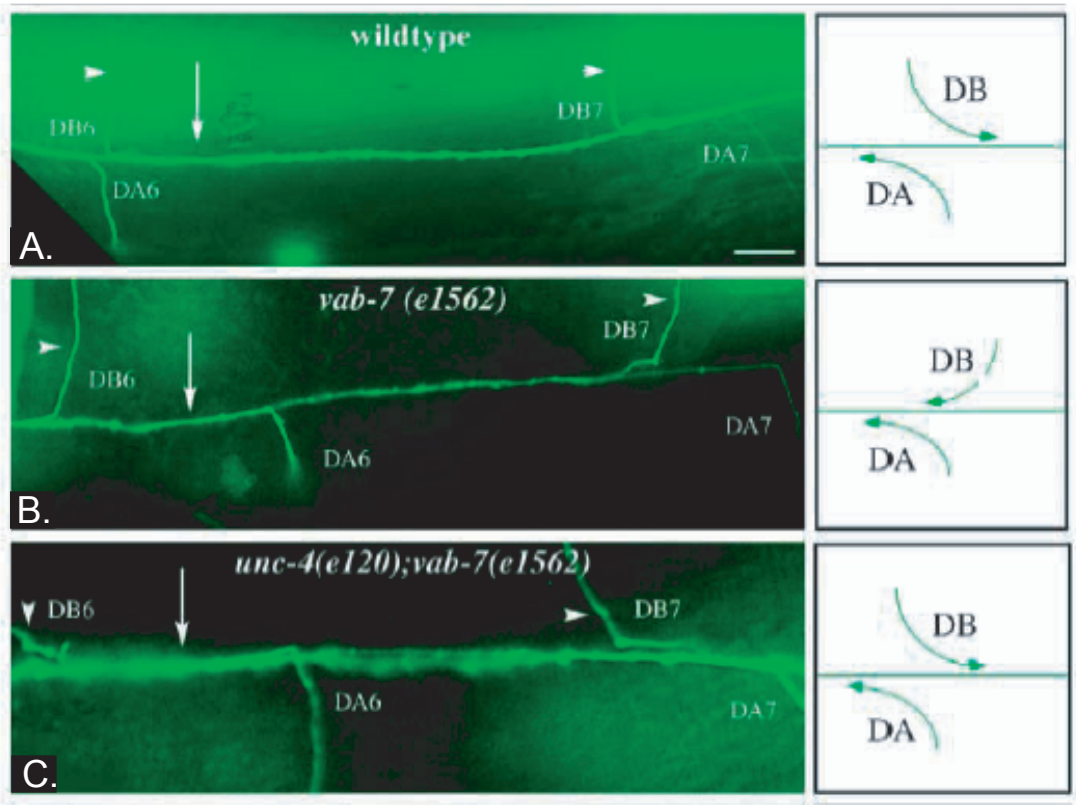

Figure 1.10. *vab-7* represses *unc-4* to specify axonal trajectory in DB motor neurons. Anterior is left, all images taken on the dorsal side of the animal. A. In wildtype animals, the DB motor neurons are directed posteriorly, while DA motor neurons project anteriorly. B. In *vab-7* mutants, DB motor neurons switch axonal polarity and are directed anteriorly, similar to the DA motor neurons. C. *unc-4; vab-7* double mutants show rescue for the axonal polarity defect, indicating that ectopic *unc-4* in the *vab-7* mutant is sufficient to alter axon trajectory. Figure adapted from Esmaeili, et al, 2002.

and assume an "Ω" conformation (White, Southgate et al. 1992). This observed phenotype is consistent with UNC-4 function in A-class motor neurons, which comprise the backward locomotory circuit (Chalfie, Sulston et al. 1985). EM reconstruction of the *unc-4(e120)* mutant revealed that a subset of VA motor neurons (VA2-10) are miswired with synaptic inputs normally reserved for their lineal sister cells, the VBs (White, Southgate et al. 1992). Specifically, VA motor neurons usually form both chemical synapses and gap junction synapses with the AVA interneuron and chemical synapses with AVD and AVE. In *unc-4* mutants, these connections are replaced with inputs from the AVB (gap junction) and PVC (chemical synapse) interneurons that are normally restricted to B-class motor neurons (Figure 1.11). The UNC-4 protein contains a conserved eh1 motif that functions to recruit the Groucho/TLE transcriptional co-repressor protein UNC-37 (Pflugrad, Meir et al. 1997; Winnier, Meir et al. 1999). Thus, we propose that UNC-4 and UNC-37 function in A-class motor neurons to repress B-class specific genes.

Consistent with this model, we have identified three B class motor neuron genes that are negatively regulated by UNC-4 and UNC-37. GFP reporters for three cell surface ion channel subunits, *acr-5* (acetylcholine receptor), *del-1* (DEG/ENaC sodium channel) and *glr-4* (glutamate receptor), are all normally expressed in VB motor neurons and are ectopically expressed in VA motor neurons in *unc-4* and *unc-37* mutants (Figure 1.12) (Winnier, Meir et al. 1999) (S. Von Stetina, D. Miller, unpublished results). Genetic experiments with loss-of-function mutations in these loci, however, have ruled out a role for these B motor neuron genes in synaptic choice (Von Stetina, Fox, et al.

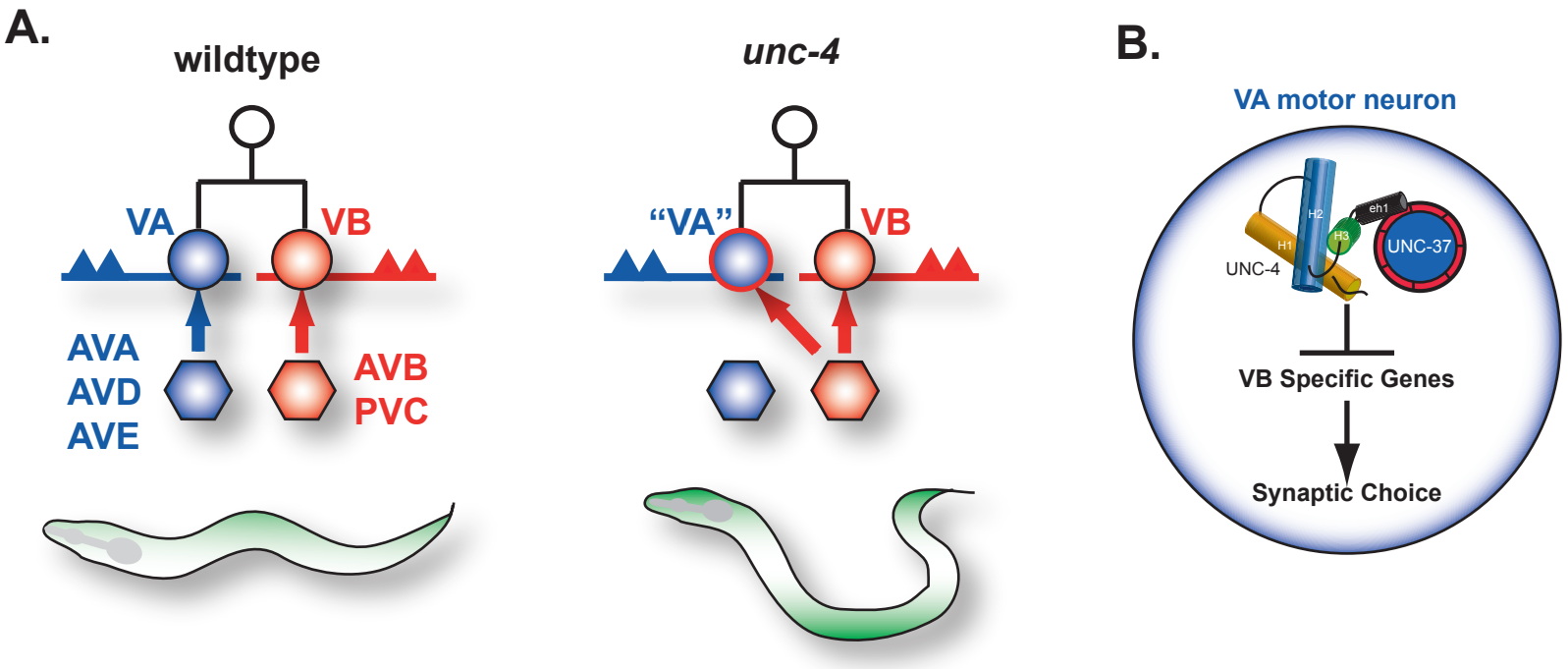

Figure 1.11. UNC-4 and UNC-37 repress VB-specific genes to specify synaptic inputs to VA motor neurons. A. Most VA and VB motor neurons arise from a common progenitor and receive inputs from separate groups of interneurons to mediate backward and forward movement, respectively. In *unc-4* mutants, which cannot move backward, a subset of VAs are miswired with inputs normally reserved for their VB sister cells. B. Model of UNC-4 action. The UNC-4 homeodomain protein and its co-repressor UNC-37/Groucho, specify pre-synaptic inputs to VA motor neurons by repressing VB-specific genes.

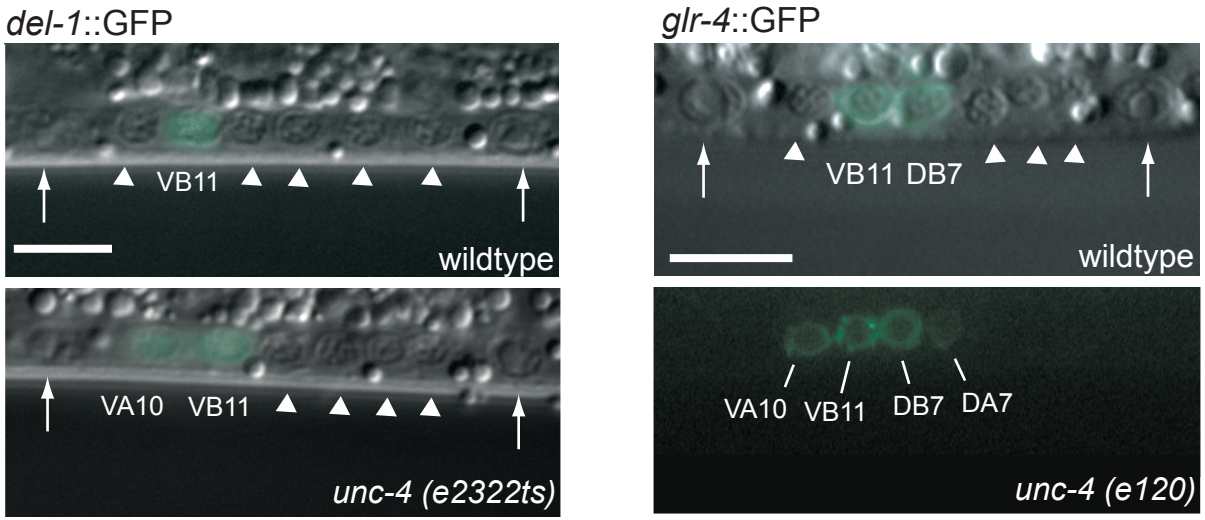

Figure 1.12. *del-1* and *glr-4* are negatively regulated by UNC-4. (Left) A GFP reporter for the DEG/ENaC subunit, *del-1*, is normally restricted to VB motor neurons in the L2 (top) but is also expressed in VA motor neurons in *unc-4* mutants (bottom). (Right) *glr-4*::GFP (glutamate receptor subunit) is expressed in DB and VB motor neurons in the wildtype and ectopically expressed in DA and VA motor neurons in *unc-4*. Arrowheads point to DIC images of motor neuron nuclei that do not express GFP. Arrows denote VNC landmarks, P9.p and P10.p ectodermal blast cells. Anterior is to left, ventral down. Scale bars represent 5 μm.

submitted). As noted below, this negative result motivated my project to identify additional *unc-4* target genes.

Neurotransmitter vesicle abundance is regulated by UNC-4

unc-4 mutants display a second phenotype in addition to the miswiring defect. UNC-4-expressing cells also exhibit a 40% reduction in synaptic vesicles. Consistent with the observed decrease in SV number, there is also a significant decrease in the levels of SV associated proteins (Figure 1.13). For example, immunostaining experiments determined that RAB-3, UNC-17, CHA-1, SNT-1 and SNB-1 proteins are all significantly reduced in *unc-4* mutants. Interestingly, this effect is post-transcriptional as a *promoter*::GFP reporter for *unc-17/cha-1* does not exhibit a reduction in GFP levels in *unc-4* mutants (Lickteig, Duerr et al. 2001), whereas both UNC-17 (VAChT) and CHA-1 (ChAT) protein levels are significantly reduced. These results suggest that UNC-4 is likely acting indirectly to regulate the levels of these proteins. We, therefore, propose that UNC-4 represses downstream genes that negatively affect the maintenance or biosynthesis of synaptic vesicles. According to this model, *unc-4* would function as a regulator of synaptic inputs as well as synaptic outputs (Figure 1.14).

The genes acting downstream of *unc-4* to regulate synaptic assembly and function are unknown. The major focus of my project has been to identify these UNC-4 targets using microarray strategies. As outlined in the forthcoming chapters, I have developed methods using Fluorescence Activted Cell Sorting (FACS) to isolate specific GFP-marked cells from *C. elegans* embryos. Using this approach, purified *unc-4*::GFP neurons were obtained and RNA extracted for application to the *C. elegans* Affymetrix array. A

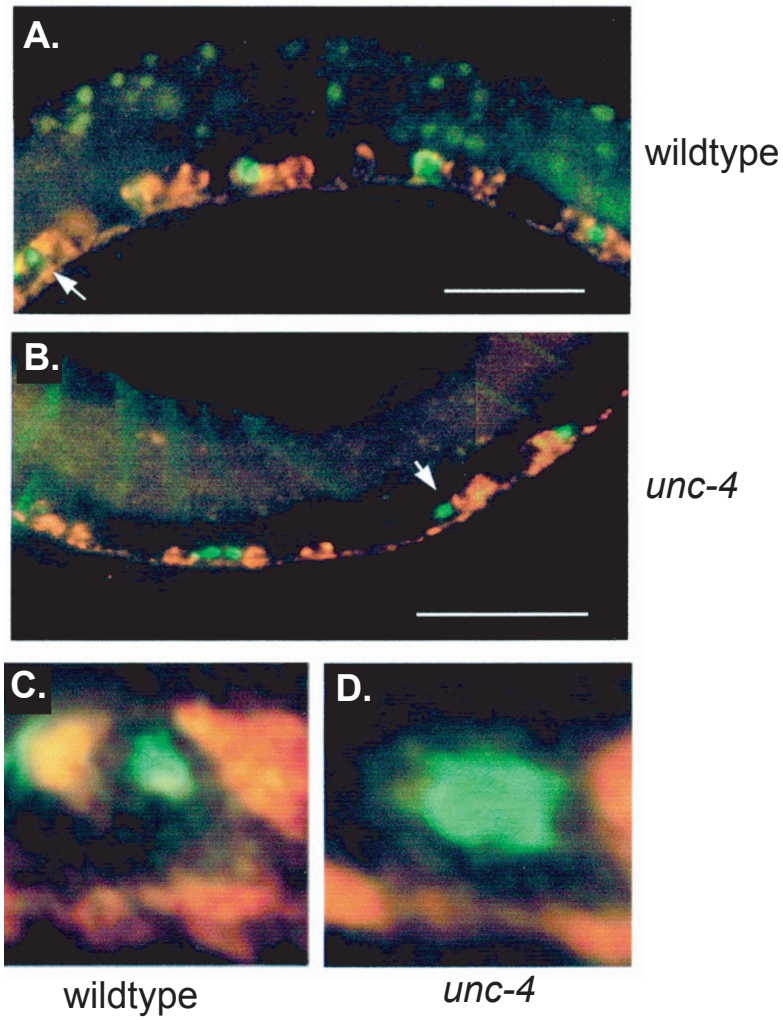

Figure 1.13. Synaptic vesicle proteins are reduced in *unc-4* mutants. All experiments performed in an *unc-104* mutant background to cluster synaptic vesicles at cell soma. Furthermore, all strains carry *unc-4*::GFP to mark A-class motor neurons. A,C. Cytoplasmic UNC-17 immunostaining (red) is bright surrounding all *unc-4*::GFP neurons (green). B, D. UNC-17 immunofluorescence is reduced or absent in *unc-4*::GFP DA and VA motor neuron cell soma. C, D. High magnification images of VA motor neurons from A, B. Scale bars represent 10μm, anterior left. Image adapted from Lickteig et al., 2001.

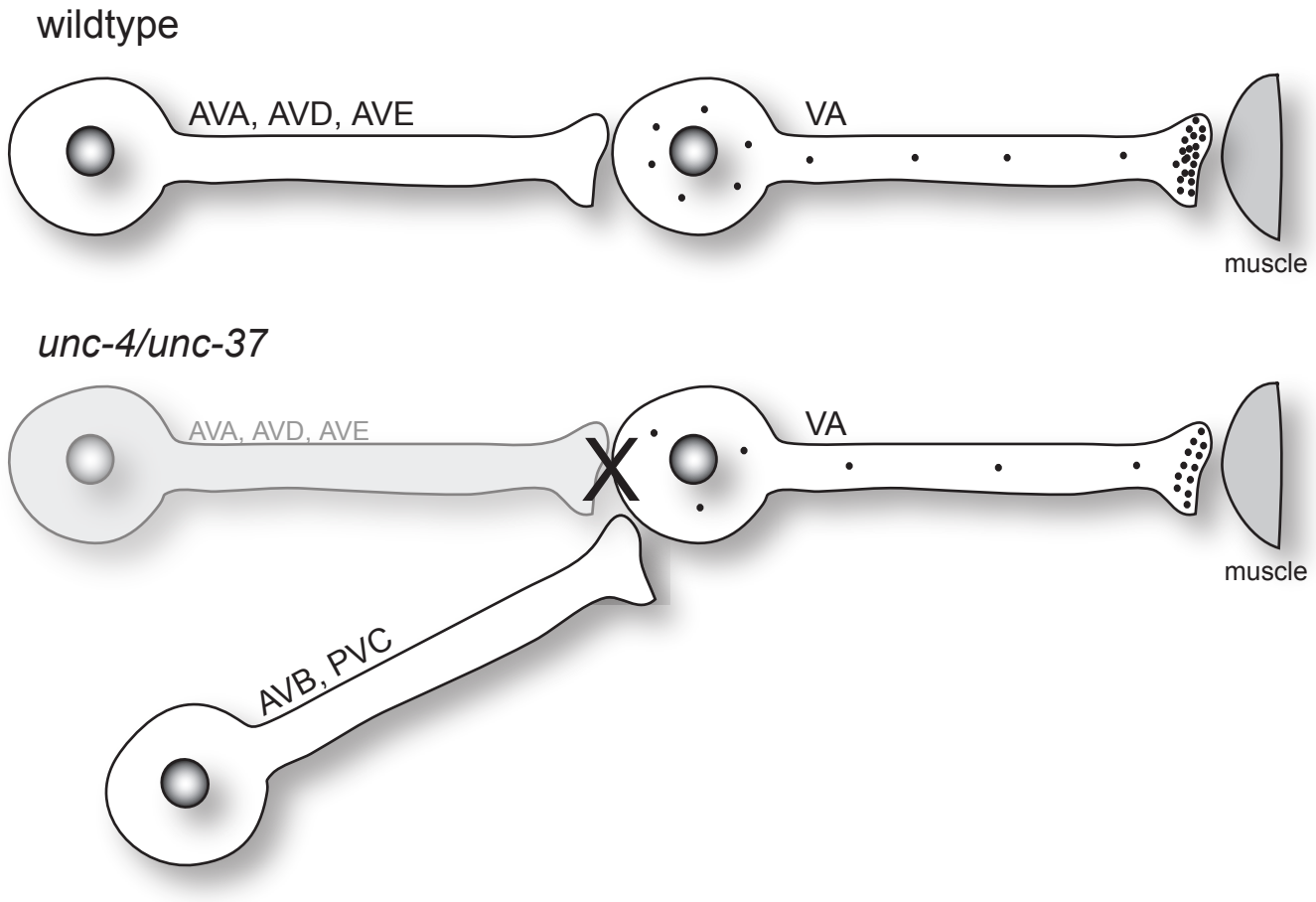

Figure 1.14. Model of *unc-4* function in VA motor neurons. (Top) Wildtype VA motor neurons receive inputs from AVA, AVD, and AVE and make chemical synapses at the NMJ. (Bottom) In the *unc-4* mutant, the VAs are miswired with inputs from AVB and PVC. VA motor neurons still make chemical synapses with the bodywall muscle, however, they exhibit reductions in the levels of neurotransmitter vesicles. Thus, *unc-4* functions to regulate both synaptic inputs and synaptic outputs in VA motor neurons. Figure adapted from Von Stetina et al., 2006.

comparison of wildtype and mutant profiles identified specific transcripts that are upregulated in *unc-4* and *unc-37* mutants. This work, in combination with results from a similar approach by Steve Von Stetina, have defined a list of ~400 candidate UNC-4 target genes that can now be tested by genetic methods for downstream roles in the *unc-4* pathway. In Chapter V below, I outline experiments firmly establishing that one of these UNC-4 regulated genes, *ceh-12*, the *C. elegans* homolog of HB9, functions in the *unc-4* pathway to regulate both wiring specificity and synaptic vesicle abundance in A-class motor neurons.

Molecules implicated in synaptic specificity

There are many integral steps necessary for a synapse to form between adjacent neurons. First, neuronal identities must be established. Second, growth cones must reach the target area and identify the correct synaptic partner. Finally, a synapse is assembled connecting the two cells, allowing for synaptic transmission to occur. As described before, much is known about the mechanisms that determine neuron fate and identity. The molecules required to guide growth cones to target regions are also well defined. The mechanisms underlying synaptic partnership, however, are poorly understood. In 1963, Roger Sperry proposed that neurons display unique combinations of cell-surface markers that are recognized by a specific partner (Sperry 1963). In support of this "lock and key" theory is the identification of many adhesion and cell surface molecules that often are differentially spliced to produce thousands of isoforms. In this section, I will

review some of the molecules that have been identified as proteins that may function to specify synaptic choice.

Neurexins/Neuroligins

Neuroligins are transmembrane proteins that contain a cleaved signal peptide, a cholinesterase-like domain, a carbohydrate attachment region, and a PDZ domain. There are three neuroligin proteins in rat and mouse; five have been identified in humans. Each neuroligin gene is capable of producing up to four alternatively spliced isoforms (Juttner and Rathjen 2005; Lise and El-Husseini 2006). The neurexins are transmembrane proteins that contain an extracellular N-terminal sequence and have a receptor-like structure. There are three mammalian neurexin genes which each give rise to two mRNAs, α-neurexin and β-neurexin. These transcripts contain multiple alternative splice sites, and have the capability of producing >1000 different transcripts. Neurexins and neuroligins interact heterophilically and recruit synaptic molecules (Lise and El-Husseini 2006). For example, neuroligin interacts with PSD-95 via its PDZ domain, thereby establishing the initial framework for post-synaptic density formation (Irie, Hata et al. 1997; Lise and El-Husseini 2006). Neurexins interact with CASK, which is required for the initial recruitment of the presynaptic vesicle machinery (Hata, Butz et al. 1996; Lise and El-Husseini 2006). Consistent with this idea, *in vitro* experiments show that interactions between β-neurexin and neuroligin are sufficient to organize presynaptic terminals in heterologous cells (Scheiffele, Fan et al. 2000). While the ability of the neurexins/neuroligins to contribute to the differentiation of pre- and post- synaptic sites is apparent, whether they determine synaptic specificity is unknown. Given the multitude

of isoforms generated through alternative splicing, however, it is reasonable to imagine that different combinations may play a role in determining the specificity of synaptic connections.

Protocadherins/Cadherins

The cadherin superfamily is comprised of transmembrane proteins that contain extracellular cadherin domains mediating calcium-dependent homophilic interactions (Suzuki 1996). The cadherin superfamily can be divided into two subgroups, the classical cadherins and the protocadherins. Classical cadherins interact with β-catenins to mediate cadherin clustering and attachment to the cytoskeleton, thereby promoting cell adhesion. In contrast, protocadherins do not interact with catenins or other cytoskeletal proteins resulting in much weaker cell-cell adhesion (Suzuki 1996). Approximately twenty classical cadherins and at least 80 different protocadherins are expressed in the central nervous system (CNS). Cadherins from both families are localized to synaptic regions, and selective expression of particular family members suggests that cadherins may be required for the differentiation and targeting of specific neuronal cell types (Junghans, Haas et al. 2005). The large number of protocadherins suggests that these molecules may be required to specify synaptic inputs. Below I will describe some of the specific examples of cadherin function in determining synaptic connectivity.

Cadherins are required for photoreceptor targeting in Drosophila

N-cadherin was identified in a genetic screen to identify mutants with defects in photoreceptor targeting. In wildtype animals, the R1-R6 photoreceptors project as a

single fascicle into the lamina where axons then defasciculate and exit the bundle to connect with specific target cells (Clandinin and Zipursky 2000). In the *N-cadherin* mutant, however, R1-R6 axons fail to defasciculate and, therefore, do not extend toward their intended target cells. R7 and R8 also exhibit targeting defects (Lee, Herman et al. 2001). The R7 and R8 receptors normally project to the medulla, which consists of three layers, M2, M3 and M6. R7 cells target the M6 layer, while R8 cells terminate in the M3 layer (Bausenwein, Dittrich et al. 1992). In the *N-cadherin* mutant, neither R7 nor R8 reach their target layers; however, this could be due to the severe defects in the structure of the medulla. An alternative model is that, since R1-R7 neurons are directed to target regions following R8 extension, mistargeting could be due to the defects observed in R8 (Lee, Herman et al. 2001). To determine if *N-cadherin* functions cell-autonomously, Lee et al., (2001) generated animals in which a single R7 neuron was mutant for *N-cadherin*, while the surrounding axons, and the target regions were wildtype. They observed that mutant R7 axons extended into the M6 region, but then retracted into the M3 region, thereby suggesting that N-cadherin was required cell-autonomously to project to the correct layer (Lee, Herman et al. 2001). Interestingly, N-cadherin is expressed in all photoreceptor neurons and their target layers, indicating that homophilic interactions are likely necessary for target layer recognition. This finding also suggests that there are probably differential downstream pathways that are activated by cadherin interactions to mediate specificity in target selection. The mechanisms in which photoreceptors choose the right cell, in the right layer, however, are still unknown.

In a related study, Lee et al., (2003) showed that the protocadherin, Flamingo (*fmi*), is also required for proper targeting of the R1-R6 photoreceptors. In *fmi* mutants,

R1-R6 axons form synapses with inappropriate partners within the lamina. Interestingly, *fmi* is transiently expressed in R1-R6 photoreceptors. Expression is high early in pupal development as the axons are extending into the lamina, with expression virtually undetectable halfway through pupal development, when synapses are forming. These findings suggest that *fmi* is critical for initial growth cone extension toward the target region; however, the authors propose that N-cadherin and the protein tyrosine phosphatase, dLar, are required for target layer recognition (Lee, Clandinin et al. 2003).

Receptor Protein Tyrosine Phosphatases (RPTP)

In the same Drosophila genetic screens used to identify N-cadherin and Flamingo, the receptor protein tyrosine phosphatase (RPTP), dLAR, was also identified (Clandinin, Lee et al. 2001). It is interesting to point out that mutations in *dlar* are very similar to those observed in *N-cadherin* mutants. The R7 axons extend to the medulla, but are misdirected, instead forming synapses in the R8 target area (Clandinin, Lee et al. 2001; Maurel-Zaffran, Suzuki et al. 2001). Given the high similarity of the *dlar* mutant phenotype to *N-cadherin*, it has been proposed that dLAR may modulate the activity of N-cadherin (Maurel-Zaffran, Suzuki et al. 2001). A second RPTP has been implicated in mistargeting; *dptp69D* mutants exhibit targeting defects in R7 similar to, but less severe than those observed in *dlar* mutants (Desai, Gindhart et al. 1996). However, the R1-R6 targeting defects differ between these two mutants. In *dlar* mutants, R1-R6 target the lamina, but do not make the proper synaptic connections, while in *dptp69D* mutants, the R1-R6 axons extend past the lamina (Desai, Gindhart et al. 1996). These results suggest

that specific RPTPs may function to modulate cell-surface markers that are required for R-cell axon termination at the intended region and proper target recognition.

Immunoglobulin (Ig) Superfamily proteins

Similar to cadherins, Ig domain proteins typically engage in homophilic interactions to mediate cell adhesion. Members of the Ig superfamily have been implicated in a wide variety of cell adhesion processes in multiple cell types. In the following sections I highlight specific examples of Ig domain-containing proteins that have known roles in synaptic choice.

Sidekicks direct synaptic targeting in the chick retina

The *sidekick* proteins are large proteins that contain 6 Ig domains, 13 fibronectin domains, a transmembrane domain, and a PDZ protein-protein interaction domain. *sidekick* was first identified in Drosophila, in a genetic screen looking for molecules involved in retinal patterning (Nguyen, Liu et al. 1997). However, the role of Sidekicks in synaptic formation has been better defined in the chick retina. Sdk-1 and Sdk-2 were identified in a screen for proteins that are differentially expressed between subsets of retinal ganglion cells (RGC) in an effort to identify candidate genes that mediate lamina-specific synapse formation in the inner plexiform layer (Yamagata, Weiner et al. 2002). Both proteins localize to non-overlapping sets of RGCs as well as to specific sublaminae in the inner plexiform layer. Sdk-1 and Sdk-2 are concentrated at synaptic sites and *in vitro* assays confirm that these proteins interact through homophilic adhesions. The authors demonstrate that Sdk+ RGCs project to Sdk+ laminae. Sdk is sufficient to

promote this interaction as overexpression of Sdk in Sdk- cells re-directs these neurons to Sdk+ laminae (Yamagata, Weiner et al. 2002). This study presents the first direct evidence that homophilic interactions of Ig proteins may play a critical role in the formation of specific connections between neuronal partners; however, as mentioned above for N-cadherin, it is unclear whether the sidekicks also mediate synaptic specificity, or only target layer recognition. Interestingly, the Sdk proteins are only localized to 2 of the 10 sublaminae, thereby suggesting that additional adhesion molecules are required for synaptic connections in the additional layers (Yamagata, Sanes et al. 2003).

SynCAM

SynCAM is an Ig domain protein that aligns pre- and post-synaptic regions through homophilic interactions (Biederer, Sara et al. 2002). In experiments similar to those described above for neurexin/neuroligin, Biederer et al., (2002) showed that expression of SynCAM in co-cultured neurons is sufficient to promote pre-synaptic differentiation. Furthermore, co-expression of SynCAM and glutamate receptors in a heterologous system was able to fully reconstitute a functional glutamatergic synapse (Biederer, Sara et al. 2002). These results indicate that SynCAM expression on the pre- and post-synaptic membranes is sufficient to initiate synapse assembly, possibly through the recruitment of synaptic proteins via its PDZ domain; however, the actual mechanism of SynCAM function is not understood (Biederer, Sara et al. 2002).

Dscam

In Drosophila, Dscam is an intriguing candidate for synaptic specificity determinant as it encodes a family of Ig domain proteins arising from ~38,000 alternatively spliced transcripts (Schmucker, Clemens et al. 2000). Dscam is highly expressed in the nervous system, and loss of the entire protein family leads to defects in axon guidance, targeting, branch specification and dendrite patterning (Schmucker, Clemens et al. 2000; Wang, Zugates et al. 2002; Hummel, Vasconcelos et al. 2003; Chen, Kondo et al. 2006). *In vitro* studies have determined that, similar to other Ig proteins, homophilic interactions are required for adhesion, suggesting that synaptic connectivity results from neuronal partners that express the same Dscam variant (Wojtowicz, Flanagan et al. 2004). To test this model, *Dscam* alleles able to generate only ~22,000 isoforms were generated (Chen, Kondo et al. 2006). Indeed, these mutants display specific defects in mechanosensory neuron axon targeting. Furthermore, re-introduction of single isoforms into the mutant alleles results in partial rescue of the axon targeting defects, indicating that specific combinations of Dscam isoforms are required to specify synaptic connectivity in these neurons (Chen, Kondo et al. 2006). Vertebrate Dscam does not undergo the extensive alternative splicing observed in Drosophila (Agarwala, Nakamura et al. 2000; Agarwala, Ganesh et al. 2001; Zipursky, Wojtowicz et al. 2006). Nevertheless, this mechanism of alternative splicing could be utilized in additional protein families and provide a means to establish the molecular diversity required to specify synaptic choice.

SYG-1 specifies synapse formation in C. elegans

SYG-1 was identified in a visual genetic screen for mutations that disrupt synaptic vesicle localization in the HSNL (hermaphrodite specific neuron, left) neuron. In wildtype animals, the synaptic vesicle marker SNB-1::YFP (synaptobrevin) fusion protein is localized at the region where the HSNL makes synaptic connections with the vulval muscles and the VC motor neurons. In *syg-1* mutants, SNB-1::YFP expression is reduced or absent at the normal site of the synapse. Shen and Bargmann (2003) show that SYG-1 functions cell autonomously in HSNL for proper synaptic vesicle localization. Furthermore, they show that a signal in the vulval epithelium is required to establish proper synaptic formation (Shen and Bargmann 2003). The same group reported the identification of SYG-2, which is expressed in the vulval epithelium and exhibits SNB-1::YFP localization defects similar to *syg-1* mutants (Shen, Fetter et al. 2004). They suggest that SYG-2 is functioning as a guidepost signal, and that interaction of SYG-1 with SYG-2 is required for synaptic vesicle accumulation in HSNL at the site of synaptic connections. *syg-1* encodes an immunoglobulin domain protein related to the mammalian NEPH protein, while *syg-2* is related to the immunoglobulin protein nephrin. Loss of these proteins in mammals leads to kidney development problems. Interestingly, NEPH and nephrin are also expressed in the nervous system; however, their role in synaptic connectivity is unknown (Shen, Fetter et al. 2004). These findings underscore the importance of local interactions between members of the Ig superfamily to determine the site of synapse formation.

Transcription factors

engrailed (en) directs axon targeting in the cockroach

In the cockroach, the sensory neuron 6m is born between 4-9 hours post hatching and first send axons into the central nervous system about 3 days later. On day 6, synaptic connections form between the 6m sensory neuron and the giant interneurons (GI) 1, 2, and 5 (Marie, Cruz-Orengo et al. 2002). The Engrailed transcription factor is expressed in 6m; in contrast, expression is never detected in the neighboring sensory neuron 6d. Sensory neurons in animals treated with *en* RNAi exhibit axon guidance defects and changes in synaptic connectivity. The 6m sensory neuron no longer makes connections with GI 1/2/5; instead, it forms connections with GI 3/6, which normally synapse with the 6d sensory neurons (Marie, Cruz-Orengo et al. 2002). Furthermore, *en* expression is necessary during the critical period of synapse formation at day 6, since RNAi of *en* at later times does not disrupt synaptic connectivity. Thus, *en* is required to specify the connectivity of the 6m sensory neuron at a specific developmental timepoint. This finding is similar to that observed in *unc-4*, in which a transcription factor functions to block the creation of alternative synaptic inputs that are normally reserved for a neighboring neuron.

brakeless (bks) represses runt (run) to regulate photoreceptor target choice

Run belongs to the Runt family of transcription factors and is normally expressed in the R7 and R8 photoreceptors which target the medulla (Kaminker, Singh et al. 2001). Bks is a zinc finger transcription factor that is expressed in all photoreceptor cells. In *bks*

mutants, the R1-R6 neurons extend past the lamina and terminate in the medulla (Rao, Pang et al. 2000; Senti, Keleman et al. 2000). In an examination of cell-type specific markers, Kaminker et al. (2002) discovered that in *bks* mutants, *run* is ectopically expressed in the R2 and R5 photoreceptors and that cell-autonomous expression of *run* in these cells leads to mistargeting of all 6 photoreceptors (Kaminker, Canon et al. 2002). The authors suggest that since R2 and R5 are the first two photoreceptors to be specified, the additional R cell axons likely follow the tracts established by R2/5. Interestingly, all of the R1-R6 photoreceptors maintain normal expression of cell-type specific markers (Kaminker, Canon et al. 2002). Thus, it appears that Brakeless blocks the inappropriate expression of the transcription factor, RUN, in order to preserve normal targeting (Kaminker, Canon et al. 2002).

unc-4 specifies pre-synaptic inputs to VA motor neurons in C. elegans

A described above, UNC-4 is a homeodomain transcription factor that is expressed in VA motor neurons where it functions to specify pre-synaptic inputs as well as to maintain neurotransmitter signaling capacity (Miller, Shen et al. 1992; White, Southgate et al. 1992; Lickteig, Duerr et al. 2001). In *unc-4* mutants, VAs are miswired with inputs normally reserved for their VB sister cells (White, Southgate et al. 1992); synaptic vesicles are also depleted at the neuromuscular junction. The downstream mechanisms that control these important events, however, are not known. **The goal of this dissertation project was to identify *unc-4* target genes that define synaptic specificity and strength.** The following chapters describe my approach to this question

and report the first successful identification of an *unc-4* target gene that regulates both of these processes.

Conclusions

The mammalian spinal cord is highly complex, potentially containing billions of neurons. Coordinated movement depends on the incorporation of these neurons into discrete circuits that drive motor activity. Although the choice of correct synaptic partners is essential to the formation of these networks, the mechanisms that control this decision are poorly understood. We have simplified this question by working with *C. elegans*, a model organism with a small, well-defined nervous system. As described in the first section of this chapter, all of the neurons and their synapses in the motor circuit have been identified by EM reconstruction. In addition, genetic studies have identified the transcription factors that specify individual neuronal fates. Importantly, many of these have conserved functions in vertebrates. This last section focused on molecules that have proposed functions in synapse formation, mostly in Drosophila and vertebrate nervous systems. Given the complexity of these systems, however, studying the formation of individual synapses *in vivo* is difficult. To overcome this problem, our lab has focused on the formation of a single set of synapses in *C. elegans*; those that form between the AVA interneurons and the VA motor neurons. The simplicity of the nematode nervous system, along with methods to profile individual cell types should allow us to identify the genetic code that defines these cells, and thereby provide insight into the programs that confer synaptic specificity. The forthcoming chapters will detail my contribution to understanding the mechanisms that lead to synaptic connectivity. Given the high degree of conservation exhibited in determining neuronal fates, it is likely that our findings in *C.*

elegans may provide insight into the mechanisms that specify synaptic choice in more complex organisms.

CHAPTER II

CELL-SPECIFIC PROFILING USING MAPCeL

Introduction

The nematode *C. elegans* arises from an invariant lineage (Sulston, Schierenberg et al. 1983), in which genetic programs are established to define individual cell types. Due to the small size of this organism, however, the isolation of individual cells to evaluate the molecular determinants of a specific tissue has been inherently difficult. To circumvent this problem the Miller lab collaborated with Kevin Strange and his group to develop methods for isolating and culturing embryonic *C. elegans* cells. Although cell culture techniques had been previously described (Bloom 1993), these methods did not support differentiation or long term viability *in vitro*, preventing the use of these cells for molecular approaches. The Miller and Strange labs developed a new protocol for the robust, large-scale culture of embryonic cells. Importantly, these cells displayed morphological, physiological and molecular traits akin to *in vivo* characteristics, thereby suggesting that the culture conditions support normal differentiation (Christensen, Estevez et al. 2002).

I participated in these studies, first as a rotation student and then as a beginning graduate student with the goal of advancing a strategy for isolating specific *C. elegans* cells for microarray profiling. Using GFP marked transgenic strains in combination with Fluorescence Activated Cell Sorting (FACS), I developed the method we have termed MAPCeL (Microarray Profiling *C. elegans* Cells). By obtaining RNA from sorted cells

and performing microarray experiments we have obtained gene expression fingerprints for specialized cell types in the nematode embryo. Extensive work validating these data suggests that this method reliably detects transcripts that are expressed in specific cells. In this chapter I will describe my contributions to the development of the cell culture technique, and the use of this technique to establish MAPCeL methods. Finally, I will describe how we used MAPCeL to profile the DA motor neurons (marked with *unc-4*::GFP) and how we confirmed the validity of these findings. The work described in this chapter has been published in *Neuron* (cell culture methods) (Christensen, Estevez et al. 2002) and *BMC Genomics* (MAPCeL) (Fox, Von Stetina et al. 2005). In later chapters I will describe the application of MAPCeL to achieve the long-term goal of my project, namely the identification of UNC-4 target genes that control synaptic specificity in the *C. elegans* motor circuit.

Materials and Methods

Nematode strains

Nematode strains were grown and maintained as previously described (Brenner, 1974) unless otherwise noted. Strains used for these experiments include the wildtype N2, NC197 (*wdIs4, unc-4*::GFP II) (Pflugrad, Meir et al. 1997), NC300 (*wdIs5, unc-4*::GFP III) (Lickteig, Duerr et al. 2001), PD4251 (*ccIs4251, myo-3*::GFP I) (Fire, Xu et al. 1998) and DP132 (*edIs6, unc-119*::GFP) (Maduro and Pilgrim 1995). Table 2.1 lists GFP reporters generated to validate microarray data.

Table 2.1. promoter::GFP fusions generated to validate *unc-4*::GFP dataset			
***promoter*::GFP fusion**	**Strain**	**Source**	**Reference**
flp-13	NY2073	Chris Li	(Kim and Li 2004)
mab-9	*mab-9*::GFP	Allison Woollard, Roger Pocock	
mig-13	CF896	Cynthia Kenyon	(Sym, Robinson et al. 1999)
nca-1	TS48	Kevin Hamming, Colin Thacker, Terry Snutch	
nlp-9	AA325	Anne Hart	(Li, Nelson et al. 1999)
rpy-1	NM946, NM986, NM987	Mike Nonet	
syg-1	VH697	Harald Hutter	
twk-30	NC698	Larry Salkoff	(Salkoff, Butler et al. 2001)
F09C3.2	NC847, NC821	Promoterome	
T19C4.5	NC843	Promoterome	
tsp-7	NC850	Promoterome	
nlp-15	HA0357	Anne Hart	(Li, Nelson et al. 1999)
F29G6.2	NC865	Promoterome	
tig-2	NC845	Promoterome	
F55C12.4	NC902, NC844	Promoterome	
trp-1	CX3587	Cori Bargmann	
nlp-21	HA0444	Anne Hart	(Nathoo, Moeller et al. 2001)
acr-14	NC956	Promoterome	

Embryonic cell isolation and cell culture

Embryos were isolated from gravid adults following lysis in a hypochlorite solution. Intact embryos were separated from debris by flotation on 30% sucrose. Eggshells were dissolved by incubation in 0.5ml chitinase (0.5U/ml in egg buffer) for 45 minutes. Following resuspension in L-15 medium supplemented with 10% FBS (L15-10) and antibiotics, the embryos were dissociated by passage through a 5µm syringe filter (Durapore). L-15 media, and egg buffer were adjusted to an osmolarity of ~340 mOsm using sucrose. Cells were plated on peanut lectin (for visualization) or poly-L-lysine (0.01%, Sigma) (for FACS) coated single-well chambered coverglasses (Nalge Nunc International) at a density of ~10 million cells/ml and maintained in L15-10 media. Cells were incubated at 25°C in a humidified chamber.

Immunofluorescence

Cells were fixed with 1% paraformaldehyde for 30 minutes, rinsed with egg buffer, and then permeabilized for 2 minutes with ice cold methanol. Permeabilized cells were incubated for 60 minutes with UNC-54 monoclonal antibody (1:2000, mouse) (Miller, Ortiz et al. 1983) or with synaptotagmin antibody (SNT-1, 1:50, rabbit) (Lickteig, Duerr et al. 2001) followed by incubation for 30 minutes with Cy3-labeled secondary antibodies.

Microscopy

Transgenic animals and cultured cells were visualized by differential interference contrast (DIC) or epifluorescence microscopy using either a Zeiss Axioplan or Axiovert

compound microscopes. Images were recorded with CCD cameras (ORCA I, ORCA ER, Hamamatsu Corporation, Bridgewater, NJ). Some images were recorded on a Zeiss 510 META confocal microscope.

FACS analysis

Sorting experiments were performed on a FACStar Plus flow cytometer (Becton Dickinson, San Jose, CA) equipped with a 488 nm argon laser. Emission filters were 530+30 nm for GFP fluorescence and 585+22 nm for propidium iodide (PI) fluorescence. The machine was flushed with egg buffer prior to sorting to enhance viability. 2 μm fluorescent beads were used to calibrate light scattering parameters for the relatively small size of *C. elegans* embryonic cells. Cells were sorted at a rate of 4000-5000 cells per second through a 70 μm nozzle.

Immediately prior to sorting, supernatant from the 24-hour cultures was removed and discarded. One milliliter of egg buffer was added to the chamber coverglass. Cells are loosely adherent to poly-L-lysine and can be easily dislodged with gentle pipetting. Three milliliters of egg buffer + cells were drawn into a 3cc syringe and the suspension filtered with a 5 μm Durapore syringe filter. PI was added to the cell suspension at a final concentration of 5 μg/ml prior to sorting. Autofluorescence levels were established by flow cytometry of cells isolated from wildtype (i.e. non-GFP) embryos. Next, wildtype cells stained with PI were used to define the sorting gate for damaged cells. GFP+ cells containing no PI were sorted to establish the intensity range of GFP fluorescence. Finally, *unc-4*::GFP cells stained with PI were gated using the parameters established above. The sorting gate for size and granularity was empirically adjusted to

exclude cell clumps and debris and to achieve ~90% enrichment for GFP-labeled cells. *unc-4*::GFP cells were collected in a 15 ml conical tube containing 1 ml of L15-10 media. Cells were pelleted using low-speed centrifugation (300xg) and either plated on peanut lectin-coated slides for visualization or used for RNA isolation (see below). Dr. Susan Barlow isolated Reference cells from 1 day old cultures of embryonic blastomeres isolated from the non-GFP wildtype strain (N2). In this case, all viable cells (i.e. non-PI stained) were collected by FACS for RNA isolation.

RNA isolation, amplification, and hybridization

RNA was prepared from FACS isolated *unc-4*::GFP cells for comparison to RNA from the wildtype reference strain (N2). Cells were pelleted using low-speed centrifugation (300 xg). The supernatant was removed and RNA was extracted with a micro-RNA isolation kit (Stratagene) using the recommended volumes for 1 million cells. Typical yields were 1 pg total RNA/cell. 100 ng of total RNA was subjected to 2 rounds of amplification, as described in the Affymetrix GeneChip Eukaryotic Small Sample Target Labeling Protocol, with the following modifications: 5 pmol (100 ng) of T7-dT primer (5'-GGCCAGTGAATTGTAATAC GACTCACTATAGGGAGGCGG-$(dT)_{24}$ -3') was used as opposed to the recommended 100 pmol. Also, RNA cleanup was achieved using the RNeasy mini kit (Qiagen); 300 µl of 100% ethanol (final concentration = 40% ethanol) was added to the sample prior to absorption to the column matrix. Eluate was passed through the column 2x prior to washing to improve yields. The BioArray High Yield RNA Transcript Labeling Kit (Enzo) was used to biotinylate the sample in the second round of amplification. 10-15 µg of labeled aRNA (amplified RNA)

was fragmented and hybridized to the Affymetrix *C. elegans* chip according to the Affymetrix Expression Analysis Technical Manual. The Agilent Bioanalyzer was used to assess RNA quality prior to labeling and to confirm fragmentation (<200bp) before hybridization.

Data Analysis

The commercially available *C. elegans* Affymetrix array was used for all experiments. This chip was designed using the December 2000 genome sequence. All probe set information is available at www.affymetrix.com as well as www.wormbase.org. *unc-4*::GFP neurons were profiled in triplicate; baseline data (all cells) were obtained from four independent experiments with wildtype embryonic cells. Hybridization intensities for each experiment were scaled in comparison to a global average signal from the same array (Hill, Brown et al. 2001). Expressed transcripts were initially identified on the basis of a "Present" call in a majority of experiments (2/3 for *unc-4*::GFP and 3/4 for wildtype cells) as determined by Affymetrix MAS 5.0 (see below). In this approach, a Mismatch (MM) value for each feature is compared to a Perfect Match (PM) value to estimate non-specific binding. This strategy, however, tends to arbitrarily exclude low intensity signals in which PM and MM values may be comparable (Irizarry, Bolstad et al. 2003; Irizarry, Hobbs et al. 2003). To avoid this bias in the detection of transcripts that might be differentially elevated in the *unc-4*::GFP data set, intensity values were normalized using RMA (Robust Multi-Array Analysis) available through GeneTraffic (Iobion), in which the MM values are not considered (Irizarry, Bolstad et al. 2003; Irizarry, Hobbs et al. 2003). Comparisons of RMA-normalized intensities for *unc-4*::GFP

vs reference cells were statistically analyzed using Significance Analysis of Microarrays software (SAM, Stanford) (Tusher, Tibshirani et al. 2001; Storey and Tibshirani 2003). A two-class unpaired analysis of the data was performed to identify genes that differ by ≥1.7-fold from the wildtype reference at a False Discovery Rate (FDR) of ≤1%. These genes were considered significantly enriched. This analysis also identified ~1600 transcripts that are depleted (1.7x, <1% FDR) in *unc-4*::GFP cells vs the wildtype reference. Although 729 of these transcripts are also scored as "present" in the *unc-4*::GFP motor neuron dataset, we attribute their detection to high expression in the small fraction (~10%) of non-GFP cells contaminating this preparation (see above). Therefore, we excluded all 729 of these wildtype-enriched transcripts from the list of present calls in the *unc-4*::GFP motor neuron data set. Finally, to compute the overall sum of Expressed Genes (EGs) in the *unc-4*::GFP data set we restored 118 *unc4::*GFP enriched genes that were initially excluded from the present list due to high mismatch signals. These considerations produce a final list of 6,217 genes that are detected in *unc-4*::GFP motor neurons.

Annotation of datasets

A Wormbase mirror was established by downloading code and databases from www.wormbase.org. Using the acedb perl module, an annotation script was generated that queries the WormBase mirror. Affymetrix (Affy) IDs have been mapped to specific transcripts in WormBase. Text files containing Affy IDs (one per line) and cosmid names are input into the script, which then searches the WormbBse mirror and matches Affy ID/cosmid name to a specific transcript. Cosmid names are used for this search

when Affy IDs have not been mapped in WormBase. This information is used to acquire other linked annotations (i.e. KOG, common name, RNAi phenotype, Expression data, Kim mountain data and Gene Ontology, etc.).

In litero *analysis*

An extensive literature search was performed using Textpresso (www.textpresso.org). The keywords "DA motor neurons" generated a list of 68 citations; a similar search was conducted using the keywords "I5 pharyngeal neuron" and "SAB neurons" that detected an additional 21 citations. Expression patterns on wormbase were also searched using the "Cell identity" function to identify genes with documented expression in DA, SAB or I5. A list of 27 genes with documented expression in DA motor neurons, the I5 pharyngeal neuron and the SAB neurons was compiled from this information (Table 2.2).

Generating transgenic promoter GFP strains

twk-30::GFP (25 ng/ul) was microinjected with the *myo-3*::dsRed2 marker (25 ng/ul) (Mello and Fire 1995). Other transgenics were generated by biolistic transformation with promoter::GFP constructs from the Promoterome project. Primer sequences for "promoterome" constructs can be found at http://vidal.dfci.harvard.edu/promoteromedb (Dupuy, Li et al. 2004). Microparticle bombardment was conducted (Praitis, Casey et al. 2001) in a BioRad Biolistic PDS-1000/He equipped with the Hepta Adapter. Gold beads (1 micron) were coated with DNA at 1 μg/μl. 100 mm NGM plates were seeded with a monolayer of ~100,000

Table 2.2. Genes with known expression in *unc-4*::GFP neurons						
Cosmid	**Gene**	**Enriched**	**Present**	**Description**	**Expression**	**Reference**
K11G12.2	*acr-2*	X	X	Acetylcholine receptor	DA	(Hallam, Singer et al. 2000)
K02B12.1	*ceh-6*		X	Transcription factor (OCT-1)	SAB	(Burglin and Ruvkun 2001)
ZC416.8b	*cha-1*	X	X	Choline Acetyltransferase	SAB, DA	J. Duerr, wormbase.org
T25F10.2	*dbl-1*		X	TGF-β	DA	(Morita, Chow et al. 1999)
E02H4.1	*del-1*			DEG/ECaC channel	SAB	(Winnier, Meir et al. 1999)
ZK512.6	*eat-4*		X	Permease	I5	(Lee, Sawin et al. 1999)
F56E3.4	*fax-1*			Hormone receptor	SAB	(Much, Slade et al. 2000)
F43C9.4	*mig-13*	X	X		DA	(Sym, Robinson et al. 1999)
C09B8.7	*pak-1*		X	p21-activated S/T kinase	DA	(Iino and Yamamoto 1998)
C02D4.2	*ser-2*			7 TM receptor	SAB	(Tsalik, Niacaris et al. 2003)
F26E4.8	*tba-1*		X	Alpha tubulin	DA	(Fukushige, Yasuda et al. 1995)
C53D6.2	*unc-129*		X	TGF-β	DA	(Colavita, Krishna et al. 1998)
ZC416.8a	*unc-17*	X	X	Vesicular amine transporter	DA	J. Duerr, wormbase.org
Y16B4A.1	*unc-3*	X	X	Transcription Factor (EBF/Olf-1)	DA	(Prasad, Ye et al. 1998)
F26C11.2	*unc-4*	X	X	Transcription Factor (Prd-like)	DA	(Miller and Niemeyer 1995)
B0273.4a	*unc-5*	X	X	Netrin receptor	DA	(Su, Merz et al. 2000)
F45E10.1a	*unc-53*		X	Nuclear pore protein	DA	(Stringham, Pujol et al. 2002)
R13A1.4	*unc-8*	X	X	DEG/ECaC channel	SAB	(Tavernarakis, Shreffler et al. 1997)
H30A04.1 a	*eat-20*		X	Fibrillin-like protein	I5	(Shibata, Fujii et al. 2000)
K02G10.4	*flp-11*			FMRF-like peptide	DA	(Kim and Li 2004)
F33D4.3	*flp-13*	X	X	FMRF-like peptide	I5	(Kim and Li 2004)
F46H5.6	*grd-7*			Groundhog (Hh family)	DA	(Aspock, Kagoshima et al. 1999)
F09C3.1	*pes-7*		X	Ras GAP	DA	(Young and Hope 1993)
F59B2.13			X	GPCR	I5	Albertson, 1995
F38E1.5	*gpa-2*			G-protein, alpha subunit	I5	(Zwaal, Mendel et al. 1997)
C06A8.9	*glr-4*		X	Glutamate channel	SAB	(Brockie, Madsen et al. 2001)
ZC196.7	*glr-5*	X	X	Glutamate channel	SAB	(Brockie, Madsen et al. 2001)

L4/adult *unc-119(ed3)* animals. For each construct, 1 'shot' was performed using a 1550psi rupture disk at 28 inches of Hg vacuum. After a 1 hr recovery period, animals were washed from the plates with 7 ml M9 buffer and transferred to 7 NGM plates (1 ml/plate). Animals were grown at 20°C for 1 week. To pick transgenic animals, one-half of the plate was 'chunked' and added to a new 100 mm NGM plate; animals with wildtype movement were transderred to 60 mm NGM plates and allowed to self. Worms derived from separate plates were considered independent lines; at least 2 lines were obtained for each construct.

Results

When I joined the Miller lab in the spring of 2001, the culture methods had been optimized to yield neurons and muscle cells *in vitro*. My initial experiments were designed to determine if these cells also expressed other cell-specific traits normally observed *in vivo*. To address this question I used a combination of immunostaining and GFP reporters to confirm expression of *in vivo* markers in specific neurons and muscle cells (Figure 2.1).

Cultured cells express cell-specific markers *in vitro*

As described above, a concern with the culturing technique was that these cells were precursor cells, and that they were not differentiating into specialized cell types. To determine if this was the case, cells were isolated from two different transgenic lines, *unc-119*::GFP which labels all neurons [222 (76%) in the embryo] (Maduro and Pilgrim

1995) and *myo-3*::GFP which labels the 81 (15% of embryonic cells) (Fire, Xu et al. 1998) body wall muscle cells. Following 24 hours in culture GFP cells were counted to establish that ~13% of cells in the *myo-3*::GFP culture were GFP+ while ~75% expressed GFP in the *unc-119*::GFP culture. These results suggest that the fraction of muscle cells and neurons arising in culture is consistent with the number of cells that comprise these tissues in the embryo.

To establish that these cells were able to differentiate *in vitro*, cultures were stained with antibodies specific for proteins expressed in muscle or neurons. For this purpose we used antibodies to UNC-54, a myosin heavy chain specific to body wall muscle cells (Miller, Ortiz et al. 1983) and synaptotagmin (SNT-1), a synaptic vesicle component that is highly expressed in neurons (Lickteig, Duerr et al. 2001). *myo-3*::GFP muscle cells were stained with the antibody for UNC-54, to confirm that UNC-54 colocalized with the *myo-3*::GFP reporter (Figure 2.1). To further confirm that these cells were differentiating into specific cell types, *unc-119*::GFP cells were cultured and stained with the antibody for UNC-54. The rationale was that since UNC-54 is specific to muscle cells we should not see staining in the *unc-119*::GFP neurons. To our surprise, however, about 2% of the GFP+ cells stained with UNC-54. Upon examination of the *unc-119*::GFP transgenic animals we detected *unc-119*::GFP expression in the 8 most anterior head muscles, which is consistent with our observations *in vitro* in which a small fraction (~2%) of *unc-119*::GFP cells also stain for UNC-54. To confirm that muscle cells did not express neuron specific markers, *myo-3*::GFP muscle cells were stained with the SNT-1 antibody. One cell (out of 390) co-expressed these two markers, suggesting that both neurons and muscle cells express distinct cell-specific markers indicative of

differentiation in culture. The Strange lab went on to perform electrophysiology experiments and showed that these excitable cells exhibit properties comparable to those obtained *in vivo* (Christensen, Estevez et al. 2002).

Next, cells were cultured from the *unc-4*::GFP transgenic line, since this was the marker we were planning to use to perform the microarray experiments looking for UNC-4 target genes. UNC-4 is a homeodomain transcription factor that is expressed in 13 embryonic motor neurons (9 DA, 3 SAB, 1 I5) (Miller and Niemeyer, 1995), or about 2% of all 550 embryonic cells. Just after dissociation, very few cells expressed GFP (~0.2% based on FACS analysis), however, after 24 hours, GFP+ cells constituted ~4% of the entire cell population. This delay in GFP expression is correlated with the observation that *unc-4*::GFP is not expressed *in vivo* until after morphogenesis (400 minutes) in embryos that are not readily dissociated by our methods (Miller and Niemeyer 1995). To confirm that these GFP+ cells exhibited properties of functional neurons, they were stained with an antibody for synaptotagmin (SNT-1). SNT-1 is a synaptic vesicle protein that is expressed in UNC-4 neurons (Lickteig, Duerr et al. 2001). I found that all *unc-4*::GFP neurons were labeled with the SNT-1 antibody, which was localized to the single process that extends from these cells (Figure 2.1). At no time did we find *unc-4*::GFP neurons that did not express SNT-1.

Having utilized morphological and immunostaining criteria to confirm that *unc-4*::GFP neurons differentiate in culture, I next adopted a microarray strategy for global analysis of gene expression in cultured *unc-4*::GFP neurons. These data were also expected to provide a reference wildtype profile for the identification of UNC-4 regulated genes in these cells (see Chapter IV).

Profiling strategy

unc-4::GFP is expressed in 13 embryonic motor neurons; (1) I5 (pharynx), (3) SAB (retrovesicular ganglion), and (9) DA (ventral nerve cord)(Miller and Niemeyer 1995). Although each of the motor neuron classes is morphologically distinct, the DA and SAB motor neurons, which constitute the majority (12/13) of *unc-4*:GFP neurons, also share several characteristics including common presynaptic inputs, anteriorly directed axonal processes, cholinergic activity, and similar defects in *unc-4* mutants (White, Southgate et al. 1986; Lickteig, Duerr et al. 2001). It is therefore reasonable to assume that many of the same genes would be expressed in both of these motor neuron classes and that these could be revealed in microarray experiments.

A schematic of our approach to profile *unc-4::*GFP cells is presented in Figure 2.2. *C. elegans* embryonic cells were cultured for 24 hr to allow differentiation of GFP-labeled motor neurons. Fluorescence Activated Cell Sorting (FACS) was used to isolate enriched (~90%) populations of *unc-4*::GFP cells. RNA was extracted, amplified, and labeled for application to the *C. elegans* Affymetrix Gene Chip.

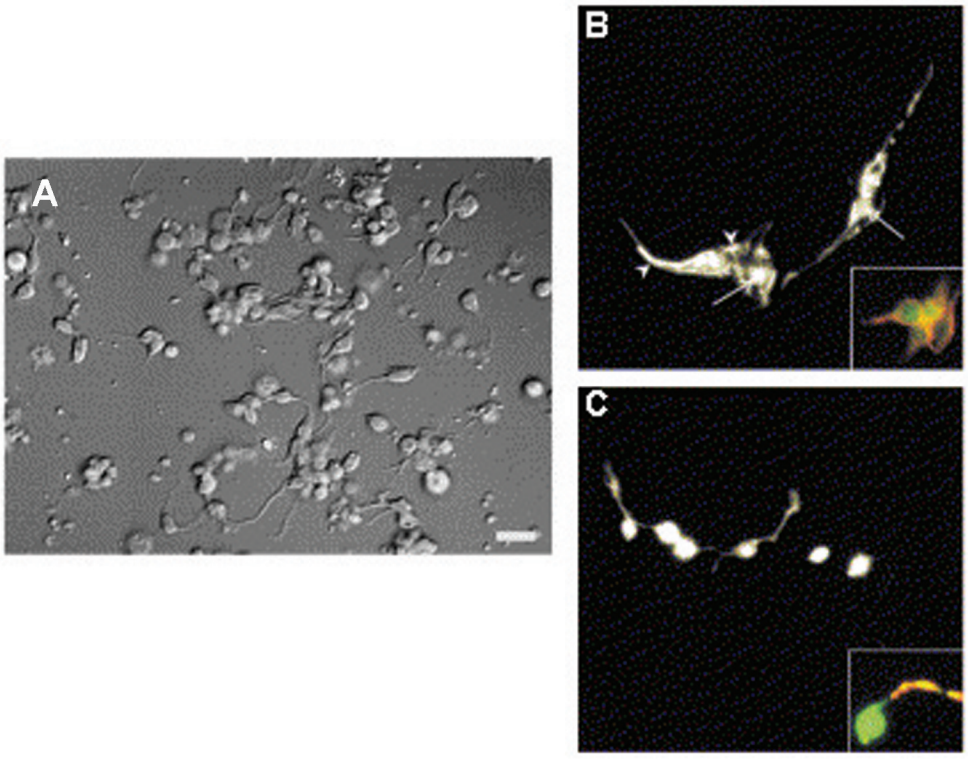

Figure 2.1. Cell-specific expression of GFP reporters in cultured cells. A. DIC image of a typical culture of C. elegans embryonic cells. Scale bar is 5 microns. B. *myo-3*::GFP expression in cultured cells. Inset: Immunolocalization of UNC-54 myosin in body wall muscle cells. C. Cultured cholinergic motor neurons expressing *unc-4*::GFP. Inset: Immunolocalization of synaptotagmin in motor neurons. Yellow indicates overlap of GFP and Cy3 fluorescence. Figure adapted from Christensen et al., 2002.

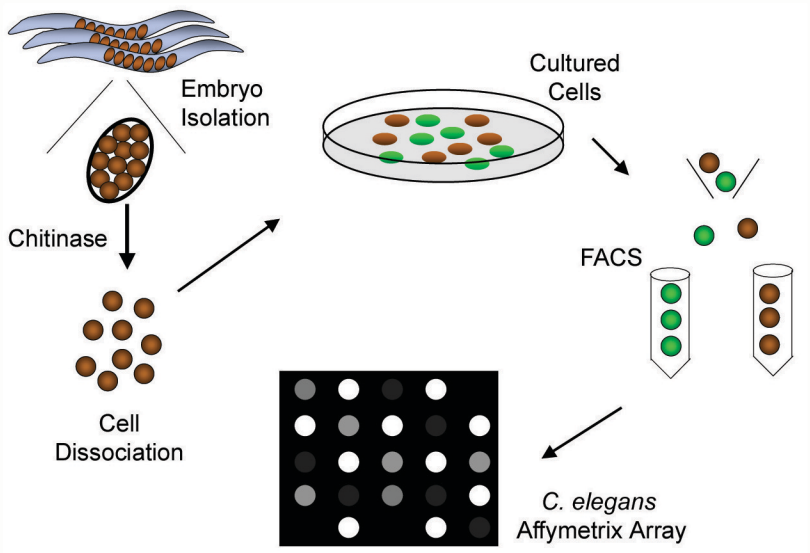

Figure 2.2. MAPCeL strategy for profiling *C. elegans* GFP neurons. Embryos are isolated from gravid adults and treated with chitinase to degrade the egg shell. Embryonic cells are cultured for 24 hours and enriched by FACS. Amplified, labeled aRNA is hybridized to the Affymetrix *C. elegans* array.

Sorting *unc-4*::GFP neurons using FACS

It is necessary to plate freshly dissociated embryonic cells on a solid substrate to promote differentiation and to prevent clumping. Although *C. elegans* neurons show extensive morphological differentiation on peanut lectin-coated glass they also adhere avidly and cannot be easily removed. We found that cells plated on poly-L-lysine coated surfaces also differentiate but can be readily dissociated from the substrate by gentle trituration. A fluorescence profile was established for cells from the non-GFP wildtype strain (N2) to identify autofluorescent intestinal cells. Because these cells autofluoresce in both the Propidium Iodide (PI) and GFP channels, they are largely restricted to the diagonal axis of this scatter plot. PI was added immediately prior to sorting to stain damaged cells (~20%). Separate experiments with PI-stained wildtype cells and with cells from *unc-4*::GFP embryos were used to establish sorting gates for PI and GFP labeled cells, respectively. As shown in Figure 2.3, viable *unc-4*::GFP neurons were simultaneously gated by light scattering parameters. This gate was established empirically to achieve ~90% enrichment of *unc-4*::GFP-labeled cells. Typically, I was able to obtain about 40,000 *unc-4*::GFP neurons from each sort.

Microarray experiments yield reproducible profiles

Data obtained from successive hybridizations of two separate arrays with the same labeled probe yielded a coefficient of determination, $R^2 = 0.99$. This result indicates that potential differences between individual Affymetrix arrays or hybridization and scanning procedures are not significant sources of error. The overall concurrence of the experimental (*unc-4*::GFP motor neurons) and Reference data is illustrated graphically in

the scatter plots shown in panels A and B of Figure 2.4. To assess the reproducibility of sample preparation methods (e.g. FACS isolation, RNA extraction, amplification, labeling, etc.), R^2 was calculated for each pairwise combination of independent samples. An average R^2 of 0.96 (n =4) was calculated for the wildtype (N2) reference samples; average R^2 was 0.92 (n =3) for the *unc-4*::GFP motor neuron data set. These values are indicative of highly similar samples and thereby show that our methods are reliable.

Detecting Expressed Genes (EGs)

We adopted specific criteria to identify transcripts in the *unc-4*::GFP MAPCeL profile that are expressed at some level in these cells. To identify this group of transcripts we started with the list of genes that had been identified as "Present" (see Materials and Methods, above) in the majority (2/3) of *unc-4*::GFP datasets by the Affymetrix MAS 5.0 software. This list was adjusted in two ways to arrive at a more accurate representation of Expressed Genes (EGs). In the first instance, transcripts that were statistically downregulated in *unc-4*::GFP motor neurons relative to the wildtype reference were removed from the "present" list as these are likely to be detected because they are actually highly enriched in contaminating the non-GFP cells (~10%). Conversely, we included transcripts that were considered enriched according to our statistical methods but originally scored as "absent" on the basis of PM vs MM signals used by Affymetrix MAS 5.0 software (see Methods). This second adjustment simply acknowledges that enriched transcripts are clearly expressed and therefore should be scored as "present." We refer to the transcripts in these modified lists as EGs (Expressed Genes). A total of 9,103 EGs were detected in the Reference data set and 6,217 EGs in the *unc-4*::GFP

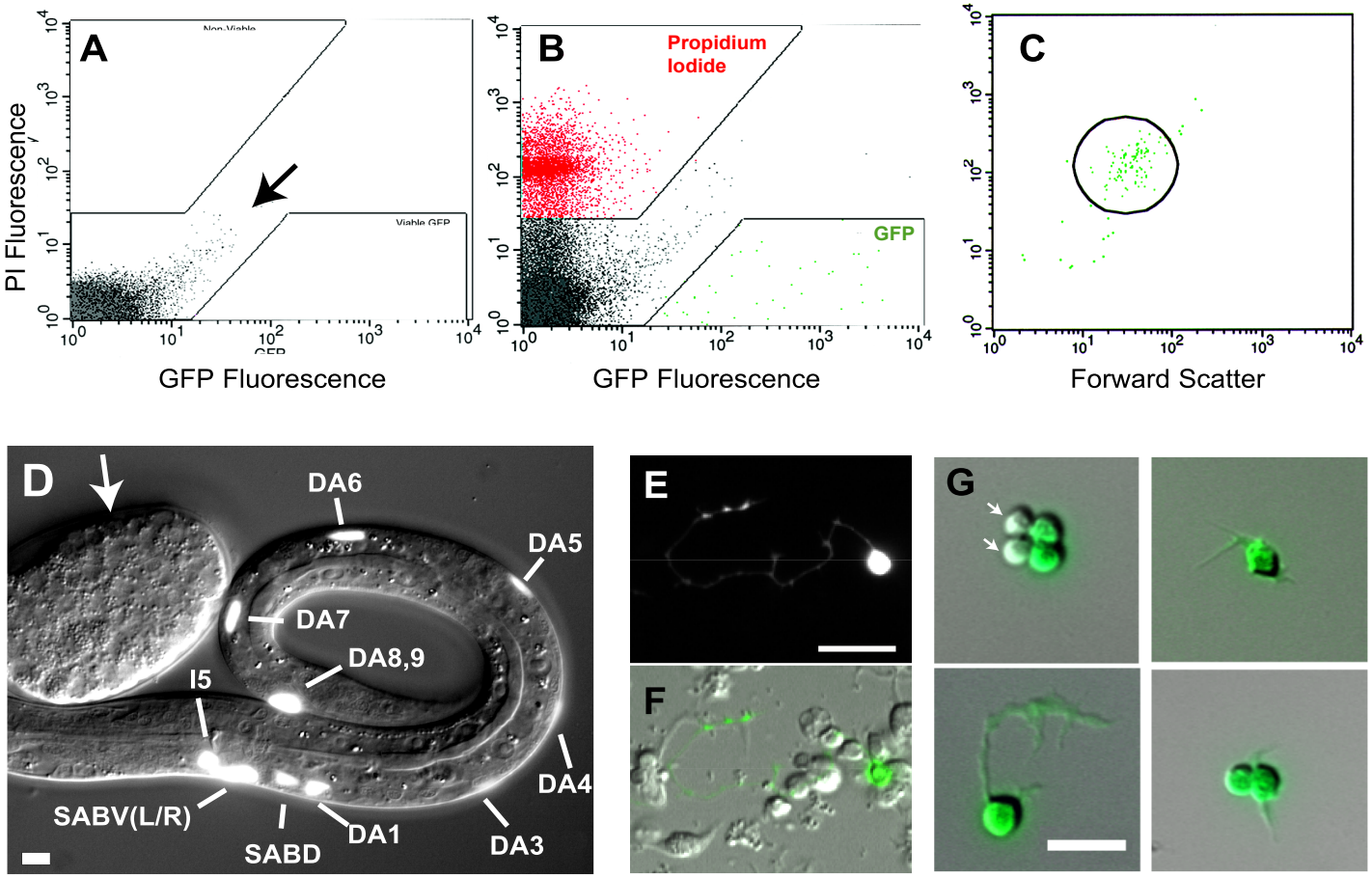

Figure 2.3. Isolation of *unc-4*::GFP neurons by FACS. A. Fluorescence intensity profile of wildtype (non-GFP) cells. Boxed areas exclude autofluroescent cells (arrow). B. *unc-4*::GFP cells are gated to exclude propidium iodide-stained (non-viable) cells. C. Light scattering gate for GFP-positive cells (circle) to exclude cell clumps and debris. D. Combined fluorescence and DIC image of *unc-4*::GFP labeled motor neurons in L1 larva. (DA2 is not visible here). Arrow points to embryo at stage (<400 minutes) prior to *unc-4*::GFP expression. E,F. Fluorescence and DIC images of 24 hr culture from *unc-4*::GFP embryos. G. *unc-4*::GFP neurons after enrichment by FACS. Arrows point to rare (~10%) non-GFP cells. Scale bars represent 5 µm.

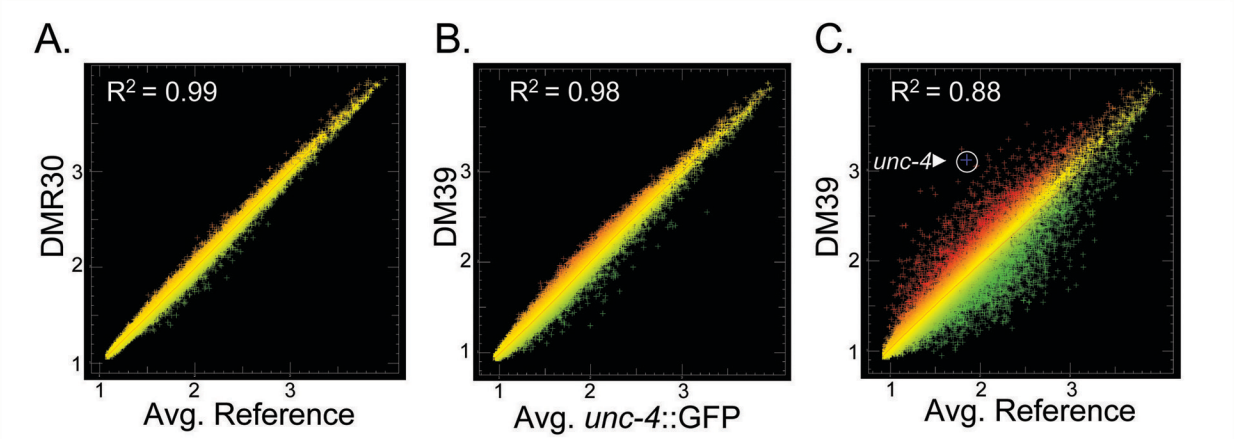

D. *unc-4*::GFP hybridizations

Chip	DM39	DM51	DM59
DM39	-	0.90	0.95
DM51	-	-	0.90

E. Reference hybridizations

Chip	DMR 28	DMR 30	DMR 32	DMR 34
DMR 28	-	0.96	0.95	0.95
DMR 30	-	-	0.97	0.97
DMR 32	-	-	-	0.94

Figure 2.4. Coefficients of Determination (R^2) for individual hybridizations. A. Scatter plot of normalized intensity values (log base 2) for representative hybridization (DMR30) from all cells (Reference) compared to average intensity of 4 Reference hybridizations. B. Scatter plot of representative *unc-4*::GFP hybridization (DM39) compared to the average intensities for all three *unc-4*::GFP hybridizations. C. Results of single *unc-4*::GFP hybridization (DM39) (red) compared to average Reference intensities (green) to identify transcripts showing differential expression. The *unc-4* transcript (arrowhead) is highly enriched (~13x) in *unc-4*::GFP neurons. D. R^2 values for all pairwise combinations of *unc-4*::GFP hybridizations. E. R^2 values for all pairwise combinations of Reference (i.e. all cells) hybridizations.

motor neuron data set. Overall 10,071 unique transcripts were detected in these experiments or about 50% of all predicted *C. elegans* ORFs (Vaglio, Lamesch et al. 2003). These results are comparable to microarray data from whole embryos that also detected about half of the predicted *C. elegans* genes (Baugh, Hill et al. 2003). Genes that are not detected may be expressed in a relatively small number of cells. This point is substantiated by our finding that 968 EGs in the *unc-4*::GFP motor neuron data set are not scored as "present" in the Reference data set. For example, the transcription factor UNC-3 is normally expressed in a small subset of embryonic neurons including the DAs (Prasad, Ye et al. 1998). The *unc-3* transcript is enriched in the *unc-4*::GFP motor neuron data set but is not detected in the Reference.

Microarray experiments identify *unc-4*::GFP enriched genes

The "*unc-4*::GFP motor neuron" dataset was generated from RNA that was pooled from the equivalent of 100,000 *unc-4*::GFP neurons. Separate pools of RNA were used for each microarray experiment. Three independent microarray experiments were performed with *unc-4*::GFP RNA. For the "Reference" data set, RNA was extracted from all embryonic cells. Dr. Susan Barlow generated four independent Reference microarray datasets (details in methods).

A scatter plot that compared the transcript levels from the *unc-4*::GFP motor neurons, and the Reference dataset (R^2=0.88) indicated that there are a subset of genes that are differentially expressed in *unc-4*::GFP neurons (Figure 2.4). To identify the list of transcripts that are significantly elevated in *unc-4*::GFP neurons we used a statistics program, SAM (Stanford), to identify all transcripts that were elevated ≥1.7x in *unc-*

4::GFP neurons when compared to the Reference sample at a False Discovery Rate (FDR) ≤1%. As expected for a gene that is selectively expressed in *unc-4*::GFP neurons, the hybridization signal for the *unc-4* transcript is highly elevated (13x) in comparison to all cells. According to these criteria 1012 genes are enriched in UNC-4 motor neurons, whereas 1596 transcripts are depleted. The threshold of ≥ 1.7x fold was defined empirically. At higher values (e.g. ≥ 2.0x), genes with known expression in these cells were excluded (e.g. *acr-2, unc-5*) (Hedgecock, Culotti et al. 1990; Hallam, Singer et al. 2000), whereas a lower threshold of ≥1.5x included significantly more false positives (e.g. muscle genes, *pat-3, sup-10*) (Hobert, Moerman et al. 1999; de la Cruz, Levin et al. 2003).

Validation of UNC-4 motor neuron genes

Information gleaned from published literature (www.textpresso.org) and from wormbase (www.wormbase.org) identified 27 genes with known expression in embryonic motor neurons that also express *unc-4*::GFP (I5, SAB, DA). We detect 21 (78%) of these genes as EGs, of which 10 (37%) are enriched (Table 2.2). In addition, a significant number of transcripts encoding core neuronal functions (e.g. axon guidance, neurotransmitter signaling, etc.) are detected in the *unc-4*::GFP data set. For example, in addition to UNC-64 (syntaxin or t-SNARE,) other components of the SNARE complex, SNB-1 (synaptobrevin or v-SNARE) and SNAP-25 (Y22F5A.3), are detected (Nonet, Saifee et al. 1998; Weimer and Jorgensen 2003; Weimer, Richmond et al. 2003). We also examined the data set for potential false positives by considering transcripts that are known to be highly expressed in other tissues but not in UNC-4 motor neurons. For

example, in the embryo, the homeodomain protein UNC-30 is exclusively detected in DD motor neurons. Expression of the GABA vesicular transporter, UNC-47, in DD motor neurons depends on *unc-30* function (Eastman, Horvitz et al. 1999). UNC-4 motor neurons are cholinergic and, as expected, neither of these GABA specific transcripts are present in the *unc-4*::GFP motor neuron data set.

The strong representation of ~80% of genes known to be expressed in I5, SAB, and DA motor neurons in the *unc-4*::GFP motor neuron dataset indicates that other previously uncharacterized transcripts in this list are also likely to be expressed in these cells *in vivo*. To test this idea, we evaluated GFP reporter lines for representative genes detected as enriched in the *unc-4*::GFP motor neuron data set (Figure 2.5). As shown in Table 2.3, 82% (15/18) of these promoter-GFP fusions show expression in UNC-4 motor neurons *in vivo*. Of the GFP reporters not detected in these neurons, one of them, T19C4.5, fails to express GFP in any cell. This finding could mean that the upstream sequence selected for this construct does not overlap the endogenous T19C4.5 gene regulatory region. In some cases, cell-specific expression of *C. elegans* genes depends on distal upstream regions, intronic sequences, or 3' domains that would not be included in these 5' promoter GFP fusions (McGhee and Krause 1997). This explanation could also account for the apparent absence of GFP expression in the *unc-4*::GFP motor neurons of the *nlp-9* and *nlp-15* GFP reporters. The validity of this data set is further substantiated by the observation that GFP expression in DA motor neurons is detected even for lower ranking genes (e.g. *syg-1*::GFP, statistical rank = 877). Thus, we believe that the transcripts listed in the *unc-4*::GFP motor neuron data set are likely to constitute an accurate representation of genes normally expressed in these cells.

Table 2.3. Expression of promoter::GFP reporters for transcripts enriched in unc-4::GFP motor neuron dataset					
Rank	**Cosmid**	**Gene**	**Protein**	**UNC-4 neuron**	**Other cells**
15	F33D4.3	*flp-13*	Neuropeptide	I5	ASE, ASG, ASK, BAG, DD, M3, M5, head neurons(Kim and Li 2004)
17	C11D2.6	*nca-1*	Ca++ channel	DA	DB, VA, VB, head/tail neurons
56	F09C3.2		Phosphatase	DA	VA, VB, VD, DB, intestine, hypodermis
98	T19C4.5		Novel		No GFP
161	T23D8.2	*tsp-7*	Tetraspanin	DA	All VNC motor neurons, head/tail neurons, touch neurons
165	CC4.2	*nlp-15*	Neuropeptide		DD, head/tail neurons, body muscles, pharyngeal muscle(Li, Kim et al. 1999)
210	F29G6.2		Novel	DA	DB, touch neurons, pharyngeal neurons, head neurons
215	F39G3.8	*tig-2*	TGF-β	DA	VA, VB, DB, body wall muscle, touch neurons, pharyngeal muscle
233	F55C12.4		Novel	DA	VB, DB, DD, AS, VD
234	E03D2.2	*nlp-9*	Neuropeptide		VA, intestine, head neurons(Li, Kim et al. 1999)
239	ZC21.2	*trp-1*	Ca++ channel	DA	DB, VA, VB
254	Y47D3B.2A	*nlp-21*	Neuropeptide	DA	DB, VA, VB, AS, body muscle, head neurons, intestine(Kim and Li 2004)
329	F36A2.4	*twk-30*	K+ channel	DA	All VNC motor neurons(Salkoff, Butler et al. 2001)
377	C18H9.7	*rpy-1*	Rapsyn	DA	VD, AS, VB, DB, body muscle
593	F43C9.4a	*mig-13*	CUB domain	DA	DB, ant. VNC motor neurons, pharyngeal/intestinal valves, hypodermis(Sym, Robinson et al. 1999)
782	T05C12.2	*acr-14*	NAChR	DA	VB, AS, DB, DD, HSN, VC4 & 5, AIY, head neurons, muscles, intestine
788	T27A1.6	*mab-9*	Transcription factor	DA	DD, DB, VD, AS
877	K02E10.8	*syg-1*	Ig domain	DA	VA, HSN, and other neurons

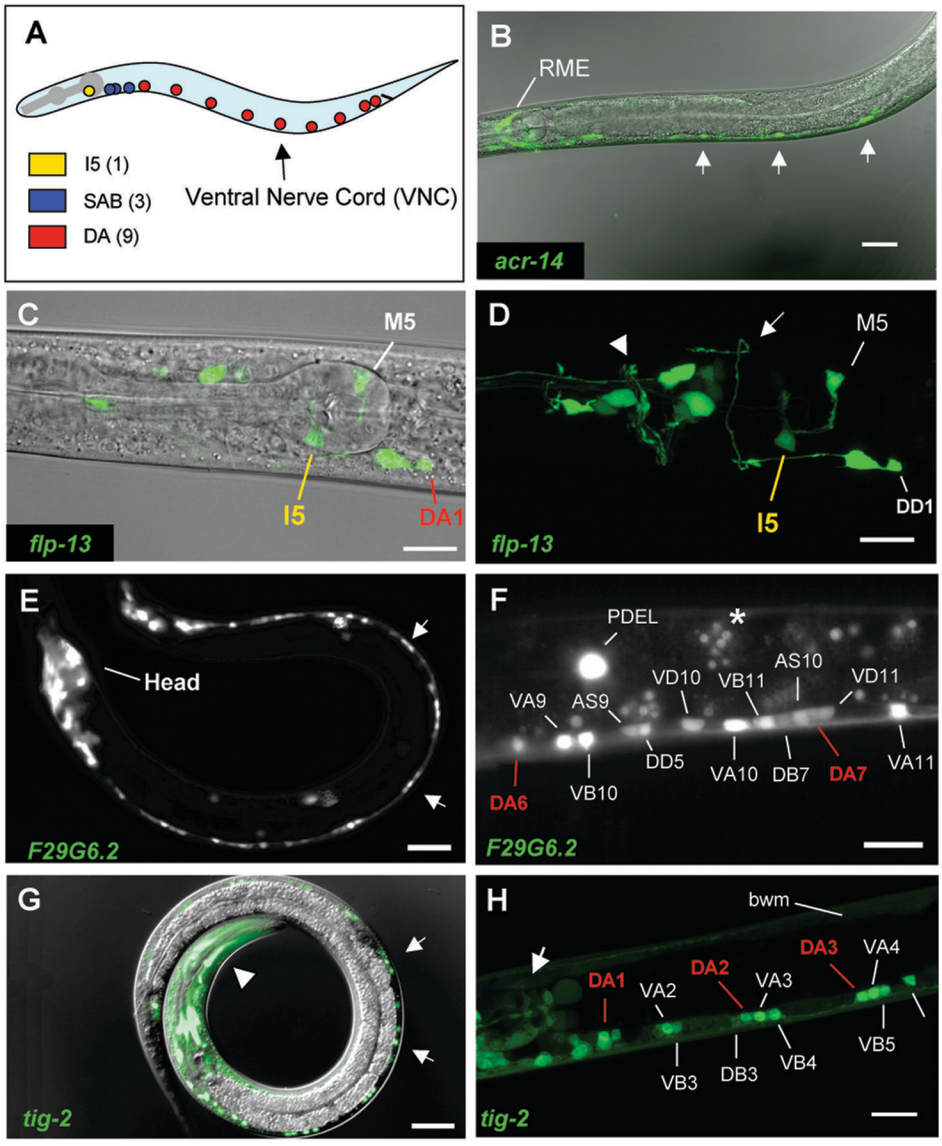

Figure 2.5. GFP reporters validate UNC-4 motor neuron genes. A. *unc-4*::GFP is expressed in 13 embryonically-derived motor neurons. Colored circles indicate approximate location of UNC-4 motor neuron soma in newly hatched L1 larva. Transgenic animals expressing GFP reporters for representative UNC-4 motor neuron genes. Anterior to left. B. *acr-14*. Confocal GFP/DIC projection. *acr-14*::GFP is expressed in RME in the head and in ventral nerve cord (VNC)motor neurons (arrows). C,D. *flp-13*. Confocal DIC/GFP image of head region (C) and matched confocal GFP projection (D). Note DD1 commissure to dorsal side (white arrow). Arrowhead marks nerve ring. E, F. F29G6.2. Arrows point to VNC motor neurons (L2 larva) (E). Posterior view of VNC showing F29G6.2::GFP expression in all VNC motor neurons. Asterisk marks gut auto-fluorescence (F). G, H. *tig-2*. DIC/GFP image of L2 larva. Note GFP expression in VNC motor neurons (arrows) and in head muscles (arrowhead) (G). Confocal projection of anterior VNC. *tig-2*::GFP is detected in A and B class motor neurons, pharyngeal muscle (arrow) and body wall muscle (bwm) (H). Scale bars are 10 microns in panels C, D, F, H and 20 microns in B, E, G.

Families of neuronal genes expressed in UNC-4 motor neurons.

Here we describe transcripts detected in the *unc-4*::GFP dataset with an emphasis on genes that are enriched in these cells and are therefore likely to encode proteins with important roles in the differentiation or function of UNC-4 motor neurons. Gene names for enriched transcripts discussed below are in bold.

Axon guidance and outgrowth

Growth cone steering and cell migration along the dorsal-ventral body axis in *C. elegans* depend on the **UNC-6/netrin** guidance cue. The **UNC-40/DCC** receptor mediates an attractive response to **UNC-6/netrin** whereas co-expression of **UNC-40/DCC** with a second **UNC-6** receptor, **UNC-5**, results in repulsion (Hedgecock, Culotti et al. 1990; Araujo and Tear 2003). The **UNC-6/netrin** signal is released from ventral ectoderm (Wadsworth, Bhatt et al. 1995) to repel growth cones expressing both **UNC-40** and **UNC-5**; this interaction is required for normal outgrowth of DA motor neuron commissures to the dorsal nerve cord (Hedgecock, Culotti et al. 1990). As expected, ***unc-5*** and ***unc-40*** transcripts are enriched in UNC-4 motor neurons. ***unc-6,*** which is known to be expressed in the I5 pharyngeal neuron, is also elevated (Wadsworth, Bhatt et al. 1995). The **CLR-1** receptor protein tyrosine phosphatase (RPTP) is proposed to inhibit attractive **UNC-6/netrin** responses via interactions with **UNC-40**. In the DA motor neurons, **CLR-1** also promotes **UNC-6/netrin** repulsion by an **UNC-40**-independent mechanism (Chang, Yu et al. 2004). As predicted by these models, the ***clr-1*** transcript is elevated in UNC-4 motor neurons. Relevant to this point, we note that the *C. elegans* Abelson tyrosine kinase ortholog, ***abl-1***, is also enriched in UNC-4 motor neurons. In Drosophila,

Abl tyrosine kinase antagonizes the axon guidance role of RPTPs in motor neurons (Wills, Bateman et al. 1999). It will be interesting to determine if **ABL-1** functions similarly in *C. elegans* and, in this case, if **ABL-1** works in opposition to **CLR-1** during DA motor axon outgrowth (Figure 2.6). We also detected axon guidance effectors ***unc-115*** and *ced-10* in our microarray array dataset. Genetic approaches have shown that ***unc-115*** (AbLIM, actin binding protein) and *ced-10* (Rac GTPase) are downstream effectors of **UNC-40** signaling and presumptive links to the cytoskeleton (Gitai, Yu et al. 2003; Struckhoff and Lundquist 2003).

Transcripts for genes with general roles in axon outgrowth are enriched in the *unc-4*::GFP motor neuron data set. These include ***unc-44*** (ankyrin-like), ***unc-76*** (novel) and ***unc-14*** (RUN domain). All three of these genes are highly expressed in the *C. elegans* nervous system. ***unc-44*** encodes multiple alternatively spliced transcripts with broad roles in axonal morphogenesis (Otsuka, Boontrakulpoontawee et al. 2002). **UNC-76** and its vertebrate homologs define a new protein class of unknown biochemical function. In *C. elegans*, ***unc-76*** mutants show axon outgrowth and fasciculation defects (Bloom and Horvitz 1997). ***unc-14*** and *unc-51* (serine/threonine kinase) mutants display similar neuronal defects with misplaced processes and enlarged abnormal varicosities (McIntire, Garriga et al. 1992). UNC-51 (EG) has been proposed to phosphorylate **UNC-14** to regulate vesicular trafficking during axonal process outgrowth (Ogura, Shirakawa et al. 1997; Lai and Garriga 2004).

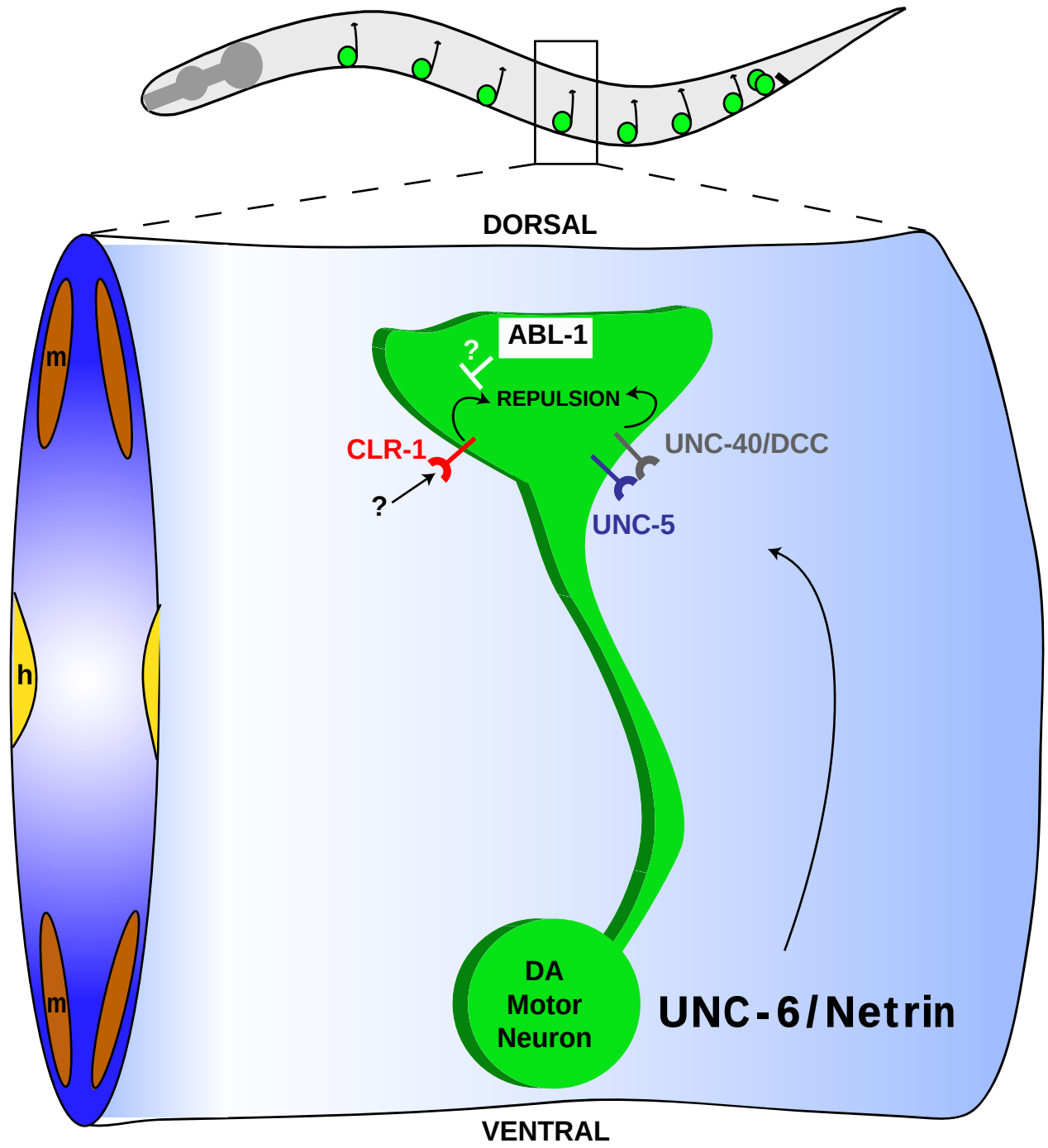

Figure 2.6. Model of DA motor neuron axon guidance. Ventrally derived UNC-6/Netrin guidance cues bind to the UNC-40/DCC and UNC-5 receptor to steer the DA motor axon toward the dorsal nerve cord. The receptor tyrosine phosphatase, CLR-1, promotes dorsal axon outgrowth via an UNC-40/DCC independent pathway (Chang, Yu et al., 2004). The transcript encoding the *C. elegans* ortholog of Abelson tyrosine kinase (ABL-1) is enriched in the *unc-4*::GFP motor neuron dataset and is proposed to antagonize CLR-1 activity.

Wingless signaling

Wingless (Wnt) signaling controls multiple developmental processes in the nervous system ranging from cell determination to axon guidance and synaptogenesis (Yoshikawa, McKinnon et al. 2003; Hirabayashi, Itoh et al. 2004). The *C. elegans* genome contains 5 Wnt genes and 4 Wnt receptors or Frizzled homologs (Korswagen 2002). One of each, ***cwn-1*** (Wnt) and ***lin-17*** (Frizzled), is enriched. Transcripts for other components of the canonical (*mig-5, mom-5, cwn-2, dsh-1, dsh-2, Y73B6BL.21*) and noncanonical (*lit-1, mom-4, par-1, tap-1*) Wnt signaling pathways are detected as EGs. Thus, UNC-4 motor neurons are presumptively competent to send as well as respond to Wnt signals. Functions for Wnt signaling in the *C. elegans* motor neuron circuit have not been defined. Possibilities include the regulation of synaptogenesis as suggested by studies of Drosophila motor neurons, which secrete Wnt to control both presynaptic and postsynaptic differentiation at the neuromuscular synapse (Packard, Koo et al. 2002). A gradient of Wnt signaling controls cell migration along the A/P axis in *C. elegans* (Whangbo and Kenyon 1999). Responsiveness to this graded Wnt signal could account for the anterior polarity of DA motor neurons in the dorsal nerve cord as suggested by the recent finding that commissural axonal polarity along the A/P axis in the vertebrate spinal cord is dependent on Wnt signaling (Lyuksyutova, Lu et al. 2003).

Nicotinic Acetylcholine Receptors (nAChRs)

The *C. elegans* genome encodes at least 27 distinct nAChR subunits (Jones and Sattelle 2004). Two of these, **ACR-2** and **UNC-63** are expressed in DA class motor neurons (Hallam, Singer et al. 2000; Culetto, Baylis et al. 2004) and are enriched in the

unc-4::GFP motor neuron data set. Expression of *unc-29* (Fleming, Squire et al. 1997) and *unc-38* (J.L. Bessereau, personal communication) in ventral cord motor neurons has been previously reported and these are also detected as EGs. *acr-12*::GFP is expressed in neurons (Gottschalk, Almedom et al. 2005), and we have validated the enrichment of ***acr-14*** with GFP reporters that confirm expression in DA motor neurons. In body muscle, **UNC-63** is an essential component of a levamisole-sensitive nACh receptor that also includes UNC-29, UNC-38, LEV-1 and LEV-8 (Culetto, Baylis et al. 2004; Towers, Edwards et al. 2005). **ACR-12** may coassemble with **UNC-63**, UNC-29, and UNC-38 to generate a related nACh receptor in UNC-4 motor neurons (Gottschalk, Almedom et al. 2005). Five additional sets of nAChR subunits are detected as EGs and a so-called "orphan" ligand-gated ion channel (LGIC) subunit, **F21A3.7**, with significant similarity to the nAChR gene family, is enriched. Despite the diversity of nAChR subunits expressed in UNC-4 motor neurons and the potentially complex array of resultant receptors, no functions have been directly assigned to nAChRs in these cells (Schafer 2002). Although loss-of-function mutations in nAChR subunits that are also expressed in muscle (i.e. *unc-29*, *unc-38*, ***unc-63***) result in locomotory defects, gene knockouts of ***acr-2*** (Y. Jin, personal communication) and ***acr-12*** (data not shown), which are exclusively expressed in neurons, do not produce obvious effects on motility or behavior. Perhaps the surprisingly large number (12) of nAChR subunit genes detected in these cells results redundancy masking defects in single gene knockout mutants. Alternatively, these nAChRs may mediate subtle aspects of motor neuron activity. This idea is consistent with models in which nAChRs act presynaptically to modulate neurotransmitter release (Jones, Sudweeks et al. 1999; Kim, Poole et al. 2001). Finally, we detect enrichment of

transcripts for proteins **RIC-3** (novel) and **LEV-10** (CUB domain) that mediate nAChR localization (Halevi, Yassin et al. 2003; Gally, Eimer et al. 2004).

Ligand-Gated Ion Channels

UNC-4 motor neurons are potentially responsive to additional classes of neurotransmitters. Enrichment of ***glr-5*** (kainate type ionotropic glutamate receptor subunit) correlates with its known expression in the SAB motor neurons (Brockie, Madsen et al. 2001). As members of the GABA/Glycine family of ligand-gated receptors, the presumptive anion channels encoded by **T27E9.9** and **Y71D11A.5** are predicted to hyperpolarize UNC-4 motor neurons and thus inhibit cholinergic activity (Lynch 2004). It may be significant that a candidate sodium/chloride-dependent glycine transporter, ***snf-5***, is enriched. (**C09E8.1**, an outlier in the sodium/chloride-dependent transporter family is also enriched.) In mammalian cells, the plasma membrane transporters GLYT1/GLYT2 remove glycine from the synaptic cleft, and in the case of GLYT2, thereby recycle glycine for reuptake into synaptic vesicles (Gomeza, Ohno et al. 2003). UNC-4 motor neurons, however, do not express the GABA/Glycine vesicular transporter, UNC-47, and are therefore, unlikely to release glycine presynaptically (McIntire, Reimer et al. 1997). In this case, the physiological function of the **SNF-5** transporter could mirror that of GLYT1, which is believed to attenuate glycinergic signaling by pumping glycine into a non-glycinergic glial cell (Gomeza, Hulsmann et al. 2003). To date, the potential function of glycinergic signaling in *C. elegans* has not been explored.

G-protein signaling

Cholinergic motor neuron activity in *C. elegans* is modulated by G-protein signaling pathways that respond to the neurotransmitters acetylcholine, serotonin (5-HT), and dopamine (Figure 2.7) (Miller, Emerson et al. 1999; Nurrish, Segalat et al. 1999; Chase, Pepper et al. 2004). In each case, acetylcholine release is either promoted by **EGL-30** ($G\alpha_q$) or inhibited by GOA-1 ($G\alpha_o$). Input to these antagonistic pathways is provided by G-protein coupled receptors (GPCRs). Pharmacological evidence suggests that a muscarinic acetylcholine receptor activates **EGL-30** to enhance ACh release at the neuromuscular synapse (Lackner, Nurrish et al. 1999; Miller, Emerson et al. 1999). The enriched muscarinic AChRs, **GAR-2** and **GAR-3** could account for this effect (Steger and Avery 2004). Similarly, the enriched 5-HT receptor, **SER-4**, is a strong candidate for the GPCR mediating the inhibitory effect of serotonin on ACh release from ventral cord motor neurons (Nurrish, Segalat et al. 1999). Dopamine may either activate or inhibit ACh release within the same cholinergic motor neuron. Activation depends on **DOP-1,** which is enriched in UNC-4 motor neurons. Inhibition is attributed to DOP-3. Expression of DOP-3 in cholinergic ventral cord motor neurons is reportedly weak and we do not detect the *dop-3* transcript in our data set (Chase and Koelle 2004; Chase, Pepper et al. 2004). UNC-4 motor neurons are also potentially responsive to GABA as we detect enrichment of a transcript (**Y41G9A.4**) encoding a metabotropic GABA type B1 receptor. GABA-dependent effects on cholinergic motor neuron activity have not been previously reported in *C. elegans*.

Genetic screens for mutations affecting neurotransmitter release have revealed a complex web of interacting components that couple G-protein signaling to synaptic

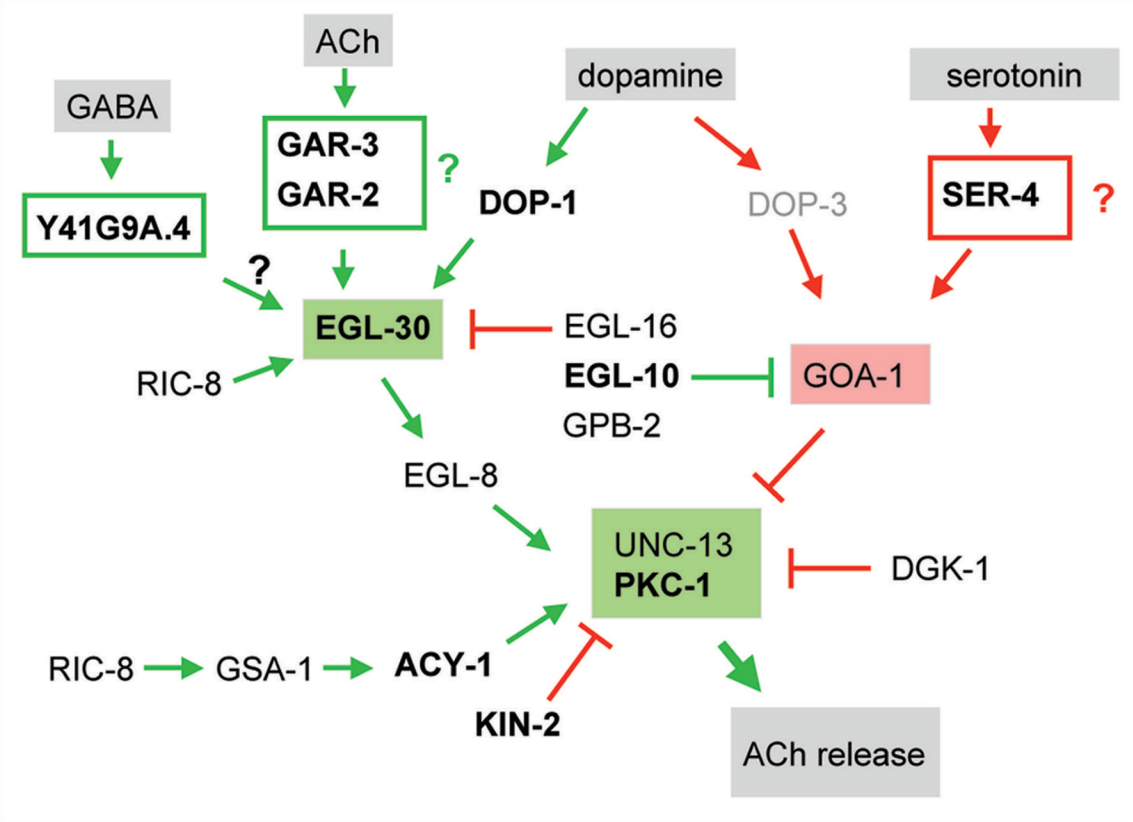

Figure 2.7. G-protein signaling pathways regulating neurotransmitter release in cholinergic motor neurons. Components shown in bold are enriched in the *unc-4*::GFP motor neuron data set. All others are EGs with the exception of the *dop-3* transcript which is not detected (light gray text). Green denotes interactions that promote acetylcholine (ACh) release and red marks the steps that inhibit synaptic vesicle fusion. Neurotransmitters are highlighted in gray boxes. This figure adapted from Reynolds, Schade, et al.,2004.

vesicle fusion (Lackner, Nurrish et al. 1999; Miller, Emerson et al. 1999; Reynolds, Schade et al. 2004; Schade, Reynolds et al. 2004) (D. Sieburth and J. Kaplan, personal communication). With the exception of *dop-3*, transcripts for all of the known components of these pathways are either enriched (***acy-1, egl-10, gpc-2, kin-2, pkc-1***) or detected as EGs (*dgk-1, egl-8, egl-16, gpb-2, gsa-1, kin-2, ric-8, unc-13)*. Lack of enrichment of some of these components is consistent with the widespread utilization of G-protein signaling pathways in *C. elegans* neurons and muscle cells (Jansen, Thijssen et al. 1999; Wilkie 1999). As noted above, these data have also revealed several additional enriched transcripts with potential roles in G-protein-dependent locomotory behavior. ***egl-47*** encodes an orphan GPCR and ***rgs-1*** an RGS protein, both of which can regulate *goa-1* signaling in the egg laying circuit (Dong, Chase et al. 2000; Moresco and Koelle 2004). RNAi of **F39B2.8**, which encodes a highly conserved but unusual protein with both serine/threonine kinase and 7-transmembrane domains, results in a locomotory defect (Keating, Kriek et al. 2003) that could be indicative of a neuromodulatory function in DA motor neurons.

Neuropeptide Signaling

The *C. elegans* genome includes a large and diverse array of genes encoding potential neuroactive peptides. GFP reporter studies indicate that these genes are predominantly expressed in neurons. Twenty-three "flp" genes encoding FMRFamide and related peptides (FaRPs) have been described. FaRPs have been shown to modulate a wide array of invertebrate neural functions (Li, Kim et al. 1999). Previously reported expression of ***flp-2, flp-4,*** and ***flp-13*** in the pharyngeal I5 neuron (Kim and Li 2004) is

confirmed by their enrichment in the *unc-4*::GFP motor neuron data set. ***flp-5*** is also elevated in these cells and 8 additional flps are detected as EGs. Specific FaRPs modulate cell excitability (***flp-13***), locomotion (*flp-1*) and feeding behavior (*flp-21*) in *C. elegans* (Nelson, Rosoff et al. 1998; Rogers, Reale et al. 2003). The inhibitory action of the **FLP-13** peptide on pharyngeal muscle activity is consistent with its expression in I5 (Rogers, Franks et al. 2001).

The *C. elegans* genome contains 37 genes encoding predicted insulin-like peptides (Pierce, Costa et al. 2001). Transcripts for two of these, ***ins-1*** and ***ins-18***, are enriched in UNC-4 motor neurons; *ins-17*, *ins-24* and *ins-30* are present but not significantly elevated relative to other cells. ***ins-1*** and ***ins-18*** have been implicated in the DAF-2 insulin receptor dependent pathways regulating growth, metabolism and lifespan (Pierce, Costa et al. 2001).

A total of 32 genes encoding other potential classes of neuropeptides have also been identified in the *C. elegans* genome. Three of these neuropeptide-like protein (nlp) genes, ***nlp-9***, ***nlp-15***, and ***nlp-21***, are enriched in UNC-4 motor neurons. An additional group of 11 nlp transcripts are detected as EGs. To date, no functions have been directly assigned to nlp genes in *C. elegans* (Nathoo, Moeller et al. 2001).

Our studies have revealed that a surprisingly large number of neuropeptide genes are transcribed in UNC-4 motor neurons. These results indicate that UNC-4 motor neurons are likely to exhibit significant neurosecretory activity. This conclusion is consistent with our finding that proteases required for neuropeptide processing and activation, **T03D8.3 (**Proprotein convertase (PC) 2 chaperone), *egl-3* (zinc carboxypeptidase) and *egl-21* (subtilisin-like proprotein convertase)] are also expressed

in these cells (Kass, Jacob et al. 2001; Jacob and Kaplan 2003; Zahn, Angleson et al. 2004). Other genes with important roles in neurosecretion are also detected. ***ric-19*** encodes a novel arfaptin-related protein that is believed to function in the Golgi in the generation of neurosecretory granules and may, through this activity and subsequent neuropeptide signaling, exert an indirect effect on ACh release from conventional synaptic vesicles (Pilon, Peng et al. 2000; Spitzenberger, Pietropaolo et al. 2003). Our finding that ***ric-19*** is highly enriched in cholinergic motor neurons could be indicative of autocrine neuropeptide modulation of ACh secretion at the neuromuscular synapse. Consistent with this idea is our finding that *ida-1*, a conserved membrane component of the dense core vesicles in which neuropeptides are typically packaged, is an EG (Cai, Fukushige et al. 2004). Finally, **UNC-31** (CAPS), a known facilitator of dense core vesicular release, is enriched (Cai, Fukushige et al. 2004). Plasma membrane fusion of both dense core vesicles and the small, clear vesicles in which classical neurotransmitters are packaged depend on a common set of calcium-activated components (Richmond and Broadie 2002), most of which are either enriched or present in these cells.

In addition to secreting neuropeptides, UNC-4 motor neurons are also likely to respond to neuropeptide signaling. Transcripts for nine putative neuropeptide receptors are enriched. RNAi of two of these, ***npr-2*** and **F59D12.1**, results in locomotory defects that could be indicative of specific functions in DA motor neurons (Keating, Kriek et al. 2003). ***npr-2*** is a close relative of *npr-1* (not detected) which has been shown to control social feeding behavior in response to the FLP-21 (not detected) peptide (Rogers, Reale et al. 2003). **F59D12.1** is most closely related to melatonin receptors but its *in vivo* ligand is unknown**.** Neuropeptides are believed to modulate secretion of classical

neurotransmitters (Richmond and Broadie 2002). Neuropeptide-specific effects on excitatory motor neuron activity in the *Ascaris* ventral nerve cord have been reported (Davis and Stretton 2001). Genetic evidence in *C. elegans* indicates that acetylcholine release at the neuromuscular junction is enhanced by neuropeptide activity (Jacob and Kaplan 2003) and that this pathway depends on the EGL-30 $G_q\alpha$ protein (Nelson, Rosoff et al. 1998). These neuropeptides may be released from neurons and also as a retrograde signal from muscle cells (Doi and Iwasaki 2002; Jacob and Kaplan 2003).

Transcription factors

In the embryo, the **UNC-4** transcription factor is exclusively expressed in I5, SAB and DA motor neurons (Miller and Niemeyer 1995). It is therefore not surprising that ***unc-4*** is one of the most highly enriched transcripts in our data set. **UNC-4** and its homologs in other species are members of the Prd-like class of homeodomain proteins and are likely to function as transcriptional repressors (Miller, Shen et al. 1992; Winnier, Meir et al. 1999). In *C. elegans*, **UNC-4** physically interacts with UNC-37, a Groucho-like transcriptional co-repressor protein (Pflugrad, Meir et al. 1997; Winnier, Meir et al. 1999). The ubiquitous expression of UNC-37 *in vivo* is consistent with our finding that the *unc-37* transcript is an EG but is not enriched in the *unc-4*::GFP motor neuron data set. **UNC-4** activity is required for normal SAB axonal outgrowth and for maintaining wildtype levels of neurotransmitter vesicles in SAB and DA motor neurons (Lickteig, Duerr et al. 2001). Downstream **UNC-4** targets that regulate these events are unknown.

A member of the highly conserved OLF-1/EBF family of transcription factors, **UNC-3** is expressed in a subset of cholinergic ventral cord motor neurons including the

DAs and in the ASI sensory neuron. ***unc-3*** mutants show defects in motor neuron axon outgrowth and in ASI function (Prasad, Ye et al. 1998). These data are consistent with the elevated level of ***unc-3*** transcript in the *unc-4*::GFP motor neuron data set. Vertebrate OLF-1/EBF proteins also control neuronal differentiation and axonal morphology in the CNS (Garel, Marin et al. 1997).

MAB-9 is a member of the T-box family of transcription factors (Pocock, Ahringer et al. 2004). Of the 20 T-box transcription factor genes in the *C. elegans* genome, only ***mab-9*** is enriched in UNC-4 motor neurons. We used a ***mab-9***::GFP reporter to confirm expression in DA motor neurons. **MAB-9** also functions in the GABAergic motor neurons to control axonal outgrowth and morphology (Huang, Cheng et al. 2002) (Pocock and Woollard, Oxford, personal communication). The role of **MAB-9** in motor neuron differentiation may be conserved as the vertebrate homolog, TBX20, is highly expressed in hindbrain and spinal motor neurons (Ahn, Ruvinsky et al. 2000; Kraus, Haenig et al. 2001).

ces-1 encodes a Snail-like transcription factor that functions in the NSM serotonergic motor neurons to block expression of the apoptotic factor, EGL-1 (Thellmann, Hatzold et al. 2003). The most closely related protein in Drosophila, *Scratch*, is widely expressed in neuroblasts whereas the vertebrate homolog is restricted to subsets of postmitotic neurons in the brain and spinal cord (Nakakura, Watkins et al. 2001). A function for **CES-1** in *C. elegans* ventral cord motor neurons has not been previously reported.

The *C. elegans* genome includes 284 genes with significant similarity to nuclear hormone receptors (NRs) (Gissendanner, Crossgrove et al. 2004). Six NR genes (***nhr-3, -***

95, -104, -116*, F41B5.9, C29G2.5**) are enriched in UNC-4 motor neurons. To date, no functions have been assigned to these genes. An additional 43 NRs are present but not enriched in this data set. Among these NRs is *daf-12*, a presumptive steroid hormone receptor gene that is widely expressed in most cells to control dauer formation and adult longevity (Ludewig, Kober-Eisermann et al. 2004). In the vertebrate spinal cord, retinoic acid is a potent inducer of specific neuronal fates (Appel and Eisen 2003). The strong similarity of ***nhr-3 (BLAST = e^{-28}) to the mammalian retinoic acid NR could be indicative of an ancient role for steroid hormone signaling in motor neuron differentiation. Significantly, *fax-1*, *unc-55* and *odr-7* regulate differentiation of specific neurons (i.e. AVK, VD, AWA respectively) (Sengupta, Colbert et al. 1994; Zhou and Walthall 1998; Much, Slade et al. 2000) and are not detected in *unc-4*::GFP motor neurons.

Five additional transcription factor mRNAs with potential functions in UNC-4 motor neuron differentiation are enriched: the GATA factor ***elt-1***, **C27C12.6** [DM (Doublesex-mab-3) Zn finger DNA binding domain]; **B0336.13** [TFIIA, a component of the basal transcription complex]; **F44E2.6** [pillin-like transcription factor]; **T08H4.3** [FLI-1 (Friend Leukemia integration 1 transcription factor) ETS domain]. Functions for these transcription factors in UNC-4 motor neurons have not been described.

Cell Adhesion Molecules

Cell adhesion molecules define the architecture and connectivity of the nervous system. The cadherin and Ig superfamily proteins are of particular interest because of their key roles in axon guidance and synaptic specificity.

The *C. elegans* genome encodes 80 Immunoglobulin (Ig) domain proteins (Hutter, Vogel et al. 2000; Rougon and Hobert 2003; Vogel, Teichmann et al. 2003). Transcripts for five Ig superfamily Cell Adhesion Molecules (IgCAMs), **SYG-1, SAX-7, C33F10.5, C53A5.13** and **RIG-3** are enriched in UNC-4 motor neurons. All of these proteins display extracellular protein interaction domains composed of Ig repeats (**SYG-1, RIG-3**) or tandem arrays of Ig and fibronectin repeats (**SAX-7**, **C33F10.5**, **C53A5.13**). **SYG-1**, **SAX-7** and **C53A5.13** all contain single-pass transmembrane domains while **C33F10.5** and **RIG-3** have consensus GPI attachment sites (Eisenhaber, Bork et al. 2000). Intercellular contact of **SYG-1** with the related Ig domain protein, SYG-2 (not detected), marks the location of a specific synapse in the egg laying circuit (Shen and Bargmann 2003; Shen, Fetter et al. 2004). We have confirmed that ***syg-1***::GFP is expressed in DA motor neurons and speculate that it may specify presynaptic sites in these cells. ***sax-7*** encodes the nematode ortholog of L1CAM/neuroglian, a key mediator of axonal pathfinding and morphology in mammals and in Drosophila (Hall and Bieber 1997; Cohen, Taylor et al. 1998). **SAX-7** is widely expressed and localizes to intercellular contacts during epithelial and gonad morphogenesis in *C. elegans*. **SAX-7** function at these sites may depend on interactions with the ankyrin-like cytoskeletal protein, **UNC-44**, which is also enriched in *unc-4*::GFP motor neurons (Chen, Ong et al. 2001). **SAX-7** may also have a role in maintaining the structure of the *C. elegans* nervous system as the adult nerve ring is disorganized in ***sax-7*** mutants (Zallen, Kirch et al. 1999). In flies and mammals, L1CAM/neuroglian forms a complex with another IgCAM, Contactin, at septate junctions associated with neuron ensheathment sites (Girault and Peles 2002; Faivre-Sarrailh, Banerjee et al. 2004). Although nematode neurons are not insulated, the

contactin-like molecule, **C33F10.5**, is enriched in UNC-4 motor neurons and therefore may have engaged L1CAM/Neuroglian in a primordial function that precedes the evolution of myelination strategies. **RIG-3** is related to klingon, a GPI-anchored protein (Vogel, Teichmann et al. 2003) that mediates homophilic interactions that define fly photoreceptor development (Butler, Ray et al. 1997). Finally, **C53A5.13** shows weak similarity to the L1CAM family and therefore may encode a nematode-specific Ig protein. The selective enrichment of this subset of IgCAMs points to specific roles for these adhesion proteins in cell-cell interactions that govern the differentiation or function of UNC-4 motor neurons.

Cadherins are single pass transmembrane proteins with large ectodomains that mediate Ca^{++} dependent homotypic interactions crucial to tissue morphogenesis (Hill, Broadbent et al. 2001). In the nervous system, cadherins are concentrated at synapses and may facilitate target recognition (Lee, Herman et al. 2001; Yamagata, Sanes et al. 2003). *C. elegans* contains 15 genes encoding proteins with cadherin-like extracellular domains (Hill, Broadbent et al. 2001). The single classical cadherin gene, *hmr-1*, is alternatively spliced to generate two transcripts, *hmr-1a* and *hmr-1b*. HMR-1a is important for epithelial morphogenesis whereas HMR-1b is necessary for axonal pathfinding, especially in D-class motor neurons (Broadbent and Pettitt 2002). *hmr-1* is not enriched, but is detected as an EG. One cadherin transcript, ***cdh-11***, is enriched in UNC-4 neurons and encodes the nematode ortholog of calsyntenin, a postsynaptically localized protein of unknown function that is highly expressed in the mammalian brain (Hintsch, Zurlinden et al. 2002). A role for **CDH-11** in the *C. elegans* nervous system has not been described. Five other cadherin transcripts (*cdh-1,-4, -5, -6, -7*) are EGs.

Transcripts for two muscle proteins, **UNC-22**, a sarcomeric protein with multiple Ig and FN repeats (Benian, Kiff et al. 1989), and **UNC-112**, a muscle cell attachment site component with pleckstrin homology domains (Rogalski, Mullen et al. 2000), and two additional proteins **AJM-1**, a novel coiled-coil constituent of apical junctions in epithelial cells (Koppen, Simske et al. 2001), and **T19D12.6**, a conserved protein with three lamininG domains, are also enriched in this dataset. Functional tests are required to define the potential roles of these genes in UNC-4 motor neurons.

Synapse-Associated Proteins

Genetic approaches in *C. elegans* have identified genes with key roles in synapse formation. In a screen to find GABAergic Synapse Defective (*syd*) genes, Yishi Jin's lab identified ***syd-1*** (rho-GAP activity with PDZ domain) and ***syd-2*** (a-Liprin, LAR interacting protein) (Zhen and Jin 1999; Hallam, Goncharov et al. 2002). Both are enriched in the *unc-4*::GFP dataset. **SYD-1** likely acts through its rho-GAP domain to specify axon identity; **SYD-2** is necessary for active zone formation. In mammals, **SYD-2** homologs interact with LAR (Leukocyte common Antigen-Related protein), a receptor protein-tyrosine phophastase (RPTP) (Serra-Pages, Medley et al. 1998). LAR activity defines the size, number and target projections of basal forebrain cholinergic neurons in the mouse (Van Lieshout et al., 2001). In Drosophila, DLAR is important for axon guidance and target recognition in the visual system (Krueger, Van Vactor et al. 1996; Clandinin, Lee et al. 2001). ***ptp-3*** encodes the *C. elegans* homolog of LAR. ***ptp-3*** is required for epidermal enclosure in the embryo and is also highly expressed in the *C. elegans* nervous system (Harrington, Gutch et al. 2002). The coincident enrichment of

syd-2 and ***ptp-3*** in UNC-4 motor neurons may be indicative of important roles in process outgrowth or target recognition in the motor neuron circuit. A second RPTP (**K07F5.6**) is also enriched but its function is unknown.

RPM-1 (Regulator of Presynaptic Morphology) is a large, highly conserved component of the perisynaptic region adjacent to the active zone. Synaptogenesis and axon outgrowth depend on **RPM-1** E3 ubiquitin ligase activity (Schaefer, Hadwiger et al. 2000; Zhen, Huang et al. 2000; Liao, Hung et al. 2004). **RPM-1** is expressed in all neurons, thus validating its detection in the *unc-4*::GFP motor neuron data set. We also detected enrichment of a nearby gene, **F07B7.12**, that is virtually identical to the ***rpm-1*** coding sequence and appears to have arisen as a recent, partial duplication of the ***rpm-1*** locus; **F07B7.12** lacks the **RPM-1** C-terminal E3 ubiquitin ligase domain and is not present in the *C. briggsae* genome (data not shown). The function of the **F07B7.12** protein is unknown.

Rapsyn (***rpy-1)*** is a post-synaptic component of the NMJ where it functions to cluster acetylcholine receptors (AChRs) (Sanes and Lichtman 1999). Enrichment of the ***rpy-1*** transcript in UNC-4 motor neurons could be related to co-expression of multiple nicotinic acetylcholine receptors (nAChRs) in these cells (see above).

lin-2*, lin-7,* and ***lin-10*** encode PDZ domain components of a protein complex that localizes the LET-23/EGF receptor during vulval development (Whitfield, Benard et al. 1999). An additional role for **LIN-10** in glutamate receptor trafficking has also been discovered (Rongo, Whitfield et al. 1998). Transcripts for two of these proteins are enriched (***lin-2*****,** ***lin-10***) and one is an EG (*lin-7)*, thereby suggesting potential roles in receptor localization in UNC-4 motor neurons.

Neurotransmitter Vesicular Release

Synaptic transmission is triggered by calcium dependent fusion of synaptic vesicles (SVs) with the presynaptic membrane to release neurotransmitters (NTs) into the synaptic cleft. Nascent SVs are generated in the soma for translocation to axonal termini where they are loaded with neurotransmitter. The arrival of an action potential stimulates exocytosis. SVs are regenerated by an endocytic process that recycles the SV membrane for reimportation of NTs in the presynaptic zone (Harris, Schuske et al. 2001). Most of the known constituents of the SV cycle are detected in the *unc-4*::GFP motor neuron data set.

Synaptic Vesicle Trafficking

Synaptic vesicles are transported from cell soma to the axon terminal via motor-dependent mechanisms. The kinesin heavy chains *unc-104* and *unc-116* are required to mediate this process (Hall and Hedgecock 1991; Byrd, Kawasaki et al. 2001) and both are detected as EGs; the kinesin light chain, ***klc-2*** is enriched. Recent reports show that UNC-116 and **KLC-2** form a functional kinesin-1 complex in neurons (Sakamoto, Byrd et al. 2004). UNC-16, Jnk-kinase interacting protein (JIP), has been proposed to interact with **UNC-14** as a molecular tether between kinesin-1 and synaptic vesicles (Byrd, Kawasaki et al. 2001; Sakamoto, Byrd et al. 2004). UNC-16 also interacts with JNK ***(jnk-1***) as well as JNK-kinase (***jkk-1***) indicating that Jun-kinase signaling is critical for trafficking of synaptic proteins. Mutations in all of these components lead to mislocalization of synaptic vesicle components.

Vesicle loading

unc-4::GFP motor neurons are excitatory and release the neurotransmitter acetylcholine. ***unc-17***, the vesicular acetylcholine transporter (VChAT) and the ACh synthetic enzyme, ***cha-1*** (choline acetyltransferase) are co-expressed in all cholinergic neurons (Rand and Nonet 1997). Neurotransmitter loading depends on an electrochemical proton gradient established by the vacuolar ATPase pump and various subunits of this complex (e.g. *unc-32*) (Sudhof 2004) are detected as EGs. Nematode orthologs of SV2 (**ZK637.1**) and SVOP (**Y51A2D.18**), two members of the 12 transmembrane domain transporter superfamily, are enriched. SV2 and SVOP functions are unknown but both are integral synaptic vesicle membrane proteins (Janz, Hofmann et al. 1998; Janz, Goda et al. 1999).

Vesicle exocytosis and neurotransmitter release

SV exocytosis is achieved via a stepwise process of vesicle docking, maturation (priming) and fusion (Weimer and Jorgensen 2003). Transcripts for most of the genes known to encode proteins involved in these events are detected in the *unc-4*::GFP motor neuron data set. Strikingly, Synaptogyrin (***sng-1***), a regulator of exocytosis (Sudhof 2004), is one of the most highly ranked genes. Components of the SNARE complex that mediate SV association with the presynaptic membrane (Richmond and Broadie 2002) are either enriched (**Y22F5A.3, SNAP-25**) or detected as EGs (K02D10.5, SNAP-25-like protein; *snb-1*, Synaptobrevin; *unc-64*, Syntaxin). Genes important for SV fusion, ***unc-18*** (Sec1p family), ***rab-3*** (GTPase associated with SV)**,** and ***unc-10*** (RIM) are enriched

in these cells, while a key regulator of the priming step, *unc-13,* is detectable as an EG. As expected, ***snt-1*** (synaptotagmin), the calcium sensor that triggers NT release, is enriched (Sudhof 2004). Other enriched synaptic transmission genes include the SV protein Synapsin (***snn-1***), and the guanine nucleotide exchange factor for Rab3 (***aex-3***) (Iwasaki, Staunton et al. 1997; Kao, Porton et al. 1999). We note that the piccolo-like protein, **F45E4.3**, a proposed component of the vesicle priming complex that includes UNC-13 and RIM (**UNC-10**) (Takao-Rikitsu, Mochida et al. 2004), is enriched in UNC-4 motor neurons. Another enriched transcript with a potential role in vesicular release, **F54G2.1**, encodes the nematode ortholog of BAP3, an UNC-13-related gene that is highly expressed in the human brain (Shiratsuchi, Oda et al. 1998; Palmer, Lee et al. 2002).

Vesicle Endocytosis

Clathrin-mediated endocytosis is the principle pathway for recycling synaptic vesicle membranes (Harris, Schuske et al. 2001; Richmond and Broadie 2002; Sudhof 2004). In the first step, clathrin adaptor proteins are recruited to the site of endocytosis by synaptic vesicle proteins. These interactions are required for the efficient recovery of both SV lipids and membrane proteins. For example, the AP180 clathrin adaptor protein, **UNC-11**, is specifically required for recycling synaptobrevin (SNB-1) (Nonet, Holgado et al. 1999). Additional components of the clathrin adaptor complexes are either enriched (***apt-2, apt-4***, ***aps-2***) or detected as EGs (*apt-1, apt-6, apt-7*, *dpy-23, tag-11)*. The accessory proteins and lipid modifying enzymes UNC-26 (Synaptojanin) and **UNC-57** (endophilin) are required for recruitment of the AP2 adaptor complex by Synaptotagmin

(**SNT-1**) (Harris, Hartwieg et al. 2000; Schuske, Richmond et al. 2003). Separation of the endocytic vesicle from the plasma membrane or vesicle fission is driven by the GTPase dynamin (*dyn-1*). Other genes that facilitate vesicle endocytosis are either enriched [***apt-10*** (Stoned B)] or EGs [F58G6.1 (amphiphysin), and *ehs-1* (EPS15)]. The clathrin coat is removed in the final stage of endocytosis to release the nascent SV. The heat-shock protein Hsc70 (*hsp-1*) and the DnaJ protein Auxilin (*dnj-25*) are critical for this process (Richmond and Broadie 2002) and both are EGs in the *unc-4*::GFP motor neuron data set. Finally, the transcript for **RME-8**, a novel J-domain protein required for endocytosis in coelomocytes and in the somatic gonad (Zhang, Grant et al. 2001) is enriched; a function for ***rme-8*** in the nervous system has not been previously reported.

TGF-β Signaling

Transcripts for three of the four known BMP-4/TGF-β peptides in *C. elegans* (Savage-Dunn 2001) are either enriched (***tig-2***) or detected as EGs (*dbl-1*, *unc-129*). Expression of *dbl-1* and *unc-129* in DA motor neurons has been previously described (Colavita, Krishna et al. 1998; Suzuki, Yandell et al. 1999) and we have used a GFP reporter to confirm ***tig-2*** expression in these cells. It is interesting to note that *dbl-1*, *unc-129*, and ***tig-2*** are also expressed in body wall muscles. In Drosophila, formation of a normal neuromuscular synapse depends on reciprocal BMP-4/TGF-β signaling between motor neurons and target muscles (McCabe, Marques et al. 2003). A comparable role for BMP/TGF-β signaling at the nematode neuromuscular synapse has not been detected in BMP signaling mutants. Perhaps, this outcome is a result of redundant BMP/TGF-β signals.

Serpentine Receptors

The members of the chemosensory receptor gene family (also known as the serpentine receptors [SR]) constitute ~6% (~1300 genes) of the *C. elegans* genome. Many of these genes have arisen from recent gene duplications, and almost one third are predicted to be pseudogenes (Robertson 2001; Stewart, Clark et al. 2005). In mammals and in *C. elegans*, G-protein coupled receptors are required for odorant discrimination (Troemel 1999). *C. elegans* can detect hundreds of different compounds, which suggests that a significant fraction of the SR receptors are utilized. Due to the large number of receptors (>500), and the relatively small number of chemosensory neurons (20-30) in *C. elegans*, each neuron is likely to express 40-50 different receptors (Sengupta, Chou et al. 1996; Troemel 1999; Robertson 2001). Transcripts for 18 SRs are enriched and 96 transcripts are detected as EGs. Because *unc-4*::GFP neurons are components of the motor circuit, it seems unlikely that SRs are functioning as odorant receptors in these cells. It will be interesting to determine if members of the SR family are widely expressed in other classes of *C. elegans* neurons.

Calcium Channels

Synaptic transmission is triggered by calcium influx via voltage gated calcium channels (Sudhof 2004). Calcium channels are composed of distinct subunits: $\alpha 1$, $\alpha 2\delta$, β, γ. Electrophysiological studies have identified distinct calcium currents; L-, N-, P-, Q-, R-, and T-type. These are largely defined by the specific type of $\alpha 1$ subunit incorporated into the channel (Catterall 2000). The ***unc-2*** gene encodes an $\alpha 1$ subunit of the N-/P-/Q-

class and is highly expressed in motor neurons. Pharmacologic studies indicate that the impaired movement shown by ***unc-2*** mutants is a consequence of presynaptic defects in neurotransmitter release at the neuromuscular junction (Mathews, Garcia et al. 2003). Our finding that ***unc-2*** is enriched in the *unc-4*::GFP motor neuron data set is consistent with this model. *unc-36* (EG) encodes an α2δ subunit and has been proposed to co-assemble with **UNC-2** on the basis of similar mutant phenotypes (Schafer, Sanchez et al. 1996). Another α2δ type subunit, **T24F1.6**, is enriched but has not been genetically characterized. A β subunit encoding transcript (*ccb-1*) is an EG. (γ subunit genes have not been identified in *C. elegans* (Bargmann 1998).

The *C. elegans* genome includes two α1-like subunit genes, ***nca-1*** and *nca-2*, that encode large so-called 4-domain calcium channel subunits (K. Hamming, C. Thacker, T. Snutch, personal communication); ***nca-1*** is enriched in UNC-4 motor neurons and a GFP reporter confirms expression in cholinergic ventral cord motor neurons (including DAs). *nca-2* is not represented on the Affymetrix Chip and therefore is not detected (data not shown). ***nca-1*** and *nca-2* are highly conserved with apparent human orthologs but their functions are unknown.

Other classes of calcium transporters with well-established roles in neuron excitability are enriched in UNC-4 motor neurons. These include channels that release calcium from internal stores (***unc-68***, ryanodine receptor) as well as transporters that remove calcium from the cytoplasm (***mca-3***, PMCA1-type calcium-transporting ATPase and ***ncx-4***, Ca^{2+}/Na^{2+} exchanger) (Thayer, Usachev et al. 2002; Strehler and Treiman 2004). Although **UNC-68** expression in *C. elegans* neurons has not been previously reported, mammalian ryanodine receptors are highly expressed in the CNS where they

co-localize with L-type voltage gated calcium channels to mediate excitation-coupled calcium release from the endoplasmic reticulum (Ouardouz, Nikolaeva et al. 2003). Lastly, ***trp-1,*** a TRPC (TRPCanonical) calcium/cation channel of the TRP (Transient Receptor Potential) superfamily, is enriched in the *unc-4*::GFP motor neuron data set, and we have confirmed its expression in UNC-4 motor neurons. In other cell types, TRP channels are gated by environmental stimuli (e.g., temperature or mechanical disturbance) but potential functions of TRPC channel in these motor neurons are unknown (Harteneck, Plant et al. 2000).

Calcium ion binding

The calcium-binding protein, calmodulin, regulates calcium-dependent signaling pathways that control multiple aspects of neuronal function including synaptic activity and gene expression (Chin and Means 2000). *C. elegans* encodes a single, highly conserved calmodulin ortholog, ***cmd-1*** and four calmodulin-like genes (Karabinos, Bussing et al. 2003). Transcripts for ***cmd-1*** and two of the calmodulin-like genes (**Y73B3A.12, F12A10.5**) are enriched in UNC-4 motor neurons. CAM kinase activity is regulated by calmodulin (Corcoran and Means 2001) and all of the canonical CAMK components, *unc-43* (CAMKII), *cmk-1* (CAMKI), and *ckk-1* (CAMKK), are detected as EGs. Another downstream effector of calmodulin is calcineurin, a heterodimeric serine/threonine phosphatase; the catalytic A subunit (*tax-6*) is an EG and the regulatory B subunit (***cnb-1***) is enriched in the *unc-4*::GFP motor neuron data set. These data are consistent with genetic evidence showing that *unc-43*/CAMKII and calcineurin are antagonistic regulators of G-protein dependent locomotion in *C. elegans* (Robatzek and

Thomas 2000; Bandyopadhyay, Lee et al. 2004). The transcript for a calcineurin regulatory protein, *rcn-1*, is detected as an EG in these cells (Bandyopadhyay, Lee et al. 2004). Thus, key conserved components of calmodulin-dependent signaling pathways are expressed in *unc-4*::GFP motor neurons.

Transcripts for other notable calcium binding proteins enriched in UNC-4 motor neurons include: **R08D7.5**, centrin/caltractin, a member of the calmodulin superfamily and component of the microtubule organizing center (Hu, Sheehan et al. 2004); ***pef-1***, serine/threonine protein phosphatase, an ortholog of PPEF/rdgC (retinal degeneration gene C) and proposed regulator of G-protein activity (Ramulu and Nathans 2001); ***spc-1***, alpha-spectrin, an actin binding and scaffolding protein (Norman and Moerman 2002); ***nex-1***, annexin, an actin and phospholipid binding protein (Creutz, Snyder et al. 1996).

Potassium Channels

Potassium channels are subdivided into three main groups on the basis of the number of transmembrane domains within each subunit: 2 TM inward rectifiers, 4 TM (2 pore) or TWIKs, and 6 TM voltage-gated channels (Miller 2000). TWIK channel encoding genes are the largest and most evolutionarily diverged group with ~40 members in the *C. elegans* genome. We find 8 members of the TWIK family enriched in UNC-4 motor neurons (***twk-6, -13, -29, -30, -40, -46, unc-58*, R05G9.28**). VNC motor neuron expression of ***twk-30*** and ***unc-58*** has been previously reported (Salkoff, Butler et al. 2001), and we have confirmed that ***twk-30***::GFP is expressed in DA motor neurons. TWIK channels are believed to set resting membrane potential and hence modulate cell excitability. A physiological requirement for multiple potentially redundant TWIK

channels in these motor neurons is unclear although this arrangement may allow for "fine tuning" of the electrical responsiveness of these cells (Salkoff, Butler et al. 2001). Two voltage gated K channels, F44A2.2 (Shab/K2v.2) and M60.5 (KQT) are detected as EGs.

Innexins

Neurons are electrically coupled by gap junctions, intercellular channels that facilitate the movement of ions and small molecules between cells. Gap junctions are multimeric membrane pores assembled from protein subunits contributed by each cell (Phelan and Starich 2001). The invertebrate gap junction is composed of innexins, which are structurally similar to vertebrate gap junction subunits, connexins. There are 25 innexin genes in *C. elegans* (Starich, Sheehan et al. 2001). Only one of these, ***unc-9***, is enriched in the *unc-4*::GFP motor neuron data set. ***unc-9*** mutants show jerky, uncoordinated movements indicative of defective function in the motor circuit (Phelan and Starich 2001). These mutant effects could arise from the disruption of gap junctions that electrically couple DA motor neurons with command interneurons and with other motor neurons (White, Southgate et al. 1986). Five additional innexin genes (*inx-1, -6, -7, -15, -22*) are detected as EGs, which could mean that UNC-4 motor neurons assemble more than one type of gap junction. It is surprising that the *unc-7* transcript is not detected in these cells as *unc-7* and ***unc-9*** mutants exhibit similar mutant phenotypes indicative of function in a common genetic pathway (Phelan and Starich 2001).

DEG/ENaC and Stomatins

DEG/ENaC sodium channels are comprised of single TM domain subunits that are believed to gate cation transport in response to mechanical force (Bianchi and Driscoll 2002). There are 21 DEG/ENaC encoding genes in *C. elegans* (Bianchi and Driscoll 2002). The transcript for one of these, ***unc-8***, is enriched, and confirms previous reports of ***unc-8*** expression in VNC motor neurons. The **UNC-8** protein has been proposed to function as a "stretch receptor" in a feed-back loop to coordinate motor neuron excitability with muscle contraction (Tavernarakis, Shreffler et al. 1997). DEG/ENaC activity in *C. elegans* touch neurons is modulated by interactions with Stomatin-like proteins (SLPs) (Goodman, Ernstrom et al. 2002). **UNC-8** physically interacts with the SLP **UNC-1** (Sedensky, Siefker et al. 2004). Consistent with this finding, the ***unc-1*** transcript is enriched in the *unc-4*::GFP motor neuron data set. In addition, the novel SLP *unc-24*, which may also modulate ***unc-8*** activity in the DA motor neurons is an EG (J. Koh, and D. Miller, unpublished data). Finally, the SLP, ***sto-6***, is enriched, as predicted by GFP expression (Zhang, Ma et al. 2004), but its function is unknown.

Discussion

Dissociated embryonic cells differentiate in culture

The use of cell culture systems to study cell biological processes has been popular for many organisms; however, the ability to culture nematode cells has remained difficult. The work of the Miller and Strange labs provided a protocol with which we can generate viable mass cultures of embryonic *C. elegans* cells. As with any *in vitro* culture

system, a major concern is that the artificial conditions introduced by the culture methods alter cell fates. While the cells resembled neurons and muscle cells morphologically *in vitro*, several experiments were performed to ensure that these cells were maintaining properties of these specialized cell types. In particular, we used antibodies directed against neuron and muscle-specific proteins to show that GFP-labeled neurons expressed these neuronal markers while excluding muscle specific proteins and vice versa. I was also able to show using the *unc-4*::GFP transgenic line, that GFP+ A-class motor neurons arise at the expected frequency *in vitro*, while exhibiting a developmental delay in GFP expression consistent with what is observed *in vivo*. Furthermore, the Strange lab performed electrophysiological measurements of cultured neurons and muscle cells and showed that these measurements were comparable to those obtained *in vivo*. The ability to culture *C. elegans* embryonic cells is an important advance for this organism that now allows for the application of cell-specific biochemical assays that have not been previously available to the worm community.

Methods to profile specific *C. elegans* cells

Previous studies have described other methods for cataloging transcripts from specific *C. elegans* cells. Comparisons of microarray data from mutant animals with either supernumerary or absent sensory neurons in the male tail have revealed genes that are preferentially expressed in these cells (Portman and Emmons 2004). However, this approach is limited to cell types that can be manipulated by specific mutants. In addition, this method may be insufficiently sensitive to detect changes in smaller subsets of cells due to high background mRNA from cells that are not affected by the mutation (S. Von

Stetina, D. Miller, unpublished data). This limitation can be overcome by enriching for mRNA from target cells. To this end, Zhang et al. (Zhang, Ma et al. 2002) used an approach similar to the strategy we developed to identify downstream genes of the MEC-3 transcription factor in *C. elegans* touch neurons (Zhang, Ma et al. 2002). However, this work did not provide a comprehensive cell-specific gene expression profile as we have obtained, possibly due to the limited enrichment (~50%) of GFP-labeled touch neurons. We have now optimized the application of nematode embryonic cell culture and FACS technology to obtain ~90% enrichment of GFP-marked neurons and muscle cells (RMF, S. Von Stetina, S. Barlow, D. Miller, unpublished data). These methods have now been successfully applied to profile other classes of *C. elegans* embryonic cells (McKay, Johnsen et al. 2003; Colosimo, Brown et al. 2004; Cinar, Keles et al. 2005).

Postembryonic analysis using mRNA tagging

The cell culture methods only allow for the isolation of embryonic cells; therefore, MAPCeL cannot be used for profiling cell types that arise postembryonically (Christensen, Estevez et al. 2002). Microarray profiles of specific larval cells, however, have been obtained by mRNA tagging. In this approach, an epitope-labeled polyA-binding protein (FLAG-PAB-1) is expressed transgenically under the control of a cell-specific promoter and mRNAs isolated by co-immunoprecipitation with anti-FLAG. This method has been used for microarray analysis of *C. elegans* body muscle cells and ciliated sensory neurons (Roy, Stuart et al. 2002; Kunitomo, Uesugi et al. 2005). Our lab has now successfully used the mRNA tagging strategy to profile specific subsets of motor neurons from *C. elegans* larvae (S. Von Stetina, RMF, J. Watson, S. Kim, P. Roy, D.

Miller, unpublished data). Thus, in principle, it should now be possible to obtain an accurate gene expression profile for virtually any *C. elegans* cell throughout development.

UNC-4 motor neurons are sensitive to a wide range of neurotransmitters and peptidergic signals

Acetylcholine (ACh) release at the DA neuromuscular junction is presumptively triggered by excitatory input from command interneurons. The strength of the DA cholinergic signal, however, may be strongly modulated by other cells that release neurotransmitters from distal locations. For example, dopamine is produced by 8 neurons, none of which are presynaptic to DA motor neurons (Sulston 1983). Dopamine, however, is a potent regulator of cholinergic secretory activity in the ventral motor circuit. The dopamine effect is mediated in part by DOP-1, a G-protein coupled receptor (GPCR) (Chase, Pepper et al. 2004). We have confirmed enrichment of the *dop-1* transcript and also detected elevated levels of transcripts encoding GPCRs for acetylcholine and serotonin, additional neurotransmitters known to modulate cholinergic motor neuron activity via G-protein signaling pathways (Nonet, Saifee et al. 1998; Chase, Pepper et al. 2004). Enrichment of a GABA metabotropic receptor transcript offers yet another mechanism for exogenous adjustment of neurotransmitter vesicular fusion in DA motor neurons. Indirect evidence indicates that acetylcholine release from ventral cord motor neurons may also be sensitive to neuropeptide signals from other neurons or muscle cells (Doi and Iwasaki 2002; Jacob and Kaplan 2003). We have established that *unc-4*::GFP motor neurons express elevated transcript levels for nine different GPCRs with significant homology to insect or mammalian neuropeptide receptors. This signaling

complexity is further compounded by the enrichment of transcripts for 18 members of the serpentine GPCR-like family in *unc-4*::GFP neurons. Ligands for this outlier group of GPCRs are unknown (Geary and Kubiak 2005).

The microarray data also reveal multiple additional classes of receptors and ion channels through which the differentiation and function of *unc-4*::GFP motor neurons could be modulated by extracellular signals (Figure 2.8). Finally, we have detected enrichment of transcripts encoding TGF-β, wingless, and several classes of neuropeptides. Thus, in addition to responding to a wide range of stimuli, *unc-4*::GFP motor neurons are also potentially capable of regulating the activities of other cells with a variety of different signals. If an organism as simple as *C. elegans* builds motor neurons with such sophisticated signaling and response mechanisms, it is tempting to speculate that neurons in other, more advanced species may have evolved even more complex pathways. It is likely, however, that the core signaling systems described here are also conserved. This prediction is underscored by our finding that approximately half of the enriched transcripts (537/1012) and 2/3 of EGs (4050/6217) detected in *unc-4*::GFP neurons have human homologs (BLAST < e^{-10}).

Applications of MAPCeL

In addition to confirming expression of genes with known roles in *unc-4*::GFP motor neuron differentiation and function, the microarray data also uncovered strong candidates for new genes governing these events. For example, DA motor axons grow dorsally in response to a ventrally provided repulsive UNC-6/netrin guidance cue (Hedgecock, Culotti et al. 1990). Recent work has shown that the receptor protein

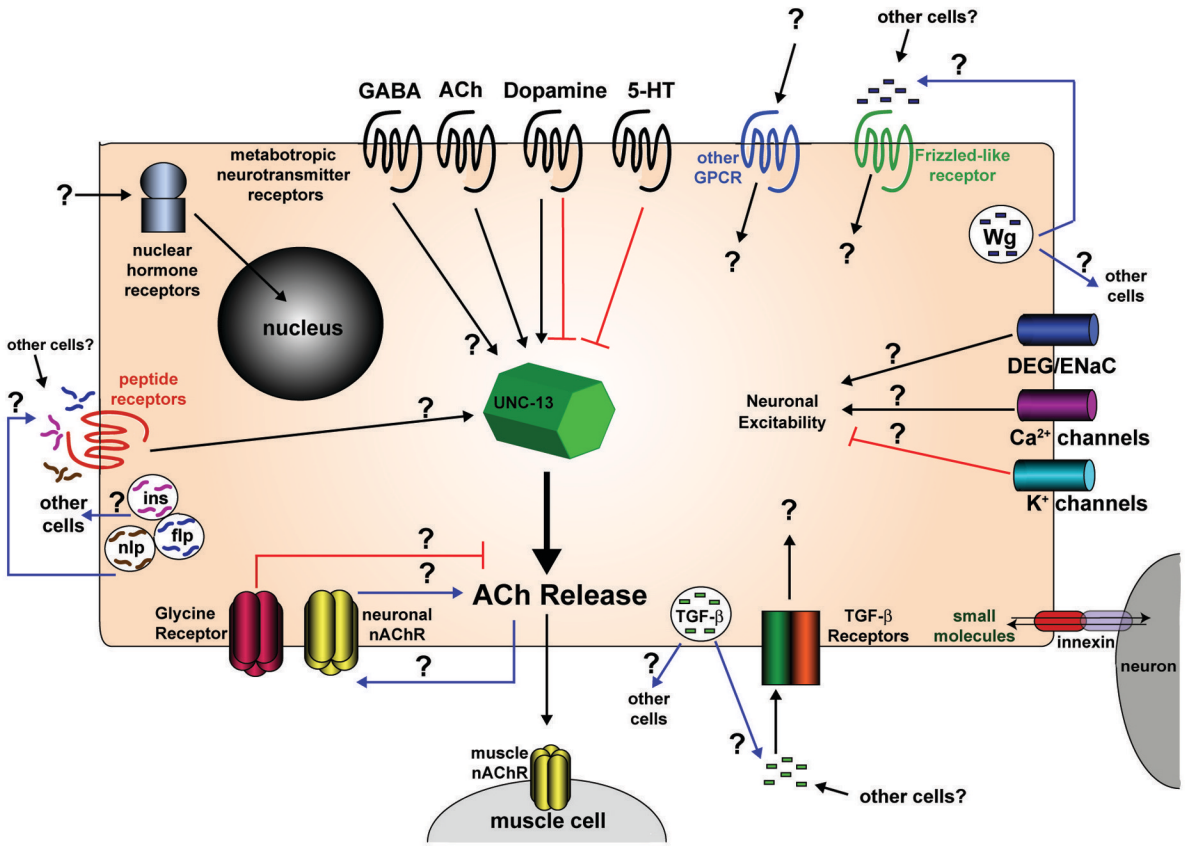

Figure 2.8. Signaling components detected in *unc-4*::GFP motor neurons.

tyrosine phosphatase (RPTP), CLR-1, positively enhances this response (Chang, Yu et al. 2004). As expected, we found that the *clr-1* transcript is enriched in the *unc-4*::GFP motor neuron data set. We also noted enrichment of *abl-1*, the *C. elegans* homolog of Abelson tyrosine kinase. By analogy to findings in Drosophila, in which Abelson tyrosinekinase functions in opposition to RPTP-dependent axon guidance (Grevengoed, Fox et al. 2003), we propose that ABL-1 antagonizes CLR-1 activity. This model predicts that either genetic ablation or RNAi of *abl-1* will suppress the DA motor axon guidance defects of *clr-1* mutants.

Another application of this strategy includes the identification of transcription factor target genes. A comparison of expression fingerprints of wildtype cells vs cells that are mutant for a specific transcription factor could reveal downstream genes (Zhang, Ma et al. 2002). For example, the UNC-4 transcription factor regulates axon morphology and synaptic strength in embryonically derived *unc-4*::GFP neurons (Lickteig, Duerr et al. 2001). UNC-4 also defines the specificity of synaptic inputs to postembryonically-derived VA motor neurons (White, Southgate et al. 1992; Miller and Niemeyer 1995; Winnier, Meir et al. 1999). We have now used a combination of MAPCeL and mRNA tagging strategies to identify candidate genes regulated by UNC-4 in these cells (see Chapter IV). Gene regulatory motifs to which transcription factors bind may also be revealed as common cis-acting sequences in cohorts of co-regulated genes (Ao, Gaudet et al. 2004).

The *C. elegans* nervous system is composed of exactly 302 neurons. The morphology and connectivity for every neuron has been defined by serial section electron microscopy to generate a detailed wiring diagram for the entire network (White,

Southgate et al. 1986). The *C. elegans* genome is similarly well defined. All 6 chromosomes are completely sequenced and the structure of over 20,000 genes described (Consortium 1998). Unique combinations of genes are likely to specify different classes of neurons and their differentiated traits. The problem now is to link the gene map with the wiring diagram. We believe that our work profiling the motor circuit using MAPCeL offers a powerful approach toward achieving this goal.

CHAPTER III

PROFILING BODY WALL MUSCLE CELLS AND THE IDENTIFICATION OF ACR-16 AS AN ESSENTIAL COMPONENT OF THE LEVAMISOLE-INSENSITIVE ACETYLCHOLINE RECEPTOR IN MUSCLE

Introduction

The sinusoidal waves that propel movement are regulated by the opposing actions of motor neurons and the muscle cells they innervate. Excitation by cholinergic neurons triggers muscle cell contraction on one side of the animal while the inhibitory GABAergic neurons stimulate muscle relaxation on the other. The rhythmic reversal of this pattern and its propagation along the length of the animal result in coordinated locomotion (Figure 3.1). To better understand the molecular mechanisms underlying regulated movement it is important to identify the genetic components that comprise the motor circuit. Chapter II describes the development of a method, MAPCeL, for obtaining microarray expression data from specific cells and its use to profile cholinergic *unc-4*::GFP motor neurons. Here I describe the use of MAPCeL to obtain a comprehensive expression profile of the muscle cells that these motor neurons innervate.

The body wall muscle cells comprise the largest class of muscle cell types in *C. elegans*; the adult contains 95 body muscle cells of which 81 are generated in the embryo (Sulston and Horvitz 1977; Sulston, Schierenberg et al. 1983). Nematode body muscle cells are striated with structural and functional similarities to the striated skeletal muscles of vertebrates (Figure 3.2) (Waterston 1988). As in vertebrate muscle, the prominent functional unit of the body muscle cell is the sarcomere, a structure composed of myosin-

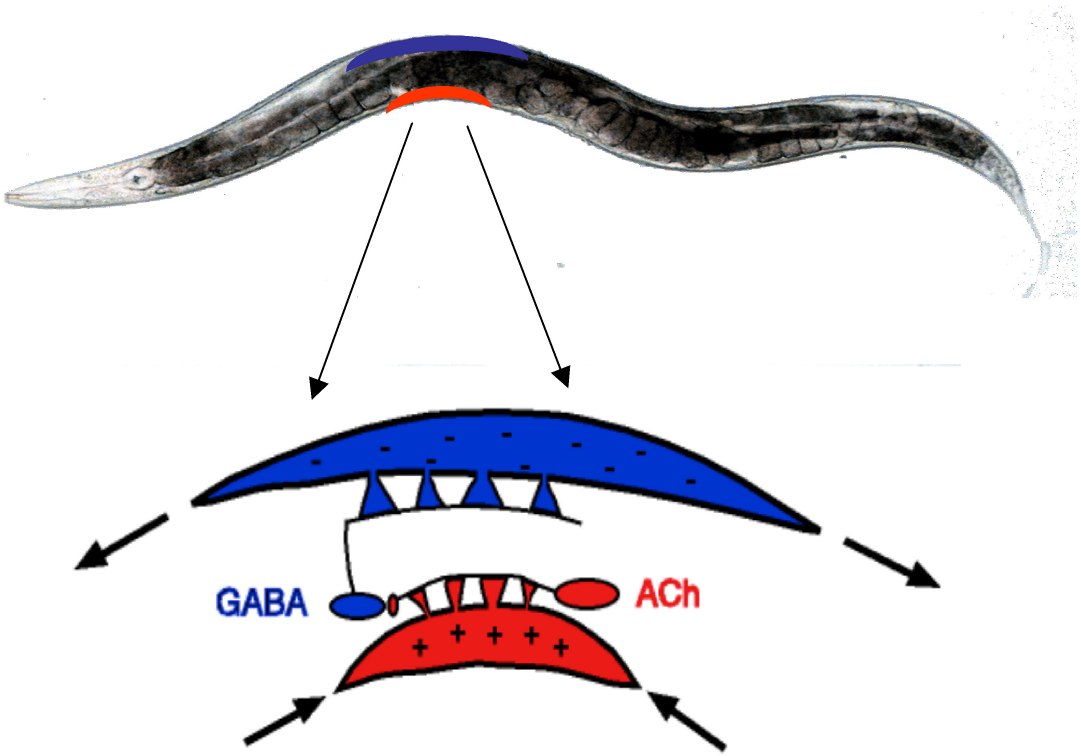

Figure 3.1. Motor neurons stimulate muscle contraction/relaxation to regulate coordinated movement. The sinusoidal movements associated with coordinated locomotion are mediated by two classes of motor neurons that stimulate muscle contraction and relaxation. The cholinergic motor neurons (red) stimulate contraction while simultaneously the GABAergic motor neurons (blue) promote relaxation on the opposite side of the animal. Figure courtesy of Janet Richmond.

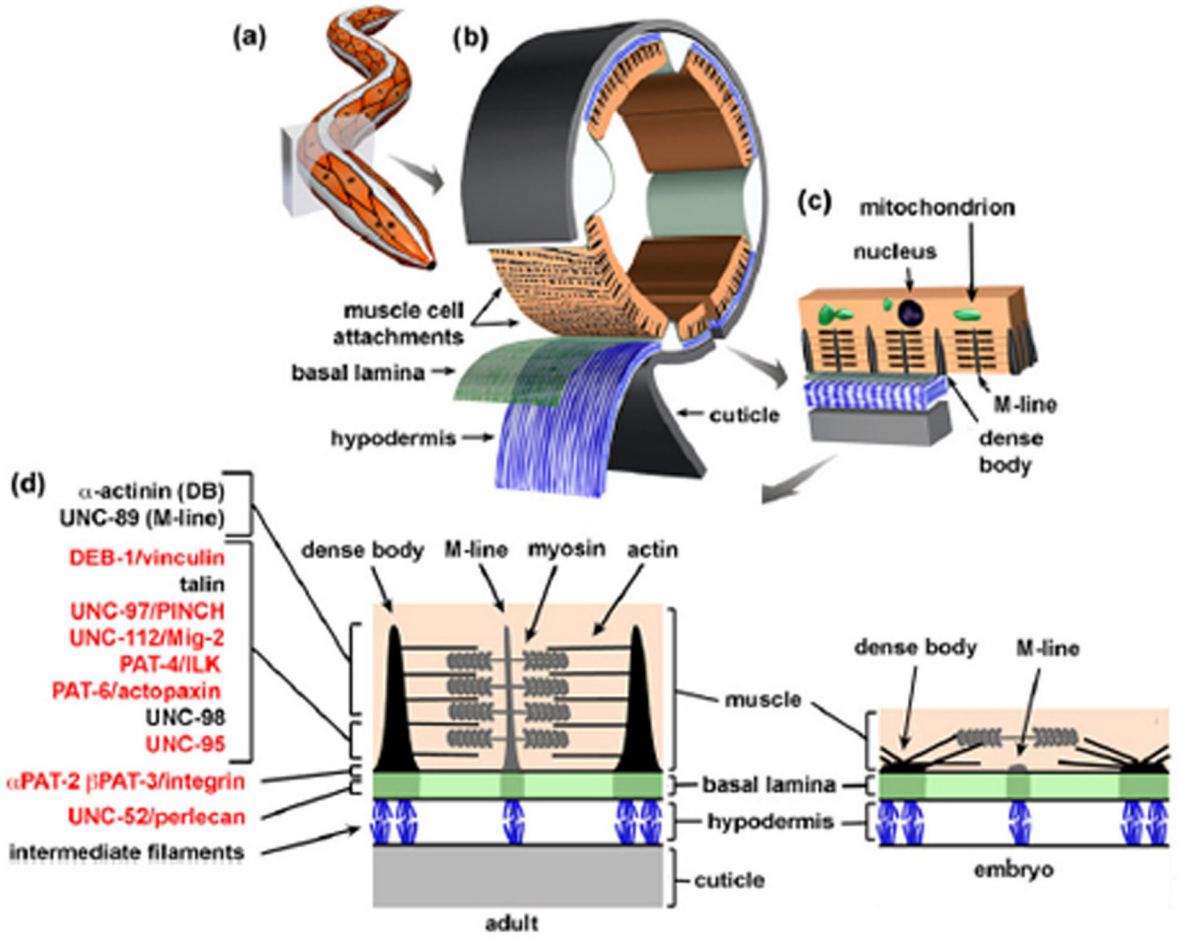

Figure 3.2. Schematic cartoon of the structure of *C. elegans* body wall muscle. A. An adult worm with four body wall muscle quadrants visible (orange). B. Cross-section of body wall muscle with basal lamina and hypodermis peeled away to reveal basement membrane and two muscle cells. C. Longitudinal section of body wall muscle cell. D. Location of muscle attachment proteins in the adult (left) and embryonic (right) body wall muscle cells. Genes in red lead to a Pat (Paralyzed at Two-fold stage) phenotype. Image adapted from Moerman and Williams, 2006.

containing thick filaments and actin-containing thin filaments. Force is generated in an ATP-dependent process driven by the myosin motor domain that drives the movement of thick filaments over thin filaments resulting in muscle contraction (Waterston 1988; Moerman and Fire 1997). Extensive research on the nematode body wall muscles has identified a large array of genes necessary for muscle assembly, development and function; many of these genes and the proteins they encode are also conserved in vertebrate muscle (Moerman and Fire 1997). To obtain a comprehensive catalog of genes expressed in *C. elegans* body wall muscles, we have profiled embryonic *myo-3*::GFP labeled muscle cells. Given the conservation of previously identified genes between nematode and vertebrate organisms, it is likely that the genes revealed by these experiments will have important roles not only in nematode muscle, but also in muscle cells of larger, more complex organisms.

In an experimental test of the reliability of our data, we collaborated with Janet Richmond (University of Illinois, Chicago) to confirm that a novel nicotinic acetylcholine receptor (nAChR) subunit gene revealed in the *myo-3::*GFP microarray profile encodes an essential component of a physiologically distinct nACh receptor in *C. elegans* body muscle cells. Three classes of ionotropic receptors have been identified at the nematode neuromuscular junction: inhibitory γ-aminobutyric acid (GABA) receptors, and two types of excitatory nAChRs that are distinguished by their sensitivity to the acetylcholine agonist, levamisole (Richmond and Jorgensen 1999). The GABA receptor is encoded by a single gene, *unc-49* (Bamber, Beg et al. 1999; Bamber, Twyman et al. 2003; Bamber, Richmond et al. 2005), while the levamisole-sensitive receptor is composed of 5 subunits (UNC-38, UNC-29, UNC-63, LEV-1, and LEV-8) (Lewis, Wu et al. 1980; Fleming,

Squire et al. 1997; Richmond and Jorgensen 1999; Culetto, Baylis et al. 2004; Towers, Edwards et al. 2005). Although the existence of a levamisole-insensitive nAChR was inferred from pharmacological and genetic data, the molecular identity of the corresponding nAChR gene(s) remained elusive. In addition to detecting the transcripts encoding the known ionotropic GABA receptor *unc-49* and most of the components of the levamisole-sensitive nAChR, the body muscle microarray profile also detected two additional nAChR subunit genes, *acr-8* and *acr-16*, that had not been previously studied. Experiments performed with the Richmond lab have established that one of these nAChR subunit genes, *acr-16*, encodes the levamisole-insensitive receptor. These findings were published in *The Journal of Biological Chemistry* (Touroutine, Fox et al. 2005).

Materials and Methods

Nematode strains

Nematode strains were maintained at 20-25°C using standard culture methods (Brenner 1974). Strains used for microarray experiments were the N2 wildtype isolate and PD4251(*ccIs4251*, *myo-3*::GFP)(Fire, Xu et al. 1998). Deletion alleles, *acr-16(ok789)* and *acr-8(ok1240)*, were obtained from the *C. elegans* knockout consortium (Bob Barstead, http://celeganskoconsortium.omrf.org/). We generated the following strains to examine the expression of the ACR-8 and ACR-16 acetylcholine receptor subunits: P*acr-8*::GFP [NC752(*wdEx263*), NC753(*wdEx264*)], and P*acr-16*::GFP [NC971(*wdEx418*), NC972(*wdEx419*)]. Additionally, over 50 transgenic GFP reporter lines were generated by our collaborator, Michael Krause (NIH/NIDDK), to validate microarray data.

Generating transgenic promoter::GFP strains to validate microarray data

Transgenic strains from the Krause lab were generated either by conventional cloning or by SOE (sequence overlap extension) methods (Hobert 2002). Promoter regions were amplified and cloned into the *BamHI* site of pPD95.67 (Fire Vector Kit 199X) or SOE was used to generate a linear *promoter*::GFP construct. Transgenic animals were created by microinjection of 23µl (5-10ng/µl) of SOE reaction with 3µl (60 ng/µl) pRF4 [*rol-6(d)]* co-injectable marker, with the exception of H22K11.4::GFP and E02H4.3::GFP, which were generated by the Miller lab using biolistic transformation. For these reporters, promoter regions were cloned into *HindIII* (H22K11.4)/PstI (E02H4.3) and *XmaI* sites of pPD95.75 GFP plasmid (1995 Fire Vector Kit) along with the *unc-119* minigene. Microparticle bombardment was conducted in a BioRad Biolistic PDS-1000/He equipped with the Hepta Adapter as follows. Gold beads (1 micron) were coated with DNA at 1 µg/µl. 100 mm NGM plates were seeded with a monolayer of ~100,000 L4/adult *unc-119 (ed3)* animals. For each construct, 1 'shot' was performed using a 1550 psi rupture disk at 28 inches of Hg vacuum. After a 1 hr recovery period, animals were washed from the plates with 7 ml M9 buffer and transferred to seven 100 mm NGM plates (1 ml/plate). Animals were grown at 20 ^{o}C for 1 week. To pick transgenic animals, one-half of the plate was 'chunked' and added to a new 100 mm NGM plate; animals with wildtype movement were picked to 60 mm NGM plates and allowed to "self". Worms derived from separate plates were considered independent lines; at least 2 lines were obtained and analyzed for each construct.

Promoter::GFP reporters for AChR subunit genes, acr-8 and acr-16

Pacr-8::GFP – A region 2,460 bp upstream of the ATG start site was generated by PCR using the primers *acr-8p1* 5'-AAGCTTTGTCAGTCTCTACGATTAC-3' and *acr-8p2* 5'-GGATCCGATGAAGCTGGAGTGAGAAG-3'. The *acr-8* PCR fragment and an *unc-119* minigene (from plasmid pDP#MM051) (Maduro and Pilgrim 1995) were subcloned into the GFP vector pPD95.75(1995 Fire Vector Kit) to produce the vector *acr-8*::GFP-*unc-119*. Four independent P*acr-8*::GFP transgenic lines were generated by microparticle bombardment, as described above, with the *acr-8*::GFP-*unc119* plasmid into *unc-119(ed3)* animals.

Pacr-16::GFP: GFP reporters were generated using SOE (Hobert 2002). Primers used for amplification of the GFP fragment are described in Hobert, 2002 (Hobert 2002). A region extending from 3000bp upstream of the *acr-16* start site to 24bp into exon one was PCR amplified with primers: *acr-16p1* 5'-CACCCTTGTGTGTCTGTGAAG-3' and *acr-16p3GFP* 5'-AGTCGACCTGCAGGCATGCAAGCTTGCGCACGAGATGAGAAG-3'. 15µl of PCR product was co-injected with 25ng/µl of the plasmid pRF4 (*rol-6*). Five independent lines of P*acr-16::GFP* were generated (Touroutine, Fox et al. 2005).

Cell Culture

C. elegans embryos were dissociated for FACS isolation of freshly dissociated *myo-3*::GFP muscle cells (M0) (see below). Embryonic cells were also cultured for 24 hr as described in Chapter II to generate the M24 *myo-3*::GFP muscle cells for FACS isolation (Christensen, Estevez et al. 2002).

FACS Analysis

FACS experiments were conducted on a FACStar Plus flow cytometer (Becton Dickinson, San Jose, CA) equipped with a 488 nm argon laser. Emission filters were 530±30 nm for GFP and 585±22 nm for Propidium Iodide (PI). The machine was flushed with egg buffer (Christensen, Estevez et al. 2002) and light scattering parameters calibrated with 2 μm beads. Sorting gates for GFP-labeled cells were established as outlined in Chapter II (Fox, Von Stetina et al. 2005). The rate of cell sorting was 4000-5000 cells per second through a 70 μm nozzle.

Freshly dissociated muscle cells were sorted immediately after embryo isolation. Following chitinase digestion, embryos were dissociated by gentle resuspension in egg buffer and passed through a 5 μm durapore filter to remove intact embryos and debris. Cells were counted on a hemocytometer and diluted to a concentration of ~10 million cells/ml. PI was added to a final concentration of 5 μg/ml. Cultured muscle cells were prepared for sorting as described in Chapter II (Fox, Von Stetina et al. 2005). Briefly, dissociated embryonic cells were incubated for 24 hours on poly-L-lysine coated one-well coverglasses in L15-10 media at a concentration of 10 million cells/ml. The supernatant was removed and the cells were washed from the substrate using egg buffer. The cell solution was filtered using a 5 μm durapore filter and PI was added to a final concentration of 5 μg/ml to mark non-viable cells. Reference datasets were generated from all embryonic cells that were either sorted just after dissociation (R0) or cultured for 24 hrs prior to sorting (R24) (Fox, Von Stetina et al. 2005).

RNA isolation, amplification, and hybridization

RNA was extracted from two populations of FACS-isolated GFP+ muscle cells for comparison to a wildtype non-GFP reference consisting of all viable embryonic cells. RNA was isolated using a Micro-RNA isolation kit (Strategene) and 100ng of total RNA was amplified using the Affymetrix GeneChip Eukaryotic Small Sample Labeling Protocol using the modifications described in Chapter II (Fox, Von Stetina et al. 2005). aRNA was biotin-labeled during the 2nd round of amplification using the BioArray High Yield RNA transcript Labeling Kit (Enzo). 15 μg of biotinylated aRNA was fragmented for hybridization to the Affymetrix *C. elegans* Array. RNA quality was assessed after fragmentation with the Agilent Bioanalyzer.

Data Analysis

All experiments were performed in triplicate with the exception of the cultured cell Reference dataset (R24), which was generated from four independent experiments. Raw signal intensities were scaled for interchip comparisons using Affymetrix MAS 5.0. Transcripts were deemed "present" if assigned a "present" call by Affymetrix MAS 5.0 in a majority of replicates for a given sample (2/3 for M0 muscle, 2/3 for M24 muscle, 2/3 for Reference R0, 3/4 for Reference R24). Raw data was normalized using RMA (Robust Multiarray Analysis) available through GeneTraffic (Iobion) and statistical analysis was performed using Significance Analysis of Microarray software (SAM, Stanford). A two-class unpaired analysis was performed to identify genes that are elevated ≥1.7 fold when compared to the Reference for each dataset, at a False Discovery Rate of ≤1.8% for M0

and ≤1.2% for the M24 experiments. For the M0 muscle dataset 780 genes were considered significantly enriched while 945 genes were enriched in the M24 muscle dataset.

To determine the list of Expressed Genes (EG) for each Experimental dataset we used the approach described in Chapter II (Fox, Von Stetina et al. 2005). Briefly, we first identified all genes that are Present in a majority of experiments for each dataset as described above. Since the sorted populations of GFP-enriched cells include about 10% non-GFP cells, transcripts from these contaminating cells are likely to be included in this list. These genes were identified as transcripts present in the muscle but showing relative enrichment in the Reference dataset obtained from all embryonic cells (879 for M0 muscle and 898 for M24 muscle). Accordingly, these "contaminating transcripts" were removed from the initial list of Present calls for the M0 and M24 *myo-3*::GFP data sets. Finally, a few transcripts enriched in the muscle samples that were excluded by MAS 5.0 on the basis of PM vs MM signals were restored to these lists (66 in M0 muscle, 223 in M24 muscle). In summary, these considerations identified 4868 EGs in the M0 muscle dataset and 5731 EGs in the M24 muscle dataset.

in litero *analysis*

Using Textpresso (www.textpresso.org), a literature search was performed using the keywords "body muscle expression," yielding a total of 61 citations (search performed 6/2004). Expression patterns were also identified using the "Cell Identity" function on WormBase (WS130 freeze, August 2004) to identify genes with expression

in body wall muscle, the anal muscles and vulval muscles. These searches identified 213 genes with expression in *myo-3*::GFP-expressing cells.

Global Analysis of microarray data

Annotation scripts were generated to extract information from WormBase using the Affy ID and cosmid name to search. Details regarding Perl scripts used for annotation can be found in Chapter II (Fox, Von Stetina et al. 2005).

Results

Strategy to profile embryonic muscle cells

We have used a microarray profiling strategy (MAPCeL – Microarray Profiling *C. elegans* Cells) to isolate RNA from embryonic muscle cells. In the embryo, *myo-3*::GFP is expressed in 81 body wall muscles and in two minor muscles, the anal depressor and sphincter (Figure 3.3A) Together, these tissues comprise ~15% of the total cell population (83/550 total embryonic cells, Figure 3.3B). *myo-3*::GFP is also expressed in a few additional larval muscle cells (e.g. vulval) that do not arise in our embryonic cultures and, therefore, are not directly profiled in these microarray experiments. Expression of *myo-3*::GFP at early stages of body muscle differentiation has allowed the isolation of two developmentally distinct populations of muscle cells. *myo-3*::GFP is initially detected in body muscle cells prior to embryonic morphogenesis. Consequently, these *myo-3*::GFP cells are readily dissociated from newly isolated embryos. The microarray profile of these freshly dissociated cells will be labeled "M0" to reference the

direct isolation of these muscle cells from embryos without culture or at "0" hr. The M0 profile is expected to detect transcripts that are highly expressed in nascent muscle cells. We have also generated transcript profiles from *myo-3*::GFP muscle cells that have been allowed to differentiate for 24 hrs in culture; the microarray profile of these cells will be referred to as "M24" muscle dataset. mRNAs isolated from these cells are expected to provide a gene expression profile of differentiated body wall muscle cells.

Isolating *myo-3*::GFP muscle cells using FACS

A schematic diagram outlining both strategies to isolate *myo-3*::GFP muscle cells is shown in Figure 3.4. Details describing the isolation of each cell population (**M0** and **M24**) are outlined below.

*Freshly dissociated **(M0)** myo-3::GFP muscle cells isolated by FACS*

For isolating early arising body muscle cells, the *myo-3*::GFP cell suspension was sorted immediately after embryo dissociation. FACS parameters for setting the GFP+ gate were established as follows. First, wildtype non-GFP embryonic cells (from N2) were used to identify a population of autofluorescent cells. These gut cells fluoresce in both the red (PI) and green (GFP) channels and can be visualized along the diagonal axis of the scatter plot in Figure 3.3C. Next, gating criteria for non-viable cells were determined by sorting wildtype cells stained with PI. These scatter plots were compared to a profile of *myo-3*::GFP embryonic cells to define the GFP sorting window (Figure 3.3D). Viable GFP-positive muscle cells were then gated according to light scattering

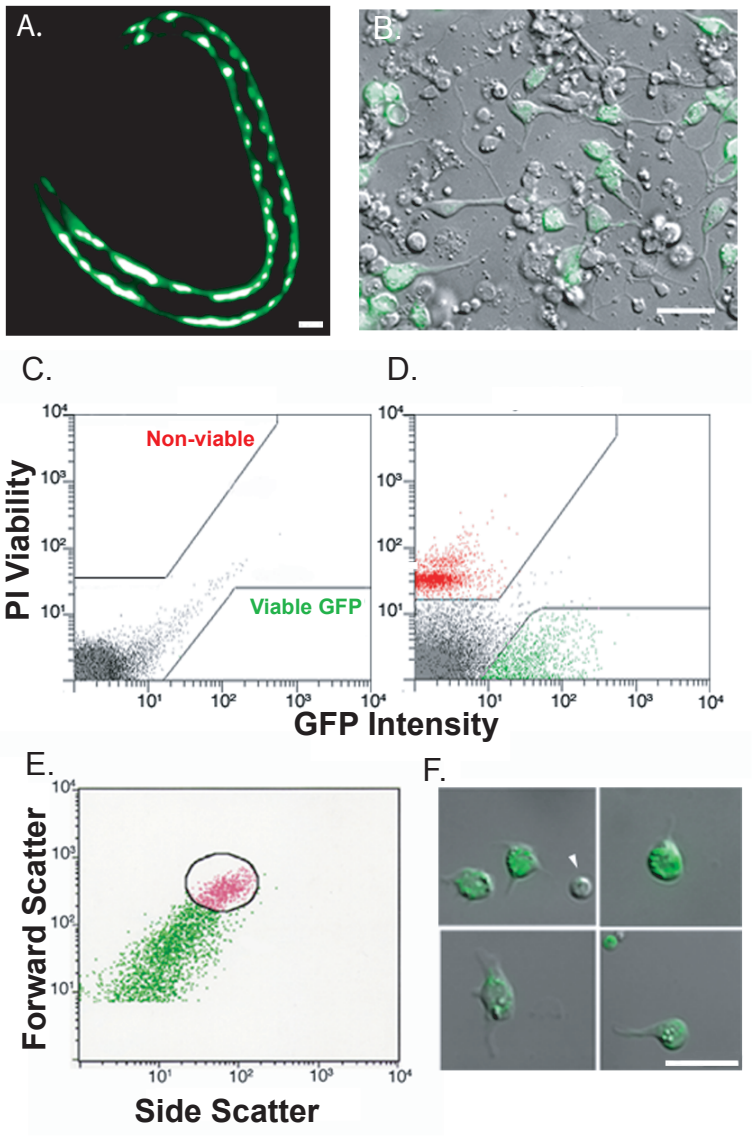

Figure 3.3. Isolation of freshly dissociated *myo-3*::GFP muscle cells using FACS. A. Fluorescence image of *myo-3*::GFP in the body wall muscle cells of a newly hatched L1 larva. B. Combined DIC and fluorescence image of a 24 hour culture of *myo-3*::GFP muscle cells. C. Fluorescence intensity profile of wildtype (non-GFP) cells. Boxed areas exclude autofluorescent cells. D. *myo-3*::GFP cells are gated to exclude propidium-iodide (PI) stained (non-viable) cells. E. Light scattering gate for GFP-positive cells (circle) to exclude cell clumps and debris. F. *myo-3*::GFP muscle cells after enrichment by FACS.

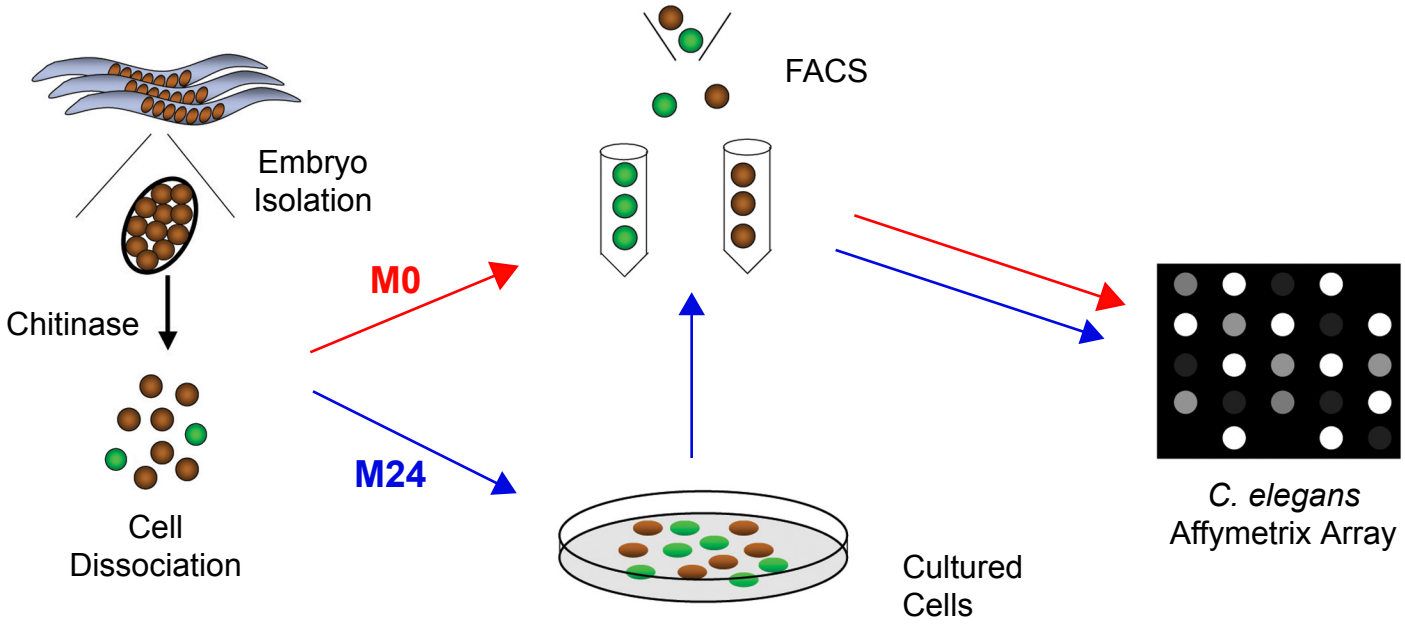

Figure 3.4. Profiling strategy for *myo-3*::GFP muscle cells. Embryos are isolated from gravid adults and treated with chitinase. For the freshly dissociated (M0) dataset (red) cells were sorted immediately after dissociation. The cultured cells dataset (M24, blue) was generated from RNA isolated from cells that had been cultured for 24 hours before sorting. RNA isolated from each set of cells was amplified and labeled prior to hybridization to the *C. elegans* Affymetrix Array.

parameters (Size – X axis, and granularity – Y axis) (Figure 3.3E) to isolate a subpopulation of cells that excludes large clumps and small debris. Direct visual inspection of *myo-3*::GFP cells isolated according to these criteria confirmed that GFP+ cells comprise ~90% of the total population for an overall 6-fold enrichment of *myo-3*::GFP cells after FACS in comparison to the intact embryo (Figure 3.3F). A typical sort yielded ~300,000 *myo-3*::GFP cells.

*Isolating cultured **(M24)** myo-3::GFP muscle cells*

The cultured cell population was isolated using the MAPCeL protocol outlined in Chapter II. We have previously shown that *myo-3::*GFP cells differentiate in culture, display a spindle-shaped morphology resembling the body wall muscle cells *in vivo* (Figure 3.3B), express muscle-specific genes, and exhibit largely normal physiological properties. In culture, *myo-3*::GFP cells constitute ~15% of all cells which is comparable to their frequency *in vivo* (83 muscle cells/550 total embryonic cells) (Christensen, Estevez et al. 2002). Direct observation confirmed that M24 *myo-3*::GFP cells constituted ~90% of sorted cells after FACS. (Figure 3.5).

Microarray results are reproducible

The coefficient of determination (R^2) was established for each set of microarray replicates. We have previously shown that the Reference dataset obtained from all cells after 24hr in culture has an average R^2 value of 0.96 (n=4) (Fox, Von Stetina et al. 2005). Similarly, in this study we found that both M0 and M24 muscle datasets, as well as the M0 Reference profiles display high R^2 values. For the M0 myo-3::GFP cells, the average

R^2 was 0.92, while the average R^2 for the M24 muscle dataset was 0.87. The M0 Reference dataset yielded an average R^2 value of 0.94. The reproducibility of these data is graphically displayed in the scatter plots shown in Figure 3.6. For example, a comparison of the average signal intensity for one M0 myo-3::GFP replicate to the average of all three M0 muscle replicates shows largely overlapping signal intensities (yellow) that cluster along the diagonal axis. In contrast, the scatter plot comparing the M0 muscle dataset to the M0 Reference ($R^2 = 0.84$) reveals significant differences in gene expression levels. Enrichment for known muscle genes is evident as transcripts for abundant muscle structural proteins *myo-3* (myosin), *unc-54* (myosin) and *unc-15* (paramyosin) (Waterston, Epstein et al. 1974; Miller, Stockdale et al. 1986; Ardizzi and Epstein 1987) are highly elevated relative to Reference data obtained from all embryonic cells (Waterston, Epstein et al. 1974; Ardizzi and Epstein 1987). Significantly, the expression level of SNAP-25, a protein highly expressed in neurons, is decreased in muscle (Figure 3.6) (Nonet, Saifee et al. 1998). These results indicate that the *myo-3*::GFP data sets are enriched for genes highly expressed in muscle cells, and not other cell types, such as neurons. This finding is further substantiated in a comparison with data generated from all neurons. We have generated MAPCeL profiles of the entire nervous system using a panneural::GFP reporter. These experiments identified ~650 genes that are highly enriched in neurons. In a comparison with our muscle microarray datasets we found only 19 genes in common between the M0 and the panneural dataset, while 48 were in common between the panneural and the M24 data.

Detecting Expressed Genes (EGs) in muscle cells

We initially identified all transcripts that are reliably detected at some level in the

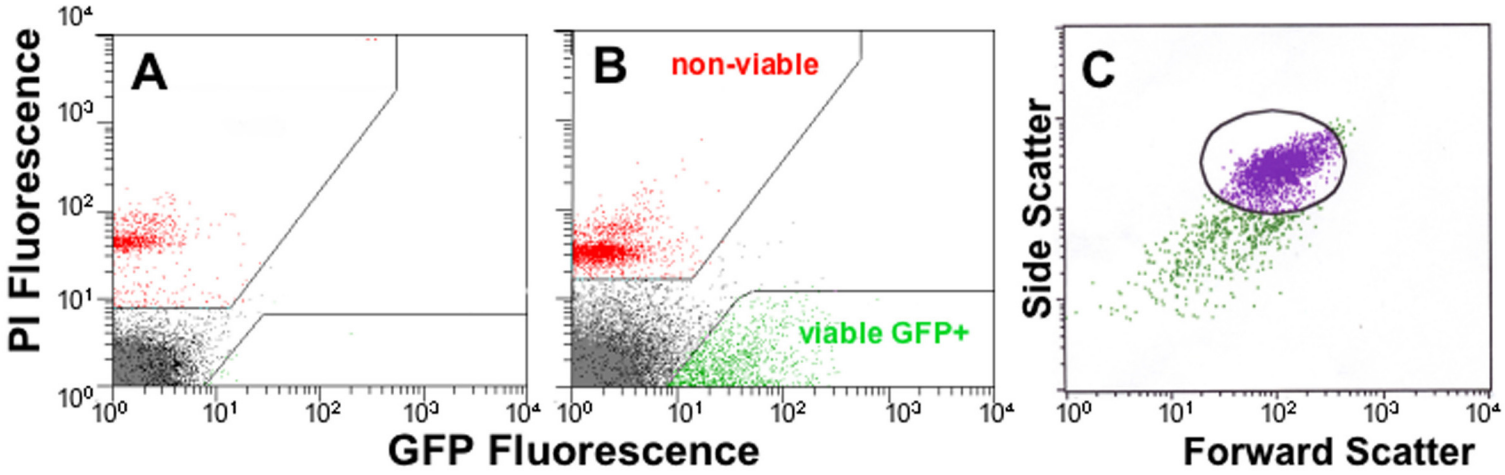

Figure 3.5. Sorting cultured *myo-3*::GFP body wall muscle cells. A. Fluorescence scatter plot of wildtype (non-GFP) cells. Propidium iodide (PI)-labeled cells are shown in red. The sorting gate in the lower right-hand corner excludes auto-fluorescent gut cells in the GFP channel. B. Fluorescence scatter plot of cultured cells from *myo-3*::GFP embryos. Note the abundant GFP-labeled cells (green). C. GFP+ cells were also gated within the circumscribed area (purple) to exclude large clumps and small debris.

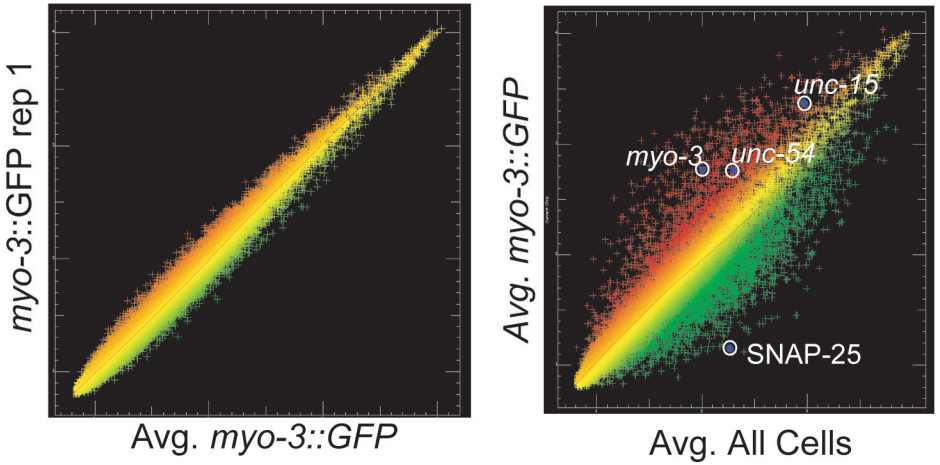

0hr

Chip	Rep2	Rep3
Rep1	0.90	0.94
Rep2		0.92

24hr

Chip	Rep2	Rep3
Rep1	0.80	0.86
Rep2		0.96

Figure 3.6. Coefficients of determination (R2) for individual hybridizations. A. Scatter plot of representative hybridization (rep-1) to the average intensities for all three *myo-3*::GFP (M24) hybridizations. B. Results of single *myo-3*::GFP hybridization (red) compared to average reference intensities (green) to identify transcripts showing differential expression. As expected, the known muscle genes *unc-54*, *myo-3*, and *unc-15* (circled) are all highly enriched in *myo-3*::GFP muscle cells. C. R2 values for all pairwise comparisons of *myo-3*::GFP M0 datasets. D. R2 values for all pairwise *myo-3*::GFP M24 datasets.

muscle data sets. As described above for the microarray profiles of embryonic A-class motor neurons, the initial lists of "present" genes for the experimental M0 and M24 data sets were adjusted to remove transcripts that could be attributed to contamination by non-GFP cells (~10%) in FACS derived *myo-3*::GFP cell populations. This final list of "Expressed Genes" or "EGs" includes 6728 unique mRNAs from the M0 and M24 populations of *C. elegans* body wall muscle cells. A total of 11,570 unique EGs are included in the sum of the Reference data sets. Overall, 12,230 transcripts were detected in these experiments. As indicated in Figure 3.7, a majority of transcripts (5,993) are detected in both muscle cells and in the Reference data set. These transcripts are likely to include "housekeeping" genes with universal roles in cell differentiation and homeostasis; for example, there are 84 ribosomal proteins detected. EGs that are selectively detected in the M0 and M24 profiles, however, are likely to provide functions that are unique to muscle cells. These "muscle-specific" genes as well as transcripts showing "enriched" expression in muscle cells relative to other embryonic cells are likely to fulfill roles unique to muscle cells and are therefore described in detail below.

Comparison of M0 and M24 muscle datasets

The experiments performed in this study profile muscle cells that differ in developmental age. The M0 set is comprised of early pre-morphogenesis embryonic cells whereas the M24 dataset profiles cells that have differentiated in culture for 24 hours. A comparison of transcripts enriched in both datasets reveals 401 common genes (Figure 3.8). Interestingly, of 39 transcripts encoding muscle structural proteins, 79%

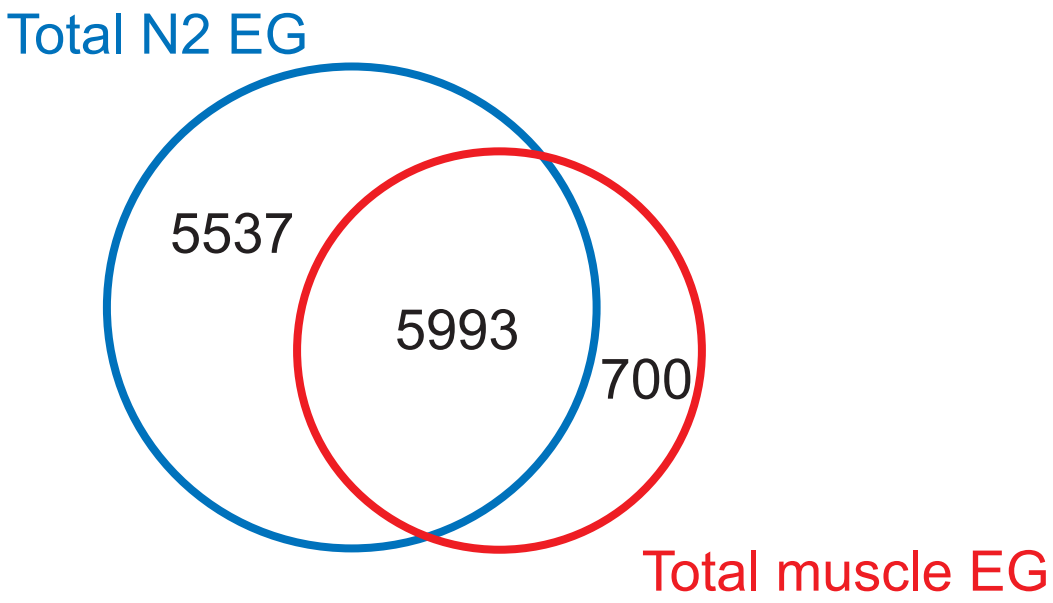

Figure 3.7. Venn diagram comparing the total number of EGs detected in the muscle datasets and the Reference datasets. 5993 genes were found common between all datasets, while 700 were exclusive to the muscle datasets and 5537 exclusive to the reference datasets.

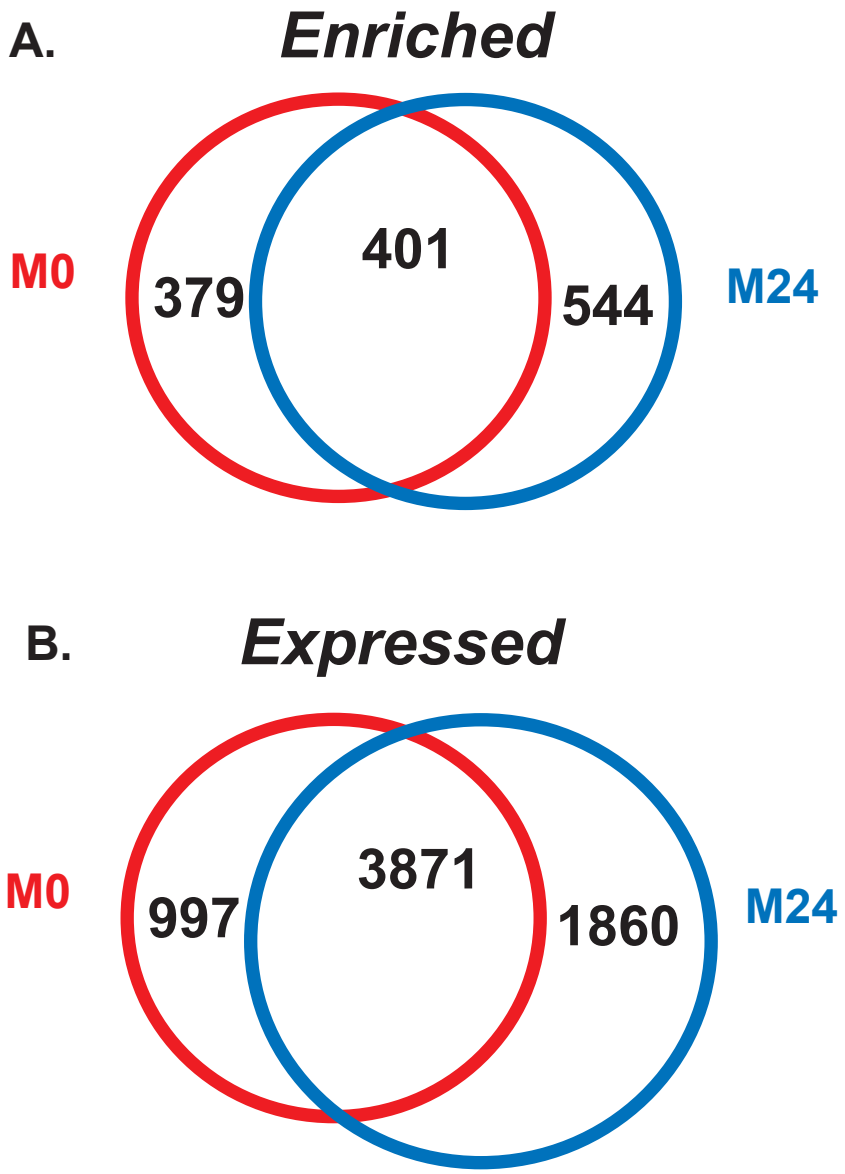

Figure 3.8. Venn diagrams comparing M0 and M24 *myo-3*::GFP datasets. A. There are 401 transcripts that are detected as enriched in both datasets while 379 are exclusive to the M0 dataset and 544 are only enriched in M24. In all, 1324 transcripts were identified as highly enriched in body wall muscle cells. B. There are 6728 genes expressed in body wall muscle cells of which 3871 are common between the two datasets. The M0 dataset contains 997 genes that are not expressed in the M24 dataset while 1860 are exclusive to the cultured cells.

(30/39) are common to both datasets (Table 3.1). This finding indicates that other genes in this list may also fulfill key roles in both nascent and fully differentiated muscle cells and may, therefore, constitute a core group of muscle function genes.

In addition to transcripts that are elevated in both data sets, we also detected genes that are selectively enriched in either the M0 or M24 profiles. Overall, 379 genes show elevated expression in the M0 data set only whereas a separate group of 544 transcripts are exclusively enriched relative to all other cells in the M24 data set. Of genes that are differentially detected in these data sets, we note that *pat-3* and *pat-6,* which are required for initial muscle assembly (Williams and Waterston 1994; Gettner, Kenyon et al. 1995; Lin, Qadota et al. 2003), are selectively enriched in the M0 profile. Conversely, *unc-70* is exclusively elevated in the M24 dataset, a result consistent with the finding that UNC-70 (β-spectrin) is expressed in all embryonic cells early in development but becomes localized to muscles and neurons at hatching (Hammarlund, Davis et al. 2000). An important note in this regard is that *unc-70* is detected as an EG in the M0 dataset. These observations suggest that other transcripts that are differentially detected in M0 vs M24 data sets may also detect genes that may be differentially expressed in development to regulate assembly and function of muscle cells. It is also possible that some of these differences could be induced by differences in the cellular environments of the M0 (intact embryo) and M24 (*in vitro* culture) muscle cells. For example, 24 genes encoding proteasome subunits show elevated expression in the M24 data set whereas none of these transcripts are enriched in the M0 profile. This finding could be indicative of the general lack of innervation of muscle cells in culture because of the removal of motor neuron activity *in vivo* results in increased muscle protein degradation via a

Table 3.1. Genes required for muscle structure and assembly identified in microarray experiments					
Rank M0	**Rank M24**	**Cosmid**	**Common Name**	**Protein**	**Function**
13	277	ZC477.9a	*deb-1*	Vinculin	Attachment protein in dense bodies
108	75	C18A11.7a	*dim-1*	Immunoglobulin protein	Myofilament organization
757	88	T11B7.4a	*eat-1*	ALP/Enigma	Muscle cell adhesion
456	357	T11B7.4a	*eat-1*	ALP/Enigma	Muscle cell adhesion
-	393	K08C7.3a	*epi-1*	Laminin	Myofilament organization
-	228	Y38C1AB.8	*frm-5*	FERM domain	Cell adhesion/migration
539	782	F01G12.5a	*let-2*	Collagen	Muscle contraction/organization
528	517	Y105E8B.1a	*lev-11*	Tropomyosin	Contractile structural protein
92	332	C36E6.3	*mlc-1*	Myosin Light Chain	Muscle development
329	184	C36E6.2	*mlc-2*	Myosin Light Chain	Muscle development
286	259	F09F7.2	*mlc-3*	Myosin Light Chain	Muscle development
235	172	T22E5.5	*mup-2*	Troponin T	Sarcomere organization, cell contraction
709	236	K12F2.1	*myo-3*	Myosin Heavy Chain	Muscle contraction
181	53	F54C1.7	*pat-10*	Troponin C	Muscle contraction
100	-	ZK1058.2	*pat-3*	Beta-integrin	Myofilament organization
425	407	C29F9.7	*pat-4*	Integrin-linked kinase	Muscle attachment, dense bodies
64	-	T21D12.4	*pat-6*	Alpha-parvin	Muscle assembly
161	233	C08D8.2b	*tmd-2*	Tropomodulin	Muscle organization
121	217	F42E11.4	*tni-1*	Troponin I	Sarcomere organization
316	235	T20B3.2	*tni-3*	Troponin I	Muscle contraction
-	886	F53A9.10a	*tnt-2*	Troponin T	Muscle contraction
174	270	C14F5.3a	*tnt-3*	Troponin T	Muscle contraction
18	307	F07A5.7	*unc-15*	Paramyosin	Thick filament component
448	576	C47E8.7	*unc-112*	Pleckstrin-homology	Dense body assembly
365	340	D1081.2	*unc-120*	MADS transcription factor	Muscle development
516	260	ZK617.1a	*unc-22*	Twitchin	Regulation of contraction
238	114	ZK721.2	*unc-27*	Troponin I	Sarcomere structure, dense body positioning
451	680	B0350.2a	*unc-44*	Ankyrin	Cell migration
311	170	F30H5.1	*unc-45*	Myosin chaperone	Myosin assembly into thick filaments
489	-	ZC101.2e	*unc-52*	Perlecan	Muscle development
-	440	F11C3.3	*unc-54*	Myosin Heavy Chain	Muscle thick filaments
295	188	C38C3.5c	*unc-60*	Cofilin	Actin filament organization
-	651	K11C4.3	*unc-70*	Beta-spectrin	Sarcomere assembly
-	193	C04F6.4a	*unc-78*	Actin-interacting protein	Actin/cofilin assembly in myofilaments
133	191	F08B6.4a	*unc-87*		Myofilament assembly
94	24	C09D1.1c	*unc-89*	Myosin light chain kinase	M-line organization
320	303	Y105E8A.6	*unc-95*	Paxillin	Organization of thick and thin filaments
172	72	F14D12.2	*unc-97*	LIM-domain of the PINCH family	Assembly of muscle attachment structures
200	528	F08C6.7	*unc-98*	C2H2 zinc finger	Dense body and M-line maintenance

proteasome-dependent mechanism (Szewczyk, Hartman et al. 2000).

1324 genes are enriched in body wall muscle cells

The following sections describe bioinformatic analysis and GFP reporter assays performed on the total number of muscle genes detected as enriched in M0 and M24 muscle cells. These experiments were conducted to validate the proposal that our microarray strategies reliably detect muscle genes in both of these populations of body muscle cells.

***In litero* analysis**

A thorough search of the literature and WormBase (www.wormbase.org) (WS130 freeze) identified 213 genes with known expression in *myo-3*::GFP muscle cells (body wall muscle, anal muscle, vulval muscle). A majority of these genes, 166 (78%), are detected as EGs in *myo-3*::GFP muscle cells whereas 91 (42%) are enriched. Because our profiles are limited to embryonic muscle cells, we also compared the microarray data to a subset of 45 genes that are listed in wormbase as expressed in embryonic muscle. This comparison was very favorable as 39 (87%) are EGs and 36 (80%) are enriched in either one or both of the M0 and M24 data sets. Significantly, of the 27 genes with known expression in the DA motor neurons (see Chapter II), only 4 are enriched in the muscle profiles (*unc-129, pak-1, del-1, syg-1*), and one of these, *unc-129*, is known to be expressed in both body muscle and DA class motor neurons (Colavita, Krishna et al. 1998).

GFP reporters verify muscle microarray profiles

To confirm muscle expression for genes with unknown spatial distributions, we collaborated with Michael Krause (NIH/NIDDK), who generated GFP reporters from a random sampling of genes in the M0 and M24 data sets. 67% (38/57) of transgenic lines generated from these reporter genes showed expression in *myo-3*::GFP muscle cells, thereby indicating that previously uncharacterized genes in these microarray data sets are also likely to be expressed in these muscle cells *in vivo*. Table 3.2 notes expression of each GFP reporter in four adult muscles (body wall muscle, anal muscle, pharyngeal muscle, vulval muscle). Given that body wall cells are the predominant muscle cell type, it is not surprising that most of the reporters show expression in this tissue. The one exception is *zig-6*::GFP which is exclusively detected in anal muscle. This finding underscores the sensitivity of our methods to transcripts that may be selectively expressed in a subset of embryonically-generated muscle cells. Of note, 22 GFP reporters were also expressed in the vulval muscles although these post-embryonically derived cells are absent from primary cultures and therefore were not directly profiled by our methods. This finding is likely to reflect underlying similarities between vulval and body wall muscle cells. Interestingly, 6 reporters show expression in all 4 muscle types and may be indicative of genes required for general muscle function (Figure 3.9). In summary, the analysis of GFP reporters constructed from the muscle-enriched datasets confirm muscle expression *in vivo* and also reveal potentially interesting examples of genes with roles common to all four major muscle types as well as other transcripts with functions that may be selectively required in specific subsets of body muscle cells.

Table 3.2. GFP reporter expression in all four muscle groups						
Cosmid Name	**Common Name**	**Promoter Size**	**BWM**	**Vul**	**Anal**	**Phg**
F45D11.15		1.3 kb				
F21H7.3		669 bp				
R04B5.5		450 bp				
Y97E10AR.2		1.5 kb				
F57B7.4	*mig-17*	3.2 kb				
C02F12.7		1.8 kb				
D1007.14	*pqn-24*	737 bp				
B0304.1	*hlh-1*	3 kb				
F09B9.4		1.9 kb				
D2007.1		963 bp				
ZK792.7		3.8 kb				
F54D8.2		1.2 kb				
T04H1.1		2.6 kb				
Y69E1A.6	*sri-19*	1.4 kb				
K12F2.1	*myo-3*	2.6 kb				
K09A9.6		4 kb				
F54D7.4	*zig-7*	4 kb				
T26E3.2	*ndx-1*	4 kb				
T28A11.21		2.2 kb				
T03G11.8	*zig-6*	4 kb				
K01A2.1		3.3 kb				
F28H1.2	*cpn-3*	1.6 kb				
H22K11.4		3 kb				
E02H4.3		3 kb				
C18B2.3		1.4 kb				
T04A6.1		952 bp				
T13B5.3		639 bp				
R05F9.6		1.2 kb				
T22A3.4		733 bp				
T12D8.9		4 kb				
Y41G9A.3		4 kb				
K06A9.3		1.5 kb				
C36E6.3	*mlc-1*	2.7 kb				
K07C11.5		2.8 kb				

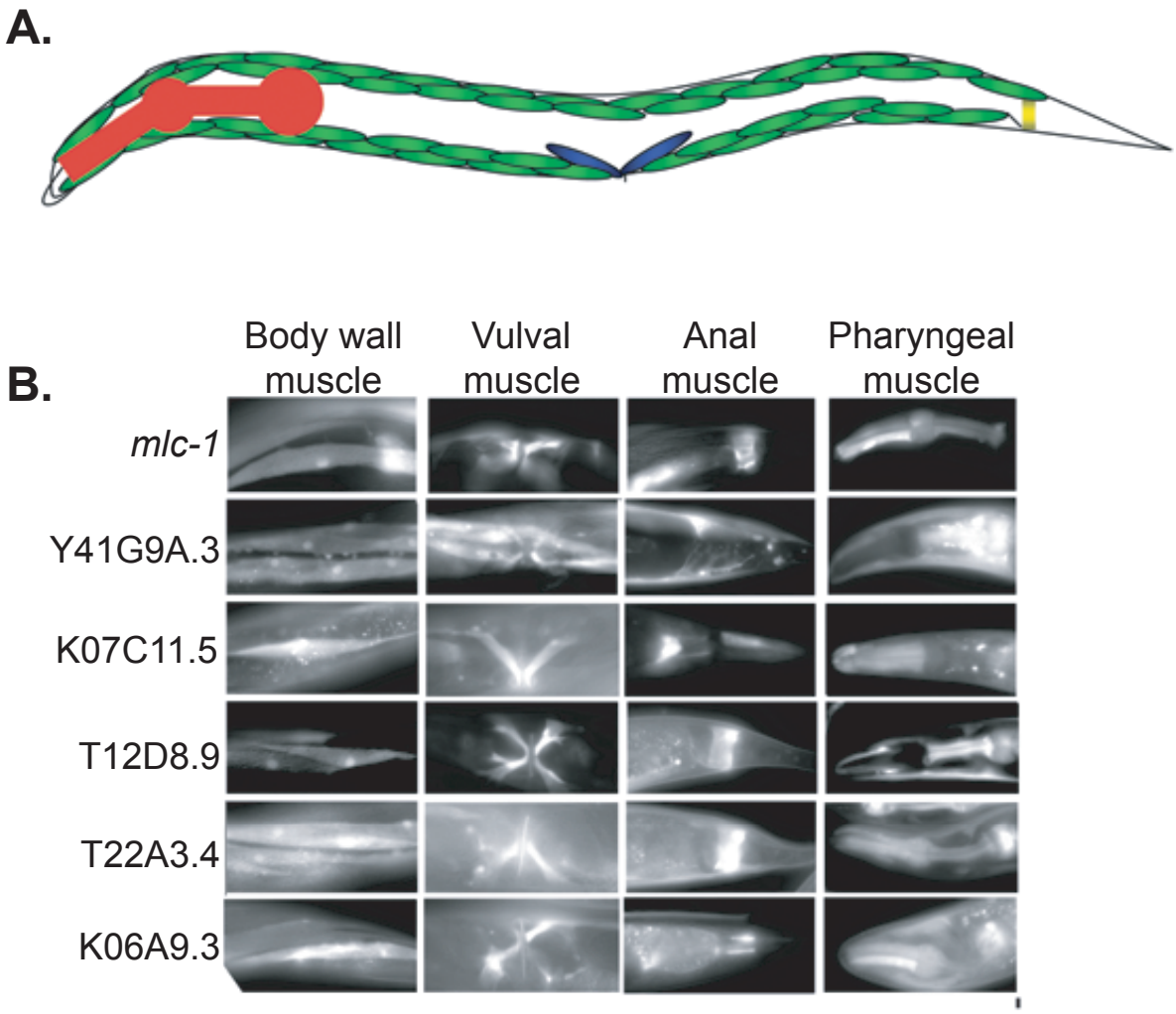

Figure 3.9. GFP reporters verify muscle genes. A. Cartoon showing major muscle groups of *C. elegans*. *myo-3*::GFP is expressed in body wall muscle (green), vulval muscle (blue) and anal muscle (yellow). Pharyngeal muscle is shown in red. B. Transgenic animals expressing GFP in all four major muscle classes. These genes are likely representative of transcripts necessary for basic muscle function.

Comparison of MAPCeL data to mRNA-tagging

The mRNA-tagging method was first introduced by Peter Roy and utilizes an epitope-tagged version of the poly-A binding protein, PAB-1, expressed under a cell-specific promoter. This allows for cross-linking of the PAB-1 to mRNA, followed by immunoprecipitation for the epitope tag, and thereby enriching for cell-specific RNAs. Dr. Roy first profiled the body wall muscle cells of the L1 larval animal. In his profile, he identified ~1,300 genes that were significantly elevated in muscle cells. In an effort to assess the data generated using these two different approaches, we compared the total list of genes detected in our muscle-enriched datasets to the list of genes enriched in the mRNA-tagging experiments. To our surprise, only 190 genes were in common between these two approaches. There are several differences between the methods used, which could account for this disparity. First, we profiled embryonic muscle whereas Dr. Roy profiled L1 larval muscle. Secondly, two separate platforms were used. We utilized the *C. elegans* Affymetrix array while they used the *C. elegans* DNA arrays manufactured in Stuart Kim's lab. Incidentally, we have now adopted the mRNA-tagging approach in our lab, and have discovered a high level of background associated with non-specific mRNA being immunoprecipitated, which could account for the differences detected. Given the extensive validation performed to verify our data, we believe that MAPCeL offers a robust system to generate accurate genes expression profiles from embryonic tissue.

Gene families enriched in muscle cells

Genetic studies in *C. elegans* have revealed a significant number of genes required for muscle structure, development and function (Moerman and Fire 1997). To

assess the potential utility of our data for expanding this catalog of muscle genes, we organized transcripts in our muscle microarray profiles according to functional categories. A sampling of these findings is presented below. Genes showing enriched transcript levels are denoted in bold type. All genes discussed in this section are listed in Table 3.3.

Muscle structure and function

The overall organization of *C. elegans* body wall muscle cells is similar to that of vertebrate skeletal muscle. The primary functional component is the sarcomere, a structure composed of myosin-containing thick filaments (A-band) that interdigitate with actin-containing thin filaments (I-band). The periodic array of tandem A-band and the I-band structures lead to the striated appearance of the body wall muscle cells. However, instead of being cross-striated as in vertebrates, the sarcomere is obliquely striated in the nematode; A-I alternations are offset ~6° from the longitudinal axis of the filaments as opposed to a 90° angle in cross-striated vertebrate muscle (Francis and Waterston 1985; Waterston 1988). The sarcomere maintains functional alignment through attachments of the thin filaments to dense bodies, which link thin filaments to the basement membrane of the cell. The thick filaments are stabilized within the sarcomere by the M-line, a specialized region in the A-band that may link adjacent thick filaments. The dense bodies and the M-line are the primary mediators of tension generated during muscle contraction (Waterston, Thomson et al. 1980). Hemidesmosomes that connect each muscle cell to the overlying cuticle transmit this force to deform the exoskeleton and thereby propel locomotion (Francis and Waterston 1985; Bartnik, Osborn et al. 1986).

Table 3.3. Gene families enriched in muscle cells				
Cosmid Name	**Common Name**	**Rank M0**	**Rank M24**	**KOG (or other description)**
Muscle Structure and Function				
K12F2.1	*myo-3*	709	236	Myosin class II heavy chain
F11C3.3	*unc-54*	-	440	Myosin class II heavy chain
Y11D7A.14		-	837	Myosin class II heavy chain
F45G2.2		-	748	Myosin class II heavy chain
C36E6.3	*mlc-1*	92	332	Myosin regulatory light chain, EF-Hand protein superfamily
C36E6.2	*mlc-2*	329	184	Myosin regulatory light chain, EF-Hand protein superfamily
F09F7.2	*mlc-3*	286	259	Myosin essential light chain, EF-Hand protein superfamily
F07A5.7	*unc-15*	18	307	Myosin class II heavy chain
ZK617.1a	*unc-22*	516	260	Projectin/twitchin and related proteins
W06H8.8	*tag-58*	171	542	Titin
T23E7.2a		716	148	Titin-related protein
F54E2.3a	*pqn-43*	6	237	Titin-related protein
T23E7.2e		22	348	Titin-related protein
K03C7.1		42	426	Titin-related protein
K03E5.5a		518	460	Titin-related protein
K07E12.1a		245	532	Titin-related protein
F21C10.7		199	-	Titin-related protein
C27B7.7		403	-	Titin-related protein
F15G9.4a	*him-4*	743	569	Hemicentin/Titin-related protein
C32E12.4		771	29	Titin-related protein
K03E6.6	*pfn-3*	65	95	Profilin
K06A4.3		587	396	Actin regulatory proteins (gelsolin/villin family)
Y71G12B.11		266	132	Talin
W03F11.6a		-	400	Actin filament-binding protein Afadin
F08A8.6	*tag-138*	-	446	Actin-binding protein SLA2/Huntingtin-interacting protein Hip1
Y66H1B.3		455	791	Actin-binding cytoskeleton protein, filamin
Y66H1B.2a		118	892	Actin-binding cytoskeleton protein, filamin
R01H10.3	*cor-1*	775	20	Actin-binding protein Coronin, contains WD40 repeats
Y105E8B.1a	*lev-11*	528	517	Actin filament-coating protein tropomyosin
F42E11.4	*tni-1*	121	217	Troponin I
ZK721.2	*unc-27*	238	114	Troponin I
T20B3.2	*tni-3*	316	235	Troponin I
T22E5.5	*mup-2*	235	172	Troponin
C14F5.3a	*tnt-3*	174	270	Troponin
F54C1.7	*pat-10*	181	53	Troponin C
ZC477.9a	*deb-1*	13	277	Alpha-catenin
ZK1058.2	*pat-3*	100	-	Integrin beta subunit (N-terminal portion of extracellular region)
C29F9.7	*pat-4*	425	407	Integrin-linked kinase
F54C1.7	*pat-10*	181	53	Calmodulin and related proteins (EF-Hand superfamily)
C47E8.7	*unc-112*	448	576	Mitogen inducible gene product (contains ERM and PH domains)
C18A11.7a	*dim-1*	108	75	Immunoglobin and related proteins
K11C4.5	*unc-68*	441	313	Ca2+ release channel (ryanodine receptor)
K11D9.2a	*sca-1*	194	30	Ca2+ transporting ATPase
C18E9.1	*cal-2*	473	537	Calmodulin and related proteins (EF-Hand superfamily)
C54E10.2		-	578	Ca2+ sensor (EF-Hand superfamily)
F21A10.1		764	646	Ca2+ sensor (EF-Hand superfamily)
K03E6.3	*ncs-3*	664	194	Ca2+ sensor (EF-Hand superfamily)
F40E10.3	*csq-1*	157	238	Calsequestrin
Dystrophin Glycoprotein Complex				
F15D3.1a	*dys-1*	265	882	Dystrophin-like protein

C33G3.1a	*dyc-1*	308	811	Muscular protein implicated in muscular dystrophy phenotype
F30A10.8a	*stn-1*	646	518	Syntrophins (type beta)
F07H5.2	*sgn-1*	275	118	Gamma/delta sarcoglycan
K01A2.1		209	631	Beta-sarcoglycan
H22K11.4		435	35	Sarcoglycan complex, alpha/epsilon subunits
F27D9.8a		91	-	
T03F7.1	*snf-11*	-	639	Sodium-neurotransmitter symporter
Transcription Factors				
Y47D3B.7	*sbp-1*	331	7	Predicted DNA-binding protein
F46G10.6	*mxl-3*	546	8	Upstream transcription factor 2/L-myc-2 protein
T20B3.3	*srh-215*	-	54	Predicted olfactory G-protein coupled receptor
T26C11.1	*tbx-41*	-	128	TBX2 and related T-box transcription factors
T04C10.4	*atf-5*	-	175	Activating transcription factor 4
C29G2.5		-	316	7-transmembrane receptor
F40G9.11	*mxl-2*	-	317	bHLHZip transcription factor BIGMAX
W07G1.3		-	334	Activating transcription factor 4
D1081.2	*unc-120*	365	340	Regulator of arginine metabolism and related MADS box-containing transcription factors
T27C4.4a	*egr-1*	-	350	Histone deacetylase complex, MTA1 component
Y46H3D.6		-	427	Hormone receptors
C33G8.6	*nhr-42*	-	513	Hormone receptors
C49D10.2		-	522	Nuclear hormone receptor
T24A6.11		-	530	Nuclear hormone receptor
F45E4.9	*hmg-5*	-	547	HMG box-containing protein
H05G16.1	*frm-3*	-	661	Rho guanine nucleotide exchange factor CDEP
T22H6.6	*gei-3*	-	668	HMG-box transcription factor Capicua and related proteins
C10G8.7	*ceh-33*	615	688	Transcription factor SIX and related HOX domain proteins
C10G8.6	*ceh-34*	358	693	Transcription factor SIX and related HOX domain proteins
B0414.2	*rnt-1*	93	702	Runt and related transcription factors
Y46H3D.7		-	708	Hormone receptors
ZC64.3a	*ceh-18*	-	709	Transcription factor OCT-1, contains POU and HOX domains
F44E2.6		-	723	Predicted pilin-like transcription factor
F41B5.9		-	848	Hormone receptors
B0304.1a	*hlh-1*	145	86	Myogenic factor/Myogenin
R13A5.5	*ceh-13*	325	-	Transcription factor zerknullt and related HOX domain proteins
F28B12.2	*egl-44*	457	-	TEF-1 and related transcription factor, TEAD family
T14G12.4a	*fkh-2*	437	-	Transcription factor of the Forkhead/HNF3 family
F38A6.3a	*hif-1*	575	-	Hypoxia-inducible factor 1/Neuronal PAS domain protein NPAS1
C37F5.1	*lin-1*	25	-	Predicted transcription factor
R03E9.1	*mdl-1*	376	-	Upstream transcription factor 2/L-myc-2 protein
Y5H2B.2a	*nhr-13*	600	-	Hormone receptors
F58G6.5a	*nhr-34*	727	-	Hormone receptors
T23H4.2	*nhr-69*	190	-	Hepatocyte nuclear factor 4 and similar steroid hormone receptors
Y68A4A.6	*srz-96*	619	-	7-transmembrane receptor
K10D3.3	*taf-11.2*	464	-	Transcription initiation factor TFIID, subunit TAF11
Y65B4BR.5a		250	-	Transcription factor containing NAC and TS-N domains
K06A9.2		532	-	Transcription factor activity
Neuromuscular Junction				
F09E8.7	*lev-1*	648	182	Acetylcholine receptor
C35C5.5	*lev-8*	86	772	Acetylcholine receptor
T08G11.5	*unc-29*	70	411	Acetylcholine receptor
F21F3.5	*unc-38*	440	432	Acetylcholine receptor
Y110A7A.3	*unc-63*	-	79	Acetylcholine receptor
ZC504.2	*acr-8*	623	733	Acetylcholine receptor
F25G6.3a	*acr-16*	-	41	Acetylcholine receptor
T21C12.1a	*unc-49*	428	-	GABA receptor
K06C4.6a	*mod-1*	-	802	Ligand-gated ion channel
C27H5.8	*glc-4*	780	-	Ligand-gated ion channel

T24D8.1		-	67	Ligand-gated ion channel
T27A1.4		201	834	Ligand-gated ion channel
Y113G7A.5		753	-	Ligand-gated ion channel
F22A3.3	*glr-8*	249	-	Glutamate-gated kainate-type ion channel receptor subunit GluR5 and related subunits
ZK867.2		593	-	Glutamate-gated kainate-type ion channel receptor subunit GluR5 and related subunits

Thick filaments are largely comprised of two myosin heavy chain proteins, MHC A and MHC B, encoded by the ***myo-3*** and ***unc-54*** genes, respectively (Miller, Ortiz et al. 1983; Miller, Stockdale et al. 1986; Waterston 1988). Interestingly, *myo-3* is enriched in both the M0 and M24 data sets whereas *unc-54* is selectively elevated in the M24 profile but detected as an EG in M0 muscle cells. This finding indicating that *myo-3* transcript levels are elevated before *unc-54* mRNA during body muscle development is consistent with the observation that MHC A protein is also more abundant than UNC-54 in early embryonic muscle cells (Epstein, Casey et al. 1993). The apparent sequential expression of *myo-3* and *unc-54* parallels their distinct roles in thick filament assembly; MHC A establishes a bipolar nucleation complex to which UNC-54 is added as the filament elongates (Miller, Ortiz et al. 1983; Epstein, Miller et al. 1985; Epstein, Ortiz et al. 1986). Differential roles in muscle development are also underscored by the findings that *myo-3* null mutants are inviable as embryos, whereas genetic ablation of *unc-54* disrupts muscle structure but does not result in lethality (Moerman, Plurad et al. 1982; Waterston 1989; Moerman and Fire 1997). Therefore, selective enrichment of *myo-3* in the M0 dataset indicates that *myo-3* may be an essential myosin gene expressed during early embryonic development to initiate thick filament assembly, whereas UNC-54 is selectively involved in thick filament elongation and muscle contraction (Miller, Ortiz et al. 1983). Two additional transcripts, **Y11D7A.14** and **F45G2.2**, with sequence similarity to the myosin heavy chain genes are elevated in the M24 data set; **Y11D7A.14** encodes an unconventional myosin that is not well-conserved relative to the other structural myosins expressed in muscle. **F45G2.2**, however, is a member of the myosin II class of striated

muscle MHCs that includes *myo-3* and *unc-54*. Potential functions for these additional myosin molecules in muscle can now be explored by genetic or RNAi methods.

The myosin light chain proteins regulate the ATPase activity of the MHCs. Three myosin light chain genes (***mlc-1, -2, -3***) are enriched in both datasets. Genetic data indicate that ***mlc-3*** is an essential muscle component whereas ***mlc-1*** and ***mlc-2*** appear to have redundant functions (Moerman and Fire 1997). Paramyosin (***unc-15***), a core component of thick filaments that interacts with MHC A (MYO-3) and MHC B (UNC-54), shows elevated transcript levels in both M0 and M24 profiles. Finally, UNC-45, a highly conserved myosin binding protein and chaperone that directs assembly of these components is enriched (Hutagalung, Landsverk et al. 2002).

Muscle structure and function also depend on a family of very large cytoplasmic proteins, that contain multiple fibronectin and immunoglobulin domains (Flaherty, Gernert et al. 2002; Ferrara, Flaherty et al. 2005). The founding member of this family, ***unc-22***, encodes "twitchin," which when mutated causes constant twitching movements (Waterston, Thomson et al. 1980; Moerman and Fire 1997). ***unc-22*** is enriched in both datasets. A second member of this family, titin, adopts an elongated structure that spans half a sarcomere (from Z line to M Line) and functions in myofibril assembly and elasticity (Gregorio, Granzier et al. 1999). In *C. elegans*, titin is somewhat smaller, and likely does not function in thick filament organization as expression is first detected after initial assembly begins in the embryo (Flaherty, Gernert et al. 2002). Titin is, however, detected before thin filaments arise and may be involved in actin assembly as it localizes to the I-band in L2/L3 larval animals (Flaherty, Gernert et al. 2002). Previous work identified a 90kb gene, that covers 6 predicted genes, and encodes three distinct titin

isoforms in *C. elegans* (Flaherty, Gernert et al. 2002). We find that one of the identified titin transcripts (**W06H8.8**) is enriched in both datasets, along with 8 transcripts that contain titin-like domains (Table 3.3).

Thin filaments are primarily composed of actin, troponin and tropomyosin. While actin genes are not enriched in the muscle data sets due to high expression levels in non-muscle cells, several actin genes (*act-2, -3, -4,* -5) are detected as EGs. In contrast, we see elevated expression of several actin-binding and regulatory proteins. Among these are members of the **Profilin (e.g. *pfn-3*)** and **Gelsolin (e.g. K06A4.3)** families, which are proposed to regulate thin filament assembly (Table 3.3) (Waterston 1988; Moerman and Fire 1997). Sarcomeres are initially assembled during embryonic development. Muscle cells add new sarcomere repeats and expand in size as the animal grows (Mackenzie, Garcea et al. 1978). The continuous growth of the contractile apparatus during development could account for the expression of key structural components (e.g. *tni-1*, troponin) in both datasets. On the other hand, as noted above, genes identified in the M0 dataset may play important roles in the initial formation or organization of the sarcomere whereas transcripts that are uniquely enriched in the M24 profile may be required for sarcomere maintenance during expansion of the body wall muscle cells.

Troponin and tropomyosin form a complex that regulates actin-myosin interactions in response to calcium (Waterston 1988; Moerman and Fire 1997). In *C. elegans*, tropomyosin is encoded by ***lev-11***, which is enriched in both datasets. Troponin is comprised of three subunits, TnI, TnT and TnC. There are four TnI genes in the nematode, of which three (***tni-1, unc-27, tni-3***) are expressed in body wall muscle (Burkeen, Maday et al. 2004). TnT is encoded by two genes, ***mup-2*** and ***tnt-3***, and ***pat-***

10 encodes TnC. Consistent with the importance of these genes in muscle function, all of them are enriched in both muscle datasets.

Myofibrils are attached to the cell membrane through dense bodies. Many components of this structure are known including the following enriched genes: vinculin (***deb-1***), talin (**Y71G12B.11a, b**), afadin (**W03F11.6a**) and β-1 integrin (***pat-3***). Previous studies have also identified ***unc-112*** and ***dim-1*** as components required for dense body assembly and maintenance, respectively (Rogalski, Mullen et al. 2000; Rogalski, Gilbert et al. 2003). All of these components are enriched in both datasets. In addition to these genes, we also identified several other actin-binding proteins that may play an integral role in the assembly of the dense bodies (Table 3.3.).

Muscle contraction is facilitated by the release of intracellular calcium stores upon stimulation by an action potential. Signals received from neurons induce the release of calcium from the sarcoplasmic reticulum. Calcium initiates myofibril contraction and is rapidly pumped back into the sarcoplasmic reticulum via an ATP-dependent calcium channel (Zwaal, Van Baelen et al. 2001). As expected, a significant number of calcium channel and calcium ion binding proteins are detected as enriched transcripts. These include ***unc-68*** and ***sca-1***. ***unc-68*** encodes the nematode homolog of the Ryanodine receptor (RyR). The primary function of the RyR is to release stored calcium from the sarcoplasmic reticulum (Maryon, Coronado et al. 1996; Maryon, Saari et al. 1998). Consistent with this finding, **UNC-68** is expressed in body wall muscle and mutations that disrupt the *unc-68* gene lead to uncoordinated movement indicative of compromised muscle function. ***sca-1*** encodes the nematode sarco-endoplasmic reticulum calcium ATPase (SERCA). The SERCA channel is responsible for removing calcium from the

cytoplasm into calcium stores (Zwaal, Van Baelen et al. 2001). We also find three genes that are predicted to function as calcium sensors (**C54E10.2, F21A10.1, *ncs-3***), as well as other components of calcium signaling including **calsequestrin** and **calmodulin** (Table 3.3).

The Dystrophin Glycoprotein Complex (DGC)

In humans, Duchenne and Becker muscular dystrophies arise from mutations in a single gene, dystrophin; these diseases are characterized by severe muscle weakening and degeneration (Muntoni, Torelli et al. 2003). Dystrophin is localized beneath the sarcolemma and is attached to actin filaments as well as to the Dystrophin glycoprotein complex (DGC) (Gieseler, Grisoni et al. 2000). This protein complex functions to stabilize the sarcolemma and prevent damage to muscle fibers induced by long-term contraction. Mutations in the *C. elegans* homolog of dystrophin (***dys-1***) lead to hyperactivity, but muscle degeneration has not been observed (Grisoni, Martin et al. 2002; Segalat 2002). Nevertheless, in *C. elegans*, as in mouse, mild MyoD (***hlh-1***) mutations in conjunction with dystrophin deficiencies act synergistically to induce muscle degeneration (Megeney, Kablar et al. 1996; Gieseler, Grisoni et al. 2000). *C. elegans* is, therefore, a useful model to study these degenerative diseases. In our microarray data, we have confirmed that most of the major components of the DGC (Grisoni, Martin et al. 2002)[***dys-1*** (Dystrophin), ***dyc-1*** (CAPON), ***stn-1*** (Syntrophin) and ***sgn-1*** (Sarcoglycan)] are enriched in *C. elegans* body wall muscle, with the exception of *dyb-1* (Dystrobrevin). Other enriched transcripts with potentially related functions include the sarcoglycan-like genes, **K01A2.1** and **H22K11.4;** a GFP reporter for

H22K11.4 confirms its expression in body wall, anal and vulval muscles. Additionally, the M0 profile detects **F27D9.8a**, a second syntrophin-like gene. Given the conservation between the nematode and vertebrate homologs of the DGC components it is likely that our data contains novel proteins that may be required to maintain muscle integrity and when mutated lead to muscle-related diseases.

Transcription Factors

Myogenesis is initiated by a family of helix-loop-helix (HLH) transcription factors that includes MyoD, myogenin, MRF-4/herculin/Myf-6, and Myf-5 (Fukushige and Krause 2005). In *C. elegans*, ***hlh-1*** encodes MyoD and is first detected at the 28 cell stage of embryogenesis in the four blastomeres (MS, C, D, AB) that give rise to the body wall muscle cells (Krause, Fire et al. 1990). Consistent with the important role of ***hlh-1*** in early myogenesis, the *hlh-1* transcript is enriched in both muscle data sets. Also enriched is the MADS transcription factor **UNC-120**. ***unc-120*** is expressed early in embryonic development in the muscle precursor cells and is predicted to regulate expression of the essential muscle components actin and myosin (www.wormbase.org); ***unc-120*** mutations result in paralysis, disorganized muscle and reduced levels of myosin and actin (Dichoso, Brodigan et al. 2000). Additionally, we detect ***ceh-13***, a member of the HOX family of transcription factors that regulate cellular differentiation in specific body regions. **CEH-13** expression in the embryo is limited to the anterior body muscles and other cell types in the head region. *ceh-13* is essential for embryonic development as null mutations are lethal. Interestingly, weaker ***ceh-13*** mutants develop normally until the elongation stage of embryogenesis, when they display a “twitching” phenotype; rare post-

hatching animals show uncoordinated movements indicative of impaired muscle function (Brunschwig, Wittmann et al. 1999).

In addition to these characterized transcription factors, we detect eight putative **nuclear hormone receptors** (NR) (see Table 3.3.). In *C. elegans,* the NR family consists of ~280 receptors that are presumptively regulated by lipophilic hormones to control a variety of processes from sex determination to lifespan (Gissendanner, Crossgrove et al. 2004). Functions for the NR transcripts showing enriched expression in our muscle data sets have not been characterized. However, recent studies of an NR gene, *nhr-40*, that is detected as an EG in both data sets, have identified a key role in muscle development. Mutations in the NR gene, *nhr-40*, lead to late embryonic/early larval arrest with irregular development of body wall muscle cells and uncoordinated locomotion (Brozova, Simeckova et al. 2006). The significance of this class of transcription factors to vertebrate muscle development is uncertain as the nematode NR sequences are not well-conserved. On the other hand, the absence of clear mammalian homologs offers the possibility of developing phylum-specific nematocides that target these diverged NR proteins.

A total of 38 transcription factors are enriched in muscle cells in these experiments. The functions of a majority of these transcription factors in muscle development have not been explored. It is also interesting that most of these transcription factors are selectively enriched in either the M0 (13) or M24 (18) data sets. This finding could mean that muscle development is orchestrated by a diverse array of transcription factors with functions that are specifically required in either early muscle precursor cells or later to regulate terminal muscle differentiation.

The neuromuscular junction

Coordinated locomotion is mediated by signaling between motor neurons and their postsynaptic muscle partners. Neurotransmitters released by the presynaptic cell induce the opening of ion channels thereby altering the local membrane potential to regulate muscle cell activity. These transmitter-gated ionotropic receptors are clustered at the synapse and open transiently in response to neurotransmitter binding. Consistent with the importance of these molecules in facilitating synaptic signals, we find a large number of ligand-gated ion channels enriched in body wall muscle cells. All of the essential subunits of the levamisole-sensitive nicotinic acetylcholine receptor (nAChR) (***lev-1, lev-8, unc-29, unc-38, unc-63***) are enriched. Two additional uncharacterized nAChR genes, ***acr-8*** and ***acr-16,*** were also detected. These genes were further tested as candidates for the levamisole-insensitive nAChR (see below). Whereas the ACh receptors trigger muscle contraction, the neurotransmitter, GABA, inhibits muscle activation. The GABA receptor gene ***unc-49*** that mediates this response is enriched. In addition to the expected ACh and GABA receptors, we also detected ionotropic receptors for other classes of neurotransmitters that have not been previously shown to regulate muscle activity. Prominent among these is *mod-1*, which encodes a serotonin-gated chloride channel required for 5HT-dependent inhibition of *C. elegans* locomotion (Ranganathan, Cannon et al. 2000). **T24D8.1** also encodes a potential 5-HT receptor. Other candidate ionotropic anion channel receptor genes include ***glc-4*** (glutamate-gated Cl- channel) **T27A1.4,** and **Y113G7A.5** (both similar to GABA-A receptor). Excitatory

responses to glutamate could be mediated by ***glr-8*** (glutamate-gated kainite-type ion channels).

P*acr-8*::GFP and P*acr-16*::GFP are expressed in body wall muscle

We generated transgenic *promoter*::GFP reporter strains of the *acr-8* and *acr-16* genes. In both cases, GFP expression was detected in body wall muscles (Figure 3.10). P*acr-8::*GFP is strongly expressed in body muscle cells, anal muscle, vulval muscle and ventral cord motor neurons. P*acr-16*::GFP is detected in body wall muscle cells (but not the vulval or anal muscles) and is also detected in a subset of neurons, notably the DB motor neurons in the ventral nerve cord. Consistent with the identification of these subunits in our microarray data from embryonic muscle cells, we see expression of both P*acr-8*::GFP and P*acr-16*::GFP in the embryo (data not shown).

ACR-16 is an essential subunit of the levamisole-insensitive AChR

In mutants which lack a functional levamisole-sensitive receptor (i.e. ***unc-63***) the body wall muscles are unresponsive to the acetylcholine agonist levamisole. However, these mutants still exhibit residual responses to acetylcholine. This finding indicates that there must be an additional levamisole-insensitive receptor functioning at the neuromuscular junction (Richmond and Jorgensen 1999). Using established electrophysiological methods to record from individual muscle cells (Richmond and Jorgensen 1999), the Richmond lab measured the evoked-responses to acetylcholine and levamisole in *acr-8(ok1240)* and *acr-16(ok789)* mutant animals. *acr-8(ok1240)* mutants displayed wildtype responses to both acetylcholine and levamisole indicating that ACR-8

is not an essential component of either acetylcholine channel. However, *acr-16 (ok789)* mutants showed a wildtype response to levamisole but acetylcholine evoked currents were absent (Figure 3.11). To confirm that the defects exhibited by the *acr-16(ok789)* mutants were due to the loss of *acr-16* and not a background mutation in the strain, the Richmond lab created mosaic animals that expressed ACR-16 (detected by a GFP co-selectable marker) in limited numbers of muscle cells. With this strain they were able to record from genetically wildtype muscle cells (GFP+), as well as *acr-16* mutant cells (GFP-) in the same animal. These experiments confirmed that GFP-expressing cells displayed wildtype levels of ACh-evoked currents whereas non-GFP and therefore *acr-16* mutant muscle cells were unresponsive. The results of these experiments confirm earlier physiological data pointing to the existence of a two pharmacologically distinct classes of body muscle ACh receptors (levamisole sensitive vs. levamisole insensitive) and firmly establish that ACR-16 is an essential component of the levamisole insensitive ACh receptor. The model that both classes of ACh receptors contribute to overall body muscle activity is supported by a genetic experiment showing that loss of both receptors in the double mutant *unc-63(x37); acr-16(ok789)* leads to more severe locomotory defects than either single mutant alone. These findings have been independently confirmed (Francis, Evans et al. 2005).

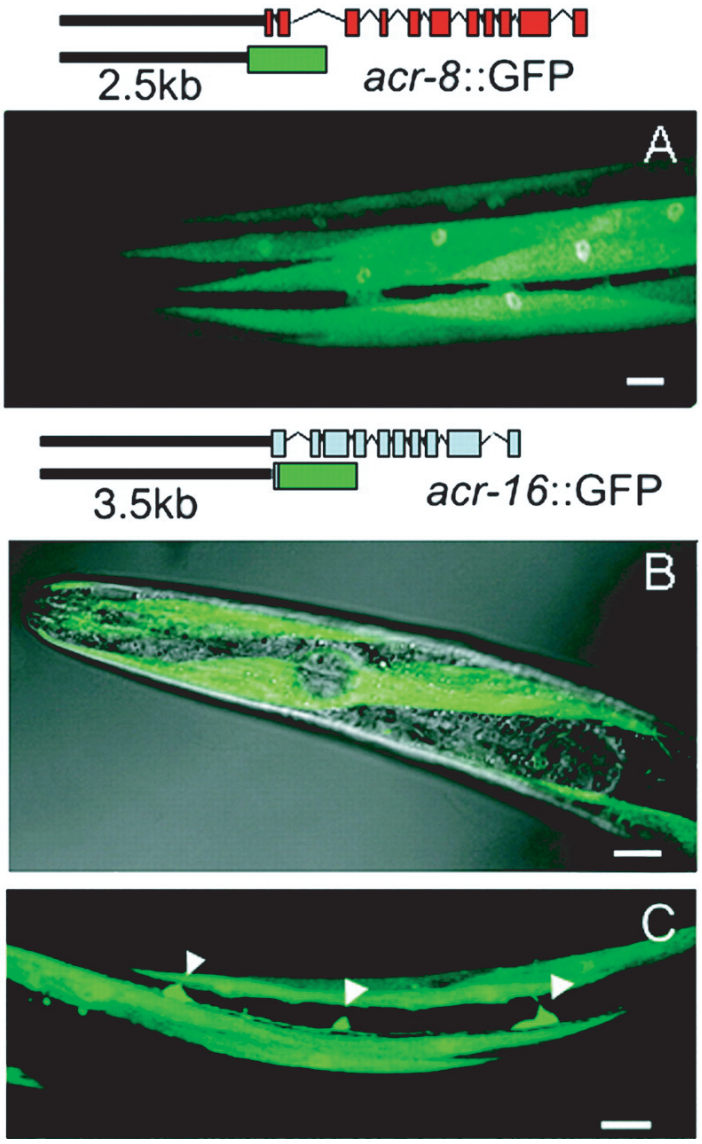

Figure 3.10. GFP reporters for *acr-8* and *acr-16* are expressed in body wall muscle cells. A. Head region showing *acr-8*::GFP expression in body muscle cells. B. Combined differential interference contrast and GFP images of *acr-16*::GFP expression in body muscle cells. The spiral disposition of the body muscle cells is due to the Rol-6 transgenic marker. C. Ventral view of the midbody region. *acr-16*::GFP was expressed in body muscles and in DB motor neurons (arrowheads) in the ventral nerve cord. All images are confocal projections. Scale bars = 10 μm.

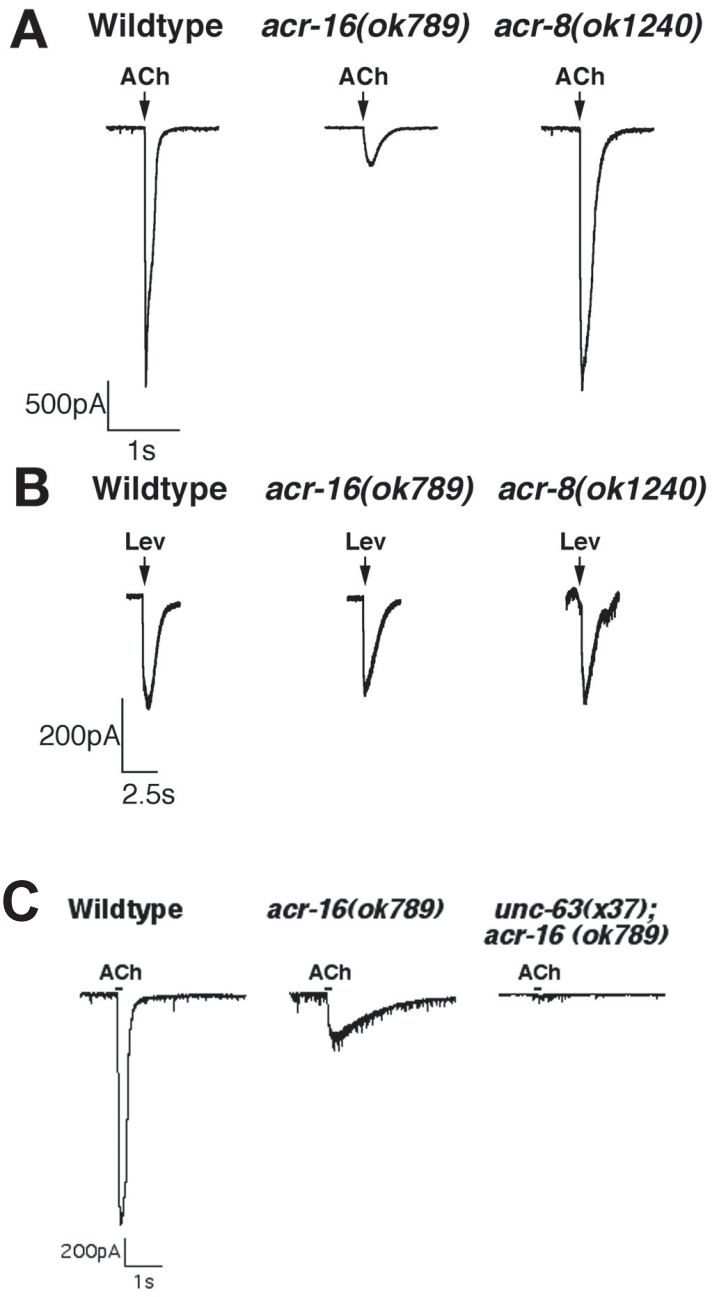

Figure 3.11. *acr-16 (ok789)* mutants reduce levamisole-resistant muscle ACh responses while *unc-63; acr-16* double mutants eliminate the muscle ACh responses. A. The representative current traces of voltage-clamped body wall muscle ACh responses (100-ms pulses of 5 x 10^{-4} M ACh) demonstrate that *acr-16(ok789)* mutants, but not *acr-8(ok1240)* mutants, had reduced ACh current amplitudes compared to the wildtype (WT). B. Responses to 100-ms pulses of 5 x 10^{-4} M levamisole. Levamisole current amplitudes were unaffected in *acr-8(1240)* and *acr-16(ok789)* mutants. C. Voltage-clamped muscle recordings demonstrate that the residual inward current elicited by 100-ms applications of ACh in *acr-16* mutants was abolished in *unc-63(x37); acr-16(ok789)* double mutants.

Discussion

Expression profiling identifies new muscle genes

Chapter II outlines a new technology, MAPCeL, that we have used to obtain gene expression profiles from specific *C. elegans* cell types. We have now applied this methodology to profile the body wall muscle cells that regulate locomotion. To gain the full complement of genes expressed in muscle we profiled *myo-3*::GFP labeled muscle cells at two different time points, immediately after dissociation from the embryo (M0) and following 24 hours in culture (M24). As expected, a significant number of genes are shared between these two data sets including most of the known structural components of the muscle sarcomere. It is also interesting, however, that an approximately equal number of genes in each data set are uniquely enriched relative to other embryonic cells in either the M0 or M24 profiles. This disparity could be due to differences in the developmental age of the profiled muscle cells. Expression of muscle sarcomere components (i.e. *myo-3* encoded MHC A) is initially noted at ~300 min of embryonic development. At this stage, myofilament proteins are diffusely distributed in the cytoplasm but can be seen to accumulate at sites adjacent to the cell membrane after muscle cells have migrated to their final locations in each body wall quadrant (~420 min). These early muscle cells (<400 min) are readily released from young embryos for FACS isolation and, therefore, constitute the majority of *myo-3*::GFP cells surveyed in the M0 data set. Differentiated muscle cells, which are not readily dissociated from older embryos by our methods, can be obtained, however, after overnight culture of these early muscle precursor cells *in vitro*. These cells are profiled in the M24 data set. It will be

interesting to determine if genes that are differentially expressed in the M0 vs M24 data sets are also required for stage-specific functions during muscle cell proliferation and differentiation in the embryo. One example of this is the identification of 38 transcription factors in these two experiments, of which only 7 are common to both the M0 and M24 datasets. The transcription factors that are differentially expressed could perform important functions in the early vs. late development of the embryonic muscle; genes identified in the M0 dataset could be required for the initial differentiation of muscle cells whereas those identified in the M24 set could be involved in cell function, growth or maintenance.

By examining the sum of genes detected as enriched we have demonstrated that each dataset, M0 and M24, contains a valid representation of genes required for body wall muscle function. Approximately 80% of known muscle genes are expressed in these datasets. An even greater fraction (90%) of muscle genes known to be expressed in the embryo are detected. In addition, we generated over 50 transgenic GFP trangenes for previously uncharacterized genes in these profiles and confirmed that close to 70% of these reporters are expressed in the body wall muscle cells. These results confirm that the microarray data sets that we have generated are largely comprised of muscle genes. With over 1300 muscle-enriched transcripts identified in these profiles, these data represent a rich resource for identifying new genes with key roles in muscle differentiation or function.

The importance of the nematode system to identify genes that have conserved functions in vertebrate animals has been well documented. Many groups have now adapted the worm to study human diseases. An example of this is the use of *C. elegans*

to study muscular dystrophy. In combination with *hlh-1*, animals mutant for *dys-1* (dystrophin) exhibit muscle wasting similar to that observed in vertebrate systems. *hlh-1* encodes the *C. elegans* homolog of MyoD, a transcription factor required for muscle differentiation (Krause, Fire et al. 1990). Contrary to the lethal phenotype of *hlh-1* in *C, elegans* (Chen, Krause et al. 1992), MyoD mutations in mice have very mild muscle defects (Rudnicki, Braun et al. 1992); however, in combination with dystrophin (mdx) they exhibit severe muscle wasting, likely due to a failure in satellite cell renewal and muscle regeneration (Megeney, Kablar et al. 1996). While satellite cells are not prevalent in *C. elegans*, the *hlh-1*(hypomorph);*dys-1* double mutants display a similar muscle degeneration phenotype (Gieseler, Grisoni et al. 2000). The mechanism in which this occurs is not understood; however, it is possible that, in combination, these genes affect the normal repair mechanisms that maintain muscle integrity. Given that we have identified most of the essential components of the Dystrophin glycoprotein complex, it is likely that the data generated in these microarray experiments may contain additional genes that are critical for muscle development and have potential roles in human muscle disease.

ACR-16 is an essential component of the levamisole-insensitive nAChR

The identification of *acr-16* as a novel component of the levamisole-insensitive acetylcholine receptor demonstrates the utility of our approach. ACR-16 is the closest nematode homolog of vertebrate α7 nicotinic acetylcholine receptor subunits, sharing ~47% identity. Given that ACR-16 was the only identified nACh receptor subunit required for the levamisole-insensitive response, ACR-16 may function as a homomeric

receptor *in vivo*. This idea is consistent with the finding that both ACR-16 and its vertebrate α7 homolog are capable of forming functional homomeric nicotinic acetylcholine receptors in heterologous cells (e.g. *Xenopus* oocytes) (Ballivet, Alliod et al. 1996) (Couturier, Bertrand et al. 1990; Seguela, Wadiche et al. 1993; Drisdel and Green 2000). α7-like acetylcholine channels are required for learning and memory functions in the human brain and defects in these genes have been linked to specific neurological disorders, including Parkinson's disease and epilepsy (Gotti and Clementi 2004). While the physiological properties of α7 nACh receptors in heterologous cells have been extensively described, the mechanisms by which these receptors are localized to their sites of action *in vivo* are poorly understood. The Richmond lab is now using genetic approaches to delineate mechanisms by which ACR-16 is trafficked to the neuromuscular junction. It seems likely that these experiments will provide insight into the regulation of vertebrate nAChR localization.

The two classes of nicotinic acetylcholine receptors, the levamisole-sensitive and the levamisole-insensitive, account for the complete response to acetylcholine exhibited by muscle cells. Interestingly, although animals mutant in both nicotinic receptors [*unc-63(x37); acr-16(ok789)*] are unresponsive to acetylcholine and exhibit severe locomotory defects, these animals retain some movement as evidenced by locomotion assays. One explanation is that there may be additional excitatory channels that could be reflective of muscarinic, peptidergic, co-transmitter, or myogenic activity. Further examination of our microarray data could provide candidate genes that may be involved in additional signaling pathways present at the neuromuscular junction. Interestingly, we detect a muscarinic acetylcholine receptor (*gar-3*) as well as three glutamate receptors (e.g. *glr-8*,

ZK867.2, F59E12.8) that could provide excitatory inputs to muscle cells. While it has not been shown that the motor neurons release glutamate, it is possible that additional locomotory information may be coming directly from the command interneurons, which are glutamatergic (Brockie, Madsen et al. 2001; Brockie, Mellem et al. 2001). In addition, evidence suggests that neuropeptide signaling plays an important role in modulating ACh release from neurons (Jacob and Kaplan 2003). In accordance with this, we detect the neuropeptide receptor, T22D1.12, as enriched, while two additional receptors are EGs. Furthermore, it has been proposed that neuropeptide signaling may regulate ACh release through retrograde signaling from muscle cells (Doi and Iwasaki 2002; Jacob and Kaplan 2003); consistent with this observation, we detect enrichment of one neuropeptide gene, *nlp-2*, and we also detect nine additional neuropeptide genes as EGs. Taken together, it is likely that further analysis of previously uncharacterized genes will uncover the additional excitatory mechanisms utilized at the neuromuscular junction.

Profiling the motor circuit using MAPCeL

In Chapter II and continued here in Chapter III, I have described my efforts to profile the cholinergic DA motor neurons and the body wall muscles they innervate. To further define the molecular properties that underlie coordinated locomotion, MAPCeL has also been used to profile the cholinergic DB motor neurons (RMF) and the GABAergic DD motor neurons (S. Barlow, L. Earls). The identification of *acr-16* from the muscle experiments shows the utility of these data for identifying new genes required for essential cellular functions. From the data generated using MAPCeL we can now

begin to identify the unique combinations of genes that are necessary to regulate the functional development of the *C. elegans* motor circuit.

CHAPTER IV

GENOMIC APPROACHES TO IDENTIFY UNC-4 TARGET GENES

Introduction

The major goal of my project was to identify genes that act downstream of the homeodomain transcription factor UNC-4. UNC-4 is required to specify pre-synaptic inputs to a subset of VA motor neurons (Miller, Shen et al. 1992). In *unc-4* mutants, VA motor neurons do not receive A-type inputs; instead, they are miswired with inputs normally reserved for their VB sister cells (White, Southgate et al. 1992). In addition, UNC-4 is required to regulate the levels of synaptic vesicles in UNC-4-expressing cells, thereby mediating the strength of synaptic output from these neurons (Lickteig, Duerr et al. 2001). These two defects lead to the inability of *unc-4* mutants to crawl backward. The genes that function downstream of UNC-4 to mediate these functions, however, have remained elusive. Genetic screens have not identified UNC-4 targets, likely due to the redundancy of target genes; therefore, we have adopted genomic approaches to identify the molecular components that act downstream of UNC-4 to regulate the specificity of synaptic input as well as the strength of synaptic output.

Previous studies from our lab suggest that UNC-4 and its cofactor, UNC-37, function as transcriptional repressors (Pflugrad, Meir et al. 1997; Winnier, Meir et al. 1999). Thus, microarray experiments were aimed at identifying genes that show elevated expression in *unc-4* and *unc-37* mutant backgrounds. Initially, a former graduate student in the lab, Stephen Von Stetina, conducted microarray experiments using RNA isolated

from the entire animal. Wildtype RNA was compared to RNA extracted from *unc-4* and *unc-37* mutants. This approach, however, failed to identify *bona fide* target genes. This result is likely due to insufficient sensitivity of the whole animal approach as UNC-4 is expressed in less than 30 of the 959 cells that comprise the post-embryonic worm (Miller and Niemeyer 1995). To overcome this problem, we established methods to isolate RNA specifically from UNC-4-expressing cells.

The previous two chapters describe my efforts to optimize MAPCeL techniques through the generation of gene expression profiles of embryonic cell-types (e.g A-class motor neurons, muscle cells) from the *C. elegans* motor circuit. In this chapter, I will describe the application of MAPCeL methodology to identify UNC-4 target genes through the isolation of embryonic *unc-4*::GFP neurons from *unc-4* and *unc-37* mutants. In parallel to this approach, Steve Von Stetina adopted an mRNA-tagging strategy (Roy, Stuart et al. 2002), to isolate mRNA directly from postembryonic UNC-4 expressing cells (VA motor neurons). Through the use of these complementary approaches we have identified ~400 potential target genes that can now be tested for roles in the UNC-4 pathway.

Materials and Methods

Nematode Strains

Nematode strains were grown and maintained at 25°C as previously described (Brenner 1974). Strains used for microarray experiments were NC300 [*wdIs5*, *unc-4*::GFP III] (Lickteig, Duerr et al. 2001), NC633 [*unc-4(e120); wdIs5*], and NC652 [*unc-37(e262); wdIs5*].

Isolation of A-class motor neuron-specific RNA preparations from unc-4 and unc-37 mutants

unc-4::GFP neurons were dissociated, cultured, and sorted as described in Chapter II. RNA was extracted, amplified and hybridized to the Affymetrix *C. elegans* array using the methods established in Chapter II.

Data Analysis

Three independent preparations of *unc-4*::GFP neurons were isolated from both *unc-4(e120)* and *unc-37(e262)* mutants; Reference data were obtained from three replicates of *unc-4*::GFP neurons in a wildtype background (see Chapter II). Comparisons of RMA-normalized intensities for *unc-4(e120)* or *unc-37(e262)* were statistically analyzed using SAM. A two-class unpaired analysis of the data was performed to identify genes that differ $\geq$1.3 fold from the *unc-4*::GFP wildtype Reference at a false discovery rate $\leq$ 63%. Due to the high degree of false positives detected by analyzing each mutant separately and the limited number of targets shared between the two datasets, we also performed normalization comparing all six mutant samples [from both *unc-4(e120)* and *unc-37(e262)*] to the *unc-4*::GFP wildtype reference. This approach provides additional statistical power for the analysis and is based on the reasonable assumption that authentic *unc-4* target genes should be de-repressed in both *unc-4* and *unc-37* mutant backgrounds. In this case, 155 genes that differed from wildtype at $\geq$1.3 fold with an FDR $\leq$ 48% were considered candidate UNC-4 target genes. All datasets were annotated using Perl scripts described in Chapter II.

Construction of GFP reporters to analyze unc-4 target genes

Overlap PCR methods were used to generate *promoter*::GFP reporters of target genes using methods previously described (Hobert 2002). PCR products were microinjected at a concentration of 25-50 ng/µl with the *rol-6(d)* co-selectable marker. Additional reporter constructs were obtained from the Promoterome project (Dupuy, Li et al. 2004) and transgenic strains were generated by bombardment using methods described in Chapters II and III. A complete list of reporter constructs, and observed expression patterns can be found in Table 4.1.

Results

Culture and isolation of *unc-4*::GFP neurons from *unc-4(e120)* and *unc-37(262)* mutants

Mutations in *unc-4* impose limited effects on the fate of A-class motor neurons. Mutant VA and DA motor neurons are morphologically indistinguishable from wildtype A-class motor neurons as they retain the usual anterior polarity and synapse with appropriate body wall muscle cells (White, Southgate et al. 1992). My results confirm that *unc-4*::GFP neurons from *unc-4* and *unc-37* mutants are morphologically similar in culture to their wildtype counterparts, a finding consistent with *in vivo* observations. *unc-4*::GFP neurons differentiate in culture, typically extend a single process as *in vivo* and constitute ~4% of all embryonic cells, a frequency consistent with the occurrence of 13 *unc-4*::GFP neurons per 550 cells in the mature embryo (Christensen, Estevez et al. 2002) (Figure 4.1). RNA from the equivalent of 100,000 FACS-isolated *unc-4*::GFP neurons was amplified and applied to the Affymetrix *C. elegans* array.

Identification of *unc-4* target genes

Microarray data were obtained from three independent preparations of RNA from *unc-4*::GFP cells in *unc-4(e120)* mutant animals. We also performed three replicate experiments with RNA from *unc-37(e262*). These data were compared to a Reference generated from RNA isolated from wildtype *unc-4*::GFP neurons (Chapter II). Consistent with the limited changes imposed by *unc-4*, we found that few genes were significantly elevated at ≥1.7x when compared to wildtype. We, therefore, reduced the stringency of our statistical analysis and looked for genes that were elevated ≥1.3x. The application of these criteria identified 62 genes elevated in *unc-4(e120)* with a FDR ≤63%, and 379 genes upregulated in *unc-37(e262)* with an FDR ≤63%. The large number of *unc-37* transcripts detected in this experiment may be attributed to the well-established role of UNC-37 as a cofactor that functions with a wide array of different classes of DNA binding transcription factors (Pflugrad, Meir et al. 1997; Calvo, Victor et al. 2001; Zhang and Emmons 2002). Reasoning that only a subset of these genes are likely also to be regulated by *unc-4*, I decided to increase the statistical power of the analysis by combining the *unc-4* and *unc-37* mutant data sets to identify genes that were elevated across all six experiments. This approach revealed 151 genes that are significantly enriched compared to the wildtype Reference and significantly reduced the overall FDR (48%).

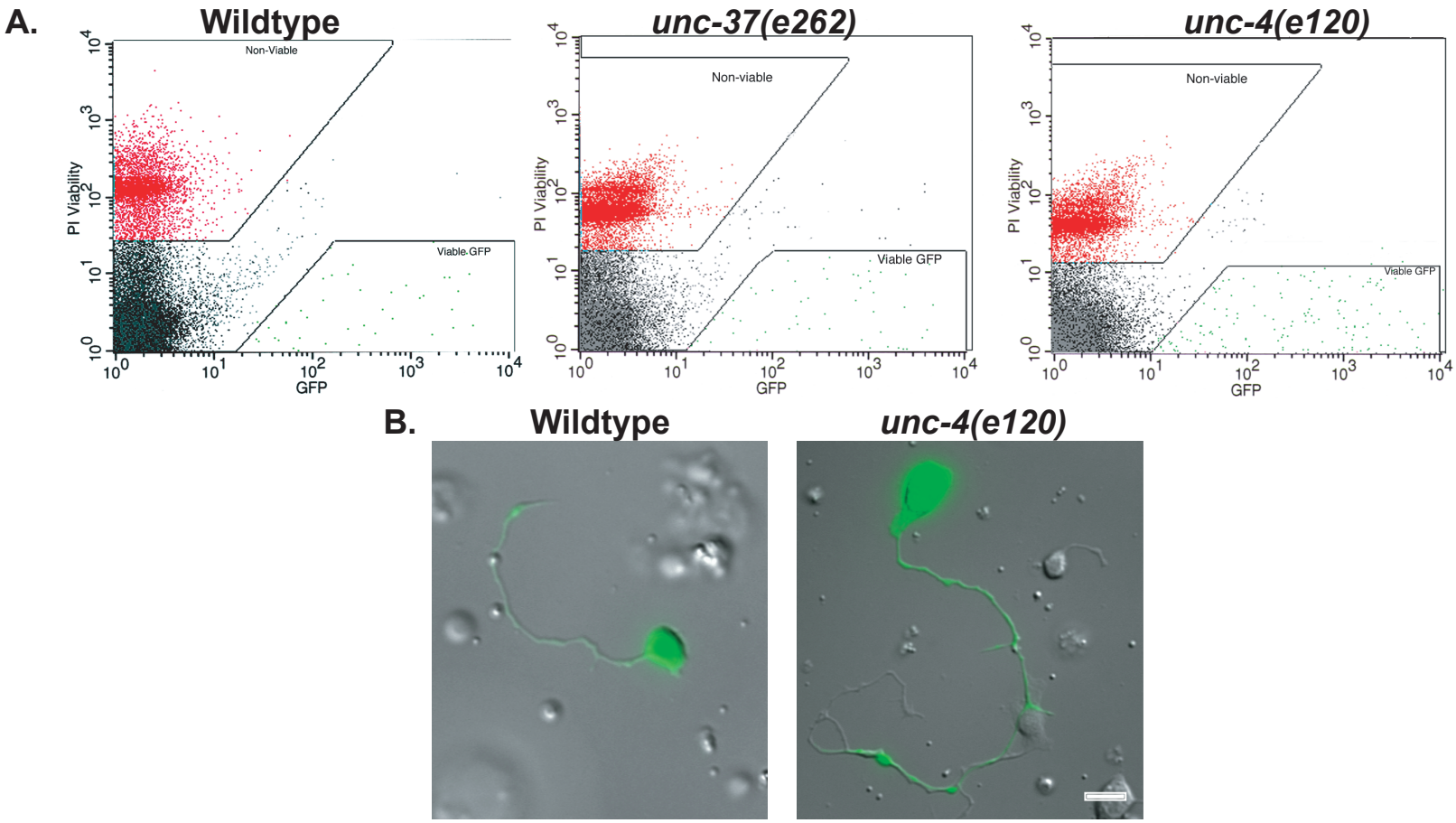

Figure 4.1. Sorting *unc-4*::GFP neurons from *unc-4(e120)* and *unc-37(e262)* mutants. A. FACS plots of *unc-4*::GFP neurons isolated from wildtype, *unc-37(e262)* and *unc-4(e120)* animals. GFP expression is indicated by the X-axis while propidium-iodide fluorescence is indicated along the Y-axis. ~30-40,000 cells were isolated per sort from each strain. B. *unc-4*::GFP neurons from *unc-4(e120)* mutant animals are identical to those isolated from wildtype animals. Scale bar = 5µm.

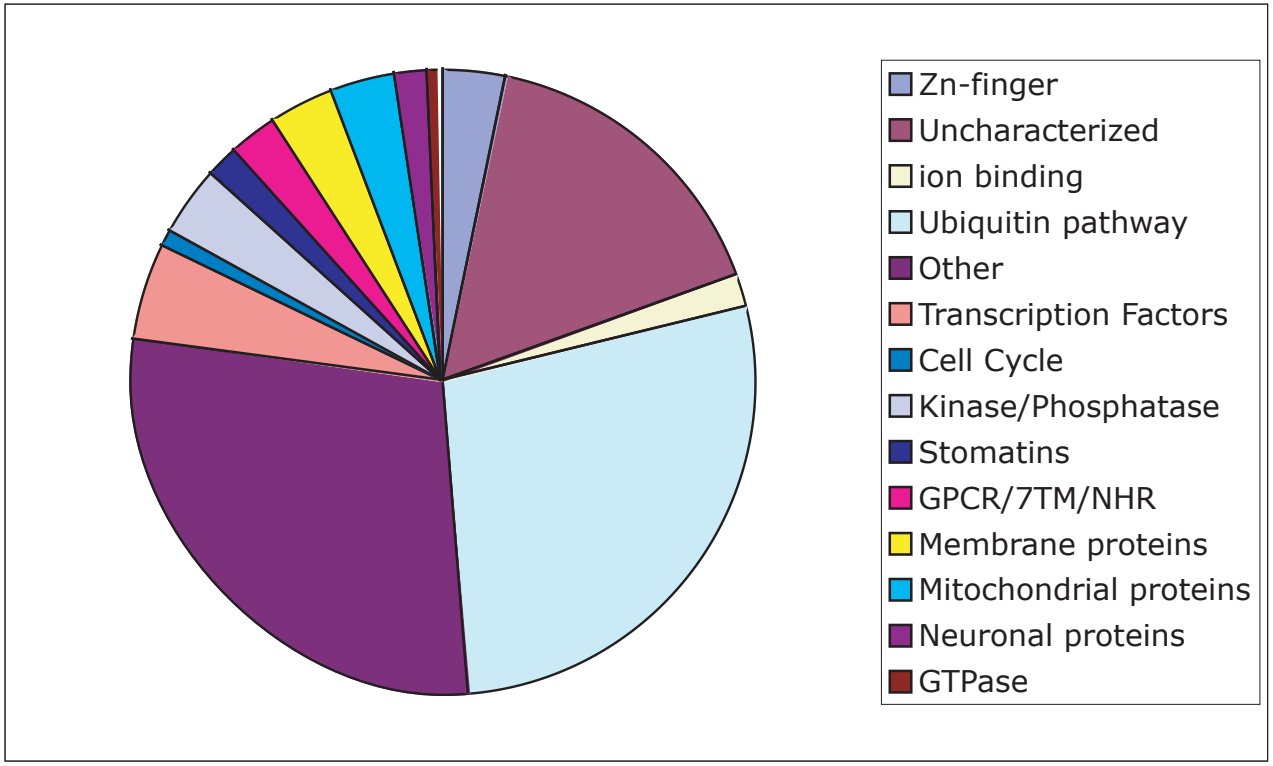

Figure 4.2. Pie chart depicting functional categories of UNC-4 target genes. 151 genes were identified as enriched in *unc-4/unc-37* mutant *unc-4*::GFP neurons. These genes were classified according to functional categories based on KOG descriptions.

A survey of candidate UNC-4 target genes

The pie chart in Figure 4.2 illustrates the different families of proteins that were identified as candidate UNC-4 target genes. This section features a subset of these genes that a review of literature indicates are plausible candidates for downstream regulators of synaptic defects in the *unc-4* pathway.

The ubiquitin-proteasome system (UPS)

~30% of the UNC-4 regulated dataset consists of components that function in the UPS to regulate protein degradation. For example, we identified 21 proteasome subunits, and 5 ubiquitin ligases. Recent studies have established broad roles for ubiquitin-dependent protein turnover in axon guidance and synaptic assembly (Murphey and Godenschwege 2002; Cline 2003; DiAntonio and Hicke 2004). An example is the Drosophila gene *highwire (hiw*), a putative ubiquitin ligase, that was identified in genetic screens for mutants with impaired walking. Loss of *hiw* also leads to an increased number of synaptic boutons as well as an overgrowth of presynaptic branches at the neuromuscular junction (Wan, DiAntonio et al. 2000). In *C. elegans*, the Hiw homolog RPM-1 (regulator of presynaptic morphology) exhibits similar defects; synaptic terminals are disorganized and frequently include multiple active zones in the presynaptic region (Schaefer, Hadwiger et al. 2000; Zhen, Huang et al. 2000). *rpm-1* mutants also display axon guidance defects (Schaefer, Hadwiger et al. 2000; Zhen, Huang et al. 2000). Data from Yishi Jin's lab indicate that RPM-1 is localized to the periactive zone adjacent to the presynaptic density where it negatively regulates a p38 MAP kinase cascade. RPM-1 achieves this outcome indirectly by targeting DLK-1, a MAPKKK in the p38 pathway,

for ubiquitin-mediated degradation (Nakata, Abrams et al. 2005). A similar mechanism has been independently confirmed in Drosophila, in which the MAP kinase JNK is effectively downregulated by Hiw activity (Collins, Wairkar et al. 2006). In this case, genetic results indicate that Hiw-controlled synaptic assembly depends on the transcription factor D-fos. A clear implication of this finding is that Hiw defines synaptic growth by regulating gene transcription. Joseph Watson in our lab has confirmed this model by detecting a battery of *rpm-1* regulated transcripts in the *C. elegans* nervous system. These experiments have demonstrated that the UPS plays an important role in modulating the levels of signaling proteins at the synapse, and misregulation of these proteins can lead to defects in synapse formation.

Most of the UPS transcripts with elevated expression in the combined *unc-4* and *unc-37* data sets encode ubiquitously expressed proteins. Nevertheless, a subset of these components, the ubiquitin ligases, (e.g. E2 and E3 ligases) have been shown to adopt tissue specific functions in other organisms (Hegde and DiAntonio 2002; d'Azzo, Bongiovanni et al. 2005) and are, therefore, stronger candidates for neuron-specific regulators of synaptic choice. As described below, one of the ubiquitin ligases, *ubc-13*, is especially attractive because its Drosophila homolog, *bendless*, controls synaptic targeting in a larval motor circuit (see below) (Muralidhar and Thomas 1993; Oh, McMahon et al. 1994).

ubc-13/bendless

ubc-13 encodes an E3 ubiquitin ligase that is most closely related to the Drosophila protein Bendless (*ben*). In Drosophila, the giant fiber (GF) extends from the

brain along the dorsal midline into the thoracic ganglion where it branches to synapse with the PSI interneuron (Muralidhar and Thomas 1993; Oh, McMahon et al. 1994) and then sends out a lateral projection to innervate the tergotrochanter muscle motor neuron (TTMmn). In this circuit, *ben* is selectively required for the creation of the synaptic connection between the GF and the TTMmn (Figure 4.3); in a *ben* mutant, the GF axon fails to make a crucial turn ("bendless") that allows it to synapse onto the TTMmn, although the PSI synapse is unaffected (Muralidhar and Thomas 1993; Oh, McMahon et al. 1994). *ben* function is also required for normal projections of the R7 photoreceptor. In *ben*, R7 photoreceptors extend projections into the medulla that are shallow and often disorganized. Similar to the GF phenotype, this defect is limited to a "bend" close to the termination site where R7 axons fail to turn at the medulla surface, a required step for generating the normal columnar innervation pattern (Oh, McMahon et al. 1994). Mosaic analysis indicates that Ben is required in the presynaptic GF where it functions to promote GF axon turning to reach the target site (Oh, McMahon et al. 1994). In contrast, the role of UNC-4 in synaptic choice is limited to the postsynaptic cell (e.g. VA motor neurons) where it regulates the formation of specific inputs but is not required for directing the trajectory of axonal outgrowth in the ventral cord. Given its strong conservation, however, *ubc-13/bendless* is an interesting candidate for a gene that could also regulate specific connections in the *C. elegans* motor circuit.

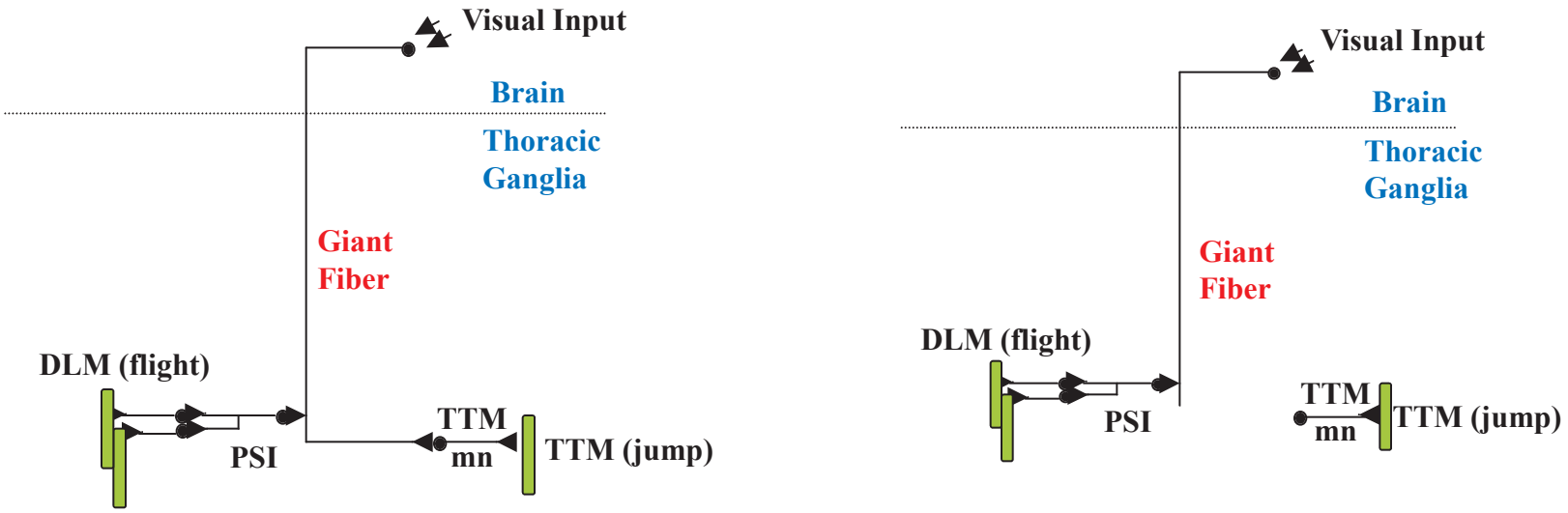

Figure 4.3. Schematic drawing of the *Drosophila* Giant Fiber (GF) in wildtype and *bendless* mutants. (Left) The GF command interneurons extend processes into the thoracic segment where it synapses with the PSI interneuron, which synapses onto the DLM motor neurons, mediating the flight response. The GF makes a second synapse onto the TTM motor neuron (TTMmn), which synapses with the TTM, mediating the jump response. (Right) In *ben* mutant animals the GF does not make the terminal bend to connect with the TTMmn. Cartoon adapted from Muraldihar and Thomas, 1993.

lin-39

LIN-39 is a member of the HOX family of homeotic transcription factors that are characterized by their role in controlling gene expression in a region-specific manner. LIN-39 is best known for its requirement in normal vulval development and in Q neuroblast migration (Clark, Chisholm et al. 1993). These LIN-39 functions are restricted to the midbody region, while other members of the HOX family control gene expression in flanking tissue domains along the anterior-posterior axis (Maloof and Kenyon 1998). VC class motor neurons undergo programmed cell death in *lin-39* mutants (Clark, Chisholm et al. 1993). The VCs arise from a lineage that also gives rise to VA and VB motor neurons but roles for LIN-39 in the development and fate of other classes of ventral cord motor neurons have not been reported. Based on GFP and lacZ reporters, LIN-39 is expressed in ventral cord motor neurons (Figure 4.4) (Wang, Muller-Immergluck et al. 1993; Wagmaister, Gleason et al. 2006) and, therefore, is a strong candidate for a gene that specifies the fates of these cells in the midbody region. Interestingly, *mab-5*, the next most posterior HOX gene, was identified in Steve Von Stetina's list of UNC-37 regulated transcripts in VA class motor neurons (see below). This finding could indicate that UNC-4 may act on different sets of genes in distinct regions of the worm to elicit its affects. In Chapter V, I will describe my work analyzing *lin-39* as a potential UNC-4 target gene.

ceh-12

CEH-12 is the nematode homolog of the HB9 homeodomain transcription factor. In the vertebrate spinal cord, HB9 specifies the motor neuron domain. HB9 represses

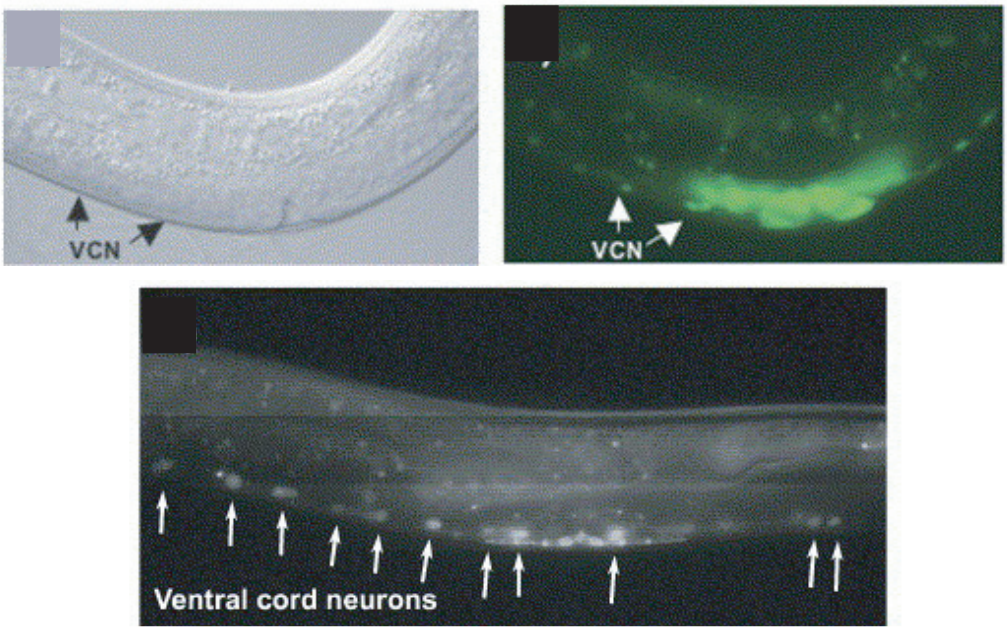

Figure 4.4. LIN-39::GFP is expressed in ventral cord motor neurons. (Top) A LIN-39::GFP translational fusion (*deIs4*) containing the entire coding sequence was expressed in ventral cord motor neurons (arrows). Right panel, DIC, Left panel, GFP. Figure from Wagmaister, Gleason et al., 2006. (Bottom) A GFP fusion protein containing only the first exon of LIN-39 is specifically expressed in the ventral cord motor neurons (arrows). Figure from Wagmaister, Miley et al., 2006.

interneuron-specific genes; loss of HB9 leads to expansion of the interneuron domain, with a consequent reduction in the motor neuron region. Conversely, overexpression of HB9 leads to an increase in the motor neuron domain (Arber, Han et al. 1999; Thaler, Harrison et al. 1999). These results suggest that HB9 functions in the vertebrate nervous system to specify motor neuron fate by blocking the adoption of interneuron fates. In flies, dHb9 is expressed in ventrally projecting motor neurons, where it represses *even-skipped*, a dorsal motor neuron marker. In *dHb9* mutants, ventrally projecting motor neurons express Eve and switch polarity to innervate dorsal muscles. *dHb9* is also expressed in serotonergic interneurons where it is required for proper axon trajectory. In this case, dHb9 does not distinguish between motor neuron and interneuron fate but instead is necessary for axonal targeting (Odden, Holbrook et al. 2002). These results from flies and from vertebrate model systems indicate that members of the HB9 family of transcription factors are conserved determinants of motor neuron fate. In *C. elegans*, CEH-12 has not been previously studied; however, given the conservation of HB9 in motor neuron development of other organisms, Steve and I focused our follow-up studies on testing the potential role of CEH-12 in the UNC-4 pathway (see Chapter V). This decision was also motivated by the finding that *ceh-12* is one of the few genes that is upregulated in both the MAPCeL and mRNA tagging microarray datasets of candidate *unc-4* and *unc-37* regulated transcripts (see below).

lin-11

lin-11 is a founding member of the LIM homeobox family of transcription factors. Elevated expression (1.3-fold) of the LIM transcription factor in the *unc-4* and *unc-37*

mutant data sets is intriguing given the conserved role of the LIM "code" in specifying the fate of postmitotic motor neurons (Tsuchida, Ensini et al. 1994; Appel, Korzh et al. 1995; Thor, Andersson et al. 1999). *lin-11* has been previously characterized in *C. elegans* for its role in vulval development where it functions to determine the primary and secondary fates of vulval precursor cells (Gupta and Sternberg 2002; Gupta, Wang et al. 2003). Furthermore, *lin-11* has an important role in specifying neuronal fate. In particular, *lin-11* is expressed in AWA chemosensory neurons where it promotes *odr-7* expression, thereby initiating AWA differentiation (Sarafi-Reinach, Melkman et al. 2001). *lin-11* is also expressed in the AIZ interneuron where it is required for AIZ function in thermoregulation (Hobert, D'Alberti et al. 1998). GFP reporter data indicates that *lin-11* is detected in some tail neurons as well as the VC motor neurons which also express *unc-4* (Hobert, D'Alberti et al. 1998; Lickteig, Duerr et al. 2001). *lin-11* mutants are characterized by a mild backward Unc phenotype which is suggestive of a role in the specification of the locomotory neurons. These data suggest that *lin-11* may be an excellent candidate to pursue, not only for the wiring defect, but also as a potential regulator of synaptic vesicle levels in the VCs.

unc-76

UNC-76 is the founding member of the FEZ (Fasciculation and Elongation protein; Zygin/Zeta-1) family of intracellular proteins, and is expressed in all nematode axons. *unc-76* was initially identified in a screen for fasciculation-defective mutants. Analysis of *unc-76* null mutants revealed additional defects in axonal bundling and elongation (Bloom and Horvitz 1997). In *C. elegans,* UNC-76 functions with a co-factor,

UNC-69. Strong loss-of function mutations in *unc-69* also lead to fasciculation defects, similar to those observed in *unc-76*. Hypomorphic or weak *unc-69* alleles and certain heteroallelic combinations of *unc-76* and *unc-69* mutants result in mislocalization of the synaptic vesicle marker, SNB-1::GFP (synaptobrevin) (Su, Tharin et al. 2006). This role may be conserved as the Drosophila homolog of UNC-76 interacts with kinesin-heavy chain to transport synaptic vesicles down the axon (Gindhart, Chen et al. 2003). These results suggest that UNC-76 and UNC-69 are required for the dual functions of regulating axonal vesicle transport as well as process outgrowth (Su, Tharin et al. 2006). Given the role of *unc-76* in synaptic vesicle trafficking, it would be interesting to determine if overexpression of *unc-76* in VA class motor neurons (the presumptive consequence of removing *unc-4* regulation) accounts for the depletion of synaptic vesicles in *unc-4* mutant neurons.

GFP reporter genes determine target gene expression

Our model is that UNC-4 is normally expressed in A-class motor neurons where it functions to repress B-class genes, thereby specifying A-type traits. Thus, we propose that an *unc-4* target gene should normally be expressed in B-class motor neurons, and show ectopic expression in the A-class motor neurons of an *unc-4* mutant. To determine the expression patterns of *unc-4* target genes, Kathie Watkins and I generated overlap PCR constructs for a subset of genes in the *unc-4* target list. Additional transgenic lines were generated using *promoter*::GFP constructs obtained from the Promoterome (Dupuy, Li et al. 2004). We have begun preliminary scoring of GFP lines; however, further analysis will be necessary to fully define the expression patterns of reporter lines.

Further genetic experiments will also be required to examine GFP reporter expression in the *unc-4* mutant background. Table 4.1 lists all reporters generated thus far and their preliminary expression patterns.

Microarray profiles generated by mRNA-tagging identify additional candidate UNC-4 target genes

The MAPCeL approach is readily applied to cells that can be directly obtained from dissocitated embryos (e.g. body muscle cells) or which can arise from these blastomeres in culture (e.g. DA motor neurons), but is not useful for larval neurons due to their inaccessibility and general failure to differentiate *in vitro*. This limitation has important implications for our effort to identify *unc-4* target genes. John White's EM reconstruction of *unc-4(e120)* revealed that only the postembryonic VA motor neurons are miswired (White, Southgate et al. 1992). Thus, candidate *unc-4* target genes identified by MAPCeL in embryonic DA motor neurons may not be regulated by *unc-4* in VA motor neurons. To overcome this problem, Steve Von Stetina adopted an mRNA-tagging approach which can be utilized to extract mRNA from specific postembryonic cells (Roy, Stuart et al. 2002). This method utilizes a FLAG-tagged polyA-binding protein (PAB-1) that is expressed under a cell-specific promoter. Transgenic animals are treated with formaldehyde to cross link epitope-tagged PAB-1 to polyA RNA and then dissociated by passage through a French Pressure cell. Cleared lysates are treated with α-FLAG antibody to immunoprecipitate the PAB-1/mRNA complex. Steve, along with Joseph Watson, optimized this approach to profile the entire L2 larval nervous system. They identified 1,562 genes (1.5x, ≤1% FDR) that were enriched in neurons, of which 445 had

Table 4.1. GFP reporters to determine *unc-4* target gene expression			
Cosmid Name	**Common Name**	**Protein**	**Expression pattern**
C30C11.2	*rpn-3*	Proteasome regulatory particle	All VNC mn, head/tail neurons
C01G6.4		E3 ubiquitin ligase	Mosaic, seems to mostly be in cholinergic mn
ZK546.2		Leucine-rich repeat	Bright intestine, mosaic – likely in most if not all VNC mn
F25H2.9	*pas-5*	Proteasome alpha subunit	Hypodermis, hard to determine if there is neuronal expression
CD4.6	*pas-6*	Proteasome alpha subunit	Mosaic, all VNC mns, head, tail and pharyngeal neurons, head and pharygeal muscle
K07D4.3	*rpn-11*	Proteasome regulatory particle	GFP expression, however these lines have not been scored.
F15B9.6		Unknown	Ventral nerve cord
F49C12.9		Unknown	GFP expression, however these lines have not been scored.
W06F12.3		Casein kinase	Anal depressor, head neurons
F15B9.6		Unknown	Ventral nerve cord
K04G2.4		Unknown	Head/tail neurons, hypodermis, head muscle
F57B9.10	*rpn-6*	Proteasome regulatory particle	GFP expression, however these lines have not been scored.
C24D10.6		Unknown	Not scored
ZK20.5	*rpn-12*	Proteasome regulatory particle	GFP expression, however these lines have not been scored.
Y42A5A.4		Protein Kinase	Head/tail neurons, one unknown VNC mn
ZC581.3		Unknown	DB mn, weak expression seen in additional mns (variable)
C13G3.1		Unknown	Head/tail neurons, faint in ventral cord
Y54G2A.31	*ubc-13*	Ubiquitin ligase	BWM, head/tail neurons, phar. muscle
M88.4		Unknown	Head/tail neurons, one unknown VNC mn, pharyngeal muscle
Y41D4B.9	*nhr-122*	Hormone receptor	Faint GFP neuron in tail
K05C4.2		Unknown	
Y34D9A.4	*spd-1*	Microtubule associated protein	Not scored
T23F2.5		Stress response protein	Not scored
Y59A8B.11	*fbxa-106*	F-box protein	
Y57E12AL.5	*mdt-6*	Transcriptional mediator	Vulva, VNC mn, head/tail neurons
C05D9.7		Unknown	Not scored
C07H6.7	*lin-39*	HOX transcription factor	No GFP
F33D11.4	*ceh-12*	HB9 transcription factor	VB mn, RID neuron, excretory gland cells, pharyngeal-intestinal valve

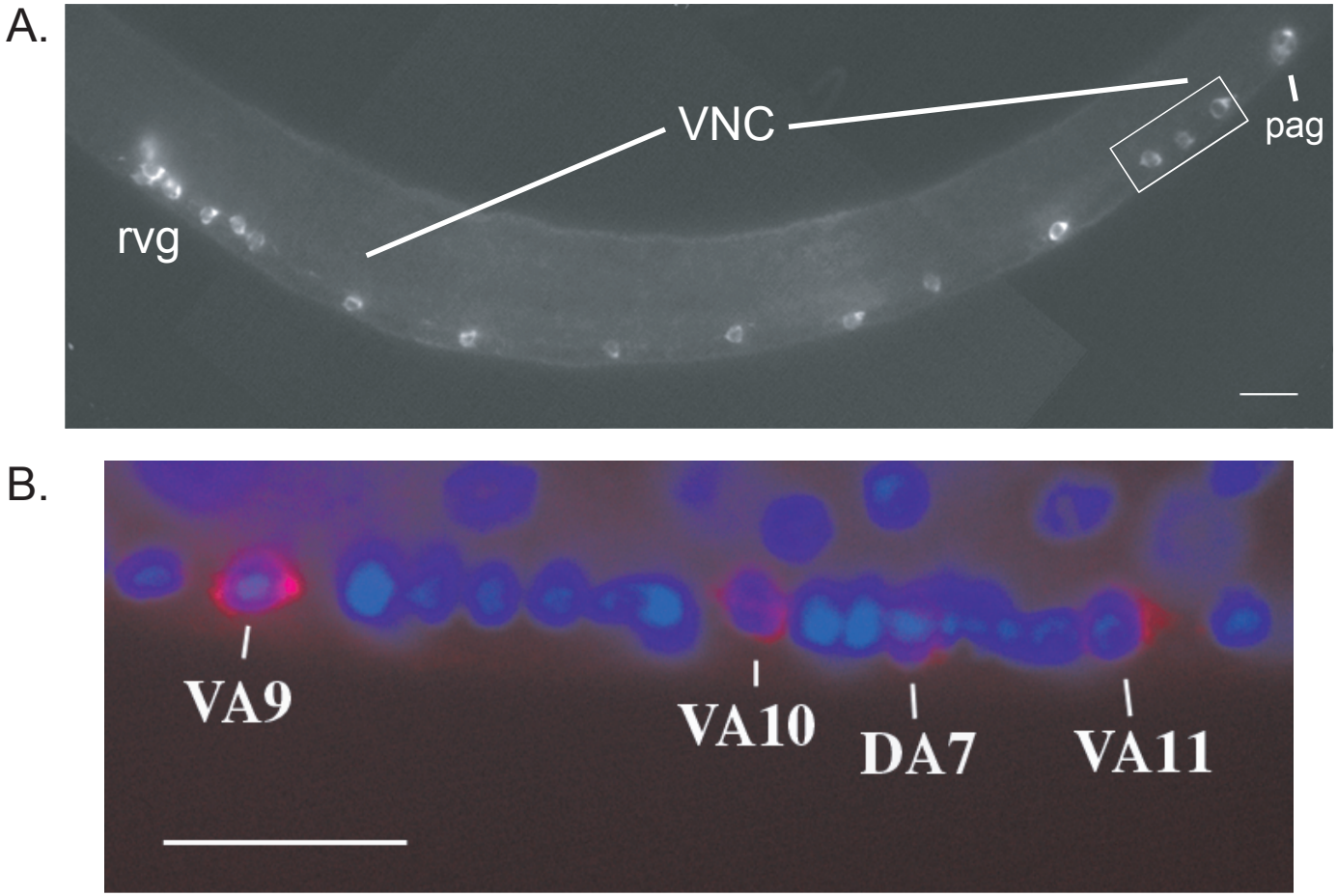

Figure 4.5. *unc-4*::3XFLAG::PAB expression in L2 larvae. A. Antibody staining detects FLAG::PAB expression in A-class neurons in the retrovesicular ganglion (rvg), ventral nerve cord (vnc), and pre-anal ganglion (pag). B. Close-up of ventral cord (boxed image in A), showing anti-FLAG staining (red) in cytoplasm surrounding only A-class nuclei (DAPI, blue). Anterior is left, ventral is down. Scale bars represent 10μm.

documented expression patterns. Of these, 91% (409) show expression in neurons. GFP reporters to previously uncharacterized genes in this data set showed a similar (>95%) high level of expression in *C. elegans* neurons. Steve and Joseph extended this method to isolate mRNA from VA motor neurons by driving expression of a 3XFLAG-PAB-1 construct with the *unc-4* promoter. As shown in Figure 4.5, this transgene is specific to VA and DA motor neurons in the ventral cord. mRNA was immunoprecipitated from mid-L2 animals, as UNC-4 is required during this developmental period to maintain normal VA inputs (Miller, Shen et al. 1992). This approach identified 412 (1.5 x, ≤1% FDR) genes enriched in A-class motor neurons, of which 89% (102/114 with expression patterns) are known to be expressed in neurons. A significant fraction of genes in this list (161) are also enriched in DA class motor neurons, including the transcription factors *unc-4* and *unc-3* (see Chapter 1). Steve then used the wild type VA profile as a Reference to identify 255 transcripts showing elevated expression in *unc-37* mutant VA class motor neurons. (For reasons that are not understood, *unc-4* mutants are incompatible with the *unc-4*::3XFLAG-PAB-1 construct and could not be used directly to generate a profile limited to *unc-4* regulated transcripts.)

A comparison of the 255 candidate *unc-37* regulated transcripts from larval VA class motor neurons vs. the MAPCeL profile of potential UNC-4 target genes that I identified revealed only six common genes (C50E3.6, *lin-11*, *sto-4*, Y39A3B.5, *odr-2* and *ceh-12*). Because *ceh-12* is a member of the HB9 family of homeodomain transcription factors with well established roles in motor neuron fate determination in mammals, birds and insects, *ceh-12* was selected from this group of candidate *unc-4* target genes for additional experiments to determine if it also specifies motor neuron fate in *C. elegans*. In

chapter V, I will describe our findings showing that *ceh-12* is indeed a *bona fide* target of UNC-4, and that it regulates synaptic choice.

Discussion

The previous two chapters outline the use of MAPCeL to profile specific motor neurons and muscle cells from the *C. elegans* embryo. These experiments were performed to establish the validity of microarray profiles of cultured *C. elegans* cells for generating reliable *in vivo* gene expression signatures of these different cell types. The ultimate goal, however, was to use these methods to solve a complex biological problem of interest to the Miller lab, i.e., the identification of UNC-4 regulated genes required for synaptic choice.

Cell-specific microarray strategies identify UNC-4 target genes

unc-4 and *unc-37* mutant *unc-4*::GFP neurons arise at the expected frequency in culture and display properties similar to wildtype *unc-4*::GFP neurons, thereby indicating that *unc-4*::GFP neurons in culture are likely to arise from the same embryonic precursor cells that generate them in the intact embryo. *unc-4::*GFP-positive neurons were isolated by FACS from these preparations and RNA extracted for application to the *C. elegans* Affymetrix Gene Chip array. *unc-4* and *unc-37* mutant profiles were compared to Reference microarray data generated from wildtype *unc-4*::GFP neurons (Chapter II). These experiments identified 151 transcripts with elevated levels in *unc-4* and *unc-37* mutant profiles.

UNC-4 is required during embryonic development in the DA motor neurons to maintain normal levels of synaptic vesicles (Lickteig, Duerr et al. 2001). UNC-4 also functions at the L2 larval stage to specify synaptic inputs to the VA motor neurons in addition to sustaining synaptic vesicle abundance (Miller, Shen et al. 1992; White, Southgate et al. 1992). Since MAPCeL profiles are limited to embryonic DA motor neurons, Steve Von Stetina used mRNA-tagging to profile larval VA motor neurons with the expectation that these were more likely to reveal *unc-4*-regulated genes that control synaptic choice. A comparison of the MAPCeL and mRNA tagging data, however, has revealed at least one gene, *ceh-12*, that is regulated by *unc-4* and *unc-37* in both DA and VA motor neurons and that also functions downstream of *unc-4* to specify presynaptic inputs. Moreover, a new assay using the gap junction marker UNC-7S::GFP has shown that ~50% of DA motor neurons are in fact miswired in *unc-4* and *unc-37* mutants (see Chapter V). Finally, my results, also presented in Chapter V, indicate that derepression of *ceh-12* in *unc-4* mutants contributes to the synaptic vesicle defect in both DA and VA class motor neurons. Taken together, these findings indicate that data obtained from both of these microarray approaches may reveal the full complement of UNC-4 target genes required to regulate the specificity of synaptic inputs as well as the strength of synaptic signaling in A-class motor neurons.

As indicated above, we have now determined that *ceh-12* functions downstream of *unc-4* to determine synaptic connectivity. *ceh-12* de-repression, however, is biased toward the posterior end of the ventral nerve cord. These results suggest that additional pathways are necessary to specify synaptic choice, especially in the anterior regions of

the animal, thereby motivating the analysis of additional targets genes that we have detected.

The Ubiquitin Proteasome System (UPS) at the synapse

Interestingly, close to 30% of the MAPCeL dataset of *unc-4* and *unc-37* regulated transcripts consists of transcripts encoding components of the UPS that targets proteins for degradation. While the high number of UPS genes in these profiles was unexpected, the overall role of the UPS in synapse formation is now well established. One of the first indications of the important role of protein turnover in neural patterning was obtained over a decade ago with the discovery that the E3 ubiquitin ligase, Bendless, is required for axonal targeting in the Drosophila jump circuit and visual system (Muralidhar and Thomas 1993; Oh, McMahon et al. 1994). Subsequent work has identified additional roles for UPS components in synaptic assembly. As described above, the E3 ubiquitin ligase Drosophila Highwire and its *C. elegans* homolog RPM-1 are important regulators of active zone formation in presynaptic areas (Schaefer, Hadwiger et al. 2000; Zhen, Huang et al. 2000). Other groups have also established the importance of the UPS in regulating synaptic function; Burbea et al. (2002) describe the regulation of the glutamate receptor, GLR-1, by the UPS at glutamatergic synapses in *C. elegans*. They show that a decrease in ubiquitination leads to an increase in GLR-1 containing synapses, while an increase in ubiquitination leads to the decrease of GLR-1 receptor expression at these synapses (Burbea, Dreier et al. 2002). Furthermore, Speese et al. (2003) have shown that the UPS functions locally at the synapse to regulate the levels of Drosophila UNC-13 (Dunc-13), a protein necessary for synaptic vesicle priming. Loss of proteasome function

causes an accumulation of Dunc-13, which leads to increased synaptic transmission, thereby increasing the strength of synaptic output (Speese, Trotta et al. 2003). These studies indicate that careful regulation of local ubiquitination events can influence the formation and function of the synapse.

EM analysis of *unc-4* mutants shows a 40% reduction in the number of synaptic vesicles located at presynaptic regions of A-class motor neurons. This effect is consistent with the decreased levels of synaptic vesicle proteins detected in these neurons by immunostaining (Lickteig, Duerr et al. 2001). The mechanism of this effect is likely to depend on a post-transcriptional event as transcription of the *unc-17-cha-1* gene, which encodes synaptic vesicle-associated proteins is not affected whereas levels of both UNC-17 and CHA-1 are reduced. Given the elevation of numerous UPS components in *unc-4* and *unc-37* mutant neurons, a facile explanation of this effect could be that UNC-4 normally represses UPS gene expression to maintain synaptic vesicle stability. Loss of *unc-4* would lead to increases in proteasome activity thereby increasing turnover of synaptic vesicle proteins. While this is an *ad hoc* model, it does provide an interesting hypothesis to further explore the nature of UNC-4 in regulating the strength of synaptic transmission (see below). Finally, it has long been hypothesized that the specificity of synapse formation depends on a "molecular address" presented by the post-synaptic membrane for recognition by the appropriate pre-synaptic partner (Sperry 1963). In this context, it seems reasonable to propose that the UPS could control the set of proteins that mediate this event. Misregulation of the UPS in *unc-4* mutants could alter levels of key surface proteins in this pathway, possibly inducing a change in synaptic partners.

CHAPTER V

CEH-12/HB9 IS A DOWNSTREAM TARGET OF UNC-4 THAT REGULATES SYNAPTIC STRENGTH AND SPECIFICITY

Introduction

As described in Chapter I, neuron progenitor domains of the vertebrate spinal cord are defined by combinatorial codes of transcription factors that specify cell fate (Lee and Pfaff 2001). The majority of the homeodomain transcription factors with this function contain a conserved eh1 (Engrailed homology) domain for interaction with members of the Groucho/TLE family of transcriptional co-repressor proteins. This complex is proposed to mediate Groucho-dependent repression of transcription factors that are normally expressed in neighboring spinal cord domains (Muhr, Andersson et al. 2001). This mechanism of cross-repression is also used to define the fates of postmitotic neurons arising from these regions (Lee and Pfaff 2001). For example, motor neurons in the MN domain express HB9 and Isl1, whereas Chx10, Lhx3 and Lhx4 mark interneurons in the adjacent V2 region. HB9 is initially expressed in motor neuron progenitors but is selectively localized to ventrally projecting motor neurons (v-MN) of the spinal cord and hindbrain following differentiation (Arber, Han et al. 1999; Thaler, Harrison et al. 1999). In HB9 mutant animals, motor neurons arise, but do not express motor neuron markers; instead, they transiently express V2 interneuron markers Lhx3/4 and Chx10. In addition to these changes in cell fate, HB9(-/-) neurons display migration and axon targeting errors indicative of defects in the assignment of motor neuron subtype identities (Arber, Han et al. 1999; Thaler, Harrison et al. 1999). Furthermore, ectopic

expression of HB9 in the V2 domain is sufficient to turn off interneuron markers and induce motor neuron differentiation (Tanabe, William et al. 1998). These findings demonstrate the requirement for transcriptional cross-repression to determine neuronal fate in the developing vertebrate spinal cord.

dHb9 also specifies motor neuron fate in Drosophila. In contrast to the broad expression of HB9 throughout the MN progenitor domain of the vertebrate spinal cord, *dHb9* is selectively expressed in a subset of motor neurons as well as in three interneurons (EW1/2/3) (Broihier and Skeath 2002; Odden, Holbrook et al. 2002). *dHb9* expression is restricted to motor neurons that project ventrally, whereas the homeodomain transcription factor Even-skipped (Eve) specifies dorsally projecting motor neurons (Landgraf, Roy et al. 1999). In a mechanism that mirrors the reciprocal-repression of transcription factors that define neuronal fates in the vertebrate spinal cord, dHB9 and Eve repress each other to specify these different subsets of motor neurons in the fly (Broihier and Skeath 2002; Odden, Holbrook et al. 2002). Loss of *dHb9* leads to defects in ventral muscle target recognition and an expansion of dorsally projecting neurons that express Eve. Conversely, mutations in *eve* lead to the ectopic expression of *dHb9* in a subset of dorsally projecting motor neurons. Furthermore, misexpression of *eve* in all postmitotic motor neurons leads to the complete elimination of *dHb9* expressing cells (Broihier and Skeath 2002). In addition to these motor neuron defects, interneuron axon projections are also affected. In summary, *dHb9* is required to specify the fates of ventrally projecting motor neurons by repressing *eve* and, in addition to this conserved function, *dHb9* directs axon targeting of a subset of interneurons.

As described in Chapter IV, we have employed two complementary microarray profiling strategies to identify genes that function downstream of the transcription factor UNC-4 in embryonic and larval A-class motor neurons. This analysis identified ~400 target genes, of which six were common between the two approaches. One of these, *ceh-12*, encodes the nematode homolog of HB9. Given the conserved role of HB9 in specifying motor neuron fate in more complex nervous systems, Steve Von Stetina and I collaborated to explore the role of *ceh-12* in the UNC-4 pathway. As outlined in this chapter, we have now shown that *ceh-12* functions downstream of UNC-4 to regulate synaptic vesicle levels in A-class motor neurons. Furthermore, we have shown that UNC-4 selectively represses *ceh-12* to specify synaptic inputs to VA motor neurons located in the posterior region of the ventral nerve cord.

Materials and Methods

Strains and genetics

Nematode strains were maintained at 20-25^{o}C using standard culture techniques (Brenner 1974). *ceh-12* deletion alleles, *gk391* and *tm1619*, were obtained from the *C. elegans* knockout consortium (Vancouver, Canada) and the National Bioresource Project (Japan), respectively. The wildtype strain was N2. All other strains used in this study are listed in Table 5.1.

Table 5.1. Strains used for *ceh-12* experiments	
Strain Name	**Genotype**
unc-4 and unc-37 alleles	
CB120	*unc-4 (e120)*
	unc-4 (e2320)
	unc-4 (e2322ts)
	unc-4 (e2323)
NC1	*unc-4 (wd1)*
CB262	*unc-37 (e262)*
ceh-12 alleles	
VC995	*ceh-12 (gk391)* 0x outcrossed
	ceh-12 (tm1619) 0x outcrossed
NC1018	*ceh-12 (gk391)* 6x outcrossed
NC1019	*ceh-12 (tm1619)* 6x outcrossed
ceh-12; unc-4 double mutants	
NC1036	*ceh-12 (gk391); unc-4 (wd1)*
NC1037	*ceh-12 (tm1619); unc-4 (e2320)*
NC1038	*ceh-12 (tm1619); unc-4 (e2322ts)*
NC1058	*ceh-12 (gk391); unc-4 (e2322ts)*
NC1078	*ceh-12 (gk391); unc-4 (e120)*
NC1108	*ceh-12 (tm1619); unc-4 (wd1)*
NC1112	*ceh-12 (gk391); unc-4 (e2320)*
NC1114	*ceh-12 (tm1619) unc-37 (e262)*
NC1115	*ceh-12 (gk391) unc-37 (e262)*
NC1153	*ceh-12 (tm1619); unc-4 (e120)*
NC1212	*ceh-12 (gk391); unc-4 (e2323)*
unc-104 strains	
NC154	*unc-104(e1265);wdIs5* (*unc-4*::GFP)
NC155	*unc-104(e1265) unc-4(e120); wdIs5*
NC1123	*ceh-12(gk391); unc-104(e1265); wdIs5*
NC1124	*ceh-12(gk391); unc-104(e1265) unc-4(e120); wdIs5*
ceh-12::GFP transgenics	
NC802	*unc-119 (ed3); wdEx310 (ceh-12*::GFP - *unc-119* minigene)
NC897	*unc-119 (ed3); wdEx376 (ceh-12*::GFP - *unc-119* minigene)
NC898	*unc-119 (ed3); wdEx377 (ceh-12*::GFP - *unc-119* minigene)
NC904	*unc-4 (e120); unc-119 (ed3); wdEx377*
NC922	*unc-37 (e262); unc-119 (ed3); wdEx376*
NC1236	*unc-37 (e262); unc-119 (ed3); wdEx310*
NC1237	*unc-4 (e120); unc-119 (ed3); wdEx310*
VA-CEH-12 transgenics	pSV47 (*unc-4*::CEH-12) and pJER1 (*myo-3*::dsRed2) were co-injected at 15 ng/ml
NC992	*wdEx448*
	pSV47, pJER1, and pCG3 (*acr-5*::YFP) were co-injected at 15 ng/ml
NC1024	*wdEx463*
NC1030	*wdEx466*
NC1046	*wdEx471*
NC1061	*wdEx478*
UNC-7::GFP strains	
EH578	*unc-7 (e5); lwEx79 (*UNC-7::GFP; *col-19*::GFP)
NC1159	*ceh-12 (gk391); unc-4 (e120); unc-7 (e5); lwEx79*
NC1160	*ceh-12 (gk391); unc-4 (e2322ts); unc-7 (e5); lwEx79*
NC1168	*unc-4 (e120); unc-7 (e5); lwEx79*
NC1192	*ceh-12 (gk391); unc-4 (e2323); unc-7 (e5); lwEx79*

NC1197	*unc-4 (wd1); unc-7 (e5); lwEx79*
NC1198	*unc-4 (e2323); unc-7 (e5); lwEx79*
NC1199	*unc-37 (e262); unc-7 (e5); lwEx79*
NC1200	*ceh-12 (gk391) unc-37 (e262); unc-7 (e5); lwEx79*
NC1202	*unc-4 (e2322ts); unc-7 (e5); lwEx79*
NC1205	*ceh-12 (gk391); unc-7 (e5); lwEx79*
NC1216	*ceh-12 (gk391); unc-4 (wd1); unc-7 (e5); lwEx79*

BLAST and phylogenetic analysis

A BLAST search using the CEH-12 protein sequence reveals that the Drosophila Hb9 protein is the highest scoring non-nematode protein, suggesting that CEH-12 is a member of the Mnx/HB9 family. Phylogenetic analysis confirms this idea. The protein sequences for Mnx/HB9 family members, UNC-4 family members, and Even-skipped family members were submitted to the EMBL-EBI ClustalW web-based server (http://www.ebi.ac.uk/clustalw/) and output generated as a Phylogram Guidetree (Figure 5.1).

Construction of ceh-12::GFP reporter lines

2.8 kilobases of promoter sequence upstream of the predicted *ceh-12* start was obtained by PCR amplification of genomic DNA using primers *ceh-12p1* (AAAACTGCAGGTAATTCGGTGCTCGACG) and *ceh-12p2* (TCCCCCCGGGCAAGGCGGAGCCCATCAC). The resulting PCR product was cloned into pCR2.1-TOPO (Stratagene). This fragment was subcloned into pPD95.75 (a gift from Andy Fire) to generate *ceh-12*::GFP. The *unc-119* minigene from MM051(Maduro and Pilgrim 1995) was cloned into *ceh-12*::GFP to make the vector suitable for biolistic transformation. Three independent transgenic lines (Table 5.1) were created by microparticle bombardment, as described (Fox, Von Stetina et al. 2005). Three additional independent lines were generated by microinjection of the *ceh-12*::GFP plasmid.

Timecourse analysis of ceh-12::GFP expression

To obtain synchronized animals, isolated embryos were allowed to hatch and crawl through a 20 μm nylon mesh onto a 100mm NGM plate seeded with OP50-1 bacteria. After 1 hr, the nylon mesh was washed with M9 buffer to rinse off hatched larvae and then transferred to a second plate for an additional 1 hr incubation. The washing and transfer procedure was repeated one additional time to generate 3 cohorts of synchronized *ceh-12*::GFP larvae. Animals were examined 3 hours post-hatching to assay *ceh-12*::GFP expression in L1 larvae. GFP fluorescence was also scored at early L2 (~20 hr post hatching) and mid-L2 (~24 hr post hatching) stages.

ceh-12 cDNA generation and transgenic expression of CEH-12

An RT-PCR reaction using 6 μg of mixed-stage N2 total RNA was used to generate *ceh-12* cDNA [primers: *ceh-12p8* (GTTTAAACTCAAGAAGAGGAAGTTG), *ceh-12p9* (GGTACCATGATGTTTTCCTCAATA)]. This 543 bp fragment was gel purified (Qiagen) and cloned into pCR2.1-TOPO (Stratagene) to create C12ORF-TOPO and used to generate pSV47 (*unc-4* promoter::CEH-12::*unc-54* 3'UTR). pSV47 was injected with pJER1 (*myo-3*::dsRed2) and pCG9 (*acr-5*::YFP) into N2 animals; five lines were obtained (Table 5.1) and examined for Unc-4 movement defects.

PCR detection of ceh-12 deletion alleles

Single worm PCR was performed as described (Plasterk 1995). *ceh-12* il and *ceh-12* ir primers were used to detect the *ceh-12 (gk391)* deletion, and F33D11.4 IL and

F33D11.4 IR primers were used to detect the *ceh-12 (tm1619)* allele. Information on deletion endpoints for *gk391* and *tm1619* can be found at www.wormbase.org.

Immunostaining with αVAB-7 antibody

Antibody staining was performed as previously described (Esmaeili, Ross et al. 2002). Briefly, adult worms were placed in 5 μl of water on a SuperPlus + charged microscope slide, and squashed under a coverslip. Slides were frozen on dry ice for 30 minutes, followed by removal of the coverslip. Animals were fixed in 5% paraformaldehyde for 20 minutes followed immediately by incubation in 100% ice-cold methanol for 4 minutes and then PBST (1x PBS with 0.2% Tween) for 4 minutes. Worms were blocked using 1% non-fat milk (in PBST) for 10 minutes, and then immediately washed with PBST for 10 minutes. Slides were incubated with primary antibody (1:50 in 1% milk solution) for 4 hours at room temperature or overnight at 4°C. Following two 30 minute washes in PBS, secondary antibody (1:1000 goat α-mouse cy3) was applied for 2 hours at room temperature. Slides were washed 2x 30 minutes in PBS, followed by application of vectashield (DAPI) and sealed for microscopic analysis.

Analysis of RAB-3 immuno-staining

Antibody staining was performed as described (Lickteig, Duerr et al. 2001). For RAB-3 antibody staining (Nonet, Staunton et al. 1997), animals were prepared using Bouin's fixative. Animals were incubated in the primary antibody (1:50) for 2 hours at room temperature followed by incubation in a Cy-3-conjugated goat α-mouse secondary antibody (1:500). RAB-3 stained animals were observed in a Zeiss Axiovert inverted

microscope equipped with a Hamamatsu ORCA-ER digital camera. Strains analyzed were wildtype, *unc-4(e120), ceh-12(gk391),* and *ceh-12(gk391);unc-4(e120)*. Thirty images were recorded per strain at an exposure time of 350 milliseconds for Cy3 fluorescence and 1000 milliseconds for GFP. *unc-4*::GFP neurons were scored according to the level of RAB-3 staining associated with each cell. ~100 GFP+ neurons were scored per strain and categorized according to fluorescence intensity: strong, weak or absent. Strong staining indicates that fluorescence completely surrounded the *unc-4*::GFP marked nucleus, whereas weak staining only partially filled the cell soma. Genotypes of specific strains were annotated with an alternative set of generic labels at the time of scoring to avoid experimental bias.

Movement Assays

To test animals for *ceh-12* suppression, 50 L4 hermaphrodites were grown overnight at 20^{o}C [or 25^{o}C for the temperature sensitive allele, *unc-4(e2322ts)*]. Samples were coded with unrelated names by a non-scorer to ensure that the study was performed blindly. The animal was tapped on the head with a platinum wire a maximum of 3 times. Backward movement was scored as: unable to back (does not move or coils immediately), initiates backing (begins sinusoidal motion backward before stopping or coiling), or sustains backward locomotion (performs backward movement for at least two sinosoidal waves).

For the *lin-39* movement assays, 50 L3 hermaphrodites were grown overnight at 25 ^{o}C. L4 Animals were tapped on the head 3 times, as described above. In this case, backward movement was scored in four categories: 1. unable to back (does not move or

coils immediately); 2. initiates backing (begins sinusoidal motion backward before stopping or coiling); 3. able to back one sinusoidal wave; 4. sustains backward locomotion (performs backward movement for at least two sinosoidal waves).

Construction of unc-7S::GFP

The *unc-7* locus encodes 2 isoforms, a long form (UNC-7L, accession #Q03412) and a shorter form, UNC-7S (Starich and Shaw, unpublished). UNC-7S and UNC-7L proteins differ only in the sequences of their predicted intracellular amino termini. Our collaborators, Todd Starich and Jocelyn Shaw, generated a transgenic line that exclusively expresses UNC-7S. An 8.6-kb region flanked by a *SalI* site located in Exon 2 of *unc-7*L (nt 14412 of cosmid R07D5) and a *BamHI* site downstream of the *unc-7* locus (nt 5788 of R07D5) was cloned into pBluescript (Stratagene). This genomic segment includes *unc-7S* promoter/regulatory elements. An in-frame GFP sequence with a translational stop was inserted at a *SalI* site in the last exon of *unc-7*, resulting in the predicted deletion of the carboxyl-terminal 17 amino acids of UNC-7S in the final expressed product. *unc-7S*::GFP and *col-19*::GFP were co-injected and transgenic animals identified by *col-19*::GFP expression in the adult hypodermis (Abrahante, Miller et al. 1998). UNC-7S::GFP puncta were diffuse in the wildtype background, but localized to tight ventral cord puncta in *unc-7* mutants; these animals were also partially rescued for the Unc-7 forward movement defect (TS and JS, unpublished data). We interpret these results to mean that UNC-7S::GFP assembles into functional gap junctions that restore locomotory activity to *unc-7* mutants.

UNC-7S::GFP antibody staining and analysis

UNC-7S::GFP transgenics were methanol-formaldehyde fixed as described (Finney and Ruvkun 1990) and incubated with monoclonal GFP antibodies (Quantum Biotechnologies) and Goat anti-Mouse IgG-Cy3. The ventral cord motor neurons between the retrovesicular ganglion (RVG) at the anterior end of the cord and the posterior preanal ganglion (PAG) of L4 and adult animals were scored for the association of anti-GFP puncta. [Motor neurons in the RVG and PAG were not scored (e.g. VA1 and VA12) because they are difficult to identify unambiguously in these ganglia.] Results were recorded for each motor neuron of each type in this interval (VA2-11, VB3-VB11, DA2-7, DB3-DB7, DD2-DD5, VD3-VD11, AS2-10, VC1-6). All scoring was performed "blindly" meaning that genotypes of each sample were unknown to the individuals performing the experiment until after scoring was completed.

The percentages of UNC-7S::GFP puncta were averaged from three *unc-4* alleles (*e120, e2322ts, e2323*) and *unc-37 (e262)* (Unc), and compared to the averages from *ceh-12; unc-4* and *ceh-12; unc-37* animals (Ceh). A two-tailed t-test was performed to determine if the average UNC-7S::GFP puncta of Unc was significantly different from the average of Ceh.

Results

CEH-12 is closely related to HB9 homeodomain protein, a known specifier of motor neuron fate

Phylogenetic analysis indicates that *ceh-12* is the closest *C. elegans* relative of the Mnx/HB9 family of homeodomain proteins (Figure 5.1). CEH-12 includes a N-terminal eh1 domain (Jimenez, Paroush et al. 1997) that is also conserved in this location in other HB9 proteins (Figure 5.1). The presence of this potential Groucho-interaction domain is consistent with the model that CEH-12 and other HB9 proteins are transcriptional repressors (William, Tanabe et al. 2003). The well-established and highly conserved role of HB9 proteins in motor neuron differentiation in other species (Arber, Han et al. 1999; Thaler, Harrison et al. 1999; Broihier and Skeath 2002) suggested to us that *ceh-12* was also likely to regulate motor neuron fate in *C. elegans* and, therefore, was a strong candidate for an *unc-4* target gene.

ceh-12::GFP is specific to VB motor neurons in the ventral cord

We have proposed that UNC-4 target genes are normally expressed in VB motor neurons in the wildtype. To test this model for *ceh-12*, we used a genomic fragment spanning 2.5 kb upstream of *ceh-12* to construct a *promoter*::GFP fusion gene. Six independent *ceh-12*::GFP transgenic lines were generated. In every case, GFP fluorescence in the ventral cord is limited to VB class motor neurons in the wildtype. *ceh-12*::GFP is also expressed in the RID neuron in the head and in the pharyngeal-intestinal valve cell and excretory gland cell (Figure 5.2).

To address whether *ceh-12* is expressed in neuronal precursor cells or restricted to postmitotic neurons, we performed a timecourse analysis to examine *ceh-12*::GFP expression starting in newly hatched L1s through mid-L2 stage animals. In wildtype animals, within 3 hr of hatching, *ceh-12*::GFP is detected in the RID head neuron, the

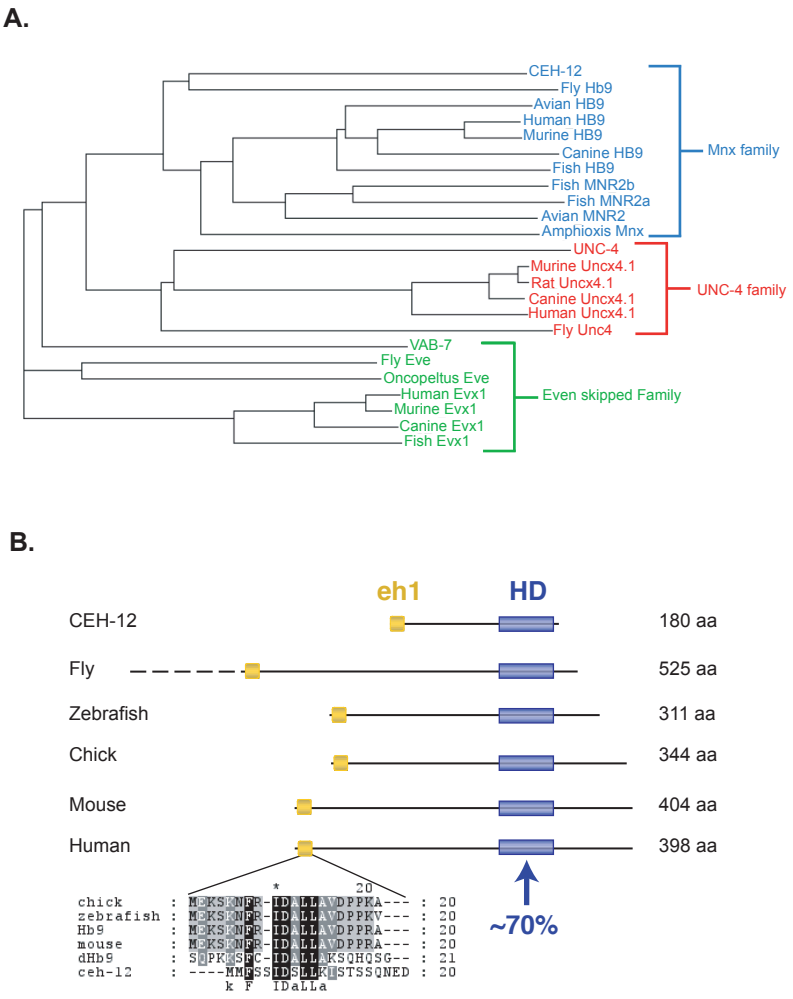

Figure 5.1. Phylogenetic analysis and domain structure of CEH-12. A. Phylogenetic tree comparing members of the Mnx/HB9, UNC-4 and Even-skipped homeodomain transcription factor families. CEH-12 is more closely related to members of the Mnx family than to other *C. elegans* homeodomain proteins. B. Genomic structures of Mnx family homeodomain genes. CEH-12 contains homeodomain (~70% identical to other species) and conserved N-terminal eh-1 Groucho interaction domain.

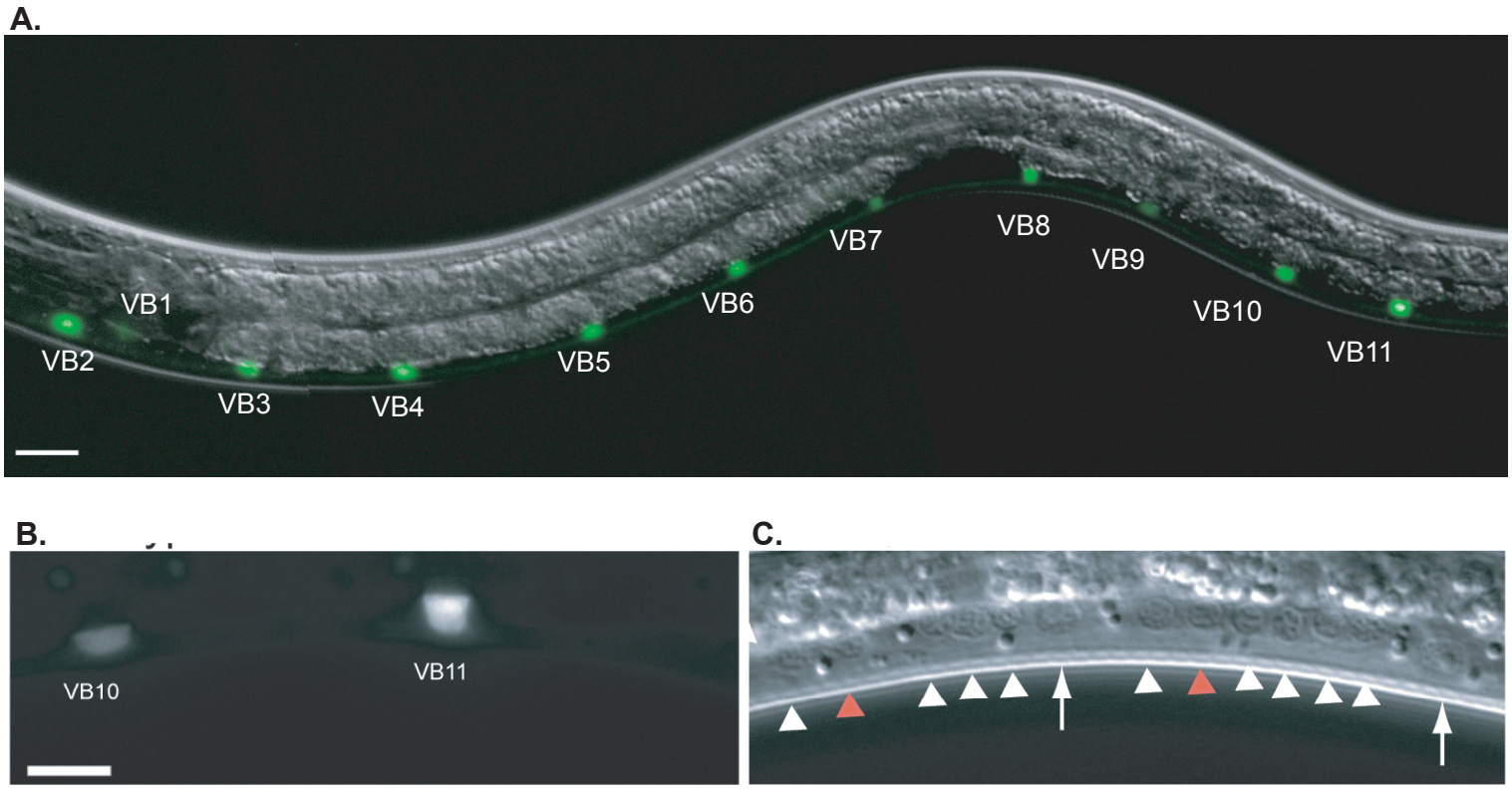

Figure 5.2. *ceh-12*::GFP is specific to VB motor neurons in the ventral nerve cord. A. A promoter-GFP reporter, *ceh-12*::GFP, is expressed in all eleven VB motor neurons and in a single head neuron, RID; occasional weak GFP expression was observed in the pharyngeal/intestinal valve cell and in the excretory gland cell (data not shown). Scale bar is 10 microns. B. Close up view of wildtype posterior ventral cord showing expression of *ceh-12*::GFP in VB motor neurons. Scale bar is 2 microns. c. White arrowheads in wildtype DIC image point to motor neuron nuclei that do not express *ceh-12*::GFP; red arrowheads denote VB10 and VB11 that express GFP in top panel. Arrows identify landmark P9.p and P10.p ectoblasts.

pharyngeal-intestinal (P-I) valve, and 1-2 excretory gland cells. Weak GFP expression was occasionally observed in 1-2 additional neurons in the tail. We found that, as the neuroblast precursors "P cells" stopped dividing (L1-L2 transition), we would see a lag in GFP expression. For example, we could observe animals in which P cells anterior to the gonad had stopped dividing, but only VB1/2 (located in the head) were expressing GFP. It was only after all ten P cells had stopped dividing that we would see expression throughout the ventral cord, indicating that *ceh-12*::GFP is expressed in postmitotic motor neurons.

CEH-12 specifies VB fate by repressing VAB-7/Eve

To determine if native *ceh-12* regulates gene expression in VB motor neurons, we assayed specific motor neuron markers in the *ceh-12* deletion alleles *tm1619* and *gk391*. Expression of VB reporters *del-1*::GFP and *acr-5*::GFP, the A-class marker *unc-4*::GFP, and the A- and B-class marker *acr-2*::GFP was unchanged (data not shown). However, immunostaining results revealed that VAB-7/Even-skipped is de-repressed in VB motor neurons in *ceh-12* mutants (Figure 5.3). VAB-7/Eve expression in the ventral nerve cord is normally restricted to DB motor neurons during the L2 larval stage in which *ceh-12*::GFP is expressed in VB motor neurons (VAB-7 is also expressed in VC motor neurons in the adult) (Figure 5.3) (Esmaeili, Ross et al. 2002). DB motor neurons extend axons to innervate dorsal muscles whereas VB motor neuron outputs are directed to ventral muscles. Ectopic VAB-7 expression in the VBs is not sufficient to impose a dorsal axonal trajectory, however, as VB motor neurons maintain ventral outputs in *ceh-12* mutants (data not shown). This finding is consistent with an earlier report that VAB-7

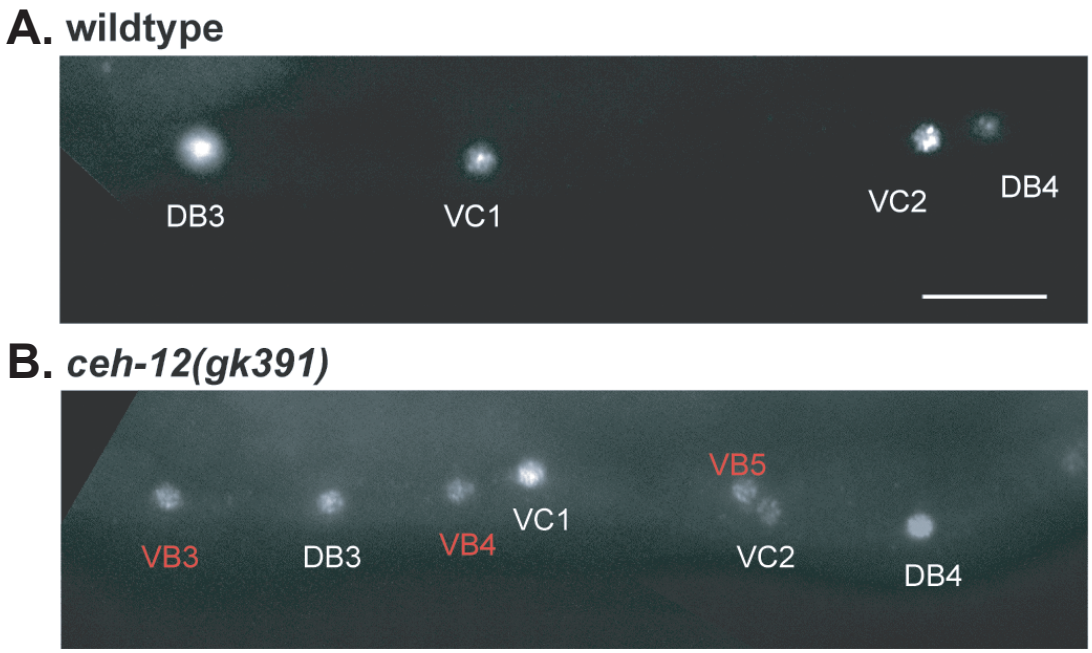

Figure 5.3. *ceh-12* represses VAB-7 to promote VB fate. A. Immunostaining of wildtype adult animals reveals VAB-7 expression in DB and VC motor neurons. B. VAB-7 is detected ectopically in VB motor neurons in *ceh-12(gk391)* mutant adult. Similar results are seen with the *ceh-12(tm1619)* allele (data not shown). Scale bar is 10 micron.

expression maintains the posterior trajectory of DB motor neurons but does not affect axon guidance along the dorsal/ventral axis. Thus, CEH-12 may repress VAB-7 to prevent VB motor neurons from adopting other DB motor neuron characteristics. Our results showing that *ceh-12*/HB9 represses VAB-7/Eve expression in VB motor neurons mirrors similar transcriptional regulation in Drosophila, in which dHB9 represses Eve in selected motor neuron classes (Broihier and Skeath 2002).

ceh-12::GFP is negatively regulated by *unc-4* and *unc-37* in posterior A-class motor neurons

Our model predicts that UNC-4 target genes are normally expressed in VB motor neurons but turned off in the VAs by the combined activity of UNC-4 and UNC-37/Groucho (Winnier, Meir et al. 1999). We have confirmed this prediction for *ceh-12* by testing *ceh-12*::GFP for *unc-4* and *unc-37* regulation (Figure 5.4). In *unc-4* and *unc-37* mutants, *ceh-12*::GFP is also expressed in A-class motor neurons (Figure 5.4). The effect is strongest for VA motor neurons in the posterior ventral nerve cord. For example, in *unc-4(e120),* 80% of VA10 neurons show ectopic *ceh-12*::GFP expression whereas only ~15% of VA7 motor neurons are affected; ectopic *ceh-12*::GFP was never detected (n = 30) in VA2 at the anterior end of the VNC (Figure 5.4). A similar bias in *ceh-12*::GFP expression was also observed for posteriorly located DA motor neurons in *unc-4* and *unc-37* mutants.

To test for the possibility that *ceh-12*::GFP is expressed transiently in anterior VA motor neurons, we performed a timecourse analysis in the *unc-4(e120)* mutant as described above for the wildtype. This experiment confirmed that early L1s, three hours post-hatching, express *ceh-12*::GFP in RID, the P-I valve, and in the excretory gland cells

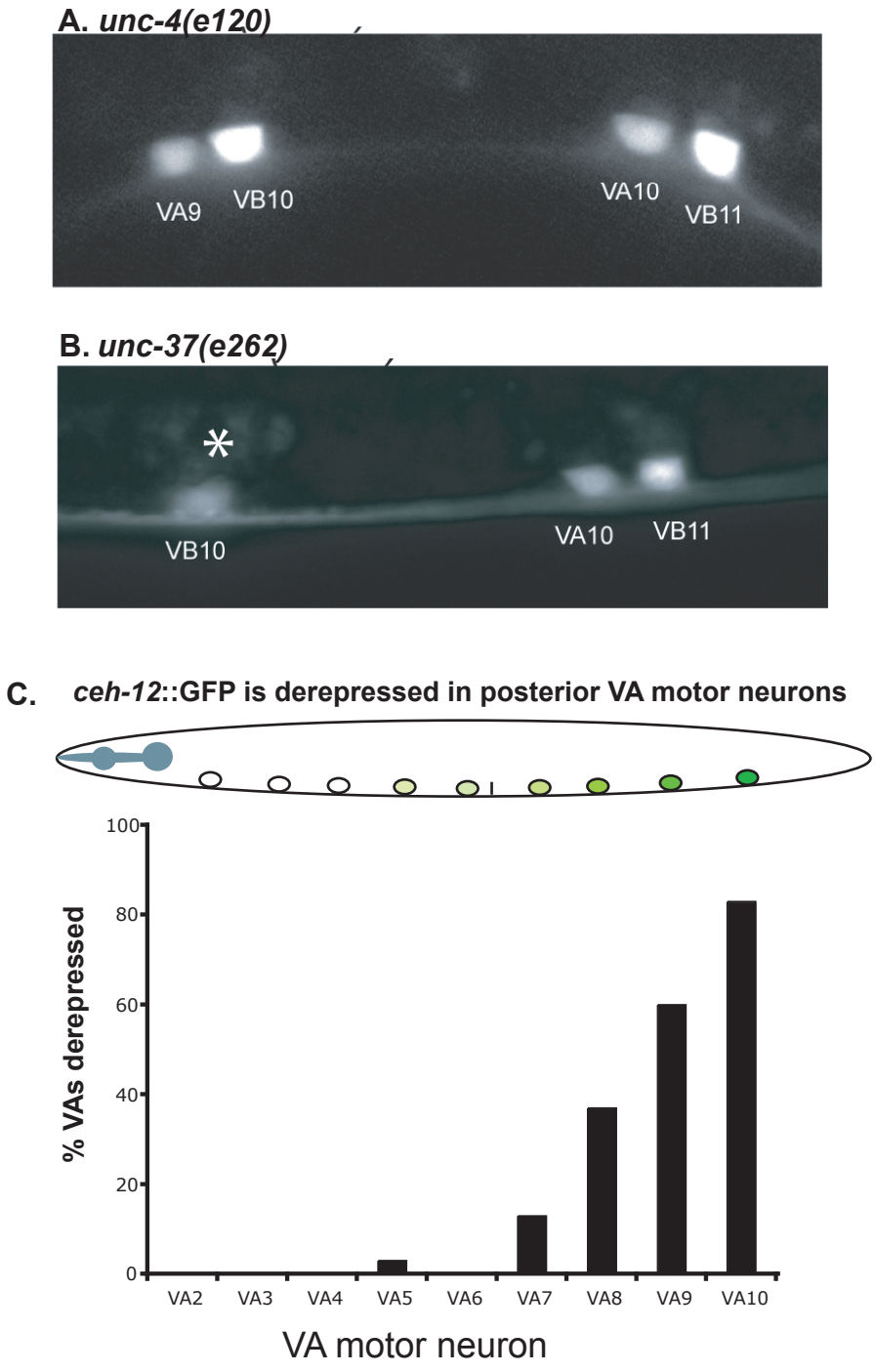

Figure 5.4. *ceh-12*::GFP is negatively regulated by UNC-4/37 in posterior VA motor neurons. A., B.Ectopic *ceh-12*::GFP expression in VA motor neurons in *unc-4* and *unc-37* mutants. All are mid-L2 stage larvae. Anterior to left, ventral down. C. *ceh-12*::GFP is preferentially de-repressed in posterior VA motor neurons in *unc-4(e120)*. n = 30.

as in the wildtype. Nevertheless, *ceh-12*::GFP was also expressed in posterior DA motor neurons with a strong GFP signal in DA7 and weaker ectopic expression in DA6, DA8 and DA9 (data not shown). This finding confirms the MAPCeL data showing that the *ceh-12* transcript is significantly elevated in DA motor neurons in *unc-4(e120)*. After the P cells had finished dividing, we could see strong GFP expression in all VBs, with equally strong expression in the posterior VA motor neurons (VA7-10); however, these experiments suggest that derepression of *ceh-12*::GFP in *unc-4(e120)* mutants is specific for posterior VA and DA motor neurons. On the basis of these results, we conclude that *ceh-12* is a strong candidate for a VB gene that is negatively regulated by the *unc-4* pathway in posterior A-class motor neurons.

CEH-12 expression in VA motor neurons induces an Unc-4-like movement defect

If *ceh-12* is sufficient to miswire VA motor neurons, then ectopic expression of CEH-12 in the VAs should result in a backward Unc defect. To test this idea, we used the *unc-4* promoter to drive CEH-12 protein expression in A-class motor neurons. These "VA-CEH-12" animals are unable to execute backward movement when stimulated by head touch and instead coil dorsally, a phenotype that resembles that of *unc-4* mutants (Figure 5.5). Because CEH-12 is predicted to act as a transcriptional repressor, this behavior could have resulted from CEH-12-dependent repression of *unc-4*. However, *unc-4*::GFP is expressed normally in A-class motor neurons in VA-CEH-12 animals. Thus, we propose that CEH-12 must be acting on other VA genes to induce the backward Unc phenotype (Figure 5.11).

***ceh-12* mutations suppress the Unc-4 backward movement defect**

Above, we showed that ectopic expression of CEH-12 in VA motor neurons is sufficient to produce an Unc-4-like backward movement defect in VA-CEH-12 worms. If de-repression of *ceh-12* in *unc-4* mutants is responsible for this phenotype, then the loss of *ceh-12* activity should result in improved backward locomotion for these animals. To test this idea, we used the *ceh-12* deletion alleles *tm1619* and *gk391* in genetic experiments with *unc-4* and *unc-37* mutants to detect "suppression" of the Unc-4 phenotype. As shown in Figure 5.6, *ceh-12(0)* affords weak but significant improvement of backward locomotion in the null allele, *unc-4(e120)*. A similar effect was observed in double mutant combinations of *ceh-12(0)* with *unc-37(e262)* (Table 5.2). Incomplete suppression of the Unc-4 phenotype by *ceh-12(0)* could be indicative of a second downstream pathway that is also de-repressed in *unc-4* mutants. We note in this regard that *ceh-12*::GFP is preferentially expressed in posterior VA motor neurons in *unc-4* mutants (Figure 5.4) although anterior VAs are also miswired. This result suggests that normal VA inputs are selectively restored to posterior VA motor neurons in *ceh-12(0)*; *unc-4(0)* double mutants whereas anterior VAs remain miswired due to the ectopic activity of a presumptive parallel pathway that functions in these cells (Figure 5.11).

The proposal that *ceh-12* functions downstream of *unc-4* in parallel to at least one additional partially redundant pathway, is also consistent with our finding that the weak or hypomorphic *unc-4* alleles, *e2323* and *e2322ts*, are strongly suppressed by *ceh-12(0)*. For example, *unc-4(e2323)* animals are unable to sustain backward movement, whereas almost all (98%) of *ceh-12(0)*; *unc-4(e2323)* animals readily execute reverse locomotion when touched on the head (Figure 5.6, Table 5.2). In this case, we propose that the

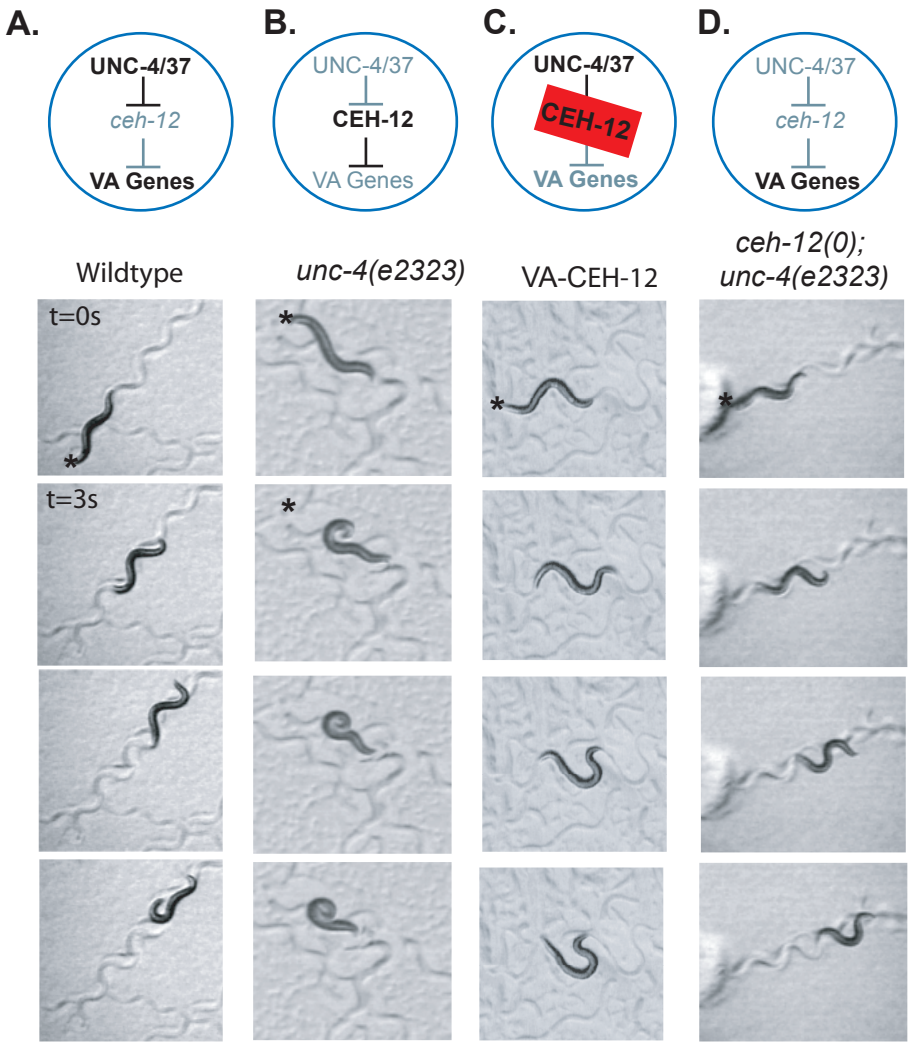

Figure 5.5. ***ceh-12*** **genetically interacts with** ***unc-4*** **to control backward locomotion.** Animals were touched on the head (asterisk) to stimulate backward locomotion. Models above movie panels indicate gene expression in VA motor neurons. A. Wildtype animals back away for 9 sec following touch. B. Mutations in *unc-4* or *unc-37* de-repress *ceh-12* and block backward locomotion. Note that the *unc-4(e2323)* animal in bottom panels coils in response to touch but cannot back. C. Transgenic expression of CEH-12 in VA motor neurons (VA-CEH-12) is sufficient to induce an Unc-4-like backing defect. D. *ceh-12(0)* restores backward movement to the hypomorphic allele, *unc-4(e2323)*.

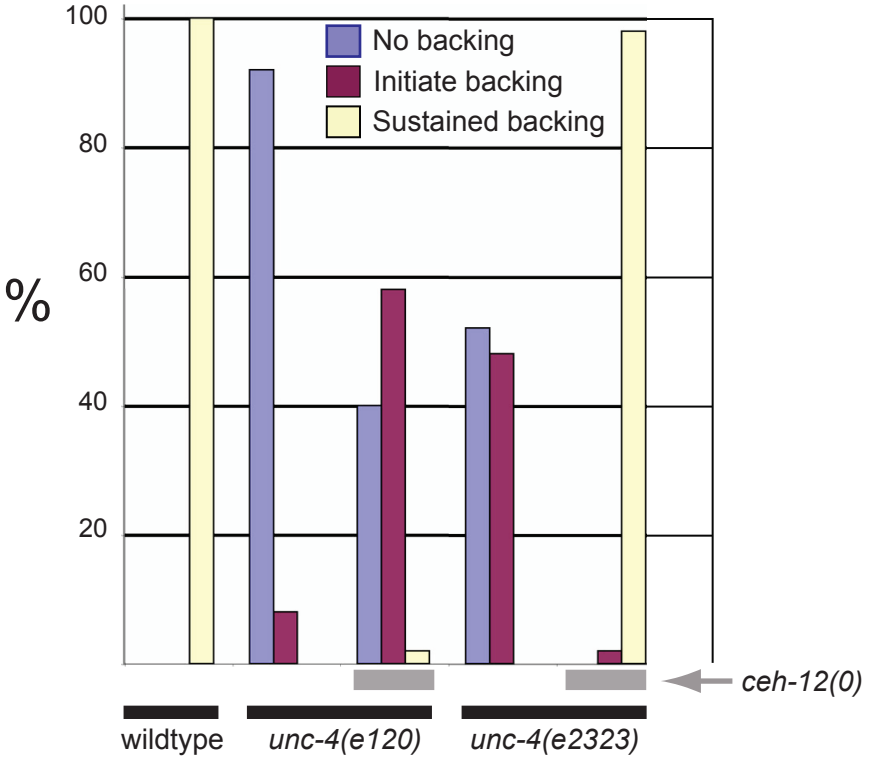

Figure 5.6. *ceh-12(0)* suppresses the Unc-4 movement defect. Quantification of Unc-4 backward movement defects reveals suppression by *ceh-12* null alleles. Individual animals of each genotype were tapped on the head to evoke backward movement and scored according to 3 phenotypes: (blue) No backing (coil immediately upon tapping); (purple) Initiate backing (but then stop); (yellow) Sustained backward movement (> 2 body bends). Note that the null allele *unc-4(e120)* is weakly suppressed by *ceh-12(0)* whereas the hypomorphic mutation, *unc-4(e2323)*, is strongly suppressed by *ceh-12(0)* (i.e. shows sustained backward movement). All results for *ceh-12(gk391)*. Similar results were obtained for *ceh-12(tm1619)* (data not shown).

residual function of these hypomorphic *unc-4* alleles prevents full de-repression of target genes and therefore limits their consequent negative effects on putative downstream VA-input genes. In this situation, subsequent elimination of *ceh-12* function in posterior VA motor neurons allows net VA motor neuron activity throughout the cord to exceed a threshold required for the restoration of backward locomotion (Figure 5.11).

Candidates that could function in parallel to *ceh-12* include *del-1* (DEG/ENaC channel subunit), *acr-5* (nicotinic ACh receptor subunit) and *glr-4* (ionotrophic Glutamate receptor); VB genes that we have previously shown to be negatively regulated in VA motor neurons by *unc-4* and *unc-37* (Winnier, Meir et al. 1999). As cell surface proteins and ion channel components, DEL-1, ACR-5, and GLR-4 are plausible synaptic determinants. Nevertheless, Steve Von Stetina determined that null alleles of these loci have no effect on the Unc-4 phenotype either alone or in combination with *ceh-12* (Table 5.2). Furthermore, he showed that *ceh-12* does not regulate the expression of these ion channel components in VB motor neurons. These genetic results rule out a role for *del-1*, *acr-5* and *glr-4* as *unc-4* target genes that regulate synaptic choice. Alternatively *unc-4* may repress these downstream genes to prevent expression of other VB traits in VA motor neurons.

UNC-4 and CEH-12 regulate the specificity of gap junctions between command interneurons and motor neurons

The wiring diagram of the *C. elegans* nervous system was originally deduced from reconstruction of serial sections photographed in the electron microscope (White, Southgate et al. 1986). A partial EM reconstruction of *unc-4(e120)* revealed the miswiring defect of selected VA motor neurons (VA2, VA3, VA10). Aberrant gap

Table 5.2. *ceh-12* suppresses the Unc-4 backward movement defect.

Strain	No Backing (%)	Initiate Backing (%)	Sustain Backing (%)	Number of animals scored
Wildtype (N2)	0	0	100	50
ceh-12(gk391)	0	4	96	50
ceh-12(tm1619)	0	6	94	50
unc-4(e120)	92	8	0	49
unc-4(e2323)	52	48	0	50
unc-4(e2322ts)	75	25	0	51
unc-37(e262)	88	12	0	49
ceh-12(gk391); unc-4(e120)	40	58	2	50
ceh-12(gk391); unc-4(e2323)	0	2	98	50
ceh-12(gk391); unc-4(e2322ts)	0	4	96	50
ceh-12(gk391); unc-37(e262)	38	40	22	50
ceh-12(tm1619); unc-4(e2322ts)	0	6	94	50
glr-4(ak78) unc-4(e120); acr-5(ok180); del-1(ok150)	96	4	0	50
ceh-12(gk391); glr-4(ak78) unc-4(e120); acr-5 (ok180); del-1(ok150)	47	45	8	49
ceh-12(tm1619); glr-4(ak78) unc-4(e120); acr-5 (ok180); del-1(ok150)	70	28	2	50

junctions with AVB are particularly prominent and are placed directly on the VA motor neuron soma, a location adjacent to the cell nucleus that is also characteristic of the usual AVB gap junctions with DB and VB motor neurons (White, Southgate et al. 1992). We have now confirmed these results with a GFP-tagged marker that allows visualization in the light microscope of gap junctions between AVB command interneurons and specific VNC motor neurons.

Invertebrate gap junctions are assembled from innexins, modular subunit proteins that function similarly to the unrelated vertebrate gap junction connexin proteins (Phelan and Starich 2001). Recently, a second vertebrate family of gap junction proteins, the pannexins, have been identified through weak sequence similarity to the innexins (Bruzzone, Hormuzdi et al. 2003; Panchin 2005). The *C. elegans* genome includes 25 innexin genes with distinct spatial and temporal patterns of expression (Starich, Sheehan et al. 2001). The *unc-7* gene encodes at least two innexin isoforms, UNC-7L and UNC-7S (Starich and Shaw, unpublished). AVB command interneurons express UNC-7S, and a GFP-tagged UNC-7S construct is expressed in distinct puncta along the ventral nerve cord. In wildtype animals, most DB and VB motor neurons are marked with UNC-7S::GFP puncta adjacent to the cell soma, whereas other motor neurons are rarely stained (Figure 5.7). This result is fully consistent with the motor circuit wiring diagram derived from EM reconstruction. On the basis of our results, we conclude that UNC-7S::GFP is a reliable marker of AVB gap junctions with specific ventral cord motor neurons.

In *unc-4(e120)* mutants, ectopic GFP puncta are consistently observed adjacent to the cell soma of nine VA motor neurons (VA2-VA10) (Figure 5.7). This result both confirms and extends the findings from the original EM reconstruction of *unc-4(e120)*.

This study was limited to portions of the anterior and posterior ventral cord where AVB gap junctions were detected for VA2, VA3 and VA10; miswiring of VA4-VA9 was inferred from the Unc-4 backward movement defect that appears to result from VA dysfunction throughout the intervening body region (White, Southgate et al. 1992).

UNC-7S::GFP puncta are similarly misplaced on VA class motor neurons in other *unc-4* alleles and in the Groucho mutant, *unc-37(e262)* (Figure 5.7) (Table 5.3). These results establish that the AVB-to-VA gap junction defect represents the *unc-4* null phenotype and confirm the essential role of UNC-37/Groucho in UNC-4 function. Surprisingly, we also observed UNC-7S::GFP puncta on DA class motor neurons (Figure 5.8) and on VA11 (Table 5.4) in *unc-4* and *unc-37* mutants (VA1 and VA12 were not scored, see Methods). The incomplete penetrance of this effect (<50%) and the limited number of DA motor neurons examined in the original EM reconstruction of *unc-4(e120)* may explain why these gap junctions with AVB were not previously observed (White, Southgate et al. 1992).

ceh-12 function is required for miswiring of posterior VA motor neurons with AVB gap junctions.

To determine if de-repression of *ceh-12* is required for the creation of ectopic AVB gap junctions with VA motor neurons, we examined the distribution of UNC-7S::GFP puncta in *ceh-12(0)*; *unc-4(e120)* double mutants. Whereas the frequency at which UNC-7S::GFP puncta are placed next to VA motor neurons in the anterior ventral cord is comparable to that of *unc-4(e120)* (i. e., 90-95%), a significant reduction is noted for posterior VA motor neurons in *ceh-12(0)*; *unc-4(e120)* animals (e.g. 30% for VA10) (Figure 5.8). This effect is confirmed by similar results showing a posterior bias for *ceh-*

Table 5.3. Quantification of UNC-7S::GFP puncta on VA motor neurons											
Strain	**n=**	**%VA2**	**%VA3**	**%VA4**	**%VA5**	**%VA6**	**%VA7**	**%VA8**	**%VA9**	**%VA10**	**%VAs**
wildtype	18-23	4	23	14	5	5	0	5	20	5	9
ceh-12(gk391)	28-34	13	16	19	6	23	4	9	30	24	11
unc-4(e120)	24-30	83	80	87	100	92	76	92	89	100	89
ceh-12(gk391; unc-4(e120)	27-45	60	82	87	88	85	70	59	50	38	69
unc-4(e2322ts)	8-10	100	90	80	100	89	100	90	80	100	92
ceh-12(gk391); unc-4(e2322ts)	7-10	60	70	100	70	80	71	70	60	30	68
unc-4(e2323)	18-30	77	83	90	86	84	83	90	75	89	87
ceh-12(gk391); unc-4(e2323	4-10	70	80	90	100	90	50	57	67	67	77
unc-37(e262)	17-20	95	79	89	89	83	94	95	74	89	88
ceh-12(gk391) unc-37(e262)	27-33	82	82	79	85	70	70	89	63	53	78
unc-4(wd1)	18-23	83	100	74	87	95	100	63	95	85	85
ceh-12(gk391); unc-4(wd1)[1]	17-20	91	100	73	91	100	70	80	80	100	87

[1] *unc-4 (wd1)* animals do not exhibit *ceh-12(0)*-mediated suppression of the miswiring phenotype in posterior VA motor neurons. The significance of this observation is unclear as the *wd1* allele is a large deletion that removes most of the *unc-4* gene as well as upstream regions that are likely to include several additional genes.

Table 5.4. Quantification of UNC-7S::GFP puncta on VA11		
Strain	**n**	**%VA11**
Wildtype	21	10
ceh-12(gk391)	34	26
unc-4(e120)	28	39
ceh-12(gk391); unc-4(e120)	39	33
unc-4(e2322ts)	10	20
ceh-12(gk391); unc-4(e2322ts)	10	20
unc-4(e2323)	27	30
ceh-12(gk391); unc-4(e2323)	9	22
unc-37(e262)	19	26
ceh-12(gk391) unc-37(e262)	30	33
unc-4(wd1)	20	10
ceh-12(gk391); unc-4(wd1)	10	30

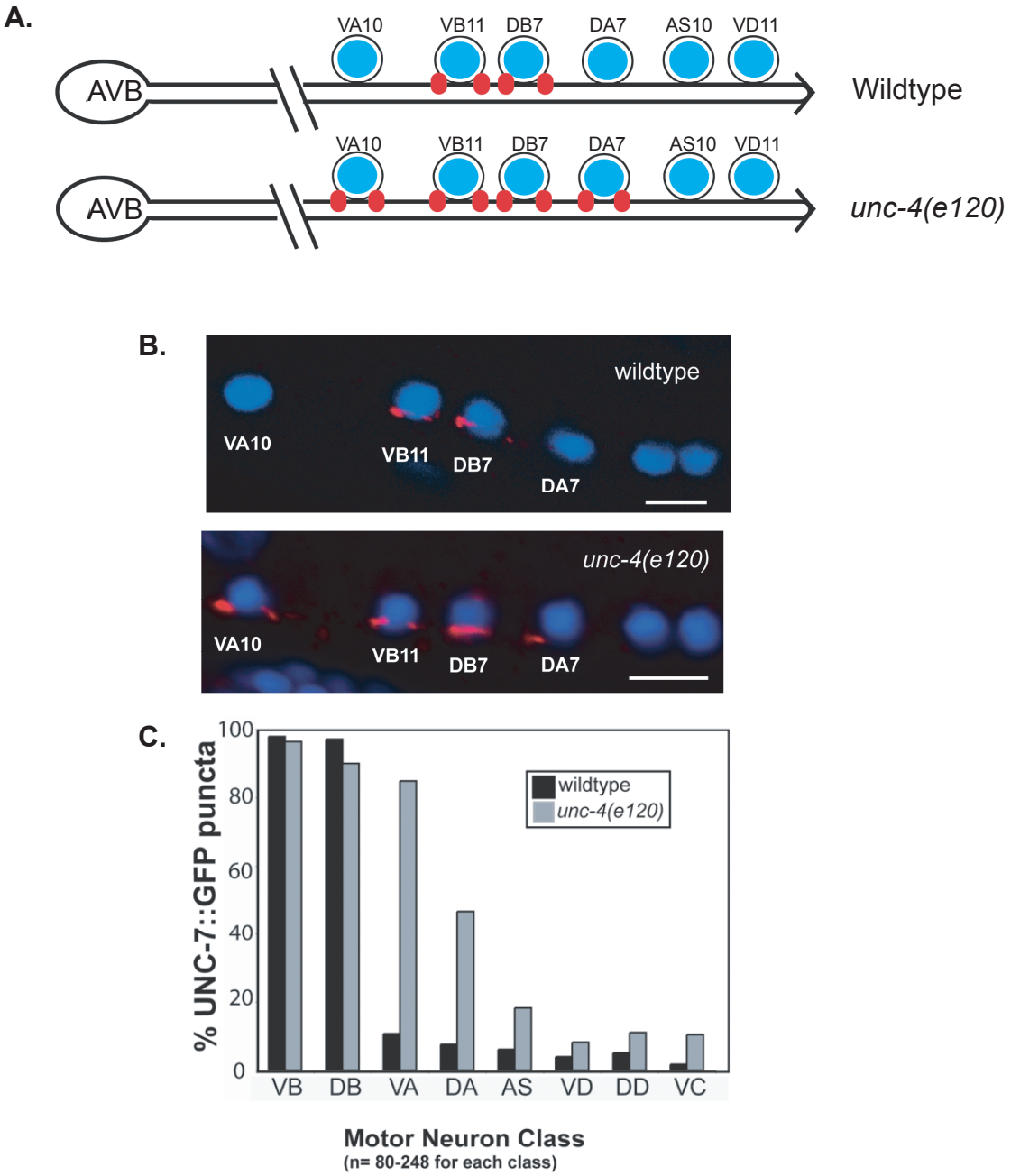

Figure 5.7. Gap junctions between command interneuron AVB and specific motor neurons are visualized with UNC-7S::GFP. A. Posterior ventral nerve cord showing gap junctions (red puncta) between AVB and soma of specific motor neurons (blue). B. Confocal images of UNC-7S::GFP puncta adjacent to motor neuron nuclei stained with DAPI. Lateral view of adult; anterior to left, ventral down. Scale bars are 5 microns. C. Quantification of UNC-7S::GFP puncta on specific motor neuron classes in wildtype and *unc-4(e120)*. UNC-7S::GFP puncta are consistently observed adjacent to DB and VB motor neurons. Most (~80%) VA motor neurons (VA2-VA10) are miswired with UNC-7S::GFP puncta in *unc-4(e120)*; DA motor neurons may also be affected (45%) (See DA7 in panel B). UNC-7S::GFP puncta are rarely associated with other motor neuron classes (AS, VD, DD, VC).

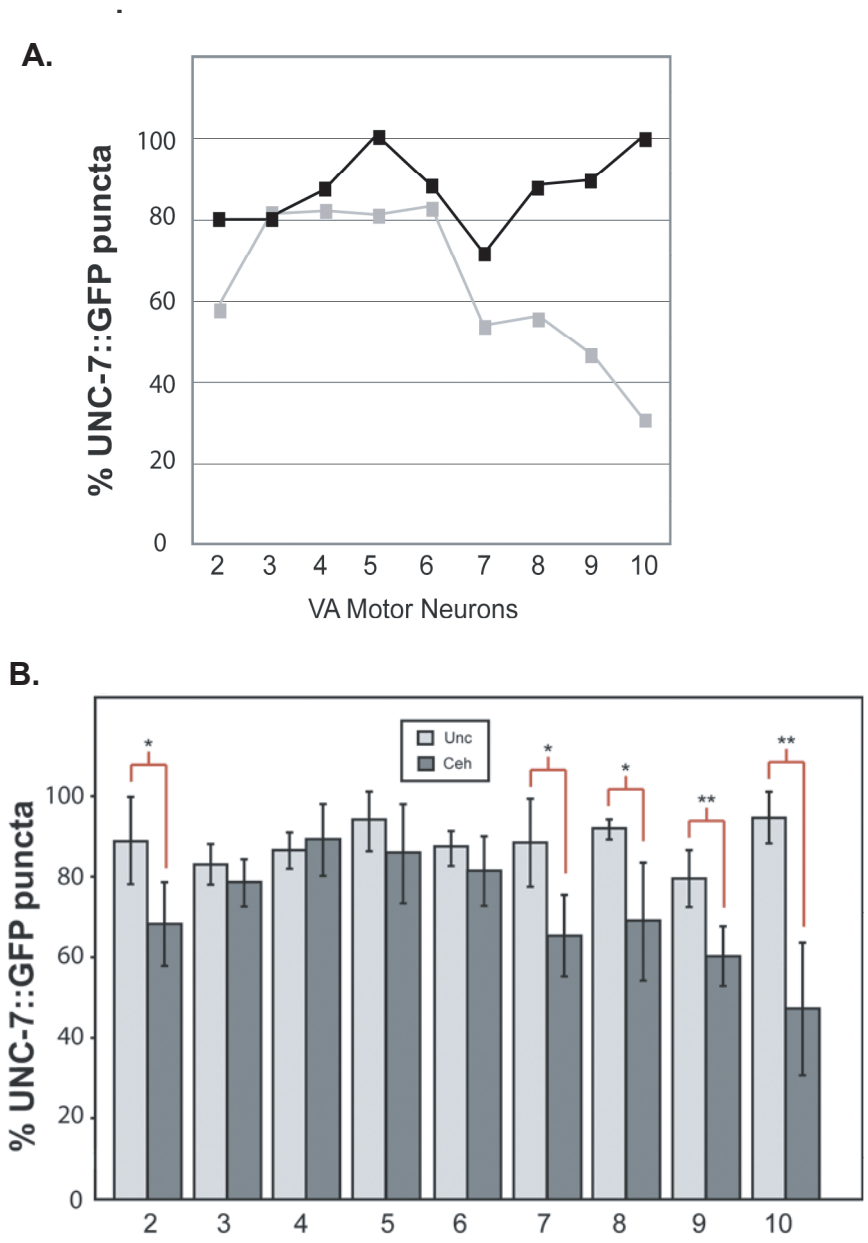

Figure 5.8. Rescue of the AVB wiring defect in *ceh-12; unc-4* is biased to posterior VA motor neurons. UNC-7S::GFP puncta were scored for VA2-VA10. A. Fraction of VAs with AVB gap junctions in *unc-4(e120)* (black boxes) vs *ceh-12(0); unc-4(e120)* (gray boxes). (n = 24 to 45 for each VA in each genotype). B. Fraction of VAs with AVB gap junctions were averaged for *unc-4 (e120, e2322ts, e2323)* and *unc-37 (e262)* mutants (Unc, light gray bars) and compared to the average of *ceh-12; unc-4* and *ceh-12; unc-37* double mutants (Ceh, dark gray bars). A statistically significant decrease in UNC-7S::GFP puncta is noted for Ceh animals in VA2 (P=0.032), VA7 (P=0.021), VA8 (P=0.021), VA9 (P=0.008), and VA10 (P=0.002). *P<0.05, **P<0.01.

12(0) rescue of the AVB gap junction miswiring defect in two additional *unc-4* alleles and in *unc-37(e262)* (Figure 5.8). The finding here that *ceh-12* is selectively required for the Unc-4 gap junction defect in the posterior ventral cord is congruent with the observation that *ceh-12*::GFP is preferentially de-repressed in posterior VA motor neurons in *unc-4* mutants (Figure 5.4). Although not directly scored by the UNC-7S::GFP assay, restoration of normal inputs (e.g. gap junctions and chemical synapses with AVA) to posterior VAs is also likely given the partial suppression of backward movement in *ceh-12(0)*; *unc-4(e120)* animals (Figure 5.6).

Do HOX genes function in the *unc-4* pathway*?*

The HOX genes are a class of homeobox transcription factors that pattern the A/P axis. In *C. elegans*, the anterior region is specified by *ceh-13*, while the midbody is patterned by *lin-39*; cell fates in the posterior region depend on two genes, *mab-5* and *egl-5* (Kenyon, Austin et al. 1997). Potential roles for HOX genes in the *unc-4* pathway were suggested by the elevation of the *lin-39* and *mab-5* transcripts respectively in the MAPCeL and mRNA tagging profiles of candidate *unc-4* target genes. This possibility seemed especially attractive as the expression domain of *lin-39* in the midbody region appears to complement expression of *ceh-12*::GFP in posterior VA class motor neurons in *unc-4* mutants. Derepression of *ceh-12*::GFP was strongest in VA7-VA10. VA7 arises from the neuronal progenitor P7, which marks the boundary for *lin-39* and *mab-5* expression, with *lin-39* being preferentially expressed in this ectoblast. Thus, we hypothesize that *lin-39* may play a role in determining synaptic choice in VA motor neurons located in the midbody region.

To assess whether the HOX genes act downstream of *unc-4* to specify cell fate, we performed movement assays to determine if mutations in these genes can suppress the Unc-4 backing defect. These experiments revealed, however, that double mutant combinations of *unc-4* (both null and hypomorphic alleles, *e120* and *e2322ts*) with *lin-39*, *mab-5* or *egl-5* do not result in a significant rescue of backward locomotion. In addition, we tested double mutant combinations of the HOX genes (*mab-5 egl-5* and *lin-39 egl-5*) and found that these also do not suppress the Unc-4 backing defect. It is quite possible that *lin-39* is affecting the midbody VA neurons, but since the wiring defect of posterior VA motor neurons are not rescued in the *lin-39;unc-4* double, there is not a measurable difference in backward movement between the *unc-4* and *unc-4;lin-39* mutants. To assess this possibility we generated a *ceh-12; unc-4; lin-39* triple mutant and tested to see if *lin-39* was able to enhance the suppression of the *ceh-12;unc-4* double mutant. Movement assays determined that the addition of *ceh-12* does not lead to further rescue of the Unc-4 backing defect. It is possible this assay may not be sufficiently sensitive to detect small changes in locomotory activity. A test that may be more informative in this case is the thrashing assay. For this test, animals are placed in liquid and the number of "thrashes" is counted; a thrash being defined as a change in direction of the midbody of the animal (Miller, Alfonso et al. 1996).

Preliminary experiments with a *lin-39 promoter*-lacZ reporter gene did not detect *unc-4* regulation *in vivo*. This result needs to be confirmed, however, by similar experiments with *lin-39*::GFP promoter constructs (Wagmaister, Gleason et al. 2006) obtained from The Eisenmann lab (U. Maryland, Baltimore). It will also be interesting to test *mab-5* for *unc-4* regulation. The normal function of *mab-5* is to promote

programmed cell death of potential VB motor neurons arising from the P11 and P12 lineages; these neurons survive in *mab-5* mutants (Kenyon 1986; Liu, Strauss et al. 2006). Whether or not the HOX genes function in the *unc-4* pathway is not resolved by these preliminary experiments. Nevertheless, it is evident that the mechanisms that influence synaptic choice are complicated and likely to include numerous, partially redundant pathways that specify synaptic connections between particular neuron pairs.

ceh-12 rescues the Unc-4 synaptic vesicle defect in VA/DA motor neurons

unc-4 mutants display a second defect in addition to the miswiring of the VA motor neurons; all neurons that normally express UNC-4 ("UNC-4 neurons") exhibit reduced numbers of synaptic vesicles (SV) in *unc-4* and *unc-37* mutants (Lickteig, Duerr et al. 2001). The loss of these neurotransmitter vesicles correlated with reduced levels of immunostaining for five SV-associated proteins; UNC-17 (vesicular acetylcholine transporter), CHA-1 (choline acetyltransferase), SNB-1 (synaptobrevin), SNT-1 (synaptotagmin) and RAB-3 (Rab3 GTPase). Having determined that ectopic *ceh-12* expression is required for the synaptic wiring defect in *unc-4* mutants, I wanted to determine if *ceh-12* is also required for the SV defect that results from inactivation of the *unc-4* pathway. To detect SV protein levels in specific ventral cord motor neurons, all experiments were performed in an *unc-104* kinesin mutant background in which SV trafficking to the synapse is blocked, such that SVs accumulate in the cell soma (Hall and Hedgecock 1991). In this way, the net SV levels in a given motor neuron can be assessed by evaluating the intensity of SV protein immunostaining in each motor neuron cell body.

In this case, for ease of identification, A-class motor neurons were marked with *unc-4::*GFP.

Initially, I confirmed that RAB-3 levels are reduced in A-class motor neurons in *unc-4(e120)* in comparison to wildtype. In the *ceh-12; unc-4* double mutant, however, wildtype levels of RAB-3 immunostaining were restored (Figure 5.9). (In *ceh-12* mutants RAB-3 immunostaining in DA and VA motor neurons is comparable to that observed in wildtype animals.) Interestingly, the restoration of wildtype levels of RAB-3 in the *ceh-12; unc-4* double mutants was not biased to posterior A-class motor neurons. This result stands in contrast to the observation reported above that *ceh-12* is selectively required for the Unc-4 miswiring defect (i.e. gap junctions with AVB) in posterior VA motor neurons. The requirement of *ceh-12* activity for RAB-3 depletion in anterior A-class motor neurons is surprising given the observation that *ceh-12*::GFP is exclusively de-repressed in posterior motor neurons in *unc-4* mutants (Figure 5.4). These findings could mean that endogenous *ceh-12* is in fact weakly derepressed in anterior VA motor neurons at levels sufficient to affect SV stability or biogenesis, but not wiring specificity. In the future, it will be important to confirm the RAB-3 results by immunostaining with additional SV markers (e.g. UNC-17, CHA-1, SNB-1, SNT-1).

ceh-12 is not required for the synaptic vesicle defect in VC motor neurons

UNC-4 is expressed in 6 different neuron classes: DA, VA, VC, SAB, I5, AVF. In addition to the A-class motor neurons, immunostaining experiments have determined that SV proteins levels are also reduced in the VC and SAB motor neurons. Given that ectopic *ceh-12*::GFP is not observed in VC and SAB motor neurons in *unc-4* mutants, we asked

if *ceh-12* activity is required for the SV defect in these cells. *unc-4*::GFP expression in the VCs is first observed in the L3 larval animal as vulval morphogenesis is initiated (Lickteig, Duerr et al. 2001). The VC synapses onto vulval muscles can be marked with GFP-tagged synaptobrevin (GFP-SNB-1) under the control of the *unc-4* promoter. The VCs exit the ventral nerve cord to target vulval muscles, such that GFP-SNB-1 puncta can be unambiguously assigned to these synapses. Lickteig et al., (2001) reported that GFP-SNB-1 localization to VC neuromuscular synapses is drastically reduced in *unc-4* mutants. I confirmed this effect by observing that most (10/11) adult animals carrying the *unc-4*::GFP-SNB-1 transgene failed to show GFP puncta in VC processes in *unc-4(120),* whereas 100% (15/15) of the wildtype animals displayed prominent GFP-SNB-1 localization to VC synapses in the vulva. In the *ceh-12; unc-4* double mutant, 100% (8/8) of the animals phenocopied *unc-4*; normal levels of GFP-SNB-1 puncta were not restored to VC motor axon nerve terminals (Figure 5.10). This result appears to rule out a role for ectopic *ceh-12* expression in the SV defect in VC class motor neurons and is consistent with the observation that *ceh-12*::GFP is not detected in the VC class motor neurons in *unc-4* or *unc-37* mutants. Again, it will be important to confirm this result with other SV marker proteins and to extend this analysis to the SAB motor neurons. Although these neurons do not express ectopic *ceh-12*::GFP in *unc-4* mutants, they do display incompletely penetrant defects in axonal morphology as well as reduced SV levels.

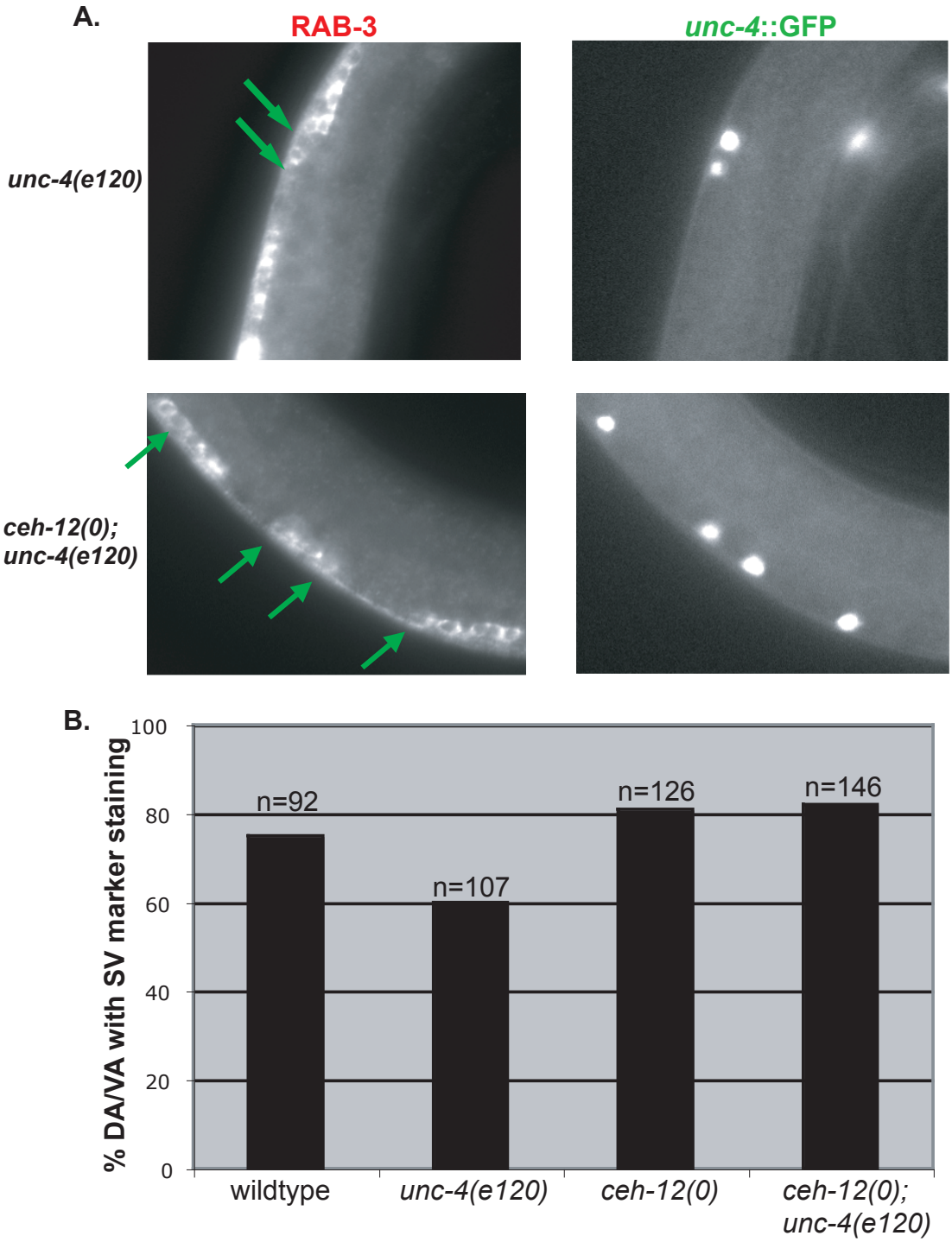

Figure 5.9. *ceh-12* suppresses the synaptic vesicle defect in *unc-4* mutants. A. RAB-3 antibody staining (left) of *unc-4*::GFP animals (right). Green arrows point to GFP+ A-type motor neurons shown on right. (Top) *unc-4* mutants stained with an antibody to RAB-3 exhibit reduced fluorescence in A-class motor neurons. (Bottom) In *ceh-12; unc-4* double mutants, RAB-3 staining is observed at wildtype levels in A-class motor neurons. B. Quantitation of SV protein levels in wildtype, *unc-4, ceh-12* and *unc-4; ceh-12* animals.

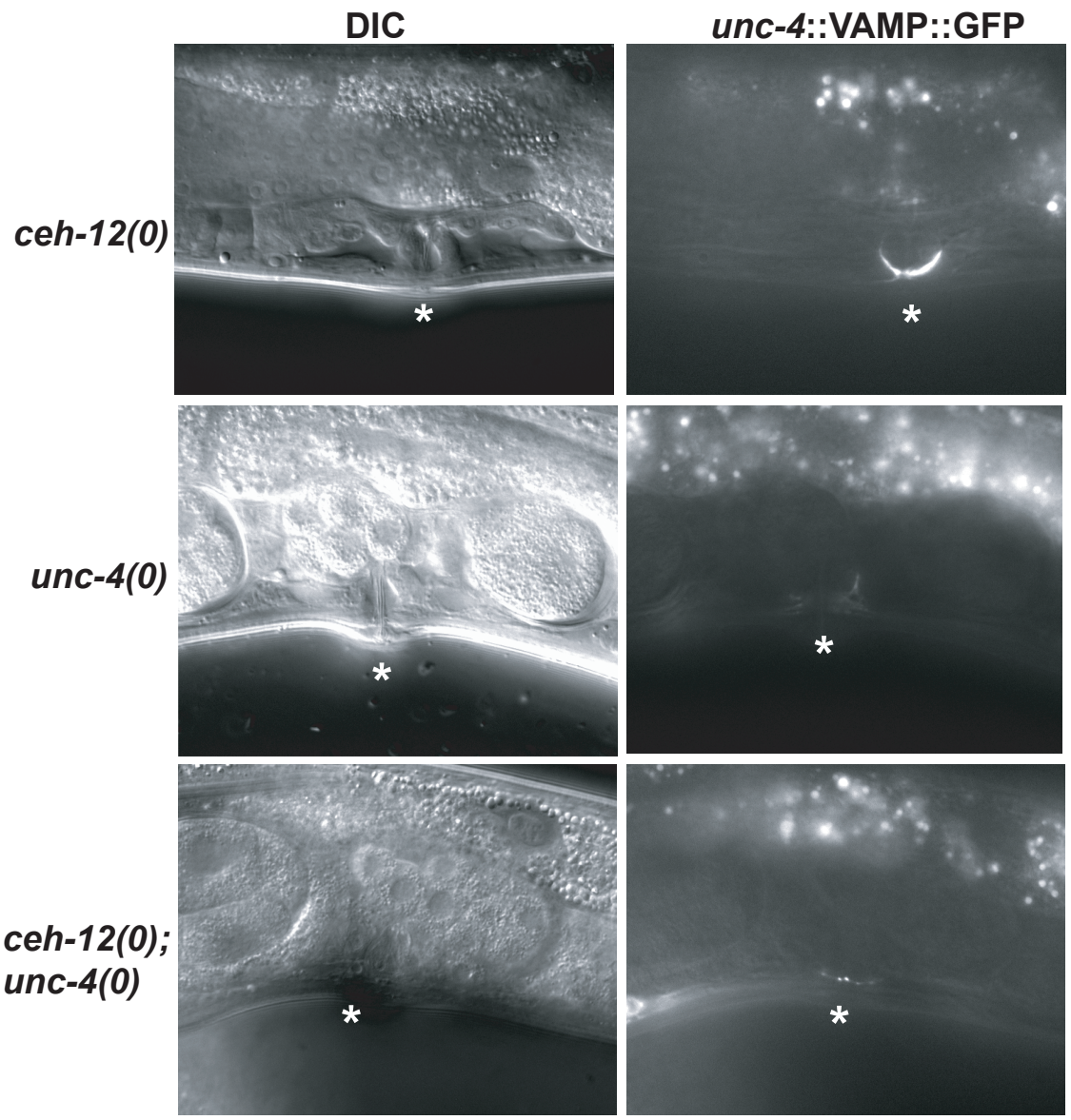

Figure 5.10. *ceh-12* does not rescue the SV defect in VC motor neurons. DIC and GFP images of *unc-4*::VAMP::GFP expression in *ceh-12(0)*, *unc-4(0)* and *ceh-12(0); unc-4(0)* mutants. Bright expression is visible in VC processes of *ceh-12* mutants, which phenocopy GFP expression in wildtype animals. In *unc-4* mutants, GFP is dramatically reduced, and often abolished in VC processes. GFP fluorescence is not restored to VC processes in the *ceh-12;unc-4* double mutant. * denotes vulva.

Discussion

My colleague Steve Von Stetina and I performed separate microarray experiments that independently identified *ceh-12*, the nematode HB9 homolog, as a target of UNC-4/UNC-37. *ceh-12* was an intriguing candidate, given its well established role in specifying motor neuron fate in other organisms (Arber, Han et al. 1999; Thaler, Harrison et al. 1999; Broihier and Skeath 2002). In flies, birds and mammals, HB9 sustains motor neuron differentiation by blocking genetic programs that drive differentiation of other neuron classes. Our work has now provided a detailed analysis of *ceh-12*/HB9 function and defined a clear role in specifying synaptic inputs as well as controlling neurotransmitter signaling capacity in *C. elegans*.

A transcriptional switch regulates synaptic input and output in *C. elegans*

Mutations in the *unc-4* homeodomain transcription factor disrupt backward locomotion (Miller, Shen et al. 1992). This movement defect may be attributed to two phenotypes: (1) VA motor neurons, which normally drive backward movement, are miswired with synaptic inputs usually reserved for VB sister cells (White, Southgate et al. 1992), and (2) *unc-4* mutant neurons exhibit a 40% reduction in synaptic vesicles (Lickteig, Duerr et al. 2001). Our model suggests that UNC-4, along with its co-repressor, UNC-37/Groucho, functions to repress VB specific genes in A-class motor neurons to specify synaptic choice as well as maintain normal levels of neurotransmitter release (Winnier, Meir et al. 1999). We have now shown that *ceh-12* is an authentic UNC-4 target gene that mediates both of these traits. *ceh-12*::GFP is specifically expressed in the VB motor neurons in the ventral nerve cord. Furthermore, we detect

ectopic *ceh-12*::GFP expression in VA and DA motor neurons in an *unc-4* mutant, which indicates that *ceh-12* is negatively regulated by *unc-4*. To determine if *ceh-12* is sufficient to induce the Unc-4 miswiring phenotype, we expressed CEH-12 ectopically in VA motor neurons. These transgenic "VA-CEH-12" animals display a backward movement defect that phenocopies *unc-4*. To determine if *ceh-12* expression in the VAs is also necessary for the backward movement defect, we asked if the loss of *ceh-12* in an *unc-4* mutant could restore normal locomotion. This genetic experiment revealed that *ceh-12* partially rescues the backing defect of an *unc-4* null mutant, but affords strong suppression of hypomorphic *unc-4* alleles. We interpret this result to mean that *ceh-12* functions in parallel to another partially redundant pathway downstream of *unc-4*. Our finding that *ceh-12* is selectively de-repressed in posterior VA motor neurons is consistent with this idea, as synaptic inputs to anterior VA motor neurons could depend on this alternative downstream pathway. The differential requirement of *ceh-12* for the specification of gap junction inputs to posterior but not anterior VA motor neurons also corroborates this model.

Having established that *ceh-12* functions downstream of *unc-4* to specify synaptic inputs, I next performed experiments to ask if *ceh-12* is also required for the second *unc-4* phenotype; the reduction of synaptic vesicle (SV) levels. A comparison of immunostaining intensities of the SV protein RAB-3 in wildtype, *unc-4*, and *ceh-12; unc-4* backgrounds clearly demonstrates that the *ceh-12* mutation rescues the synaptic vesicle defect observed in *unc-4* mutants. In contrast to the result above, in which *ceh-12* is selectively required for miswiring VA motor neurons in the posterior nerve cord, we do not see a posterior bias in the rescue of synaptic vesicle levels; SV levels are restored to

VA motor neurons throughout the ventral nerve cord in *ceh-12;unc-4* double mutants. This result is surprising given that *ceh-12::GFP* is selectively derepressed in the posterior VAs of *unc-4* mutants.

There are at least two possibilities to explain this. The first is that *ceh-12* may be acting non cell-autonomously to regulate synaptic vesicle levels. A model suggesting that HB9 has a non cell-autonomous function has been presented in Drosophila, where Lim3 is de-repressed in a dHB9 mutant in neurons that do not express dHB9 in the wildtype. The authors propose that *dHb9*-expressing cells must release a signal to these adjacent cells that restricts expression of Lim3 (Broihier and Skeath 2002). A plausible scenario to explain the apparent non cell-autonomous effect of *ceh-12* on SV levels could depend on a secreted signaling molecule that promotes SV stability or biogenesis. Perhaps the *ceh-12* expression in posterior A-type motor neurons is sufficient to block release of this signal resulting in reduced levels of SVs in all A-class motor neurons. Whether or not these motor neurons secrete signaling molecules has not been determined, but our microarray data suggests that these cells should have this capability. For example, DA motor neurons express transcripts encoding wingless (*cwn-1, 2*) as well as a Frizzled receptor (*lin-17*) (see Chapter II). Recent work has shown that mutations in Wnt signaling in the mammalian brain modulates neurotransmitter release (Ahmad-Annuar, Ciani et al. 2006). To test the idea of *ceh-12* performing non cell-autonomous functions we could ectopically express CEH-12 in a neighboring neuron (i.e. VD motor neurons) and examine the VA/DA motor neurons for reductions in SV numbers. To fully establish a non cell-autonomous role, however, we will need to identify additional *ceh-12* target

genes, and determine if they are expressed ectopically in additional cell types (i.e. not VBs) in the *ceh-12* mutant.

A second possibility is that the endogenous *ceh-12* gene is in fact ectopically expressed in A-class motor neurons in the anterior ventral nerve cord, but at very low levels that are not detectable with the *ceh-12*::GFP reporter gene. Perhaps the mechanism that regulates SV levels is more sensitive to *ceh-12* activity than the miswiring defect. Our model in Figure 5.11 predicts that *ceh-12* is de-repressed at high levels in the posterior VAs, with decreasing expression in the more anterior VA motor neurons. To determine if there are low levels of CEH-12 expressed in the anterior VA motor neurons it will be necessary to generate a CEH-12-specific antibody. With this tool it should be possible to determine the validity of this hypothesis. This model seems more plausible than a non cell-autonomous function for *ceh-12*, given the observation that the SV levels in VC motor neurons are not restored in *ceh-12;unc-4* mutants. As noted in the Results section, these findings are preliminary, and it will be necessary to test additional SV protein markers to confirm the observations obtained using the RAB-3 antibody.

A transcriptional cascade alters gap junction formation in VA motor neurons

One of the advantages of using *C. elegans* is that every synaptic connection in the nervous system has been characterized using EM reconstruction (White, Southgate et al. 1986). Unfortunately, this method is labor intensive and impractical for extensive use. To overcome this limitation we collaborated with Todd Starich and Jocelyn Shaw (Univ. Minnesota) to use UNC-7S::GFP as a specific marker of gap junctions between the AVB

interneuron and ventral cord motor neurons. With the acquisition of this strain, we can now score specific synapses in multiple animals at the light microscope.

The experiments described in this chapter show that the innexin, UNC-7S, is expressed in AVB command interneurons and assembles into gap junctions with B-class motor neurons. Genetic data suggest that these gap junctions are likely to be heterotypic and also include the innexin UNC-9 (Starich and Shaw, unpublished data). The ectopic gap junctions between AVB and A-class motor neurons that appear in *unc-4* mutants may have a similar subunit composition, as *unc-9* is the most abundant innexin transcript expressed in A-class motor neurons (Fox, Von Stetina et al. 2005) (S. Von Stetina, RMF and D. Miller, unpublished data). It follows that UNC-9 is also a likely candidate for assembly into gap junctions between VA and AVA command interneurons in the wildtype (White, Southgate et al. 1986). Gap junctions with AVB tend to be located on the motor neuron soma whereas gap junctions with AVA are more often distributed along the length of the motor neuron partner (White, Southgate et al. 1986). Thus, *unc-4* may orchestrate the assembly of UNC-9 into gap junctions at particular locations within A-class motor neurons and with selected presynaptic partners. Although gap junctions have been previously thought to provide a largely developmental role in the generation of neural networks in higher vertebrates, recent evidence suggests that these "electrical" synapses are also important for neural function in adult nervous systems (Bennett and Zukin 2004). This view is consistent with ultrastructural and immunochemical data showing that gap junctions are widely distributed in the mature mammalian brain and spinal cord (Rash, Staines et al. 2000). As the mechanisms that control the specificity of gap junction assembly in the vertebrate CNS are unknown (Hestrin and Galarreta 2005),

the discovery of downstream genes that regulate gap junction placement in *C. elegans* could provide targets for molecular studies in more complex nervous systems. Moreover, the joint regulation by *unc-4* (or *ceh-12*) of the specificity of chemical and electrical synapse formation (White, Southgate et al. 1992) is indicative of a common nexus for pathways controlling the assembly of both types of synapses.

UNC-4 regulates downstream pathways that function regionally along the A/P axis to control synaptic inputs to VA motor neurons

Our findings indicate that *ceh-12* functions in parallel with at least one additional pathway in VA motor neurons to control input specificity (Figure 5.11). *unc-4* regulation of *ceh-12* is restricted to VA motor neurons in the posterior region of the ventral nerve cord. Because anterior VA motor neurons are also miswired in *unc-4* mutants, we have proposed that the presumptive downstream pathway functioning in parallel to *ceh-12* may be selectively de-repressed in anterior VAs (Figure 5.11). An interesting consequence of this mode of regulation is a mechanism in which the common inputs shared by all VA motor neurons in *unc-4* mutants (e.g. gap junction with AVB) are defined by different stoichiometric ratios of these gene regulatory pathways in each member of the VA class. The rostro-caudal axis of these effects could be indicative of a role for HOX gene function. It is noteworthy that combinatorial expression of HOX proteins defines distinct motor neuron pools distributed along the anterior-posterior axis of the vertebrate spinal cord (Dasen, Tice et al. 2005). In *C. elegans*, the HOX protein LIN-39, for example, is selectively required for specifying cell fates in the midbody region (Salser, Loer et al. 1993) and is thus a candidate for a gene that could modulate the readout of *unc-4* activity along the A/P axis. This model is consistent with our microarray results showing that

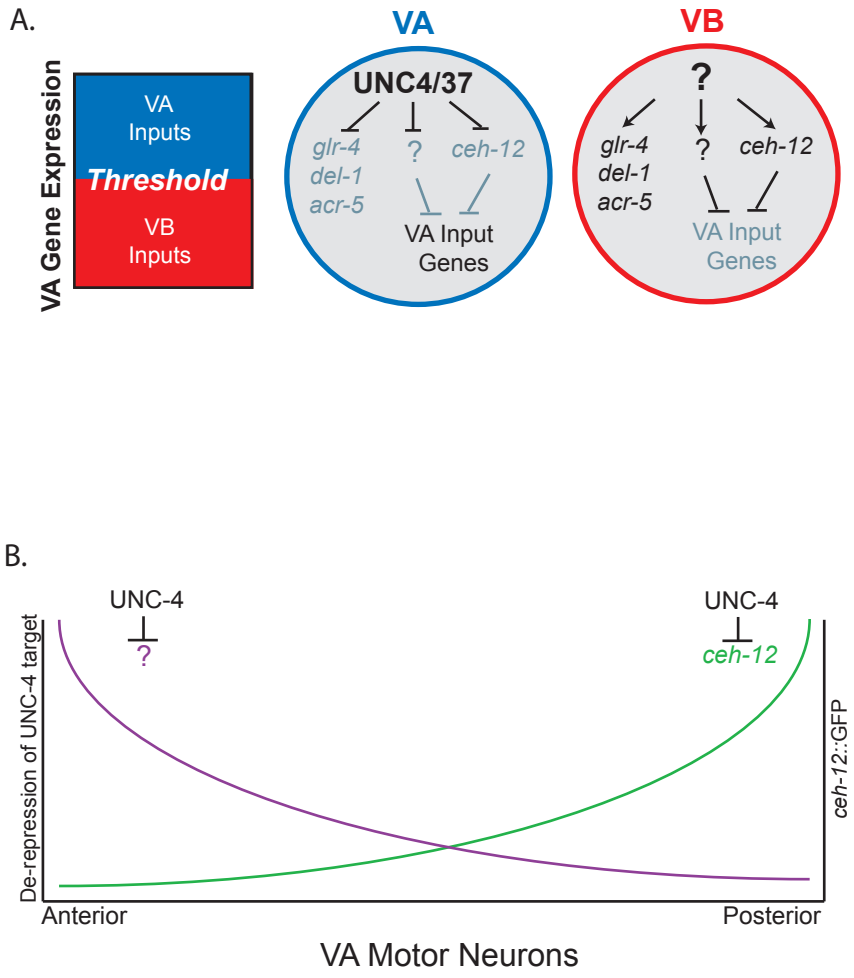

Figure 5.11. Model of UNC-4 function to regulate input to VA class motor neurons. A. A-type synaptic inputs are imposed when VA gene expression exceeds a specific threshold. In VA motor neurons, the UNC-4/UNC-37(Groucho) complex blocks expression of VB genes (*glr-4, del-1, acr-5*) that do not affect synaptic choice and at least two other VB genes, *ceh-12* and an unknown target (?), that repress VA input genes. VB motor neurons do not express UNC-4 and therefore the level of VA gene expression is not sufficient to specify A-type synapses to these cells. B. UNC-4 target gene expression is biased along the A/P axis. *ceh-12* is preferentially repressed by UNC-4 in posterior VA motor neurons whereas an as yet unidentified *unc-4* target gene (?) regulates synaptic choice anteriorly.

transcript levels for *lin-39* and *mab-5* (the next most posterior HOX gene) are elevated in A class motor neurons in *unc-4* or *unc-37* mutants. Preliminary experiments that fail to detect suppression of the Unc-4 phenotype by *lin-39* and *mab-5*, however, would appear to rule out a model in which VA inputs depend on *unc-4* repression of *lin-39* and *mab-5* in VA motor neurons.

To address the components of the parallel pathways that are necessary for input specificity it is necessary to identify additional target genes. Other *unc-4* regulated genes should be represented in the microarray profiles that we have obtained from *unc-4* and *unc-37* mutant A-class motor neurons (Chapter IV). Furthermore, downstream targets that function in parallel to *ceh-12* may be revealed by RNAi tests to detect genes that enhance *ceh-12*-dependent suppression of the Unc-4 phenotype (i.e. improved backward locomotion).

Negative gene regulation specifies motor neuron fate

Groucho functions as a co-repressor protein in concert with DNA-specific transcription factors (Chen and Courey 2000). Repression is mediated by Groucho binding to specific protein interaction domains. For example, a short peptide tag, the eh1 sequence, tethers homeodomain proteins to Groucho (Jimenez, Paroush et al. 1997). A role for this interaction in motor neuron differentiation was initially established in *C. elegans,* where the nematode homolog of Groucho, UNC-37, binds to the eh1 region of the UNC-4 homeodomain to prevent VA motor neurons from expressing genes normally reserved for their lineal siblings, the VB motor neurons (Pflugrad, Meir et al. 1997; Winnier, Meir et al. 1999). The molecular elements of this mechanism are highly

conserved as the carboxy-terminal region of human Groucho can also interact with UNC-4 to mediate this outcome in *C. elegans* (Winnier, Meir et al. 1999). Groucho binding to eh1-containing HD proteins is widely employed in the generation of distinct neural fates in the developing vertebrate spinal cord. In this setting, HD proteins in adjacent progenitor domains utilize Groucho to repress each other and thereby delineate sharply defined boundaries between neuroblasts destined to assume distinct morphological and functional fates. When one of these transcription factors is disabled by mutation, its transcription factor target is ectopically expressed, thereby inducing local neuroblasts to adopt differentiated traits of the adjacent domain (Muhr, Andersson et al. 2001). Our findings in *C. elegans* indicate that this mechanism may also be required to distinguish the fates of post-mitotic motor neurons; genetic ablation of *unc-4* results in ectopic expression in VA motor neurons of CEH-12/HB9, which in turn imposes VB-type synaptic inputs. In this case, transcriptional repression is asymmetric as CEH-12/HB9 does not repress UNC-4. We have previously reported a related mechanism involving UNC-4 that distinguishes the fates of embryonic DA and DB motor neurons (Esmaeili, Ross et al. 2002). VAB-7, a homolog of the Evenskipped (Eve) HD protein, functions in DB motor neurons to block expression of UNC-4, which is normally restricted to the DAs. In *vab-7* mutants, ectopic UNC-4 induces DB motor neurons to assume the anteriorly directed axonal trajectory of DA motor neurons. Repression may be reciprocal in this instance as UNC-4 utilizes UNC-37/Groucho to block VAB-7 expression in DA motor neurons. The fact that DA and DB motor neurons are generated by separate lineages (Von Stetina, Treinin et al. 2006) indicates that this mechanism of "cross-repression" is not limited to motor neurons that arise from common progenitors. As DA

and DB motor neurons express a number of shared traits (i.e. dorsal process outgrowth and cholinergic function), this mode of negative gene regulation may be utilized in this setting to diversify a shared genetic program. A similar model may explain our finding that DA motor neurons and VA11, neither of which are lineal sisters to VB motor neurons, express CEH-12 and are miswired with VB type inputs (i.e. gap junctions) in *unc-4* and *unc-37* mutants. The substantially higher frequency of this defect in VA motor neurons that are born to sister VBs (Figure 5.8), however, could mean that UNC-4 function is required in this case to repress a VB-specific program that is potentially triggered in the common mother cell (White, Southgate et al. 1992).

CEH-12 and HB9 specify motor neuron fate

Our results showing that *ceh-12* allows VB motor neuron fate by repressing VAB-7/Eve parallels earlier observations that HB9 regulates motor neuron differentiation in flies, birds and mammals. In Drosophila, dHB9 is expressed in a subset of ventrally projecting motor neurons, where it represses the dorsal motor neuron determinant, Eve, and blocks the adoption of a dorsal axon trajectory. Eve, in turn, opposes ventral fates in dorsal motor neurons by reciprocally repressing dHB9 in a Groucho-dependent mechanism (Broihier and Skeath 2002). Interestingly, HB9 is also restricted to ventrally projecting motor neurons in the vertebrate spinal cord, where it acts to prevent expression of markers for interneurons arising from the adjacent V2 progenitor domain. In this case, ectopic expression of HB9 in V2 neuroblasts is sufficient to drive expression of motor neuron markers as well as impose motor neuron-like morphological characteristics (i.e. ventral axonal projections) (Arber, Han et al. 1999; Thaler, Harrison et al. 1999). This

dual function of HB9 to block as well as activate expression of motor neuron-specific traits is similar to our finding that CEH-12 inhibits VA motor neuron differentiation while simultaneously promoting a specific VB trait. Together, these observations suggest that the key role of HB9 function in motor neuron differentiation is evolutionarily ancient. In this regard, we note that UNCX4.1 is strongly expressed in the V3 neural progenitor domain immediately adjacent to the MN region in which HB9 resides (Mansouri, Yokota et al. 1997). It will be interesting to determine if UNCX4.1 functions in the V3 domain to block HB9 expression.

CHAPTER VI

DISCUSSION AND FUTURE DIRECTIONS

Discussion

The goal of this dissertation project was to identify genes that specify synaptic choice in the *C. elegans* motor circuit. The work presented here outlines the development of a new method (MAPCeL) for gene expression profiling of specific cell types from the *C. elegans* embryo, and provides examples of the application of this method to complex biological problems. MAPCeL provides a significant advance in the area of expression profiling as it is now possible to obtain a genetic fingerprint of each embryonic cell type. This discussion will feature the role of these methods in identifying key functional components of the *C. elegans* motor circuit. In addition, I will discuss the successful application of MAPCeL technology to the discovery of an UNC-4 target gene required to specify synaptic choice. This finding suggests a model in which a conserved transcriptional code is responsible for defining motor neuron fate in the *C. elegans* motor circuit. In addition, we have now discovered a novel role for these proteins in establishing the pattern of synaptic connectivity.

Profiling the motor circuit

The Miller lab has now applied two complementary profiling strategies, mRNA-tagging and MAPCeL, to catalog the transcriptional profiles of specific cells in the motor

circuit. In my work, I initiated the development of MAPCeL to identify genes expressed in embryonic body muscle cells (Touroutine, Fox et al. 2005) (Chapter III). The method was then employed to profile embryonic A-type ventral cord motor neurons (Fox, Von Stetina et al. 2005). These data revealed a remarkably diverse array of receptors and neuroactive signaling components in these excitatory motor neurons. It will be interesting to compare this profile of cholinergic motor neurons to MAPCeL data obtained by Dr. Susan Barlow, a postdoc in the Miller lab, of embryonic D-class GABAergic motor neurons. Because MAPCeL is restricted to cells that arise in the embryo (Christensen, Estevez et al. 2002), Steve Von Stetina and Joseph Watson have applied mRNA-tagging (Roy, Stuart et al. 2002) to identify transcripts enriched in larval neurons. Initially, this method was utilized to profile gene expression throughout the larval nervous system. Next, mRNA tagging data were obtained from postembryonic A-class motor neurons (e.g VA motor neurons). A manuscript describing these results and a comparison to MAPCeL profile that I generated of the embryonic nervous system is now in preparation. With these tools in hand, it is now possible to apply them to specific biological questions. Below, I will summarize the joint application of MAPCeL and mRNA tagging to identify *unc-4* target genes. Ongoing projects in the Miller lab that are also using these methods include the application of MAPCeL to identify targets of the Aristaless transcription factor (ALR-1) in embryonic GABAergic motor neurons (Laurie Earls). Sarah Anthony is using mRNA-tagging to profile the DD and VD motor neurons in search of genes required for synaptic remodeling; DD motor neurons undergo a switch in synaptic polarity (from ventral muscle to dorsal muscle) in the late L1 larvae (White, Albertson et al. 1978; Walthall and Plunkett 1995). Finally, Clay Spencer is developing constructs for

profiling the command interneurons with the expectation that these data will reveal genes that mediate the creation of specific interneuron-motor neuron connections. In each case, the functional roles of transcripts identified in these data sets can be tested by genetic methods (e.g. RNAi) to identify genes with key roles in these processes. An example of the utility of these data is the identification of ACR-16 as an essential subunit of the elusive levamisole-insensitive acetylcholine receptor at the neuromuscular junction (Touroutine, Fox et al. 2005) (Chapter III). It seems likely that many additional biological questions can be potentially addressed by exploiting these cell-specific gene expression profiles. With this possibility in mind, the Miller lab is assembling a database to catalog the cell-specific fingerprints emerging from these experiments.

Microarray strategies identify transcription factor target genes

A long-standing question in the Miller lab has been: What are the downstream targets of *unc-4* that specify synaptic choice? Genetic screens have failed to identify these factors (perhaps due to redundancy; see below) and microarray experiments that queried gene expression throughout the animal were insufficiently sensitive to detect genes that were significantly regulated by *unc-4* in A-class motor neurons (S. Von Stetina, PhD dissertation, 2005). To solve this problem, Steve Von Stetina and I developed cell-specific microarray strategies to identify UNC-4 target genes. Given that available evidence indicates that UNC-4 functions with UNC-37/Groucho to repress downstream target genes (Pflugrad, Meir et al. 1997; Winnier, Meir et al. 1999), we focused our search on transcripts that were upregulated in *unc-4* or *unc-37* mutant A-class motor neurons in comparison to wildtype. Together, our combined data sets have identified

~400 candidate *unc-4* target genes. The discovery of such a large number of potential *unc-4*-regulated genes was surprising, given the limited effect of the *unc-4* mutation on VA motor neuron fate. One explanation for this result is that the mechanism of synaptic specificity is more complex and depends on UNC-4 regulation of multiple downstream genes. Our discovery that one of these UNC-4 target genes, *ceh-12*/Hb9, is partially responsible for downstream effect of *unc-4* activity is consistent with this idea. This finding points to the existence of additional *unc-4* regulated genes. In the future, these should be identified by genetic and RNAi tests of other candidate UNC-4-regulated transcripts identified in these microarray data (see Future Directions below).

A conserved transcriptional code specifies motor neuron fate in *C. elegans*

The use of transcriptional repression to determine neuronal fate is a common theme throughout evolution. This phenomenon was first characterized in the developing vertebrate spinal cord, which is patterned by the cross-repressive actions of transcription factors. Each neuronal progenitor domain expresses a unique "code" of transcriptional repressors, which function to prevent the adoption of alternative neuronal fates (Lee and Pfaff 2001). This mechanism is preserved in the determination of postmitotic motor neuron fates where the LIM-code specifies motor neuron subtypes (Shirasaki and Pfaff 2002). In the Drosophila nervous system, motor neuron identities are also defined by transcriptional repression. For example, ventrally projecting motor neurons express *dHb9* and *Nkx6,* thereby preventing *eve* expression and the adoption of dorsal motor neuron fate (Broihier and Skeath 2002; Broihier, Kuzin et al. 2004). Conversely, *eve* represses *dHb9*

and *Nkx6* to prevent ventral motor neuron traits. We have now shown that transcriptional repression also defines motor neuron classes in the *C. elegans* ventral nerve cord.

Each cholinergic motor neuron class is defined by expression of a specific transcription factor. The A-class motor neurons (DA/VA) express UNC-4 (Miller and Niemeyer 1995), whereas the VBs and DBs (i.e. B-class motor neurons) are characterized by expression of *ceh-12* and *vab-7*, respectively. Loss of *unc-4* leads to the adoption of B-class traits; VAs are miswired to receive B-type synaptic inputs (Miller, Shen et al. 1992; White, Southgate et al. 1992) and express the VB marker *ceh-12,* and DA motor neurons ectopically express the B-class markers *ceh-12* and *vab-7*. We have shown here that *ceh-12* promotes VB fate by repressing the DB marker *vab-7*. VAB-7 is normally expressed in DB motor neurons where it functions to regulate axonal trajectory by repressing A-class genes. Loss of *vab-7* leads to the ectopic expression of *unc-4* and a reversal in DB axon polarity from posterior to anterior (Esmaeili, Ross et al. 2002). Taken together, these findings reveal an intricate mechanism of transcriptional cross-repression that governs the individual fates of ventral cord motor neuron classes. In addition, the conserved roles of these transcription factors in motor circuit fate determination in insects, birds and mammals suggest that the pathways that we are uncovering in *C. elegans* may have been preserved through evolution to control the differentiation of these more complex nervous systems (Figure 6.1). Furthermore, with the identification of *ceh-12* and its role in the *unc-4* pathway, we have now uncovered a novel role for the HB9 family of transcription factors in defining interneuron to motor neuron synaptic connectivity. It will be interesting to determine if HB9 has a similar function in the vertebrate nervous system.

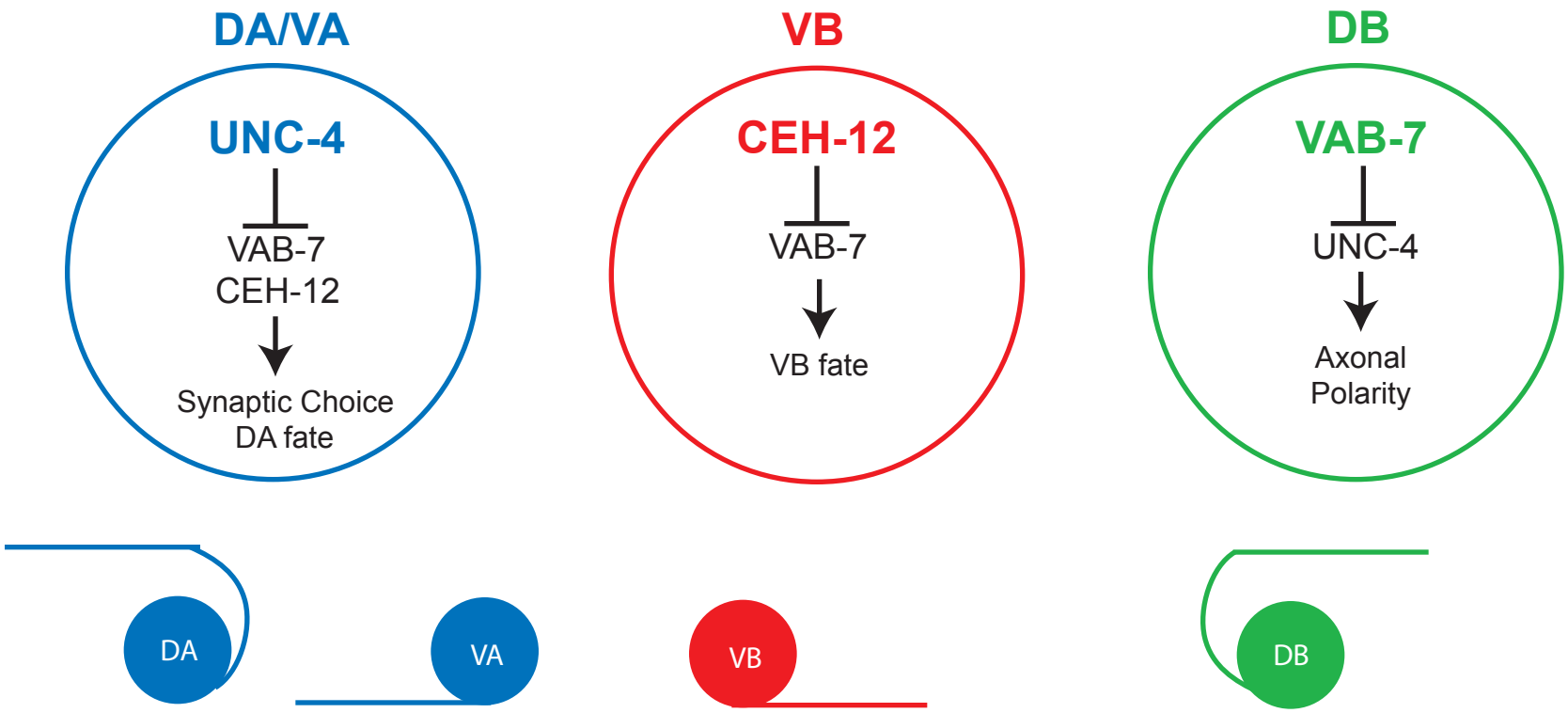

Figure 6.1. A transcriptional code defines motor neuron fate in *C. elegans*. The DA/VA motor neurons express UNC-4 and specify A-class fate by repressing VAB-7 and CEH-12. VB motor neuron fate is determined by the repression of VAB-7 by CEH-12. VAB-7 functions in DB motor neurons to prevent A-class traits by repressing UNC-4.

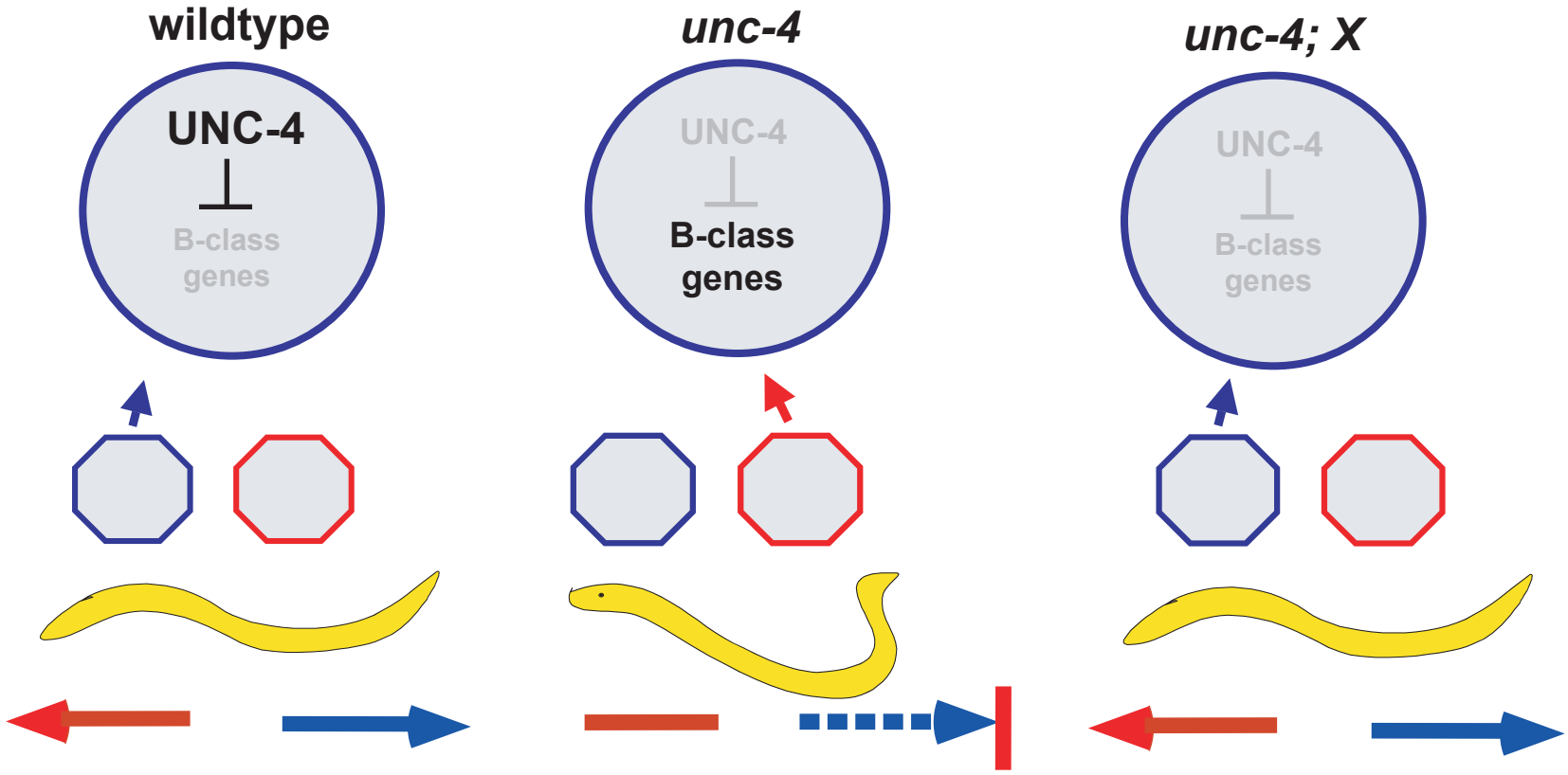

Figure 6.2. Model of *unc-4* function in VA motor neurons. A. In wildtype VA motor neurons UNC-4 normally represses B-class genes to specify A-type inputs. B. In *unc-4* mutants, B-class genes are expressed ectopically inducing B-type inputs resulting in defective backward locomotion. C. In *unc-4;target gene X* double mutants, A-type inputs should be restored by the loss of B-input genes, leading to suppression of the *unc-4* backing defect. Light gray text denotes loss of gene function.

Future Directions

Experiments to test candidate *unc-4* target genes for roles in synaptic function

Microarray data described in this work have identified ~400 candidate UNC-4 target genes. RNAi experiments can now be used to identify transcripts from this list that interact with *unc-4*. The results of genetic experiments with *ceh-12* have lead to useful strategies for specifically sensitizing this screen for *unc-4* targets. For example, weak *ceh-12* suppression of *unc-4* null alleles is consistent with our model of at least one additional pathway that functions in parallel to *ceh-12*. Thus, in the *ceh-12(0); unc-4(0)* background, RNAi of *bona fide* UNC-4 target genes in this additional pathway should result in enhanced suppression of the Unc-4 movement defect (Figure 6.2). Previous attempts at feeding bacterial RNAi clones, however, were met with limited success due to the inherent insensitivity of neurons to RNAi. To overcome this problem, we will use a recently isolated RNAi hypersensitive strain, *eri-1;lin-15b*, which substantially increases the effectiveness of RNAi in neurons (Wang, Kennedy et al. 2005).

In our working model, UNC-4 functions in A-class motor neurons to repress B-class genes (Figure 1.11). If this hypothesis is correct, then an authentic UNC-4 target gene should normally be expressed in B-class motor neurons. To examine the expression patterns of UNC-4 target genes identified in the RNAi screen, *promoter*::GFP reporters will be generated and analyzed for expression in ventral cord motor neurons (Table 4.1). These reporters will then be examined in *unc-4*/*unc-37* mutant backgrounds to detect ectopic expression in A-class motor neurons (VA/DA motor neurons). Target genes that satisfy these criteria are also expected to regulate the motor neuron selectivity of gap junctions with AVB. As reported in Chapter V, UNC-7S::GFP labels gap junctions

between the AVB interneuron and the B-class motor neurons (VB/DB). This marker also labels ectopic gap junctions with A-class motor neurons in *unc-4* mutants. Genetic ablation of an UNC-4 target gene that regulates synaptic specificity (e.g. *ceh-12*) should rescue this miswiring defect, as detected by loss of UNC-7S::GFP puncta on A-class motor neurons. These genes can be further tested for their role in regulating SV levels using a series of antibody staining experiments previously established in our lab by Kim Lickteig (Lickteig, Duerr et al. 2001)

Genetic strategies to identify additional *unc-4* pathway genes

Judsen Schneider, a graduate student in the Miller lab, has performed a genetic screen to identify mutants that can enhance suppression of the Unc-4 backward movement defect of the *ceh-12(0);unc-4(0)* double mutant. A pilot screen isolated two strong suppressors, *wd76* and *wd77*, that restore backward locomotion to *unc-4(0)* in a *ceh-12(0)*-dependent manner. The identification of these Unc-4 suppressor genes should provide insight into the pathway that functions downstream of UNC-4. Jud has also adopted a candidate gene approach in which he is testing a specific transcription factor, *cog-1* for a role in the *unc-4* pathway. In Drosophila, the COG-1 homolog, *Nkx6* functions in parallel with *dHb9* to specify the fate of ventrally projecting motor neurons (Broihier, Kuzin et al. 2004). Thus, Jud has used a genetic test to ask if *cog-1* functions in parallel to *ceh-12* in *C. elegans* motor neurons. *cog-1* was initially identified from mutant alleles that disrupt vulval development (Palmer, Inoue et al. 2002). Of particular relevance to our model that UNC-4 blocks expression of genes normally restricted to a lineal sister, VB motor neurons, is the recent discovery that COG-1 is required in ASER sensory neurons to prevent expression of traits usually reserved for its functional sister

neuron, ASEL (Chang, Johnston et al. 2003). Jud has now determined that *cog-1::GFP* is also expressed in the VA and VB motor neurons in the ventral nerve cord. Although *cog-1* does not enhance the *ceh-12(0)* dependent suppression of Unc-4 and therefore is unlikely to function downstream of *unc-4* to regulate synaptic choice, Jud's work has revealed the intriguing finding that the double mutant *ceh-12; cog-1* displays a synthetic backward Unc phenotype (neither mutation alone displays an obvious movement defect) (J. Schneider, D. Miller, unpublished). This result indicates that *cog-1* and *ceh-12* are likely to function in parallel to specify a motor neuron specific trait that is required for normal locomotion. The evolutionary significance of this finding is intriguing given the parallel roles of *dHb9* and *Nkx6* in fly motor neuron differentiation. Jud is now examining cell-type specific markers in *cog-1* mutants to determine the role of COG-1 in establishing motor neuron fate and its potential role in the UNC-4 pathway.

Does the signaling capacity of VA motor neurons regulate input specificity or *vice versa*?

Since *unc-4* regulates two distinct properties associated with synaptic function, i.e. synaptic strength and input specificity, it will be important to determine if these phenotypes arise from a common mechanism, or whether independent pathways contribute to these defects. We have now shown that the *unc-4* regulated gene, *ceh-12* is required for both defects (although preliminary evidence indicates that SV stability may be more sensitive to *ceh-12* activity than VA input specificity). The problem now is to identify additional genes downstream of *ceh-12* (e.g "gene x") that affect both or only one of these processes. A related possibility is that one of these *unc-4* (and *ceh-12*) dependent defects indirectly triggers the other. For example, does evident loss of

cholinergic signaling capacity in VA motor neurons with reduced numbers of synaptic vesicles induce input miswiring? In principle, this question could be addressed by using the UNC-7S::GFP marker to assess the specificity of VA inputs (i.e. gap junctions with AVB?) in animals deficient for cholinergic signaling (e.g. *cha-1* mutants) but wildtype for *unc-4*. The alternative possibility that normal inputs to the VAs are required for maintaining SV levels could be addressed by genetically ablating AVA, AVD and AVE by transgenic expression of human caspase ICE with the *nmr-1* promoter (Zheng, Brockie et al. 1999).

Role of *ceh-12* in modulating neurotransmitter release

In this work, we have identified *ceh-12* as a downstream component of the *unc-4* pathway necessary for synaptic input as well as the strength of synaptic output. Mutations in *ceh-12* are sufficient to rescue the reduction of synaptic vesicles observed in the *unc-4* mutant; however, the mechanism in which SV levels are modulated is still unknown. Lickteig et al. (2001) determined that SV levels are regulated at a post-transcriptional level. Thus, we propose that ectopic *ceh-12* in *unc-4* mutants is repressing a "gene x" that normally promotes SV stability or biogenesis. If *ceh-12* functions as a transcriptional repressor, as proposed in this model, then the "gene x" transcript should be downregulated in our microarray profiles of *unc-4* and *unc-37* mutant A-class motor neurons. We can use RNAi to directly test these candidate genes for effects on SV levels in *unc-4* mutants.

SV regulation in VC motor neurons

Our preliminary experiments examining RAB-3 expression in VA and DA motor neurons suggest that *ceh-12(0)* alone is sufficient to restore normal SV levels to A-class motor neurons. The SV defect in VC motor neurons is not rescued in the *ceh-12; unc-4* double mutant, however, which indicates that a different effector molecule functions downstream of *unc-4* in VC motor neurons to regulate synaptic vesicle abundance. One possibility is that a different transcription factor is de-repressed in the VCs to turn down the machinery necessary to stabilize SVs. An attractive candidate for this function is *lin-11*, which is expressed in VC motor neurons (Hobert, D'Alberti et al. 1998; Lickteig, Duerr et al. 2001). Examination of *lin-11* expression in an *unc-4* mutant should determine whether *lin-11* is regulated by *unc-4*; *lin-11*::GFP expression should be brighter in the *unc-4* mutant. Analysis of SV protein levels in the *unc-4;lin-11* double mutant would determine if this transcription factor is sufficient to stabilize SVs. As another approach to this question, we could use RNAi to test candidate *unc-4* and *unc-37* target genes identified in the microarray experiments for suppression of the SV defect in VC motor neurons. A rationale for this experiment is that some subset of UNC-4-regulated genes destabilize synaptic vesicles in VC motor neurons but not in the VAs. We currently have a Synaptobrevin::GFP (GFP-SNB-1) that is highly expressed in the VC motor neuron processes that innervate the vulva. In the *unc-4* mutant, ~100% of animals display a complete loss of GFP-SNB-1 in the VC processes. By visually screening animals treated with RNAi directed against our microarray targets, we should be able to identify candidates required for regulating SV levels in these cells, as evidenced by the restoration of GFP-SNB-1 in the VCs.

BIBLIOGRAPHY

Abrahante, J. E., E. A. Miller, et al. (1998). "Identification of heterochronic mutants in Caenorhabditis elegans. Temporal misexpression of a collagen::green fluorescent protein fusion gene." Genetics **149**(3): 1335-51.

Agarwala, K. L., S. Ganesh, et al. (2001). "Cloning and functional characterization of DSCAML1, a novel DSCAM-like cell adhesion molecule that mediates homophilic intercellular adhesion." Biochem Biophys Res Commun **285**(3): 760-72.

Agarwala, K. L., S. Nakamura, et al. (2000). "Down syndrome cell adhesion molecule DSCAM mediates homophilic intercellular adhesion." Brain Res Mol Brain Res **79**(1-2): 118-26.

Ahmad-Annuar, A., L. Ciani, et al. (2006). "Signaling across the synapse: a role for Wnt and Dishevelled in presynaptic assembly and neurotransmitter release." J Cell Biol **174**(1): 127-39.

Ahn, D. G., I. Ruvinsky, et al. (2000). "tbx20, a new vertebrate T-box gene expressed in the cranial motor neurons and developing cardiovascular structures in zebrafish." Mech Dev **95**(1-2): 253-8.

Ao, W., J. Gaudet, et al. (2004). "Environmentally induced foregut remodeling by PHA-4/FoxA and DAF-12/NHR." Science **305**(5691): 1743-6.

Appel, B. and J. S. Eisen (2003). "Retinoids run rampant: multiple roles during spinal cord and motor neuron development." Neuron **40**(3): 461-4.

Appel, B., V. Korzh, et al. (1995). "Motoneuron fate specification revealed by patterned LIM homeobox gene expression in embryonic zebrafish." Development **121**(12): 4117-25.

Araujo, S. J. and G. Tear (2003). "Axon guidance mechanisms and molecules: lessons from invertebrates." Nat Rev Neurosci **4**(11): 910-22.

Arber, S., B. Han, et al. (1999). "Requirement for the homeobox gene Hb9 in the consolidation of motor neuron identity." Neuron **23**(4): 659-74.

Ardizzi, J. P. and H. F. Epstein (1987). "Immunochemical localization of myosin heavy chain isoforms and paramyosin in developmentally and structurally diverse muscle cell types of the nematode Caenorhabditis elegans." J Cell Biol **105**(6 Pt 1): 2763-70.

Aspock, G., H. Kagoshima, et al. (1999). "Caenorhabditis elegans has scores of hedgehog-related genes: sequence and expression analysis." Genome Res **9**(10): 909-23.

Ballivet, M., C. Alliod, et al. (1996). "Nicotinic acetylcholine receptors in the nematode Caenorhabditis elegans." J Mol Biol **258**(2): 261-9.

Bamber, B. A., A. A. Beg, et al. (1999). "The Caenorhabditis elegans unc-49 locus encodes multiple subunits of a heteromultimeric GABA receptor." J Neurosci **19**(13): 5348-59.

Bamber, B. A., J. E. Richmond, et al. (2005). "The composition of the GABA receptor at the Caenorhabditis elegans neuromuscular junction." Br J Pharmacol **144**(4): 502-9.

Bamber, B. A., R. E. Twyman, et al. (2003). "Pharmacological characterization of the homomeric and heteromeric UNC-49 GABA receptors in C. elegans." Br J Pharmacol **138**(5): 883-93.

Bandyopadhyay, J., J. Lee, et al. (2004). "Regulation of calcineurin, a calcium/calmodulin-dependent protein phosphatase, in C. elegans." Mol Cells **18**(1): 10-6.

Bargmann, C. I. (1998). "Neurobiology of the Caenorhabditis elegans genome." Science **282**(5396): 2028-33.

Bartnik, E., M. Osborn, et al. (1986). "Intermediate filaments in muscle and epithelial cells of nematodes." J Cell Biol **102**(6): 2033-41.

Baugh, L. R., A. A. Hill, et al. (2003). "Composition and dynamics of the Caenorhabditis elegans early embryonic transcriptome." Development **130**(5): 889-900.

Bausenwein, B., A. P. Dittrich, et al. (1992). "The optic lobe of Drosophila melanogaster. II. Sorting of retinotopic pathways in the medulla." Cell Tissue Res **267**(1): 17-28.

Benian, G. M., J. E. Kiff, et al. (1989). "Sequence of an unusually large protein implicated in regulation of myosin activity in C. elegans." Nature **342**(6245): 45-50.

Bennett, M. V. and R. S. Zukin (2004). "Electrical coupling and neuronal synchronization in the Mammalian brain." Neuron **41**(4): 495-511.

Bianchi, L. and M. Driscoll (2002). "Protons at the gate: DEG/ENaC ion channels help us feel and remember." Neuron **34**(3): 337-40.

Biederer, T., Y. Sara, et al. (2002). "SynCAM, a synaptic adhesion molecule that drives synapse assembly." Science **297**(5586): 1525-31.

Bloom, L. (1993). Genetic and molecular analysis of genes required for axon outgrowth in Caenorhabditis elegans. Cambridge, MA, Massachusetts Institute of Technology.

Bloom, L. and H. R. Horvitz (1997). "The Caenorhabditis elegans gene unc-76 and its human homologs define a new gene family involved in axonal outgrowth and fasciculation." Proc Natl Acad Sci U S A **94**(7): 3414-9.

Brenner, S. (1974). "The genetics of *Caenorhabditis elegans*." Genetics **77**: 71-94.

Broadbent, I. D. and J. Pettitt (2002). "The C. elegans hmr-1 gene can encode a neuronal classic cadherin involved in the regulation of axon fasciculation." Curr Biol **12**(1): 59-63.

Brockie, P. J., D. M. Madsen, et al. (2001). "Differential expression of glutamate receptor subunits in the nervous system of Caenorhabditis elegans and their regulation by the homeodomain protein UNC-42." J Neurosci **21**(5): 1510-22.

Brockie, P. J., J. E. Mellem, et al. (2001). "The C. elegans glutamate receptor subunit NMR-1 is required for slow NMDA-activated currents that regulate reversal frequency during locomotion." Neuron **31**(4): 617-30.

Broihier, H. T., A. Kuzin, et al. (2004). "Drosophila homeodomain protein Nkx6 coordinates motoneuron subtype identity and axonogenesis." Development **131**(21): 5233-42.

Broihier, H. T. and J. B. Skeath (2002). "Drosophila homeodomain protein dHb9 directs neuronal fate via crossrepressive and cell-nonautonomous mechanisms." Neuron **35**(1): 39-50.

Brozova, E., K. Simeckova, et al. (2006). "NHR-40, a Caenorhabditis elegans supplementary nuclear receptor, regulates embryonic and early larval development." Mech Dev.

Brunschwig, K., C. Wittmann, et al. (1999). "Anterior organization of the Caenorhabditis elegans embryo by the labial-like Hox gene ceh-13." Development **126**(7): 1537-46.

Bruzzone, R., S. G. Hormuzdi, et al. (2003). "Pannexins, a family of gap junction proteins expressed in brain." Proc Natl Acad Sci U S A **100**(23): 13644-9.

Burbea, M., L. Dreier, et al. (2002). "Ubiquitin and AP180 regulate the abundance of GLR-1 glutamate receptors at postsynaptic elements in C. elegans." Neuron **35**(1): 107-20.

Burglin, T. R. and G. Ruvkun (2001). "Regulation of ectodermal and excretory function by the C. elegans POU homeobox gene ceh-6." Development **128**(5): 779-90.

Burkeen, A. K., S. L. Maday, et al. (2004). "Disruption of Caenorhabditis elegans muscle structure and function caused by mutation of troponin I." Biophys J **86**(2): 991-1001.

Butler, S. J., S. Ray, et al. (1997). "klingon, a novel member of the Drosophila immunoglobulin superfamily, is required for the development of the R7 photoreceptor neuron." Development **124**(4): 781-92.

Byrd, D. T., M. Kawasaki, et al. (2001). "UNC-16, a JNK-signaling scaffold protein, regulates vesicle transport in C. elegans." Neuron **32**(5): 787-800.

Cai, T., T. Fukushige, et al. (2004). "Insulinoma-Associated Protein IA-2, a Vesicle Transmembrane Protein, Genetically Interacts with UNC-31/CAPS and Affects Neurosecretion in Caenorhabditis elegans." J Neurosci **24**(12): 3115-24.

Calvo, D., M. Victor, et al. (2001). "A POP-1 repressor complex restricts inappropriate cell type-specific gene transcription during Caenorhabditis elegans embryogenesis." Embo J **20**(24): 7197-208.

Cameron, S., S. G. Clark, et al. (2002). "PAG-3, a Zn-finger transcription factor, determines neuroblast fate in C. elegans." Development **129**(7): 1763-1774.

Catterall, W. A. (2000). "Structure and regulation of voltage-gated Ca2+ channels." Annu Rev Cell Dev Biol **16**: 521-55.

Chalfie, M., J. E. Sulston, et al. (1985). "The neural circuit for touch sensitivity in *Caenorhabitis elegans*." J. Neurosci **5**: 956-964.

Chalfie, M., Y. Tu, et al. (1994). "Green fluorescent protein as a marker for gene expression." Science **263**: 802-805.

Chalfie, M. and J. White (1988). The nervous system. The nematode *Caenorhabditis elegans*. W. B. Wood. Cold Spring Harbor, New York, Cold Spring Harbor Laboratory Press**:** 337-391.

Chang, C., T. W. Yu, et al. (2004). "Inhibition of netrin-mediated axon attraction by a receptor protein tyrosine phosphatase." Science **305**(5680): 103-6.

Chang, S., R. J. Johnston, Jr., et al. (2003). "A transcriptional regulatory cascade that controls left/right asymmetry in chemosensory neurons of C. elegans." Genes Dev **17**(17): 2123-37.

Chase, D. L. and M. R. Koelle (2004). "Genetic Analysis of RGS Protein Function in Caenorhabditis elegans." Methods Enzymol **389**: 305-20.

Chase, D. L., J. S. Pepper, et al. (2004). "Mechanism of extrasynaptic dopamine signaling in Caenorhabditis elegans." Nat Neurosci **7**(10): 1096-103.

Chen, B. E., M. Kondo, et al. (2006). "The molecular diversity of Dscam is functionally required for neuronal wiring specificity in Drosophila." Cell **125**(3): 607-20.

Chen, G. and A. J. Courey (2000). "Groucho/TLE family proteins and transcriptional repression." Gene **249**(1-2): 1-16.

Chen, L., M. Krause, et al. (1992). "Body-wall muscle formation in Caenorhabditis elegans embryos that lack the MyoD homolog hlh-1." Science **256**: 240-243.

Chen, L., B. Ong, et al. (2001). "LAD-1, the Caenorhabditis elegans L1CAM homologue, participates in embryonic and gonadal morphogenesis and is a substrate for fibroblast growth factor receptor pathway-dependent phosphotyrosine-based signaling." J Cell Biol **154**(4): 841-55.

Chin, D. and A. R. Means (2000). "Calmodulin: a prototypical calcium sensor." Trends Cell Biol **10**(8): 322-8.

Christensen, M., A. Estevez, et al. (2002). "A primary culture system for functional analysis of C. elegans neurons and muscle cells." Neuron **33**(4): 503-14.

Cinar, H., S. Keles, et al. (2005). "Expression profiling of GABAergic motor neurons in Caenorhabditis elegans." Curr Biol **15**(4): 340-6.

Clandinin, T. R., C. H. Lee, et al. (2001). "Drosophila LAR Regulates R1-R6 and R7 Target Specificity in the Visual System." Neuron **32**(2): 237-48.

Clandinin, T. R. and S. L. Zipursky (2000). "Afferent growth cone interactions control synaptic specificity in the drosophila visual system." Neuron **28**(2): 427-36.

Clark, S. G., A. D. Chisholm, et al. (1993). "Control of cell fates in the central body region of C. elegans by the homeobox gene lin-39." Cell **74**(1): 43-55.

Clark, S. G. and C. Chiu (2003). "C. elegans ZAG-1, a Zn-finger-homeodomain protein, regulates axonal development and neuronal differentiation." Development **130**(16): 3781-94.

Cline, H. (2003). "Synaptic plasticity: importance of proteasome-mediated protein turnover." Curr Biol **13**(13): R514-6.

Cohen, N. R., J. S. Taylor, et al. (1998). "Errors in corticospinal axon guidance in mice lacking the neural cell adhesion molecule L1." Curr Biol **8**(1): 26-33.

Colavita, A., S. Krishna, et al. (1998). "Pioneer axon guidance by UNC-129, a C. elegans TGF-beta." Science **281**(5377): 706-9.

Collins, C. A., Y. P. Wairkar, et al. (2006). "Highwire restrains synaptic growth by attenuating a MAP kinase signal." Neuron **51**(1): 57-69.

Colosimo, M. E., A. Brown, et al. (2004). "Identification of thermosensory and olfactory neuron-specific genes via expression profiling of single neuron types." Curr Biol **14**(24): 2245-51.

Consortium, T. C. e. S. (1998). "Genome Sequence of the nematode *C. elegans*: A platform for investigating biology." Science **282**: 2012-2018.

Corcoran, E. E. and A. R. Means (2001). "Defining Ca2+/calmodulin-dependent protein kinase cascades in transcriptional regulation." J Biol Chem **276**(5): 2975-8.

Couturier, S., D. Bertrand, et al. (1990). "A neuronal nicotinic acetylcholine receptor subunit (alpha 7) is developmentally regulated and forms a homo-oligomeric channel blocked by alpha-BTX." Neuron **5**(6): 847-56.

Creutz, C. E., S. L. Snyder, et al. (1996). "Identification, localization, and functional implications of an abundant nematode annexin." J Cell Biol **132**(6): 1079-92.

Culetto, E., H. A. Baylis, et al. (2004). "The caenorhabditis elegans unc-63 gene encodes a levamisole-sensitive nicotinic acetylcholine receptor alpha subunit." J Biol Chem.

d'Azzo, A., A. Bongiovanni, et al. (2005). "E3 ubiquitin ligases as regulators of membrane protein trafficking and degradation." Traffic **6**(6): 429-41.

Dasen, J. S., B. C. Tice, et al. (2005). "A Hox regulatory network establishes motor neuron pool identity and target-muscle connectivity." Cell **123**(3): 477-91.

Davis, R. E. and A. O. Stretton (2001). "Structure-activity relationships of 18 endogenous neuropeptides on the motor nervous system of the nematode Ascaris suum." Peptides **22**(1): 7-23.

de la Cruz, I. P., J. Z. Levin, et al. (2003). "sup-9, sup-10, and unc-93 may encode components of a two-pore K+ channel that coordinates muscle contraction in Caenorhabditis elegans." J Neurosci **23**(27): 9133-45.

Desai, C. J., J. G. Gindhart, et al. (1996). " Receptor tyrosine phospatases are required for motor axon guidance in the Drosophila embryo." Cell **84**: 599-609.

DiAntonio, A. and L. Hicke (2004). "Ubiquitin-dependent regulation of the synapse." Annu Rev Neurosci **27**: 223-46.

Dichoso, D., T. Brodigan, et al. (2000). "The MADS-Box factor CeMEF2 is not essential for Caenorhabditis elegans myogenesis and development." Dev Biol **223**(2): 431-40.

Doi, M. and K. Iwasaki (2002). "Regulation of retrograde signaling at neuromuscular junctions by the novel C2 domain protein AEX-1." Neuron **33**(2): 249-59.

Dong, M. Q., D. Chase, et al. (2000). "Multiple RGS proteins alter neural G protein signaling to allow C. elegans to rapidly change behavior when fed." Genes Dev **14**(16): 2003-14.

Driscoll, M. and J. Kaplan (1997). Mechanotransduction. C. elegans II. T. B. D. A. Riddle, B. J. Meyer, and J. R. Priess. Cold Spring Harbor, NY, Cold Spring Harbor Press**:** 645-677.

Drisdel, R. C. and W. N. Green (2000). "Neuronal alpha-bungarotoxin receptors are alpha7 subunit homomers." J Neurosci **20**(1): 133-9.

Dupuy, D., Q. R. Li, et al. (2004). "A First Version of the Caenorhabditis elegans Promoterome." Genome Res **14**(10B): 2169-75.

Eastman, C., H. R. Horvitz, et al. (1999). "Coordinated transcriptional regulation of the unc-25 glutamic acid decarboxylase and the unc-47 GABA vesicular transporter by the Caenorhabditis elegans UNC-30 homeodomain protein." J Neurosci **19**(15): 6225-34.

Eberhart, J., M. E. Swartz, et al. (2002). "EphA4 constitutes a population-specific guidance cue for motor neurons." Dev Biol **247**(1): 89-101.

Eisenhaber, B., P. Bork, et al. (2000). "Automated annotation of GPI anchor sites: case study C. elegans." Trends Biochem Sci **25**(7): 340-1.

Epstein, H. F., D. L. Casey, et al. (1993). "Myosin and paramyosin of Caenorhabditis elegans embryos assemble into nascent structures distinct from thick filaments and multi-filament assemblages." J Cell Biol **122**(4): 845-58.

Epstein, H. F., D. M. Miller, 3rd, et al. (1985). "Myosin and paramyosin are organized about a newly identified core structure." J Cell Biol **100**(3): 904-15.

Epstein, H. F., I. Ortiz, et al. (1986). "The alteration of myosin isoform compartmentation in specific mutants of Caenorhabditis elegans." J Cell Biol **103**(3): 985-93.

Ericson, J., S. Thor, et al. (1992). "Early stages of motor neuron differentiation revealed by expression of homeobox gene islet-1." Science **256**: 1555-1560.

Esmaeili, B., J. M. Ross, et al. (2002). "The C. elegans even-skipped homologue, vab-7, specifies DB motoneurone identity and axon trajectory." Development **129**(4): 853-862.

Faivre-Sarrailh, C., S. Banerjee, et al. (2004). "Drosophila contactin, a homolog of vertebrate contactin, is required for septate junction organization and paracellular barrier function." Development **131**(20): 4931-42.

Ferrara, T. M., D. B. Flaherty, et al. (2005). "Titin/connectin-related proteins in C. elegans: a review and new findings." J Muscle Res Cell Motil **26**(6-8): 435-47.

Finney, M. and G. Ruvkun (1990). "The unc-86 gene product couples cell lineage and cell identity in C. elegans." Cell **63**: 895-905.

Fire, A., S. Xu, et al. (1998). "Potent and specific genetic interference by double-stranded RNA in Caenorbditis elegans." Nature **391**: 806 - 810.

Flaherty, D. B., K. M. Gernert, et al. (2002). "Titins in C.elegans with unusual features: coiled-coil domains, novel regulation of kinase activity and two new possible elastic regions." J Mol Biol **323**(3): 533-49.

Fleming, J. T., M. D. Squire, et al. (1997). "Caenorhabditis elegans levamisole resistance genes lev-1, unc-29, and unc-38 encode functional nicotinic acetylcholine receptor subunits." J Neurosci **17**(15): 5843-57.

Fox, R. M., S. E. Von Stetina, et al. (2005). "A gene expression fingerprint of C. elegans embryonic motor neurons." BMC Genomics **6**(1): 42.

Francis, G. R. and R. H. Waterston (1985). "Muscle organization in Caenorhabditis elegans: localization of proteins implicated in thin filament attachment and I-band organization." J Cell Biol **101**(4): 1532-49.

Francis, M. M., S. P. Evans, et al. (2005). "The Ror receptor tyrosine kinase CAM-1 is required for ACR-16-mediated synaptic transmission at the C. elegans neuromuscular junction." Neuron **46**(4): 581-94.

Fujioka, M., B. C. Lear, et al. (2003). "Even-skipped, acting as a repressor, regulates axonal projections in Drosophila." Development **130**(22): 5385-400.

Fukushige, T. and M. Krause (2005). "The myogenic potency of HLH-1 reveals wide-spread developmental plasticity in early C. elegans embryos." Development **132**(8): 1795-805.

Fukushige, T., H. Yasuda, et al. (1995). "Selective expression of the tba-1 alpha tubulin gene in a set of mechanosensory and motor neurons during the development of Caenorhabditis elegans." Biochim Biophys Acta **1261**(3): 401-16.

Gally, C., S. Eimer, et al. (2004). "A transmembrane protein required for acetylcholine receptor clustering in Caenorhabditis elegans." Nature **431**(7008): 578-82.

Garces, A. and S. Thor (2006). "Specification of Drosophila aCC motoneuron identity by a genetic cascade involving even-skipped, grain and zfh1." Development **133**(8): 1445-55.

Garel, S., F. Marin, et al. (1997). "Family of Ebf/Olf-1-related genes potentially involved in neuronal differentiation and regional specification in the central nervous system." Developmental Dynamics **210**(3): 191-205.

Geary, T. G. and T. M. Kubiak (2005). "Neuropeptide G-protein-coupled receptors, their cognate ligands and behavior in Caenorhabditis elegans." Trends Pharmacol Sci **26**(2): 56-8.

Gettner, S. N., C. Kenyon, et al. (1995). "Characterization of beta pat-3 heterodimers, a family of essential integrin receptors in C. elegans." J Cell Biol **129**(4): 1127-41.

Gieseler, K., K. Grisoni, et al. (2000). "Genetic suppression of phenotypes arising from mutations in dystrophin-related genes in Caenorhabditis elegans." Curr Biol **10**(18): 1092-7.

Gindhart, J. G., J. Chen, et al. (2003). "The kinesin-associated protein UNC-76 is required for axonal transport in the Drosophila nervous system." Mol Biol Cell **14**(8): 3356-65.

Girault, J. A. and E. Peles (2002). "Development of nodes of Ranvier." Curr Opin Neurobiol **12**(5): 476-85.

Gissendanner, C. R., K. Crossgrove, et al. (2004). "Expression and function of conserved nuclear receptor genes in Caenorhabditis elegans." Dev Biol **266**(2): 399-416.

Gitai, Z., T. W. Yu, et al. (2003). "The netrin receptor UNC-40/DCC stimulates axon attraction and outgrowth through enabled and, in parallel, Rac and UNC-115/AbLIM." Neuron **37**(1): 53-65.

Gomeza, J., S. Hulsmann, et al. (2003). "Inactivation of the glycine transporter 1 gene discloses vital role of glial glycine uptake in glycinergic inhibition." Neuron **40**(4): 785-96.

Gomeza, J., K. Ohno, et al. (2003). "Deletion of the mouse glycine transporter 2 results in a hyperekplexia phenotype and postnatal lethality." Neuron **40**(4): 797-806.

Goodman, M. B., G. G. Ernstrom, et al. (2002). "MEC-2 regulates C. elegans DEG/ENaC channels needed for mechanosensation." Nature **415**(6875): 1039-42.

Gotti, C. and F. Clementi (2004). "Neuronal nicotinic receptors: from structure to pathology." Prog Neurobiol **74**(6): 363-96.

Gottschalk, A., R. B. Almedom, et al. (2005). "Identification and characterization of novel nicotinic receptor-associated proteins in Caenorhabditis elegans." Embo J **24**(14): 2566-78.

Gregorio, C. C., H. Granzier, et al. (1999). "Muscle assembly: a titanic achievement?" Curr Opin Cell Biol **11**(1): 18-25.

Grevengoed, E. E., D. T. Fox, et al. (2003). "Balancing different types of actin polymerization at distinct sites: roles for Abelson kinase and Enabled." J Cell Biol **163**(6): 1267-79.

Grisoni, K., E. Martin, et al. (2002). "Genetic evidence for a dystrophin-glycoprotein complex (DGC) in Caenorhabditis elegans." Gene **294**(1-2): 77-86.

Gupta, B. P. and P. W. Sternberg (2002). "Tissue-specific regulation of the LIM homeobox gene lin-11 during development of the Caenorhabditis elegans egg-laying system." Dev Biol **247**(1): 102-15.

Gupta, B. P., M. Wang, et al. (2003). "The C. elegans LIM homeobox gene lin-11 specifies multiple cell fates during vulval development." Development **130**(12): 2589-601.

Halevi, S., L. Yassin, et al. (2003). "Conservation within the RIC-3 gene family. Effectors of mammalian nicotinic acetylcholine receptor expression." J Biol Chem **278**(36): 34411-7.

Hall, D. H. and E. D. Hedgecock (1991). "Kinesin-related gene unc-104 is required for axonal transport of synaptic vesicles in C. elegans." Cell **65**: 837-847.

Hall, S. G. and A. J. Bieber (1997). "Mutations in the Drosophila neuroglian cell adhesion molecule affect motor neuron pathfinding and peripheral nervous system patterning." J Neurobiol **32**(3): 325-40.

Hallam, S., E. Singer, et al. (2000). "The C. elegans NeuroD homolog cnd-1 functions in multiple aspects of motor neuron fate specification." Development **127**(19): 4239-4252.

Hallam, S. J., A. Goncharov, et al. (2002). "SYD-1, a presynaptic protein with PDZ, C2 and rhoGAP-like domains, specifies axon identity in C. elegans." Nat Neurosci **5**(11): 1137-46.

Hammarlund, M., W. S. Davis, et al. (2000). "Mutations in beta-spectrin disrupt axon outgrowth and sarcomere structure." J Cell Biol **149**(4): 931-42.

Harrington, R. J., M. J. Gutch, et al. (2002). "The C. elegans LAR-like receptor tyrosine phosphatase PTP-3 and the VAB-1 Eph receptor tyrosine kinase have partly redundant functions in morphogenesis." Development **129**(9): 2141-53.

Harris, T. W., E. Hartwieg, et al. (2000). "Mutations in synaptojanin disrupt synaptic vesicle recycling." J Cell Biol **150**(3): 589-600.

Harris, T. W., K. Schuske, et al. (2001). "Studies of synaptic vesicle endocytosis in the nematode C. elegans." Traffic **2**(9): 597-605.

Harteneck, C., T. D. Plant, et al. (2000). "From worm to man: three subfamilies of TRP channels." Trends Neurosci **23**(4): 159-66.

Hata, Y., S. Butz, et al. (1996). "CASK: a novel dlg/PSD95 homolog with an N-terminal calmodulin-dependent protein kinase domain identified by interaction with neurexins." J Neurosci **16**(8): 2488-94.

Hedgecock, E. M., J. G. Culotti, et al. (1990). "The unc-5, unc-6, and unc-40, guide circumferential migrations of pioneer axons and mesodermal cells on the nematode epidermis." Neuron **2**: 61-85.

Hegde, A. N. and A. DiAntonio (2002). "Ubiquitin and the synapse." Nat Rev Neurosci **3**(11): 854-61.

Helmbacher, F., S. Schneider-Maunoury, et al. (2000). "Targeting of the EphA4 tyrosine kinase receptor affects dorsal/ventral pathfinding of limb motor axons." Development **127**(15): 3313-24.

Hestrin, S. and M. Galarreta (2005). "Electrical synapses define networks of neocortical GABAergic neurons." Trends Neurosci **28**(6): 304-9.

Hill, A. A., E. L. Brown, et al. (2001). "Evaluation of normalization procedures for oligonucleotide array data based on spiked cRNA controls." Genome Biol **2**(12): RESEARCH0055.

Hill, E., I. D. Broadbent, et al. (2001). "Cadherin superfamily proteins in Caenorhabditis elegans and Drosophila melanogaster." J Mol Biol **305**(5): 1011-24.

Hintsch, G., A. Zurlinden, et al. (2002). "The calsyntenins--a family of postsynaptic membrane proteins with distinct neuronal expression patterns." Mol Cell Neurosci **21**(3): 393-409.

Hirabayashi, Y., Y. Itoh, et al. (2004). "The Wnt/beta-catenin pathway directs neuronal differentiation of cortical neural precursor cells." Development **131**(12): 2791-801.

Hobert, O. (2002). "PCR fusion-based approach to create reporter gene constructs for expression analysis in transgenic C. elegans." Biotechniques **32**(4): 728-30.

Hobert, O., T. D'Alberti, et al. (1998). "Control of neural development and function in a thermoregulatory network by the LIM homeobox gene lin-11." J Neurosci **18**(6): 2084-96.

Hobert, O., D. G. Moerman, et al. (1999). "A conserved LIM protein that affects muscular adherens junction integrity and mechanosensory function in Caenorhabditis elegans." J Cell Biol **144**(1): 45-57.

Hu, H., J. H. Sheehan, et al. (2004). "The Mode of Action of Centrin: BINDING OF Ca2+ AND A PEPTIDE FRAGMENT OF Kar1p TO THE C-TERMINAL DOMAIN." J Biol Chem **279**(49): 50895-903.

Huang, X., H. J. Cheng, et al. (2002). "MAX-1, a novel PH/MyTH4/FERM domain cytoplasmic protein implicated in netrin-mediated axon repulsion." Neuron **34**(4): 563-76.

Huber, A. B., A. Kania, et al. (2005). "Distinct roles for secreted semaphorin signaling in spinal motor axon guidance." Neuron **48**(6): 949-64.

Hummel, T., M. L. Vasconcelos, et al. (2003). "Axonal targeting of olfactory receptor neurons in Drosophila is controlled by Dscam." Neuron **37**(2): 221-31.

Hutagalung, A. H., M. L. Landsverk, et al. (2002). "The UCS family of myosin chaperones." J Cell Sci **115**(Pt 21): 3983-90.

Hutter, H., B. E. Vogel, et al. (2000). "Conservation and novelty in the evolution of cell adhesion and extracellular matrix genes." Science **287**(5455): 989-94.

Iino, Y. and M. Yamamoto (1998). "Expression pattern of the C. elegans P21-activated protein kinase, CePAK." Biochem Biophys Res Commun **245**(1): 177-84.

Irie, M., Y. Hata, et al. (1997). "Binding of neuroligins to PSD-95." Science **277**(5331): 1511-5.

Irizarry, R. A., B. M. Bolstad, et al. (2003). "Summaries of Affymetrix GeneChip probe level data." Nucleic Acids Res **31**(4): e15.

Irizarry, R. A., B. Hobbs, et al. (2003). "Exploration, normalization, and summaries of high density oligonucleotide array probe level data." Biostatistics **4**(2): 249-64.

Iwasaki, K., J. Staunton, et al. (1997). "aex-3 encodes a novel regulator of presynaptic activity in C. elegans." Neuron **18**(4): 613-22.

Jacob, T. C. and J. M. Kaplan (2003). "The EGL-21 carboxypeptidase E facilitates acetylcholine release at Caenorhabditis elegans neuromuscular junctions." J Neurosci **23**(6): 2122-30.

Jansen, G., K. L. Thijssen, et al. (1999). "The complete family of genes encoding G proteins of Caenorhabditis elegans." Nat Genet **21**(4): 414-9.

Janz, R., Y. Goda, et al. (1999). "SV2A and SV2B function as redundant Ca2+ regulators in neurotransmitter release." Neuron **24**(4): 1003-16.

Janz, R., K. Hofmann, et al. (1998). "SVOP, an evolutionarily conserved synaptic vesicle protein, suggests novel transport functions of synaptic vesicles." J Neurosci **18**(22): 9269-81.

Jimenez, G., Z. Paroush, et al. (1997). "Groucho acts as a corepressor for a subset of negative regulators, including Hairy and Engrailed." Genes Dev **11**(22): 3072-82.

Jin, Y., R. Hoskins, et al. (1994). "Control of type-D GABAergic neuron differentiation by C. elegans UNC-30 homeodomain protein." Nature **372**: 780-783.

Jones, A. K. and D. B. Sattelle (2004). "Functional genomics of the nicotinic acetylcholine receptor gene family of the nematode, Caenorhabditis elegans." Bioessays **26**(1): 39-49.

Jones, S., S. Sudweeks, et al. (1999). "Nicotinic receptors in the brain: correlating physiology with function." Trends Neurosci **22**(12): 555-561.

Junghans, D., I. G. Haas, et al. (2005). "Mammalian cadherins and protocadherins: about cell death, synapses and processing." Curr Opin Cell Biol **17**(5): 446-52.

Juttner, R. and F. G. Rathjen (2005). "Molecular analysis of axonal target specificity and synapse formation." Cell Mol Life Sci **62**(23): 2811-27.

Kaminker, J. S., J. Canon, et al. (2002). "Control of photoreceptor axon target choice by transcriptional repression of Runt." Nat Neurosci **5**(8): 746-50.

Kaminker, J. S., R. Singh, et al. (2001). "Redundant function of Runt Domain binding partners, Big brother and Brother, during Drosophila development." Development **128**(14): 2639-48.

Kania, A., R. L. Johnson, et al. (2000). "Coordinate roles for LIM homeobox genes in directing the dorsoventral trajectory of motor axons in the vertebrate limb." Cell **102**(2): 161-73.

Kao, H. T., B. Porton, et al. (1999). "Molecular evolution of the synapsin gene family." J Exp Zool **285**(4): 360-77.

Karabinos, A., I. Bussing, et al. (2003). "Functional analysis of the single calmodulin gene in the nematode Caenorhabditis elegans by RNA interference and 4-D microscopy." Eur J Cell Biol **ban**(11): 557-63.

Kass, J., T. C. Jacob, et al. (2001). "The EGL-3 proprotein convertase regulates mechanosensory responses of Caenorhabditis elegans." J Neurosci **21**(23): 9265-72.

Keating, C. D., N. Kriek, et al. (2003). "Whole-genome analysis of 60 G protein-coupled receptors in Caenorhabditis elegans by gene knockout with RNAi." Curr Biol **13**(19): 1715-20.

Kenyon, C. (1986). "A gene involved in the development of the posterior body region of C. elegans." Cell **46**(3): 477-87.

Kenyon, C. J., J. Austin, et al. (1997). "The dance of the Hox genes: patterning the anteroposterior body axis of Caenorhabditis elegans." Cold Spring Harb Symp Quant Biol **62**: 293-305.

Kim, J., D. S. Poole, et al. (2001). "Genes affecting the activity of nicotinic receptors involved in Caenorhabditis elegans egg-laying behavior." Genetics **157**(4): 1599-610.

Kim, K., M. E. Colosimo, et al. (2005). "The UNC-3 Olf/EBF protein represses alternate neuronal programs to specify chemosensory neuron identity." Dev Biol **286**(1): 136-48.

Kim, K. and C. Li (2004). "Expression and regulation of an FMRFamide-related neuropeptide gene family in Caenorhabditis elegans." J Comp Neurol **475**(4): 540-50.

Koppen, M., J. S. Simske, et al. (2001). "Cooperative regulation of AJM-1 controls junctional integrity in Caenorhabditis elegans epithelia." Nat Cell Biol **3**(11): 983-91.

Korswagen, H. C. (2002). "Canonical and non-canonical Wnt signaling pathways in Caenorhabditis elegans: variations on a common signaling theme." Bioessays **24**(9): 801-10.

Kraus, F., B. Haenig, et al. (2001). "Cloning and expression analysis of the mouse T-box gene tbx20." Mech Dev **100**(1): 87-91.

Krause, M., A. Fire, et al. (1990). "CeMyoD accumulation defines the body wall muscle cell fate during C. elegans embryogenesis." Cell **63**: 907-919.

Krueger, N. X., D. Van Vactor, et al. (1996). "The transmembrane tyrosine phosphatase DLAR controls motor axon guidance in Drosophila." Cell **84**(4): 611-22.

Kunitomo, H., H. Uesugi, et al. (2005). "Identification of ciliated sensory neuron-expressed genes in Caenorhabditis elegans using targeted pull-down of poly(A) tails." Genome Biol **6**(2): R17.

Labrador, J. P., D. O'Keefe, et al. (2005). "The homeobox transcription factor even-skipped regulates netrin-receptor expression to control dorsal motor-axon projections in Drosophila." Curr Biol **15**(15): 1413-9.

Lackner, M. R., S. J. Nurrish, et al. (1999). "Facilitation of synaptic transmission by EGL-30 Gqalpha and EGL-8 PLCbeta: DAG binding to UNC-13 is required to stimulate acetylcholine release." Neuron **24**(2): 335-46.

Lai, T. and G. Garriga (2004). "The conserved kinase UNC-51 acts with VAB-8 and UNC-14 to regulate axon outgrowth in C. elegans." Development **131**(23): 5991-6000.

Landgraf, M., S. Roy, et al. (1999). "even-skipped determines the dorsal growth of motor axons in Drosophila." Neuron **22**(1): 43-52.

Layden, M. J., J. P. Odden, et al. (2006). "Zfh1, a somatic motor neuron transcription factor, regulates axon exit from the CNS." Dev Biol **291**(2): 253-63.

Lee, C. H., T. Herman, et al. (2001). "N-cadherin regulates target specificity in the Drosophila visual system." Neuron **30**(2): 437-50.

Lee, R. C., T. R. Clandinin, et al. (2003). "The protocadherin Flamingo is required for axon target selection in the Drosophila visual system." Nat Neurosci **6**(6): 557-63.

Lee, R. Y., E. R. Sawin, et al. (1999). "EAT-4, a homolog of a mammalian sodium-dependent inorganic phosphate cotransporter, is necessary for glutamatergic neurotransmission in caenorhabditis elegans." J Neurosci **19**(1): 159-67.

Lee, S. K. and S. L. Pfaff (2001). "Transcriptional networks regulating neuronal identity in the developing spinal cord." Nat Neurosci **4 Suppl**: 1183-91.

Lewis, J. A., C.-H. Wu, et al. (1980). "The Genetics of Levamisole Resistance n the Nematode Caenorhabditis Elegans." Genetics **95**(August): 905-928.

Lewis, J. A., C. H. Wu, et al. (1980). "Levamisole-resistant mutants of the nematode Caenorhabditis elegans appear to lack pharmacological acetylcholine receptors." Neuroscience **5**(6): 967-89.

Li, C., K. Kim, et al. (1999). "FMRFamide-related neuropeptide gene family in Caenorhabditis elegans." Brain Res **848**(1-2): 26-34.

Li, C., L. S. Nelson, et al. (1999). "Neuropeptide gene families in the nematode Caenorhabditis elegans." Ann N Y Acad Sci **897**: 239-52.

Liao, E. H., W. Hung, et al. (2004). "An SCF-like ubiquitin ligase complex that controls presynaptic differentiation." Nature.

Lickteig, K. M., J. S. Duerr, et al. (2001). "Regulation of neurotransmitter vesicles by the homeodomain protein UNC- 4 and its transcriptional corepressor UNC-37/groucho in Caenorhabditis elegans cholinergic motor neurons." J Neurosci **21**(6): 2001-14.

Lin, X., H. Qadota, et al. (2003). "C. elegans PAT-6/actopaxin plays a critical role in the assembly of integrin adhesion complexes in vivo." Curr Biol **13**(11): 922-32.

Lise, M. F. and A. El-Husseini (2006). "The neuroligin and neurexin families: from structure to function at the synapse." Cell Mol Life Sci **63**(16): 1833-49.

Liu, H., T. J. Strauss, et al. (2006). "Direct regulation of egl-1 and of programmed cell death by the Hox protein MAB-5 and by CEH-20, a C. elegans homolog of Pbx1." Development **133**(4): 641-50.

Ludewig, A. H., C. Kober-Eisermann, et al. (2004). "A novel nuclear receptor/coregulator complex controls C. elegans lipid metabolism, larval development, and aging." Genes Dev **18**(17): 2120-33.

Lynch, J. W. (2004). "Molecular structure and function of the glycine receptor chloride channel." Physiol Rev **84**(4): 1051-95.

Lyuksyutova, A. I., C. C. Lu, et al. (2003). "Anterior-posterior guidance of commissural axons by Wnt-frizzled signaling." Science **302**(5652): 1984-8.

Mackenzie, J. M., Jr., R. L. Garcea, et al. (1978). "Muscle development in Caenorhabditis elegans: mutants exhibiting retarded sarcomere construction." Cell **15**(3): 751-62.

Maduro, M. and D. Pilgrim (1995). "Identification and cloning of unc-119, a gene expressed in the Caenorhabditis elegans nervous system." Genetics **141**(3): 977-88.

Maloof, J. N. and C. Kenyon (1998). "The Hox gene lin-39 is required during C. elegans vulval induction to select the outcome of Ras signaling." Development **125**(2): 181-90.

Mansouri, A., Y. Yokota, et al. (1997). "Paired-related murine homeobox gene expressed in the developing sclerotome, kidney, and nervous system." Developmental Dynamics **210**: 53-65.

Marie, B., L. Cruz-Orengo, et al. (2002). "Persistent engrailed Expression Is Required to Determine Sensory Axon Trajectory, Branching, and Target Choice." J Neurosci **22**(3): 832-41.

Maryon, E. B., R. Coronado, et al. (1996). "unc-68 encodes a ryanodine receptor involved in regulating C. elegans body-wall muscle contraction." J Cell Biol **134**(4): 885-93.

Maryon, E. B., B. Saari, et al. (1998). "Muscle-specific functions of ryanodine receptor channels in Caenorhabditis elegans." J Cell Sci **111 (Pt 19)**: 2885-95.

Mathews, E. A., E. Garcia, et al. (2003). "Critical residues of the Caenorhabditis elegans unc-2 voltage-gated calcium channel that affect behavioral and physiological properties." J Neurosci **23**(16): 6537-45.

Maurel-Zaffran, C., T. Suzuki, et al. (2001). "Cell-Autonomous and -Nonautonomous Functions of LAR in R7 Photoreceptor Axon Targeting." Neuron **32**(2): 225-35.

McCabe, B. D., G. Marques, et al. (2003). "The BMP homolog Gbb provides a retrograde signal that regulates synaptic growth at the Drosophila neuromuscular junction." Neuron **39**(2): 241-54.

McGhee, J. D. and M. Krause (1997). Transcription Factors and Transcriptional Regulation. C. elegans II. T. B. D. A. Riddle, B. J. Meyer, and J. R. Priess. Cold Spring Harbor, NY, Cold Spring Harbor Press**:** 147-184.

McIntire, S. L., G. Garriga, et al. (1992). "Genes necessary for directed axonal elongation or fasciculation in C. elegans." Neuron **8**: 307-322.

McIntire, S. L., E. Jorgensen, et al. (1993). "Genes required for GABA function in Caenorhabditis elegans." Nature **364**: 334-337.

McIntire, S. L., R. J. Reimer, et al. (1997). "Identification and characterization of the vesicular GABA transporter." Nature **389**: 870-876.

McKay, S. J., R. Johnsen, et al. (2003). "Gene expression profiling of cells, tissues, and developmental stages of the nematode C. elegans." Cold Spring Harb Symp Quant Biol **68**: 159-69.

Megeney, L. A., B. Kablar, et al. (1996). "MyoD is required for myogenic stem cell function in adult skeletal muscle." Genes Dev **10**(10): 1173-83.

Melkman, T. and P. Sengupta (2005). "Regulation of chemosensory and GABAergic motor neuron development by the C. elegans Aristaless/Arx homolog alr-1." Development **132**(8): 1935-49.

Mello, C. and A. Fire (1995). "DNA transformation." Methods in Cell Biology **48**: 451-482.

Miller, C. (2000). "An overview of the potassium channel family." Genome Biol **1**(4): REVIEWS0004.

Miller, D., III, I. Ortiz, et al. (1983). " Differential localization of two myosins within nematode thick filaments." Cell **34**: 477 -490.

Miller, D. M., III and C. J. Niemeyer (1995). "Expression of the *unc-4* homeoprotein in *Caenorhabditis elegans* motor neurons specifies presynaptic input." Development **121**: 2877-2866.

Miller, D. M., III, F. Stockdale, et al. (1986). "Immunological identification of the genes encoding the four myosin heavy chains of Caenorhabditis elegans." Proc. Nat. Acad. Sci. USA **83**: 2305-230.

Miller, D. M., M. M. Shen, et al. (1992). "C. elegans unc-4 gene encodes a homeodomain protein that determines the pattern of synaptic input to specific motor neurons." Nature **355**(6363): 841-5.

Miller, K. G., A. Alfonso, et al. (1996). "A genetic selection for Caenorhabditis elegans synaptic transmission mutants." Proc Natl Acad Sci U S A **93**(22): 12593-8.

Miller, K. G., M. D. Emerson, et al. (1999). "Goalpha and diacylglycerol kinase negatively regulate the Gqalpha pathway in C. elegans." Neuron **24**(2): 323-33.

Moerman, D. G. and A. Fire (1997). Muscle: Structure, Function and Development. C. elegans II. D. Riddle, T. Blumenthal, B. Meyer and J. Priess. Cold Spring Harbor, NY, Cold Spring Harbor Laboratory Press**:** 417-470.

Moerman, D. G., S. Plurad, et al. (1982). "Mutations in the unc-54 myosin heavy chain gene of Caenorhabditis elegans that alter contractility but not muscle structure." Cell **29**: 773-781.

Mongan, N. P., H. A. Baylis, et al. (1998). "An extensive and diverse gene family of nicotinic acetylcholine receptor alpha subunits in Caenorhabditis elegans." Receptors Channels **6**(3): 213-28.

Moresco, J. J. and M. R. Koelle (2004). "Activation of EGL-47, a Galphao-coupled receptor, inhibits function of hermaphrodite-specific motor neurons to regulate Caenorhabditis elegans egg-laying behavior." J Neurosci **24**(39): 8522-30.

Morita, K., K. L. Chow, et al. (1999). "Regulation of body length and male tail ray pattern formation of Caenorhabditis elegans by a member of TGF-beta family." Development **126**(6): 1337-47.

Much, J. W., D. J. Slade, et al. (2000). "The fax-1 nuclear hormone receptor regulates axon pathfinding and neurotransmitter expression [In Process Citation]." Development **127**(4): 703-12.

Muhr, J., E. Andersson, et al. (2001). "Groucho-mediated transcriptional repression establishes progenitor cell pattern and neuronal fate in the ventral neural tube." Cell **104**(6): 861-73.

Muntoni, F., S. Torelli, et al. (2003). "Dystrophin and mutations: one gene, several proteins, multiple phenotypes." Lancet Neurol **2**(12): 731-40.

Muralidhar, M. G. and J. B. Thomas (1993). "The Drosophila bendless gene encodes a neural protein related to ubiquitin-conjugating enzymes." Neuron **11**(2): 253-66.

Murphey, R. K. and T. A. Godenschwege (2002). "New roles for ubiquitin in the assembly and function of neuronal circuits." Neuron **36**(1): 5-8.

Nakakura, E. K., D. N. Watkins, et al. (2001). "Mammalian Scratch: a neural-specific Snail family transcriptional repressor." Proc Natl Acad Sci U S A **98**(7): 4010-5.

Nakata, K., B. Abrams, et al. (2005). "Regulation of a DLK-1 and p38 MAP kinase pathway by the ubiquitin ligase RPM-1 is required for presynaptic development." Cell **120**(3): 407-20.

Nathoo, A. N., R. A. Moeller, et al. (2001). "Identification of neuropeptide-like protein gene families in Caenorhabditiselegans and other species." Proc Natl Acad Sci U S A **98**(24): 14000-5.

Nelson, L. S., M. L. Rosoff, et al. (1998). "Disruption of a neuropeptide gene, flp-1, causes multiple behavioral defects in Caenorhabditis elegans." Science **281**(5383): 1686-90.

Nguyen, D. N., Y. Liu, et al. (1997). "The sidekick gene, a member of the immunoglobulin superfamily, is required for pattern formation in the Drosophila eye." Development **124**(17): 3303-12.

Nonet, M. L., A. M. Holgado, et al. (1999). "UNC-11, a Caenorhabditis elegans AP180 homologue, regulates the size and protein composition of synaptic vesicles." Mol Biol Cell **10**(7): 2343-60.

Nonet, M. L., O. Saifee, et al. (1998). "Synaptic transmission deficits in Caenorhabditis elegans synaptobrevin mutants." Journal of Neuroscience **18**(1): 70-80.

Nonet, M. L., J. E. Staunton, et al. (1997). "Caenorhabditis elegans rab-3 mutant synapses exhibit impaired function and are partially depleted of vesicles." Journal of Neuroscience **17**(21): 8061-73.

Norman, K. R. and D. G. Moerman (2002). "Alpha spectrin is essential for morphogenesis and body wall muscle formation in Caenorhabditis elegans." J Cell Biol **157**(4): 665-77.

Nurrish, S., L. Segalat, et al. (1999). "Serotonin inhibition of synaptic transmission: Galpha(0) decreases the abundance of UNC-13 at release sites." Neuron **24**(1): 231-42.

Odden, J. P., S. Holbrook, et al. (2002). "Drosophila HB9 is expressed in a subset of motoneurons and interneurons, where it regulates gene expression and axon pathfinding." J Neurosci **22**(21): 9143-9.

Ogura, K., M. Shirakawa, et al. (1997). "The UNC-14 protein required for axonal elongation and guidance in Caenorhabditis elegans interacts with the serine/threonine kinase UNC-51." Genes Dev **11**(14): 1801-11.

Oh, C. E., R. McMahon, et al. (1994). "bendless, a Drosophila gene affecting neuronal connectivity, encodes a ubiquitin-conjugating enzyme homolog." J. of Neuroscience **14**: 3166-3179.

Otsuka, A. J., P. Boontrakulpoontawee, et al. (2002). "Novel UNC-44 AO13 ankyrin is required for axonal guidance in C. elegans, contains six highly repetitive STEP blocks separated by seven potential transmembrane domains, and is localized to

neuronal processes and the periphery of neural cell bodies." J Neurobiol **50**(4): 333-49.

Ouardouz, M., M. A. Nikolaeva, et al. (2003). "Depolarization-induced Ca2+ release in ischemic spinal cord white matter involves L-type Ca2+ channel activation of ryanodine receptors." Neuron **40**(1): 53-63.

Packard, M., E. S. Koo, et al. (2002). "The Drosophila Wnt, wingless, provides an essential signal for pre- and postsynaptic differentiation." Cell **111**(3): 319-30.

Palmer, R. E., T. Inoue, et al. (2002). "Caenorhabditis elegans cog-1 locus encodes GTX/Nkx6.1 homeodomain proteins and regulates multiple aspects of reproductive system development." Dev Biol **252**(2): 202-13.

Palmer, R. E., S. B. Lee, et al. (2002). "Induction of BAIAP3 by the EWS-WT1 chimeric fusion implicates regulated exocytosis in tumorigenesis." Cancer Cell **2**(6): 497-505.

Panchin, Y. V. (2005). "Evolution of gap junction proteins--the pannexin alternative." J Exp Biol **208**(Pt 8): 1415-9.

Pflugrad, A., J. Y. Meir, et al. (1997). "The Groucho-like transcription factor UNC-37 functions with the neural specificity gene unc-4 to govern motor neuron identity in C. elegans." Development **124**(9): 1699-709.

Phelan, P. and T. A. Starich (2001). "Innexins get into the gap." Bioessays **23**(5): 388-96.

Pierce, S. B., M. Costa, et al. (2001). "Regulation of DAF-2 receptor signaling by human insulin and ins-1, a member of the unusually large and diverse C. elegans insulin gene family." Genes Dev **15**(6): 672-86.

Pilon, M., X. R. Peng, et al. (2000). "The diabetes autoantigen ICA69 and its Caenorhabditis elegans homologue, ric-19, are conserved regulators of neuroendocrine secretion." Mol Biol Cell **11**(10): 3277-88.

Plasterk, R. H. (1995). "Reverse genetics: from gene sequence to mutant worm." Methods Cell Biol **48**: 59-80.

Pocock, R., J. Ahringer, et al. (2004). "A regulatory network of T-box genes and the even-skipped homologue vab-7 controls patterning and morphogenesis in C. elegans." Development **131**(10): 2373-85.

Portman, D. S. and S. W. Emmons (2004). "Identification of C. elegans sensory ray genes using whole-genome expression profiling." Dev Biol **270**(2): 499-512.

Praitis, V., E. Casey, et al. (2001). "Creation of low-copy integrated transgenic lines in Caenorhabditis elegans." Genetics **157**(3): 1217-26.

Prasad, B. C., B. Ye, et al. (1998). "*unc-3*, a gene required for axonal guidance in *Caenorhabditis elegans*, encodes a member of the O/E family of transcription factors." Development **125**: 1561-1568.

Ramulu, P. and J. Nathans (2001). "Cellular and subcellular localization, N-terminal acylation, and calcium binding of Caenorhabditis elegans protein phosphatase with EF-hands." J Biol Chem **276**(27): 25127-35.

Rand, J. and M. Nonet (1997). Synaptic Transmission. C. elegans II. T. B. D. A. Riddle, B. J. Meyer, and J. R. Priess. Cold Spring Harbor, NY, Cold Spring Harbor Press**:** 611-643.

Ranganathan, R., S. C. Cannon, et al. (2000). "MOD-1 is a serotonin-gated chloride channel that modulates locomotory behaviour in C. elegans." Nature **408**(6811): 470-5.

Rao, Y., P. Pang, et al. (2000). "brakeless is required for photoreceptor growth-cone targeting in Drosophila." Proc Natl Acad Sci U S A **97**(11): 5966-71.

Rash, J. E., W. A. Staines, et al. (2000). "Immunogold evidence that neuronal gap junctions in adult rat brain and spinal cord contain connexin-36 but not connexin-32 or connexin-43." Proc Natl Acad Sci U S A **97**(13): 7573-8.

Reynolds, N. K., M. A. Schade, et al. (2004). "Convergent, RIC-8 Dependent G{alpha} Signaling Pathways in the C. elegans Synaptic Signaling Network." Genetics.

Richmond, J. E. and K. S. Broadie (2002). "The synaptic vesicle cycle: exocytosis and endocytosis in Drosophila and C. elegans." Curr Opin Neurobiol **12**(5): 499-507.

Richmond, J. E. and E. M. Jorgensen (1999). "One GABA and two acetylcholine receptors function at the C. elegans neuromuscular junction [In Process Citation]." Nat Neurosci **2**(9): 791-7.

Robatzek, M. and J. H. Thomas (2000). "Calcium/calmodulin-dependent protein kinase II regulates Caenorhabditis elegans locomotion in concert with a G(o)/G(q) signaling network." Genetics **156**(3): 1069-82.

Robertson, H. M. (2001). "Updating the str and srj (stl) families of chemoreceptors in Caenorhabditis nematodes reveals frequent gene movement within and between chromosomes." Chem Senses **26**(2): 151-9.

Rogalski, T. M., M. M. Gilbert, et al. (2003). "DIM-1, a novel immunoglobulin superfamily protein in Caenorhabditis elegans, is necessary for maintaining bodywall muscle integrity." Genetics **163**(3): 905-15.

Rogalski, T. M., G. P. Mullen, et al. (2000). "The UNC-112 gene in Caenorhabditis elegans encodes a novel component of cell-matrix adhesion structures required for integrin localization in the muscle cell membrane." J Cell Biol **150**(1): 253-64.

Rogers, C., V. Reale, et al. (2003). "Inhibition of Caenorhabditis elegans social feeding by FMRFamide-related peptide activation of NPR-1." Nat Neurosci **6**(11): 1178-85.

Rogers, C. M., C. J. Franks, et al. (2001). "Regulation of the pharynx of Caenorhabditis elegans by 5-HT, octopamine, and FMRFamide-like neuropeptides." J Neurobiol **49**(3): 235-44.

Rongo, C., C. W. Whitfield, et al. (1998). "LIN-10 Is a Shared Component of the Polarized Protein Localization Pathways in Neurons and Epithelia." Cell **94**: 751-759.

Rougon, G. and O. Hobert (2003). "New insights into the diversity and function of neuronal immunoglobulin superfamily molecules." Annu Rev Neurosci **26**: 207-38.

Roy, P. J., J. M. Stuart, et al. (2002). "Chromosomal clustering of muscle-expressed genes in Caenorhabditis elegans." Nature **418**(6901): 975-9.

Rudnicki, M. A., T. Braun, et al. (1992). "Inactivation of MyoD in mice leads to up-regulation of the myogenic HLH gene Myf-5 and results in apparently normal muscle development." Cell **71**(3): 383-90.

Sakamoto, R., D. T. Byrd, et al. (2004). "The C. elegans UNC-14 RUN Domain Protein Binds to the Kinesin-1/UNC-16 Complex and Regulates Synaptic Vesicle Localization." Mol Biol Cell.

Salkoff, L., A. Butler, et al. (2001). "Evolution tunes the excitability of individual neurons." Neuroscience **103**(4): 853-9.

Salser, S. J., C. M. Loer, et al. (1993). "Multiple HOM-C gene interactions specify cell fates in the nematode central nervous system." Genes Dev **7**(9): 1714-24.

Sanes, J. R. and J. W. Lichtman (1999). "Development of the vertebrate neuromuscular junction." Annu Rev Neurosci **22**: 389-442.

Sarafi-Reinach, T. R., T. Melkman, et al. (2001). "The lin-11 LIM homeobox gene specifies olfactory and chemosensory neuron fates in C. elegans." Development **128**(17): 3269-81.

Savage-Dunn, C. (2001). "Targets of TGF beta-related signaling in Caenorhabditis elegans." Cytokine Growth Factor Rev **12**(4): 305-12.

Schade, M. A., N. K. Reynolds, et al. (2004). "Mutations that Rescue the Paralysis of C. elegans ric-8 (Synembryn) Mutants Activate the G{alpha}s Pathway and Define a Third Major Branch of the Synaptic Signaling Network." Genetics.

Schaefer, A. M., G. D. Hadwiger, et al. (2000). "rpm-1, a conserved neuronal gene that regulates targeting and synaptogenesis in C. elegans." Neuron **26**(2): 345-56.

Schafer, W. R. (2002). "Genetic analysis of nicotinic signaling in worms and flies." J Neurobiol **53**(4): 535-41.

Schafer, W. R., B. M. Sanchez, et al. (1996). "Genes affecting sensitivity to serotonin in Caenorhabditis elegans." Genetics **143**(3): 1219-30.

Scheiffele, P., J. Fan, et al. (2000). "Neuroligin expressed in nonneuronal cells triggers presynaptic development in contacting axons." Cell **101**(6): 657-69.

Schmucker, D., J. C. Clemens, et al. (2000). "Drosophila Dscam is an axon guidance receptor exhibiting extraordinary molecular diversity." Cell **101**(6): 671-84.

Schuske, K. R., J. E. Richmond, et al. (2003). "Endophilin is required for synaptic vesicle endocytosis by localizing synaptojanin." Neuron **40**(4): 749-62.

Sedensky, M. M., J. M. Siefker, et al. (2004). "A stomatin and a degenerin interact in lipid rafts of the nervous system of Caenorhabditis elegans." Am J Physiol Cell Physiol **287**(2): C468-74.

Segalat, L. (2002). "Dystrophin and functionally related proteins in the nematode Caenorhabditis elegans." Neuromuscul Disord **12 Suppl 1**: S105-9.

Seguela, P., J. Wadiche, et al. (1993). "Molecular cloning, functional properties, and distribution of rat brain alpha 7: a nicotinic cation channel highly permeable to calcium." J Neurosci **13**(2): 596-604.

Sengupta, P., J. H. Chou, et al. (1996). "odr-10 encodes a seven transmembrane domain olfactory receptor required for responses to the odorant diacetyl." Cell **84**(6): 899-909.

Sengupta, P., H. A. Colbert, et al. (1994). "The C. elegans gene odr-7 encodes an olfactory-specific member of the nuclear receptor superfamily." Cell **79**: 971-980.

Senti, K., K. Keleman, et al. (2000). "brakeless is required for lamina targeting of R1-R6 axons in the Drosophila visual system." Development **127**(11): 2291-301.

Serra-Pages, C., Q. G. Medley, et al. (1998). "Liprins, a family of LAR transmembrane protein-tyrosine phosphatase-interacting proteins." J Biol Chem **273**(25): 15611-20.

Shan, G., K. Kim, et al. (2005). "Convergent genetic programs regulate similarities and differences between related motor neuron classes in Caenorhabditis elegans." Dev Biol **280**(2): 494-503.

Sharma, K., A. E. Leonard, et al. (2000). "Genetic and epigenetic mechanisms contribute to motor neuron pathfinding." Nature **406**(6795): 515-9.

Sharma, K., H. Z. Sheng, et al. (1998). "LIM homeodomain factors Lhx3 and Lhx4 assign subtype identities for motor neurons." Cell **95**(6): 817-28.

Shen, K. and C. I. Bargmann (2003). "The immunoglobulin superfamily protein SYG-1 determines the location of specific synapses in C. elegans." Cell **112**(5): 619-30.

Shen, K., R. D. Fetter, et al. (2004). "Synaptic specificity is generated by the synaptic guidepost protein SYG-2 and its receptor, SYG-1." Cell **116**(6): 869-81.

Sherr, E. H. (2003). "The ARX story (epilepsy, mental retardation, autism, and cerebral malformations): one gene leads to many phenotypes." Curr Opin Pediatr **15**(6): 567-71.

Shibata, Y., T. Fujii, et al. (2000). "EAT-20, a novel transmembrane protein with EGF motifs, is required for efficient feeding in Caenorhabditis elegans." Genetics **154**(2): 635-46.

Shirasaki, R., J. W. Lewcock, et al. (2006). "FGF as a target-derived chemoattractant for developing motor axons genetically programmed by the LIM code." Neuron **50**(6): 841-53.

Shirasaki, R. and S. L. Pfaff (2002). "Transcriptional codes and the control of neuronal identity." Annu Rev Neurosci **25**: 251-81.

Shiratsuchi, T., K. Oda, et al. (1998). "Cloning and characterization of BAP3 (BAI-associated protein 3), a C2 domain-containing protein that interacts with BAI1." Biochem Biophys Res Commun **251**(1): 158-65.

Speese, S. D., N. Trotta, et al. (2003). "The ubiquitin proteasome system acutely regulates presynaptic protein turnover and synaptic efficacy." Curr Biol **13**(11): 899-910.

Sperry, R. W. (1963). "Chemoaffinity in the orderly growth of nerve fiber patterns and connections." Proc Natl Acad Sci U S A **50**: 703-710.

Spitzenberger, F., S. Pietropaolo, et al. (2003). "Islet cell autoantigen of 69 kDa is an arfaptin-related protein associated with the Golgi complex of insulinoma INS-1 cells." J Biol Chem **278**(28): 26166-73.

Starich, T., M. Sheehan, et al. (2001). "Innexins in C. elegans." Cell Commun Adhes **8**(4-6): 311-4.

Starich, T. A., R. K. Herman, et al. (1993). "Molecular and genetic analysis of unc-7, a Caenorhabditis elegans gene required for coordinated locomotion." Genetics **133**: 527-541.

Steger, K. A. and L. Avery (2004). "The GAR-3 muscarinic receptor cooperates with calcium signals to regulate muscle contraction in the Caenorhabditis elegans pharynx." Genetics **167**(2): 633-43.

Stewart, M. K., N. L. Clark, et al. (2005). "High genetic diversity in the chemoreceptor superfamily of Caenorhabditis elegans." Genetics **169**(4): 1985-96.

Storey, J. D. and R. Tibshirani (2003). "Statistical significance for genomewide studies." Proc Natl Acad Sci U S A **100**(16): 9440-5.

Strehler, E. E. and M. Treiman (2004). "Calcium pumps of plasma membrane and cell interior." Curr Mol Med **4**(3): 323-35.

Stringham, E., N. Pujol, et al. (2002). "unc-53 controls longitudinal migration in C. elegans." Development **129**(14): 3367-79.

Stromme, P., M. E. Mangelsdorf, et al. (2002). "Mutations in the human ortholog of Aristaless cause X-linked mental retardation and epilepsy." Nat Genet **30**(4): 441-5.

Struckhoff, E. C. and E. A. Lundquist (2003). "The actin-binding protein UNC-115 is an effector of Rac signaling during axon pathfinding in C. elegans." Development **130**(4): 693-704.

Su, C. W., S. Tharin, et al. (2006). "The short coiled-coil domain-containing protein UNC-69 cooperates with UNC-76 to regulate axonal outgrowth and normal presynaptic organization in Caenorhabditis elegans." J Biol **5**(4): 9.

Su, M., D. C. Merz, et al. (2000). "Regulation of the UNC-5 netrin receptor initiates the first reorientation of migrating distal tip cells in Caenorhabditis elegans." Development **127**(3): 585-94.

Sudhof, T. C. (2004). "The synaptic vesicle cycle." Annu Rev Neurosci **27**: 509-47.

Sulston, J. E. (1983). "Neuronal cell lineages in the nematode Caenorhabditis elegans." Cold Spring Harbor Symposia on Quantitative Biology **48**(Pt 2): 443-52.

Sulston, J. E. and H. R. Horvitz (1977). "Post-embryonic cell lineages of the nematode, *Caenorhabditis elegans*." Dev. Biol. **56**: 110-156.

Sulston, J. E., E. Schierenberg, et al. (1983). "The embryonic cell lineage of the nematode Caenorhabditis elegans." Developmental Biology **100**(1): 64-119.

Suzuki, S. T. (1996). "Protocadherins and diversity of the cadherin superfamily." J Cell Sci **109 (Pt 11)**: 2609-11.

Suzuki, Y., M. D. Yandell, et al. (1999). "A BMP homolog acts as a dose-dependent regulator of body size and male tail patterning in Caenorhabditis elegans." Development **126**(2): 241-50.

Sym, M., N. Robinson, et al. (1999). "MIG-13 positions migrating cells along the anteroposterior body axis of C. elegans." Cell **98**(1): 25-36.

Szewczyk, N. J., J. J. Hartman, et al. (2000). "Genetic defects in acetylcholine signalling promote protein degradation in muscle cells of Caenorhabditis elegans." J Cell Sci **113 (Pt 11)**: 2003-10.

Takao-Rikitsu, E., S. Mochida, et al. (2004). "Physical and functional interaction of the active zone proteins, CAST, RIM1, and Bassoon, in neurotransmitter release." J Cell Biol **164**(2): 301-11.

Tanabe, Y., C. William, et al. (1998). "Specification of motor neuron identity by the MNR2 homeodomain protein." Cell **95**(1): 67-80.

Tavernarakis, N., W. Shreffler, et al. (1997). "*unc-8*, a DEG/ENaC family member, encodes a subunit of a candidate mechanically gated channel that modulates *C. elegans* locomotion." Neuron **18**: 107-119.

Thaler, J., K. Harrison, et al. (1999). "Active suppression of interneuron programs within developing motor neurons revealed by analysis of homeodomain factor HB9." Neuron **23**(4): 675-87.

Thayer, S. A., Y. M. Usachev, et al. (2002). "Modulating Ca2+ clearance from neurons." Front Biosci **7**: d1255-79.

Thellmann, M., J. Hatzold, et al. (2003). "The Snail-like CES-1 protein of C. elegans can block the expression of the BH3-only cell-death activator gene egl-1 by antagonizing the function of bHLH proteins." Development **130**(17): 4057-71.

Thor, S., S. G. Andersson, et al. (1999). "A LIM-homeodomain combinatorial code for motor-neuron pathway selection." Nature **397**(6714): 76-80.

Touroutine, D., R. M. Fox, et al. (2005). "acr-16 encodes an essential subunit of the levamisole-resistant nicotinic receptor at the Caenorhabditis elegans neuromuscular junction." J Biol Chem **280**(29): 27013-21.

Towers, P. R., B. Edwards, et al. (2005). "The Caenorhabditis elegans lev-8 gene encodes a novel type of nicotinic acetylcholine receptor alpha subunit." J Neurochem **93**(1): 1-9.

Troemel, E. R. (1999). "Chemosensory signaling in C. elegans." Bioessays **21**(12): 1011-20.

Tsalik, E. L., T. Niacaris, et al. (2003). "LIM homeobox gene-dependent expression of biogenic amine receptors in restricted regions of the C. elegans nervous system." Dev Biol **263**(1): 81-102.

Tsuchida, T., M. Ensini, et al. (1994). "Topographic organization of embryonic motor neurons defined by expression of LIM homeobox genes." Cell **79**: 957-970.

Tucker, M., M. Sieber, et al. (2005). "The Caenorhabditis elegans aristaless orthologue, alr-1, is required for maintaining the functional and structural integrity of the amphid sensory organs." Mol Biol Cell **16**(10): 4695-704.

Tusher, V. G., R. Tibshirani, et al. (2001). "Significance analysis of microarrays applied to the ionizing radiation response." Proc Natl Acad Sci U S A **98**(9): 5116-21.

Vaglio, P., P. Lamesch, et al. (2003). "WorfDB: the Caenorhabditis elegans ORFeome Database." Nucleic Acids Res **31**(1): 237-40.

Vogel, C., S. A. Teichmann, et al. (2003). "The immunoglobulin superfamily in Drosophila melanogaster and Caenorhabditis elegans and the evolution of complexity." Development **130**(25): 6317-28.

Von Stetina, S. E., M. Treinin, et al. (2006). "The motor circuit." Int Rev Neurobiol **69**: 125-67.

Wacker, I., V. Schwarz, et al. (2003). "zag-1, a Zn-finger homeodomain transcription factor controlling neuronal differentiation and axon outgrowth in C. elegans." Development **130**(16): 3795-805.

Wadsworth, W. G., H. Bhatt, et al. (1995). "Neuroglia and pioneer axons express UNC-6 to provide global and local netrin cues for guiding migrations in *Caenorhabditis elegans*." Neuron **16**: 35-46.

Wagmaister, J. A., J. E. Gleason, et al. (2006). "Transcriptional upregulation of the C. elegans Hox gene lin-39 during vulval cell fate specification." Mech Dev **123**(2): 135-50.

Walthall, W. W. and J. A. Plunkett (1995). "Genetic transformation of the synaptic pattern of a motoneuron class in *Caenorhabditis elegans*." J. Neuroscience **15**: 1035-1043.

Wan, H. I., A. DiAntonio, et al. (2000). "Highwire regulates synaptic growth in Drosophila." Neuron **26**(2): 313-29.

Wang, B. B., M. M. Muller-Immergluck, et al. (1993). "A homeotic gene cluster patterns the anteroposterior body axis of C. elegans." Cell **74**(1): 29-42.

Wang, D., S. Kennedy, et al. (2005). "Somatic misexpression of germline P granules and enhanced RNA interference in retinoblastoma pathway mutants." Nature **436**(7050): 593-7.

Wang, J., C. T. Zugates, et al. (2002). "Drosophila Dscam is required for divergent segregation of sister branches and suppresses ectopic bifurcation of axons." Neuron **33**(4): 559-71.

Wang, M. M. and R. R. Reed (1993). "Molecular cloning of the olfactory neuronal transcription factor Olf-1 by genetic selection in yeast." Nature **364**(6433): 121-6.

Waterston, R. H. (1988). Muscle. The Nematode Caenorhabditis elegans. W. B. Wood. Cold Spring Harbor, NY, Cold Spring Harbor Laboratory Press**:** 281-335.

Waterston, R. H. (1989). "The minor myosin heavy chain, mhcA, of Caenorhabditis elegans is necessary for the initiation of thick filament assembly." Embo J **8**(11): 3429-36.

Waterston, R. H., H. F. Epstein, et al. (1974). "Paramyosin of Caenorhabditis elegans." J Mol Biol **90**(2): 285-90.

Waterston, R. H., J. N. Thomson, et al. (1980). "Mutants with altered muscle structure of Caenorhabditis elegans." Dev Biol **77**(2): 271-302.

Weimer, R. M. and E. M. Jorgensen (2003). "Controversies in synaptic vesicle exocytosis." J Cell Sci **116**(Pt 18): 3661-6.

Weimer, R. M., J. E. Richmond, et al. (2003). "Defects in synaptic vesicle docking in unc-18 mutants." Nat Neurosci **6**(10): 1023-30.

Westmoreland, J. J., J. McEwen, et al. (2001). "Conserved function of Caenorhabditis elegans UNC-30 and mouse Pitx2 in controlling GABAergic neuron differentiation." J Neurosci **21**(17): 6810-9.

Whangbo, J. and C. Kenyon (1999). "A Wnt signaling system that specifies two patterns of cell migration in C. elegans." Mol Cell **4**(5): 851-8.

White, J. G., D. G. Albertson, et al. (1978). "Connectivity changes in a class of motoneurone during the development of a nematode." Nature **271**: 764-766.

White, J. G., E. Southgate, et al. (1992). "Mutations in the *Caenorhabditis elegans unc-4* gene alter the synaptic input to ventral cord motor neurons." Nature **355**: 838-841.

White, J. G., E. Southgate, et al. (1976). "Structure of the ventral nerve cord of *Caenorhabditis elegans*." Phil. Trans.R. Soc. Lond. **B275**: 327-348.

White, J. G., E. Southgate, et al. (1986). "The structure of the nervous system of the nematode *Caenorhabditis elegans*." Phil. Trans. R. Soc. Lond. **B314**: 1-340.

Whitfield, C. W., C. Benard, et al. (1999). "Basolateral localization of the Caenorhabditis elegans epidermal growth factor receptor in epithelial cells by the PDZ protein LIN-10." Mol Biol Cell **10**(6): 2087-100.

Wilkie, T. M. (1999). "G proteins, chemosensory perception, and the C. elegans genome project: An attractive story." Bioessays **21**(9): 713-7.

William, C. M., Y. Tanabe, et al. (2003). "Regulation of motor neuron subtype identity by repressor activity of Mnx class homeodomain proteins." Development **130**(8): 1523-36.

Williams, B. D. and R. H. Waterston (1994). "Genes critical for muscle development and function in Caenorhabditis elegans identified through lethal mutations." J Cell Biol **124**(4): 475-90.

Wills, Z., J. Bateman, et al. (1999). "The tyrosine kinase Abl and its substrate enabled collaborate with the receptor phosphatase Dlar to control motor axon guidance." Neuron **22**(2): 301-12.

Winnier, A. R., J. Y. Meir, et al. (1999). "UNC-4/UNC-37-dependent repression of motor neuron-specific genes controls synaptic choice in Caenorhabditis elegans." Genes Dev **13**(21): 2774-2786.

Wojtowicz, W. M., J. J. Flanagan, et al. (2004). "Alternative splicing of Drosophila Dscam generates axon guidance receptors that exhibit isoform-specific homophilic binding." Cell **118**(5): 619-33.

Yamagata, M., J. R. Sanes, et al. (2003). "Synaptic adhesion molecules." Curr Opin Cell Biol **15**(5): 621-32.

Yamagata, M., J. A. Weiner, et al. (2002). "Sidekicks: synaptic adhesion molecules that promote lamina-specific connectivity in the retina." Cell **110**(5): 649-60.

Yoshikawa, S., R. D. McKinnon, et al. (2003). "Wnt-mediated axon guidance via the Drosophila Derailed receptor." Nature **422**(6932): 583-8.

Young, J. M. and I. A. Hope (1993). "Molecular markers of differentiation in Caenorhabditis elegans obtained by promoter trapping." Develop. Dynamics **196**: 124-132.

Zahn, T. R., J. K. Angleson, et al. (2004). "Dense core vesicle dynamics in Caenorhabditis elegans neurons and the role of kinesin UNC-104." Traffic **5**(7): 544-59.

Zallen, J. A., S. A. Kirch, et al. (1999). "Genes required for axon pathfinding and extension in the C. elegans nerve ring." Development **126**(16): 3679-92.

Zhang, H. and S. W. Emmons (2002). "Caenorhabditis elegans unc-37/groucho Interacts Genetically With Components of the Transcriptional Mediator Complex." Genetics **160**(2): 799-803.

Zhang, S., C. Ma, et al. (2004). "Combinatorial marking of cells and organelles with reconstituted fluorescent proteins." Cell **119**(1): 137-44.

Zhang, Y., B. Grant, et al. (2001). "RME-8, a conserved J-domain protein, is required for endocytosis in Caenorhabditis elegans." Mol Biol Cell **12**(7): 2011-21.

Zhang, Y., C. Ma, et al. (2002). "Identification of genes expressed in C. elegans touch receptor neurons." Nature **418**(6895): 331-5.

Zhen, M., X. Huang, et al. (2000). "Regulation of presynaptic terminal organization by C. elegans RPM-1, a putative guanine nucleotide exchanger with a RING-H2 finger domain." Neuron **26**(2): 331-43.

Zhen, M. and Y. Jin (1999). "The liprin protein SYD-2 regulates the differentiation of presynaptic termini in C. elegans." Nature **401**(6751): 371-5.

Zheng, Y., P. J. Brockie, et al. (1999). "Neuronal control of locomotion in C. elegans is modified by a dominant mutation in the GLR-1 ionotropic glutamate receptor." Neuron **24**(2): 347-61.

Zhou, H. M. and W. W. Walthall (1998). "UNC-55, an orphan nuclear hormone receptor, orchestrates synaptic specificity among two classes of motor neurons in Caenorhabditis elegans." J Neurosci **18**(24): 10438-44.

Zipursky, S. L., W. M. Wojtowicz, et al. (2006). "Got diversity? Wiring the fly brain with Dscam." Trends Biochem Sci **31**(10): 581-8.

Zwaal, R. R., J. E. Mendel, et al. (1997). "Two neuronal G proteins are involved in chemosensation of the Caenorhabditis elegans Dauer-inducing pheromone." Genetics **145**(3): 715-27.

Zwaal, R. R., K. Van Baelen, et al. (2001). "The sarco-endoplasmic reticulum Ca2+ ATPase is required for development and muscle function in Caenorhabditis elegans." J Biol Chem **276**(47): 43557-63.